

1962

Molecular configurations of some of the solvated compounds of the Grignard system

Galen Dean Stucky
Iowa State University

Follow this and additional works at: <https://lib.dr.iastate.edu/rtd>

 Part of the [Physical Chemistry Commons](#)

Recommended Citation

Stucky, Galen Dean, "Molecular configurations of some of the solvated compounds of the Grignard system " (1962). *Retrospective Theses and Dissertations*. 2328.
<https://lib.dr.iastate.edu/rtd/2328>

This Dissertation is brought to you for free and open access by the Iowa State University Capstones, Theses and Dissertations at Iowa State University Digital Repository. It has been accepted for inclusion in Retrospective Theses and Dissertations by an authorized administrator of Iowa State University Digital Repository. For more information, please contact digirep@iastate.edu.

This dissertation has been 63-3006
microfilmed exactly as received

STUCKY, Galen Dean, 1936-
MOLECULAR CONFIGURATIONS OF SOME OF
THE SOLVATED COMPOUNDS OF THE GRIGNARD
SYSTEM.

Iowa State University of Science and Technology
Ph.D., 1962
Chemistry, physical
University Microfilms, Inc., Ann Arbor, Michigan

MOLECULAR CONFIGURATIONS OF SOME OF THE
SOLVATED COMPOUNDS OF THE GRIGNARD SYSTEM

by

Galen Dean Stucky

A Dissertation Submitted to the
Graduate Faculty in Partial Fulfillment of
The Requirements for the Degree of
DOCTOR OF PHILOSOPHY

Major Subject: Physical Chemistry

Approved:

Signature was redacted for privacy.

In Charge of Major Work

Signature was redacted for privacy.

Head of Major Department

Signature was redacted for privacy.

Dean of Graduate College

Iowa State University
Of Science and Technology
Ames, Iowa

1962

TABLE OF CONTENTS

	Page
ABSTRACT	v
INTRODUCTION	1
Literature Review	2
RMgX	2
RMgX·solvent	3
R ₂ Mg	13
Purpose	16
Computer Programs	18
STRUCTURE OF Mg ₄ Br ₆ O·4(C ₄ H ₁₀ O)	21
Literature Review	21
Preparation	26
Properties and Analyses	30
Properties	30
Chemical analysis	33
Thermogravimetric analysis	36
Infrared analysis	39
Comparison with MgBr ₂ ·diethylether	54
Summary of the analytical results	55
Space Group Determination	56
Collection and Correction of Intensity Data	58
Lorentz polarization	58
Absorption	60
Collection of data on the G.E. XRD5 diffractrometer	64

	Page
Decomposition	69
Streak	69
Anomalous dispersion	76
Background	77
Computer programming for correction of raw data	78
Solution of Structure	79
Two-dimensional Patterson	82
Three-dimensional Patterson	94
Least squares and Fourier analysis	104
Discussion of Structure	119
STRUCTURE OF $C_6H_5MgBr \cdot 2(C_4H_{10}O)$	141
Preparation, Purification and Properties	141
Growth of Single Crystals	146
Low temperature apparatus	146
Experimental techniques for growing single crystals	146
Space Group and Lattice Constants	148
Collection of Data	151
Correction of Data	153
Solution of Structure	153
General procedure	153
Initial considerations	154
Patterson calculations	156
Two-dimensional Fourier and least squares analysis	166

	Page
Three-dimensional Fourier and least squares analysis	176
Discussion of Structure	186
DIPHENYLMAGNESIUMDIETHERATE	202
Preparation and Purification	204
Properties and Collection of Data	206
Space Group Determination	209
Packing Considerations	217
Molecular Configuration	218
Nuclear Magnetic Resonance Results	220
Data Processing	229
Vector Maps	232
Least Squares Analysis and Electron Density Projections	249
$C_6H_5MgBr \cdot n(C_4H_8O)$	250
SUMMARY	254
LITERATURE CITED	258
ACKNOWLEDGEMENTS	264

ABSTRACT

Structural investigations of the solvated compounds $\text{Mg}_4\text{Br}_6 \cdot 4(\text{C}_4\text{H}_{10}\text{O})$ and $\text{C}_6\text{H}_5\text{MgBr} \cdot 2(\text{C}_4\text{H}_{10}\text{O})$ were undertaken by means of x-ray diffraction techniques. In addition, initial structural studies were made on $(\text{C}_6\text{H}_5)_2\text{Mg} \cdot 2(\text{C}_4\text{H}_{10}\text{O})$ and the space group and lattice constants were determined for an oxy salt of the Grignard reagent solvated with tetrahydrofuran.

$\text{Mg}_4\text{Br}_6 \cdot 4(\text{C}_4\text{H}_{10}\text{O})$ was found to possess tetragonal symmetry; the lattice constants based on a primitive unit cell are:

$$\begin{aligned} a &= b = 10.68 \text{ \AA} \\ c &= 15.34 \text{ \AA} \end{aligned}$$

There are two $\text{Mg}_4\text{Br}_6 \cdot 4(\text{C}_4\text{H}_{10}\text{O})$ species per unit cell.

Systematic absences indicated the space group $P\bar{4}2_1c$.

The structural analysis proceeded through a complete three-dimensional Fourier. The bromine atoms form an octahedron approximately 4.5 angstroms on an edge about the origin with the magnesium atoms in alternating faces of the octahedron, forming a tetrahedron of magnesium atoms. The magnesiums are five-fold coordinated to three bromines, a "basic" oxygen atom at the origin, and to an ether group packed against the face of the bromine octahedron. The only model compatible with the Fourier and least squares analysis and with packing considerations involves a disordered structure

in which the ether carbons can be packed in three equivalent ways against the faces of the octahedron formed by the bromine atoms. Packing considerations strongly imply that the ether oxygens are trigonally coordinated to the magnesium atom and that only two of the three possible ether orientations are utilized in the crystal.

$C_6H_5MgBr \cdot 2(C_4H_{10}O)$, a liquid at room temperature, was isolated by successive recrystallizations at low temperatures. The lattice constants for this orthorhombic system were found to be

$$\begin{aligned} a &= 12.25 \text{ \AA} \\ b &= 12.81 \text{ \AA} \\ c &= 11.02 \text{ \AA} \end{aligned} .$$

The space group was uniquely determined to be $P2_12_12_1$, and the observed density and chemical analysis both suggested 4 molecules of $C_6H_5MgBr \cdot 2(C_4H_{10}O)$ per unit cell. Three-dimensional Patterson and two-dimensional Fourier analyses revealed that the basic molecular unit consisted of the phenyl group, the ether oxygens, and the bromine atom tetrahedrally coordinated to a single-magnesium atom. There was no evidence of intermolecular interaction between the monomeric molecules of $C_6H_5MgBr \cdot 2(C_4H_{10}O)$. Because of experimental difficulties in obtaining the data the carbon positions were not located by least squares refinement. Three-dimensional Fourier results implied, however, that the ether molecules are tetrahedrally

coordinated to the magnesium atom, although additional three-dimensional work will be needed to confirm the structural aspects relating to the carbon atoms. Since the magnesium-magnesium, magnesium-bromine, and bromine-bromine distances eliminate the possibility of $R_2Mg \cdot MgX_2$ type structures in the crystal, it would be surprising if recent proposals which disregarded the presence of the molecular species $RMgX \cdot 2ether$ in solution are correct.

$(C_6H_5)_2Mg \cdot 2(C_4H_{10}O)$ has monoclinic symmetry and lattice constants (1st setting) of

$$\begin{aligned} a &= 14.21 \text{ \AA} \\ b &= 17.69 \text{ \AA} \\ c &= 7.87 \text{ \AA} \end{aligned} \quad \gamma = 91^\circ 24'$$

The observed extinctions

$$\{hkl\} \quad h + l = 2n + 1$$

gave possible space groups of $B2$, $B 2/m$, or Bm . The ratio of ether groups to phenyl groups of one to one was confirmed by nuclear magnetic resonance studies. Density measurements made on the NMR samples gave $\rho = 1.09 \text{ gms/cm}^3$. This corresponds to four molecules of $(C_6H_5)_2Mg \cdot 2(C_4H_{10}O)$ per unit cell. Intensity data were taken of $\{hk0\}$ and $\{hkl\}$ reflections. No structural interpretation was found for these data.

The lattice constants and space group of a salt obtained by the oxidation of a solution of phenylmagnesium bromide in tetrahydrofuran were determined by x-ray techniques.

The lattice constants obtained (2nd setting) were

$$\begin{aligned} a &= 8.05 \text{ \AA} \\ b &= 9.89 \text{ \AA} \\ c &= 20.73 \text{ \AA} \end{aligned} \quad \gamma = 95^\circ 20'$$

The only extinctions were $\{h0l\}$ $l = 2n + 1$ implying a space group of Pc or $P2/c$.

INTRODUCTION

The most important of all organometallic compounds during the past sixty years has undoubtedly been the Grignard reagent, RMgX . This is true not only for the organic chemist who has used the Grignards as an intermediate for the preparation of a wide variety of organic products, but also for any scientist who wishes to study the interesting physical aspects of the organometallic compounds inasmuch as the majority of all other types of organometallics are prepared using the Grignard reagent.

In spite of a great deal of research and speculation, the exact nature of the Grignard reagent has not been established. This has been primarily due to experimental difficulties. This first problem involves the extreme reactivity of the reagent to such compounds as water, carbon dioxide, oxygen, organic halides, esters, some inorganic halides, aldehydes, ketones, amides, acids, and halogens. A comprehensive treatment of the reactions of the Grignard reagent is given by Kharasch and Reinmuth (1). The second problem arises because of the difficulty in isolating the pure Grignard from its solvent and in working with the intractable unsolvated material after isolation is achieved.

To familiarize the reader with the properties of the Grignard reagent, a literature review is given next. This is

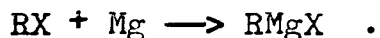
followed by a statement of the purpose of this research.

Literature Review

In view of the large amount of literature concerning the nature of the Grignard reagent, no attempt will be made to give a complete review. The reader is referred to Yoffé and Nesmeyanov (2), Rochow, Hurd, and Lewis (3), Coates (4), Runge (5), Kharasch and Reinmuth (1) for a comprehensive list of references. The research abstracted below seemed to have the most direct bearing on the solution of the compositional and structural problems involved in the Grignard system. In the discussion which follows R represents an alkyl or aryl group and X one of the halogens; Cl, Br, or I.

RMgX

Preparation The preparation of some of the unsolvated RMgX compounds can be accomplished with difficulty by the reaction (6)



Another method is to remove the solvent under reduced pressures and at temperatures 150° or higher (1).

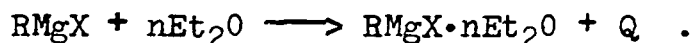
Properties and constitution The properties of the unsolvated reagents indicate they are polymeric. They are non-volatile, infusible, and for all practical purposes insoluble

in all but polar solvents such as ethers, furans, and tertiary amines, all of which probably form solvated complexes with Grignards. This is all that is definitely known about the physical properties of the unsolvated Grignard reagents.

RMgX·solvent

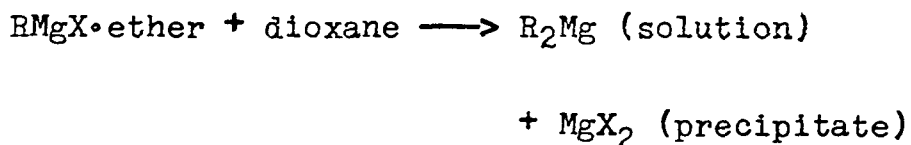
Preparation The solvated reagents are much simpler to prepare. The reaction is the same as for the unsolvated material but is generally carried out in diethylether, tetrahydrofuran, or dimethylaniline at room temperature.

Properties and constitution The properties of the solvated Grignard reagent indicate strong coordination of the ether. Tschelinzeff (7) and Lifschitz and Kalberer (8) found the following heats of solvation in kilocalories for the reactions (see Table 1)



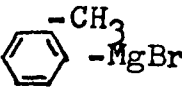
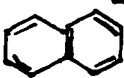
From this it is obvious that proposed structures of the Grignard reagent in ether solution must take into account the coordination of the ether.

On the basis of the reaction

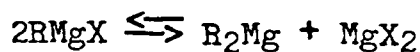


Schlenk and Schlenk (9) proposed that equilibria of the type

Table 1. Heats of solvation of Grignard reagents in kilocalories^a

Compound	Q ₁	Q ₂	Q ₃	Q ₄	Q total
N-C ₃ H ₇ MgI	6.63	5.66	.50	---	12.79
C ₂ H ₅ MgI	6.69	5.57	.23	---	12.46
C ₆ H ₅ MgBr	8.69	2.32	.83	.40	12.24
 -MgBr	7.45	3.40	.56	---	11.41
 -MgBr	7.15	3.21	.83	---	11.19

^aQ_n = heat of solvation by adding the nth ether molecule.



existed in the Grignard solution. Noller and White (10) showed that this method did not give true values of the positions of such an equilibrium or of the time for equilibrium to be reached. It is almost certain that the Grignard reagent is not as simply formulated as proposed by Schlenk and Schlenk (9), but is highly associated and complex in solution.

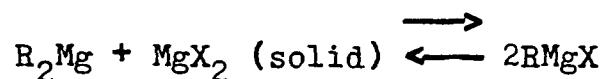
Evans and Pearson (11) noted an electrophoretic effect for aromatic Grignards. In addition, the dark color of the ether solution and a pronounced Tyndall effect also brought them to the conclusion that the aromatic Grignards

are partly colloidal in nature. The aliphatic Grignards on the other hand form true solutions. The difference between alkyl and aromatic Grignards was assigned to the greater coordinating power of the benzene. Evans and Pearson also found from electrolytic measurements that magnesium was present in both the anion and cation portions of the molecule and that several equivalents of R^- and X^- were transported per Faraday. The cation is small but highly coordinated to the ether while the anion is large but does not interact with the solvent and so carries the most current. They noted that if $ZnCl_2$ was added to $RMgX$ there was an instantaneous conversion to R_2Zn . The conclusion was that if MgX_2 was added to a solution of R_2Mg there would be instantaneous exchange between the reagents.

Dessy et al. (12) and Dessy and Handler (13) did carry out the exchange experiment to investigate this equilibrium. Their procedure was to tag anhydrous magnesium bromide with Mg^{28} or Mg^{25} and then to add .5 molar Mg^*Br_2 to a .5 molar solution of $(C_6H_5)_2Mg$ to give a solution, which chemically is indistinguishable from a one molar solution of phenyl magnesiumbromide. After some time dioxane was added and the magnesium bromide precipitated. The supernatant liquid was found to be .5 molar in magnesium and .01 molar in bromine. When Mg^{28} was used, Dessy and Handler (13) found only 7% exchange after 36 hours. When Mg^{25} was used complete exchange

was observed in all cases. This was attributed to impurities in the Mg^{25} .

These results are very similar to those obtained by Garrett et al. (14) for cadmium. They found no exchange between diethylcadmium and cadmium bromide in tetrahydrofuran. However, Garrett et al. measured the solubility of MgCl_2 in diethylether solution of $(\text{C}_2\text{H}_5)_2\text{Mg}$ and did not reach the same conclusions as Dessy and Handler (13). At 0° and 15° C the solubility of MgCl_2 was one mole MgCl_2 per mole of $(\text{C}_2\text{H}_5)_2\text{Mg}$, indicating an equilibrium



At -31° C the ratio of $\text{MgCl}_2/\text{R}_2\text{Mg}$ was 1.6 which was taken to imply the formation of $\text{RMgX}\cdot\text{MgX}_2$. No reaction was obtained at -79° C.

Dessy and Handler (13) also carried out exchange experiments using ethylmagnesiumbromide. They found, using electrolytic methods, that for this compound the magnesium which plates out at the cathode originated with the diethylmagnesium while the largest portion of the magnesium at the anode came from the magnesiumbromide. The basic cation was concluded to be RMg^+ . From the results it was concluded that the structure of the Grignard reagent was basically solvated $\text{R}_2\text{Mg}\cdot\text{MgX}_2$ to the exclusion of a species of the type $\text{RMgX}\cdot\text{solvent}$. Dessy and Handler's results are difficult to reconcile with NMR

studies of the aluminum and zinc dialkyls. $[\text{Al}(\text{CH}_3)_3]_2$ is a dimer as determined by cryoscopic measurements and infrared spectra. The dimer has also been observed in the vapor from 100° to 160° (4) and is present in the crystalline phase (15). Nevertheless NMR studies at room temperature distinguish only one kind of methyl group which indicates rapid exchange of methyl groups. Similar work (16) on mixtures of $(\text{CH}_3)_2\text{Zn}$, $(\text{CH}_3)_2\text{Cd}$, and $(\text{CH}_3)_3\text{Al}$ also showed the presence of only one methyl group at room temperature.

The results of Dessy et al. (12) and Dessy and Handler (13) are also at odds with those found by Korshunov et al. (17) and Sinotova et al. (18). Korshunov et al. studied the systems $\text{C}_6\text{H}_5\text{MgBr}-\text{C}_6^*\text{H}_6$ (I) and $\text{C}_2\text{H}_5\text{MgBr}-\text{C}_2^*\text{H}_5\text{Br}$ (II) using C^{14} as the tracer. (I) exchanged only to an extent of 5.0% at 80°C during 12 hours. (II) however gave complete exchange. They studied the effect of solvent and found exchange increased as the polarity of the solvent increased, i.e. the exchange in (II) was faster in ether than in benzene.

Sinotova et al. observed fast isotopic exchange of phenyl groups between $(\text{C}_6\text{H}_5)_2\text{Mg}$ and the Grignard reagent in ether. They discovered rapid isotopic exchange in the systems $(\text{C}_6\text{H}_5)_2\text{Hg}-\text{C}_6^*\text{H}_5\text{HgBr}$ -pyridine and $(\text{C}_6\text{H}_5)_2\text{Hg}-\text{C}_6^*\text{H}_5\text{HgBr}$ -dioxane.

There is also the observation by Schlenk and Schlenk (9) that a compound with a molecular weight corresponding to $\text{RMgX} \cdot 2(\text{C}_4\text{H}_{10}\text{O})$ crystallized out of solution at low temperatures.

If this is true, this molecular form must have some existence in solution. In addition, Cope (19) has observed that the percentage of diphenylmagnesium in solution as measured by dioxane precipitation increases with temperature, indicating some type of temperature dependent equilibrium.

Slough and Ubbelohde (20) concerned themselves with the thermodynamics of the Grignard system. They discovered that the Grignard reagent was photosensitive and extremely reactive toward oxygen. For example they found the degree of association of phenylmagnesiumbromide at 15° C is 1.85. In the presence of oxygen the degree of association at 15° C is 5.98. The degree of association decreased as the temperature increased and the concentration decreased. The degree of association of the various Grignard reagents varies widely as illustrated in Table 2.

Slough and Ubbelohde make two postulates concerning the bonding in arylmagnesium halides which because of their relation to the structure of phenylmagnesiumbromide bear repeating here. In the compound KC_8 the graphite rings apparently act as acceptor groups (21). A similar occurrence for phenylmagnesiumbromide would imply polarization bonding between the phenyl groups and the bromine atoms as in Figure 1a. The second postulate concerns the use of the pi orbitals of the phenyl group analogously to that found by Rundle and Goring (22) for the silver ion and aromatic groups.

Figure 1. Models proposed by Slough and Ubbelohde (20)
for $C_6H_5MgBr \cdot 2(C_4H_{10}O)$

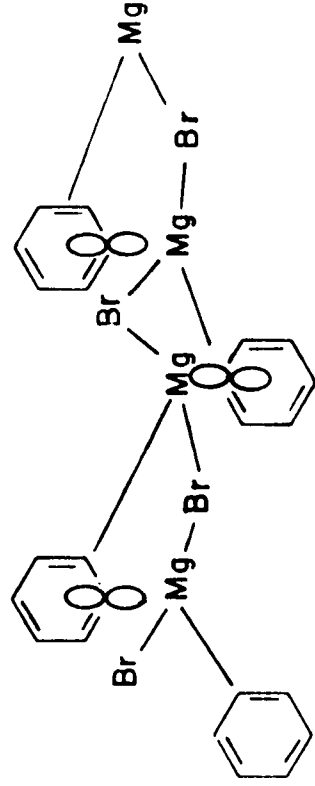
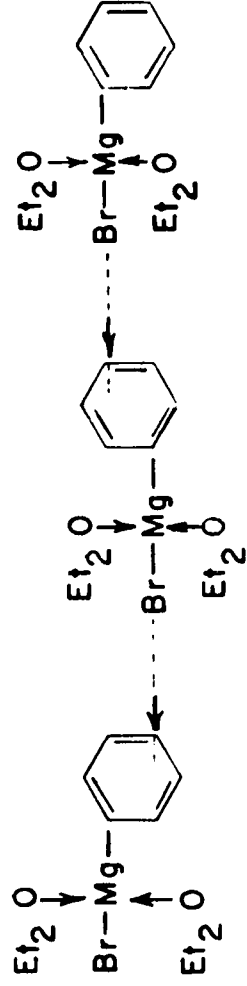
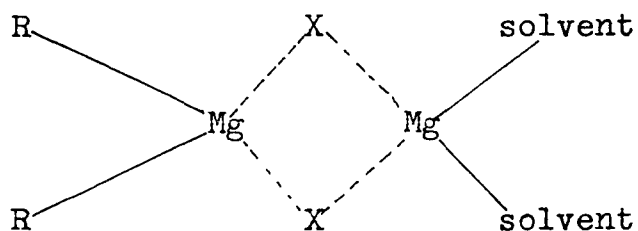


Table 2. Association of Grignard reagents

Compound	Concentration moles/liter	Degree of association	
		15° C	20° C
phenylmagnesiumbromide	.331	1.97	1.77
ortho-tolylmagnesiumbromide	.413	1.38	1.39
para-tolylmagnesiumbromide	.368	1.80	----
	.566	2.03	1.82
p-methoxyphenylmagnesium- bromide	.327	1.10	1.03
cyclohexylmagnesiumbromide	.324	2.93	2.94
	.669	4.14	3.33
cyclohexylmagnesiumchloride	.551	1.28	1.29
MgBr ₂	.071	----	1.05

The magnesium atom would make use of its tetrahedral orbitals as shown in Figure 1b.

Aston and Bernhard (23) noted that dimethylmagnesium reacted with acetone about fifty times as fast as methylmagnesiumiodide. Furthermore the reaction of methylmagnesiumbromide was first order with respect to the Grignard and independent of the acetone concentration. On this basis the argument was made that there is no appreciable amount of free dialkylmagnesium in solution and that the Grignard may be represented by a skeletal structure of



The infrared spectra of several of the Grignard reagents is given by Plum (24) and Zeil (25). Plum found three bands at about 780, 910 and 4250 cm^{-1} which were characteristic of the Grignard reagent.

Several forms of crystalline Grignard compounds have been reported. These are listed in Table 3. The variation of degree of solvation should be noted.

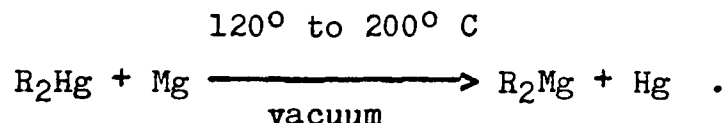
Table 3. Crystalline Grignard reagents

Compound	Reference
$\text{CH}_3\text{MgI} \cdot (\text{C}_5\text{H}_{11})_2\text{O}$	26
$\alpha\text{-C}_{10}\text{H}_7\text{MgBr} \cdot 3(\text{C}_4\text{H}_{10}\text{O})$	27
$(\text{C}_6\text{H}_5)_3\text{CMgBr} \cdot 2(\text{C}_4\text{H}_{10}\text{O})$	28
$\text{C}_2\text{H}_5\text{MgI} \cdot 2(\text{C}_4\text{H}_{10}\text{O})$	29
$\text{C}_6\text{H}_5\text{MgBr} \cdot 2(\text{C}_4\text{H}_{10}\text{O})$	29
$\text{C}_{10}\text{H}_7\text{MgBr} \cdot 1(\text{C}_4\text{H}_{10}\text{O})$	29

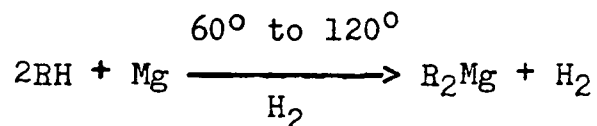
R₂Mg

The structures of the dialkyl and diaryl magnesium compounds are also unsolved. These compounds have physical properties similar to the Grignards in that they are infusible and insoluble in all solvents except those with strongly electronegative groups. The alkyl members sublime (30); however, no successful sublimation of the diaryls is reported.

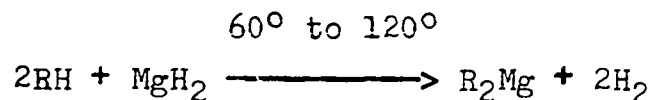
Preparation The preparation of the R₂Mg compounds can be carried out by the following reaction (31)



Dioxane precipitates MgBr₂ from a solution of RMgBr leaving R₂Mg (27). A third method is through either of the reactions (32)



or



Properties and constitution Some very careful work on the physical properties of the organometallic compounds of Cd, Zn, and Mg was done by Strohmeier (33, 34). A major

contribution of his work was the separation and isolation of pure crystalline forms of these compounds. With some minor adaptations his apparatus was used in this research for the purification of phenylmagnesiumbromide and diphenylmagnesium. He was not able to sublime diphenylmagnesium but did so in the case of both diphenylcadmium and diphenylzinc. The solubility and dipole moments which Strohmeier measured are listed in Tables 4 and 5.

The organomagnesium compounds are not ionic as they do not conduct an electric current. Rochow et al. (3) point out that $[(C_6H_5)_3C]_2Mg$ is colorless in ether as is the covalent $(C_6H_5)_3CH$, while the ionic $(C_6H_5)_3C^-Na^+$ is a bright red due to the $C_6H_5C^-$ ion.

In comparing the dialkylmagnesium compounds with those of beryllium, Gilman and Brown (30) have noted that dimethylmagnesium through di-n-butyl-magnesium are solids which sublime with difficulty. Gilman and Brown also found the solubility of dimethylmagnesium to be .08 moles/liter of diethylether which was less than that of $(C_2H_5)_2Mg$ or $(C_4H_{10})_2Mg$. They obtained crystals from a solution of dimethylmagnesium in ether but did not analyze them. These reagents were all highly inflammable in air. Gilman and Brown were unable to sublime or ether distill diphenylmagnesium or phenylmagnesiumbromide.

The decomposition products of the dialkylmagnesiums

Table 4. Comparison of the solubility of some organometallics

Solvent	CdPh ₂		ZnPh ₂		MgPh ₂		Mg(C ₂ H ₅) ₂	
	g/l	mol/l	g/l	mol/l	g/l	mol/l	g/l	mol/l
Heptane	.37	.0014	4.2	.019	.0001	-----	.099	.0012
Benzene	16	.06	79	.36	.11	.0006	1.3	.016
Dioxane	42.7	1.75	159	.72	42.9	.24	∞	-----
Diethylether	60.5	.22	∞	---	∞	---	165	2.0

Table 5. Comparison of the dipole moments of some organometallics

Solvent	HgPh ₂ μ(D)	CdPh ₂ μ(D)	ZnPh ₂ μ(D)	MgPh ₂ μ(D)
Benzene	.2	.6	.8	---
Dioxane	.4	1.4	2.7	4.9

include the series of compounds $C_nH_{2n}Mg$ as byproducts (35, 36) indicating metal-carbon double bond character. Diphenylmagnesium decomposes into metallic magnesium, biphenyl, and other organic byproducts (37).

Schlenk (29) has reported crystals of $(C_2H_5)_2Mg \cdot 2(C_4H_{10}O)$ and $(C_6H_5)_2Mg \cdot 2(C_4H_{10}O)$. Some interesting crystalline products with the formula $Li[MgPh_3]$ are formed by the reaction of phenyllithium with diphenylmagnesium (38).

Purpose

The purpose of this research is to provide some insight into the structural features of the Grignard reagents by means of x-ray diffraction techniques. In connection with this the following points are of interest:

1. From the results of Dessy *et al.* (12), Dessy and Handler (13), Slough and Ubbelohde (20) and others the Grignard

reagent is probably associated in the liquid state. A structural investigation of phenylmagnesiumbromide would show whether or not the solid is associated and if so the nature of this association. The bonding in polymeric phenylmetallic compounds has not yet been studied by x-ray diffraction techniques.

2. In conjunction with the normal association of the Grignard reagent is the observation by Slough and Ubbelohde (20) that the association is greatly increased by the addition of oxygen. To determine the nature of this association, an oxidation product of phenylmagnesiumbromidedietherate was isolated and studied.
3. The water molecule utilizes an sp^2 type hybrid bonding in $CuCl_2 \cdot 2H_2O$ as determined by neutron diffraction techniques (39). The question is whether the greater electropositive character and steric effects of the ether group will allow a similar configuration in Grignards, or if tetrahedral sp^3 hybrid orbitals of the oxygen will be used.

The Grignard system which was chosen was that of phenylmagnesiumbromide. The phenyl organic group was chosen because very little is known about the interaction of this organic species with the metal atom in organometallic compounds. The bromine atom was chosen for crystallographic reasons. In compounds containing benzene rings the interpretation of the structure is sometimes easier if a heavy atom

such as bromine is present. Phenylmagnesiumbromide has also been one of the most widely used and studied Grignard reagents.

Three compounds are intimately connected with the phenylmagnesiumbromide system, the oxidation product $\text{Mg}_4\text{Br}_6\text{O}\cdot 4(\text{C}_4\text{H}_{10}\text{O})$, phenylmagnesium bromide, and diphenylmagnesium.

Computer Programs

The IBM 650, Iowa State Cyclone, and IBM 704 computers were used in this work. The 650 and Cyclone were on the campus of Iowa State University. The 704 of the Midwestern University Research Association at Madison, Wisconsin, was used via a data link.

The initial work was carried out on the IBM 650, a smaller amount on the Cyclone, and the remainder, about half, on the IBM 704. The basic programs necessary for crystallography are a non-linear least squares and a Fourier program, the latter preferably three dimensional. These were available for both the IBM 650 and 704. The 650 least squares program by M. E. Senko and D. H. Templeton of the University of California* as modified by D. E. Williams and D. R. Fitzwater

*Senko, M. E. and Templeton, D. H. Department of Chemistry, University of California, Berkeley, California. L.S. for IBM 650. Private communication. ca. 1958.

of Iowa State University* was modified a second time to make use of the expansion of the memory of the 650 from 2000 to 4000 words. A patch was also written to allow for the symmetry of the space group $P\bar{4}2_1c$. The least squares program for the 704 was written by W. R. Busing and H. A. Levy (40) of the Oak Ridge National Laboratory. The modifications of this program for the "Frito" data link and for the treatment of observed and unobserved data were written by R. D. Willett**. One minor addition was written for this program to permit the calculation of anisotropic temperature factors for atoms in special positions for $Mg_4Br_6O_{0.4}(C_4H_{10}O)$. The Fourier program used for the IBM 650 was "TDF2" written by D. R. Fitzwater***. The Fourier program used for the 704 was "MIFR 1", written by W. G. Sly and D. P. Shoemaker (41) of the Massachusetts Institute of Technology.

Acknowledgements for miscellaneous programs for purposes such as data correction, Patterson sharpening, statistical tests, and weighting are made in the appropriate

*Williams, D. E. and Fitzwater, D. R. Department of Chemistry, Iowa State University, Ames, Iowa. L.S. IIM for IBM 650. Private communication. ca. 1958.

**Willett, R. D. Department of Chemistry, Washington State University, Pullman, Washington. Busing patches. Private communication. ca. 1961.

***Fitzwater, D. R. Department of Chemistry, Iowa State University, Ames, Iowa. TDF2. Private communication. ca. 1958.

experimental section. One program which proved invaluable in terms of time saved transformed Busing and Levy's binary structure factor output (40) into decimal structure factors properly scaled and in a format appropriate for input into Sly and Shoemaker's 704 Fourier program (41). The program, LSSRT, also generated redundant data as needed, sorted the data, and performed specified rejection tests. It was co-authored by D. R. Fitzwater*.

*Fitzwater, D. R. Department of Chemistry, Iowa State University, Ames, Iowa. LSSRT. Private communication. ca. 1961.

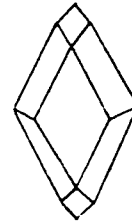
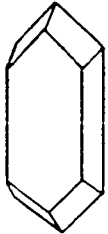
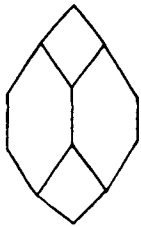
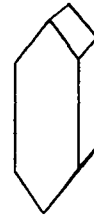
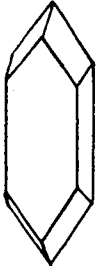
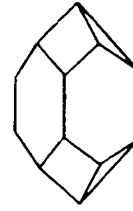
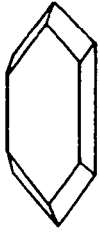
STRUCTURE OF $\text{Mg}_4\text{Br}_6\text{O}\cdot 4(\text{C}_4\text{H}_{10}\text{O})$

Literature Review

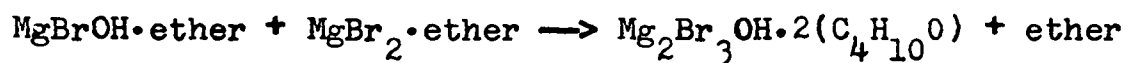
Runge (5) mentions the preparation of compounds of the type RMgX by the evaporation of the solvent in which these compounds are prepared. During the initial attempts to prepare crystals of phenylmagnesiumbromide by this method, clear polyhedral crystals were obtained. The habit of some of these crystals is illustrated in Figure 2. It was found that the crystals were also formed if dry oxygen was passed over the solution. In view of the theories which had been proposed regarding the association of the Grignard reagent and the observed increase in association with oxygen contamination, it was decided to investigate the structural properties of these crystals.

Holyrod (42) in 1904 prepared "clear colourless crystals having the form either of octahedra or of combinations of the octahedra and cube" by passing acetylene dried over phosphorus pentoxide over a diethylether solution of phenylmagnesiumbromide. He reported 53.00% bromine and 10.86% magnesium. He found 8.44 cc of CO_2 evolved when the material was decomposed with water and an electric spark passed through the resulting gaseous mixture. $\text{Mg}_2\text{Br}_3\text{C}_8\text{H}_{21}\text{O}_3$ would require 8.73 cc of CO_2 , 52.85% Br, and 10.72% Mg.

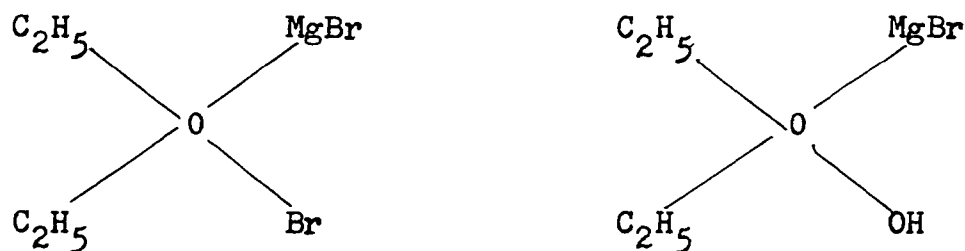
Figure 2. Habit of some crystals of $\text{Mg}_4\text{Br}_6 \cdot 0.4(\text{C}_4\text{H}_{10}\text{O})$



Holyrod suggested the formula $\text{Mg}_2\text{Br}_3\text{OH}\cdot 2(\text{C}_4\text{H}_{10}\text{O})$, the acetylene serving merely to evaporate the ether



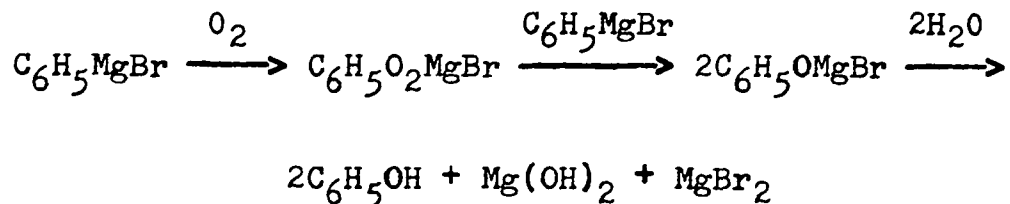
Following some work of Zelinsky (43) he proposed the structure



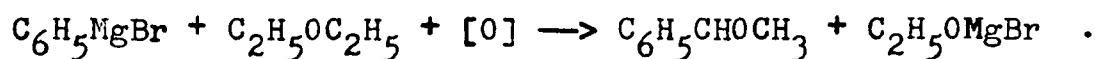
for this double salt.

Nesmeyanow (44) passed CO_2 free air over a diethyl-ether solution of phenylmagnesiumbromide and obtained large crystals. The analysis of the crystals gave 52.72% bromine and 10.73% magnesium. He concluded the crystals were the same as those prepared by Holyrod.

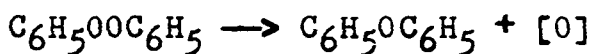
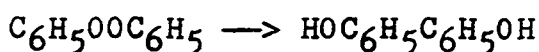
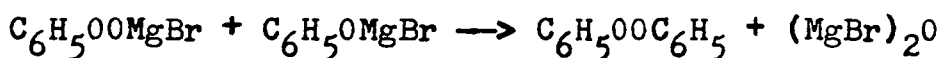
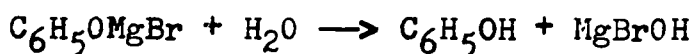
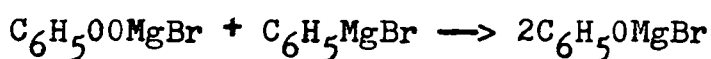
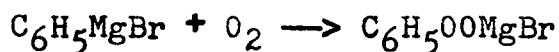
Wuyts (45) describes the oxidation of phenylmagnesium-bromide by



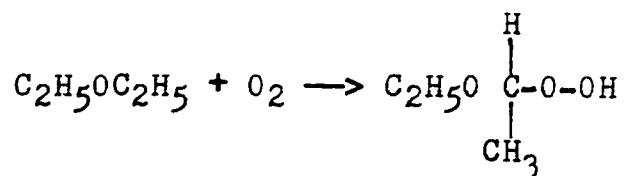
and also



Porter and Steel (46) believed that things were more complicated and used the equations below to describe the oxidation process.



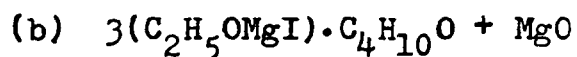
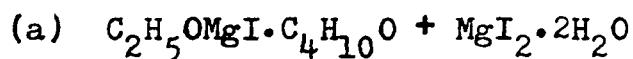
Gilman and Wood (47) noted than in diethylether solutions of arylmagnesium halides, large quantities of $\text{C}_6\text{H}_5\text{CHOHCH}_3$ formed as a result of the auto-oxidation of ethyl ether.



The d-ethoxyethylhydrogen peroxide formed by this reaction

decomposes into acetaldehyde, mono-ethyl acetal, acetic acid, ethyl alcohol and CO_2 . Acetaldehyde and its acetal then react with $\text{C}_6\text{H}_5\text{MgBr}$ to give $\text{C}_6\text{H}_5\text{CHOHCH}_3$. The point of interest here is the confirmation of Wuyt's suggestion that the oxidation of the ether may be as important as the oxidation of the Grignard reagent (45).

Meisenheimer (48) obtained crystals by the air oxidation of $\text{C}_2\text{H}_5\text{MgI}$ in diethyl ether solution. His analysis implied a formula $\text{C}_2\text{H}_5\text{OMgI} \cdot 1$ ether or perhaps something with less iodide and higher magnesium content. He postulated the following mixture.



Slough and Ubbelohde (20), while investigating association complexes of aromatic Grignard reagents by measuring the halogen/basicity ratio of the oxidation products, concluded that Meisenheimer's Mg-O-R linkages were not involved in the products of the oxidation of the Grignard solution.

Preparation

A 1.5 normal solution of $\text{C}_6\text{H}_5\text{MgBr}$ in diethylether was prepared in a closed system under a nitrogen atmosphere. The

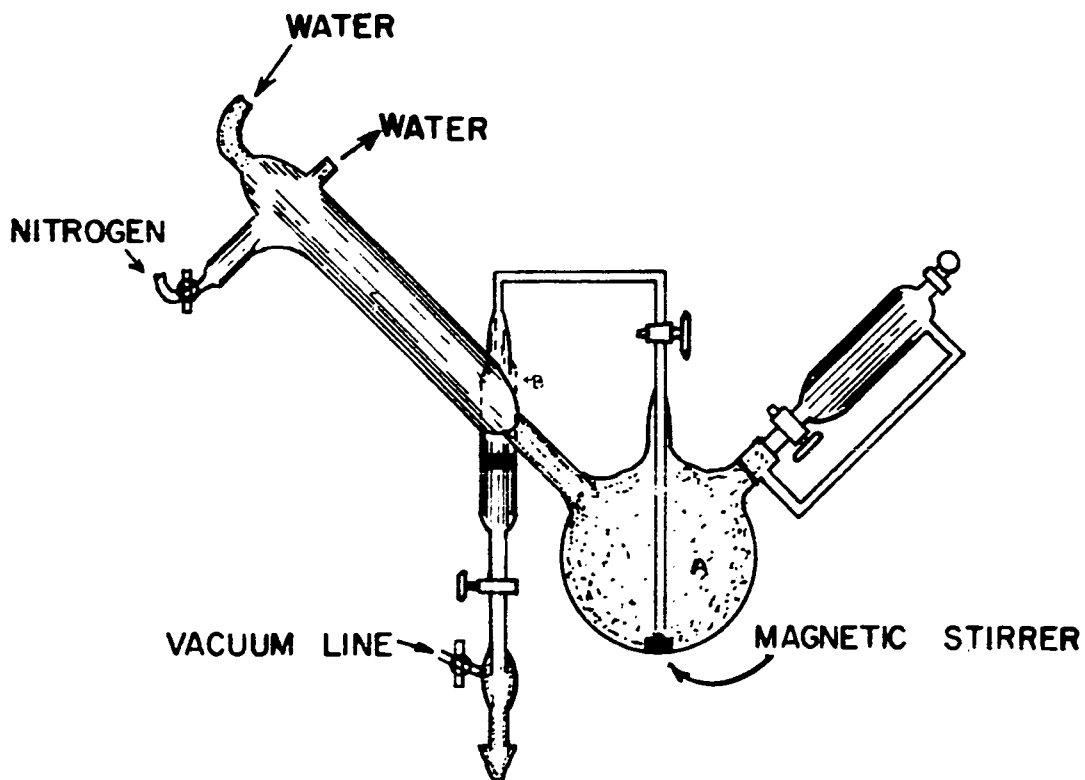
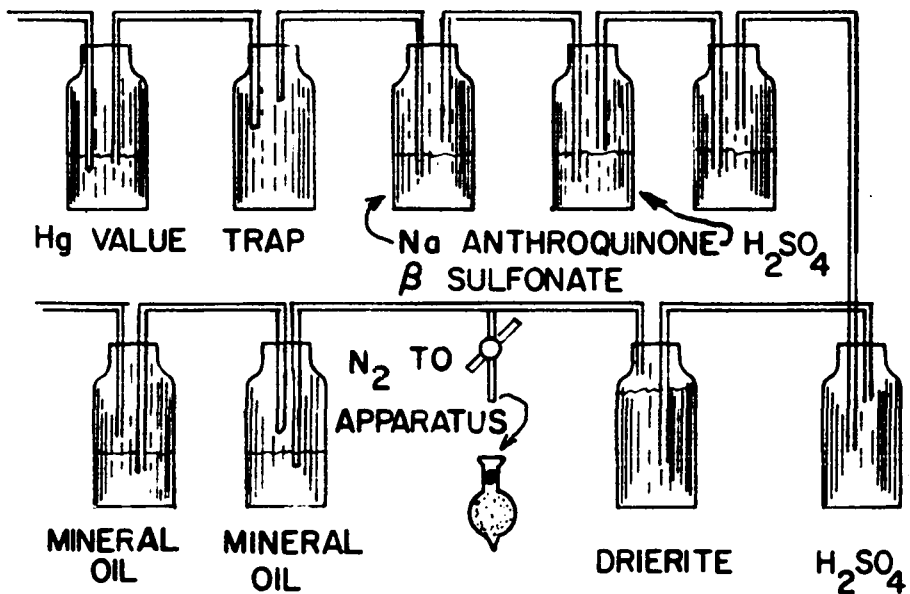
best procedure was to use the nitrogen system in Figure 3a. The sodium anthroquinone β sulfonate solution removes oxygen from the system and is prepared according to Fieser (49). The mineral oil solutions act as valves and are essential because of the large pressure fluctuations in the system due to the diethyl ether. It is convenient to dry the preparation apparatus (Figure 3b) using a vacuum, in which case care must be taken to close the stopcock to the mineral oil valves. The H_2SO_4 bottles, drierite, and $CaCl_2$ drying tube were sufficient to remove the water from the nitrogen.

The preparation apparatus (Figure 3b) needs little explanation. The reagent prepared in A was allowed to stand for one hour and then filtered through the sintered glass filter in B into a suitable receptacle. All of the apparatus was vacuum dried using an infrared lamp.

The receptacles for this experiment were made from $3/4$ inch glass tubing fitted with ground glass ball joints. The female end of the ball joint was sealed off and the male end fitted with a three to five mm inside diameter stopcock. The ball joint was held tightly together by an appropriate metal clamp. The use of stopcock lubricant was kept to a minimum; however Dow Corning silicone lubricant was used where necessary. The containers were attached to the transfer line by means of a T connection which permitted their evacuation and drying with a vacuum pump and infrared lamp.

Figures 3a and 3b. Equipment used for preparation of Grignard reagent

NITROGEN



After transferring the Grignard solution, the stopcock was opened just enough to allow passage of dry nitrogen into the container. The containers were then disconnected from the transfer line and allowed to stand, with the stopcock opened as described, in the atmosphere of the laboratory. The vapor pressure of diethylether at 20° C is 445 mm so that evaporation takes place quite rapidly and large crystals form in as little as six hours. By increasing the temperature of the solution to 60° C, occasionally well formed rhombohedral needle crystals were found growing with the polyhedral crystals. These needle crystals grew both independently and as outgrowths of the polyhedral crystals. X-ray diffraction patterns of these two different forms of crystals were identical.

A process which worked equally well in preparing the crystals was to leave the containers connected to the transfer line and to pass oxygen over the solution. The oxygen was commercial tank oxygen which was dried by first passing it through two phosphorus pentoxide towers and then filtering it with glass wool. Crystals began to form in as little as two hours.

Properties and Analyses

Properties

The crystals were found to be soft and very hygroscopic, decomposing rapidly in air with the evolution of heat.

Upon standing the crystals turned white and then into a paste. After washing the crystals with carbon tetrachloride and then storing in a tightly sealed container which contained air as an atmosphere, a definite odor of diethylether was observed.

One of the most difficult problems in connection with crystals of a compound of this nature is that of transferring the crystals. For the early chemical analyses the main interest was in the Br/Mg ratio. The bonding energy of Mg to Br is sufficiently large that one would not expect Br to be easily displaced. A sample which had completely reacted with the atmosphere should then have the same Br/Mg ratio as a pure sample. This was later confirmed. For these reasons the transference of samples in a dry box for which reasonable precautions had been taken to insure a dry and inert atmosphere was satisfactory for chemical analysis.

For crystallographic analysis the problem is more difficult. A major factor for any external decomposition effect is the larger area/volume ratio of the crystal in comparison to say the larger mass of a chemical analysis sample. The time involved for the transfer of a single crystal with a maximum dimension of .4 mm to a soft glass, thin walled capillary with a comparable diameter is generally longer than that for an aggregate sample transfer. For chemical analysis the crystals can be grown in the sample container so that no transfer at all is needed. For

$\text{Mg}_4\text{Br}_6 \cdot 0.4(\text{C}_4\text{H}_{10}\text{O})$ there is evidence from thermogravimetric analysis that the ether of crystallization is not tightly held which means that decomposition which was observed to occur in apparently the driest dry-box could be explained by the loss of ether of crystallization rather than by the assumption that the dry-box was unsatisfactory. In addition it was found that $\text{Mg}_4\text{Br}_6 \cdot 0.4(\text{C}_4\text{H}_{10}\text{O})$ decomposes in the x-ray beam and the effect was undoubtedly attributed to "poor" transfers in early work with this compound thus adding to the difficulty in evaluating a given transfer technique.

A satisfactory technique for preparing samples for chemical and thermogravimetric analysis was to grow the crystals in a small ampule, decant the mother liquor, evacuate the ampule, partially fill it with argon dried over phosphorus pentoxide and then to seal it off.

When transfers made in a dry-box using nitrogen dried first over sulfuric acid and then over phosphorus pentoxide failed to give satisfactory samples for x-ray analysis, attempts were made to transfer the crystals under some inert liquids. Semi-success was obtained with mineral oil. Ultimately the best procedure was the use of a combination of argon dried over sulfuric acid and P_2O_5 , and petroleum jelly to cover the crystals. The dry-box was swept out first for 24 hours with dry nitrogen, then two hours with argon. P_2O_5 trays were placed in the dry-box before the above operations.

The containers containing the crystals were kept covered as much as possible and any crystal removed from the mother liquor was quickly covered with petroleum jelly before transferring to German thin walled, soft glass capillaries .2 mm in radius. The capillaries were sealed with pyseal and then upon removal from the dry-box quickly resealed with a microburner attachment for a gas-oxygen torch.

The density was found by the flotation method using isopropyl iodide ($d = 1.703 \text{ gms/cm}^3$) and normal propyliodide ($d = 1.747 \text{ gms/cm}^3$). The density as determined at 27° C was found to be 1.73 gms/cm^3 .

Chemical analysis

Several chemical analyses were made on the samples by the Ames Laboratory Analytical Chemistry Group I under Dr. C. V. Banks. These results are given in Table 6.

Table 6. Chemical analysis of $\text{Mg}_4\text{Br}_6\text{O}\cdot 4(\text{C}_4\text{H}_{10}\text{O})$, No. 1

Sample	Element determined	Determination 1	Determination 2	Averages
1	% Br	52.72	52.69	52.71
1	% Mg	8.79	8.76	8.78
2	% Br	53.40	53.32	53.36
2	% Mg	8.58	8.62	8.60
3	% Br	53.31	53.31	53.31
3	% Mg	7.79	7.79	7.79
Average % Br = $53.13 \pm .28$				
Average % Mg = $8.39 \pm .40$		Br/Mg = 1.92		

At the time these samples were submitted carbon and hydrogen analyses were not available. The ratio of bromine to magnesium indicates $Mg_n Br_{2n}$ as a major constituent of the crystal.

Crystallographic analysis later showed that the ratio of bromine to magnesium given above was incorrect and instead was three to two. Neither initial crystallographic evidence nor electrostatic considerations ruled out the formula $Mg_6 Br_4 O \cdot 4(C_4 H_{10} O)$ rather than $Mg_2 Br_3 OH \cdot 2(C_4 H_{10} O)$. As indicated in the literature review, phenoxy and ethoxy groups were also possible constituents. Because of the discrepancy between chemical analysis and crystallographic results it was decided to reanalyze the crystals. This chemical analysis was made on two samples. The first sample contained crystals which had been allowed to react completely with the atmosphere, the second consisted of the pure crystals. The results of the chemical analysis of these two samples are given in Table 7. The values given for C' and H' were found after the material had been allowed to stand in a dessicator in a dry-box for 24 hours. The ratio of bromine to magnesium for the pure crystals is 1.45 and for the reacted material 1.48. These values are in close agreement with the crystallographic ratio of 1.5. The comparison of the observed percentages and those calculated for $Mg_2 Br_3 OH \cdot 2(C_4 H_{10} O)$ and for $Mg_4 Br_6 O \cdot 4(C_4 H_{10} O)$ are given in Table 8.

Table 7. Chemical analysis of $\text{Mg}_4\text{Br}_6\text{O}\cdot 4(\text{C}_4\text{H}_{10}\text{O})$, No. 2

Sample	Element determined	Determination 1	Determination 2	Determination 3	Averages
Pure crystal	% Br	51.22	51.22	-----	51.22
	% Mg	10.76	10.76	-----	10.76
	% C	20.72	20.38	-----	20.55
	% H	4.03	4.10	-----	4.04
	% C'	21.97	22.02	21.92	21.97
	% H'	4.41	4.25	4.31	4.32
Reacted crystals	% Br	58.46	58.36	-----	58.41
	% Mg	12.02	12.03	12.02	12.02
	% C	.24	.37	-----	.30
	% H	5.62	5.86	-----	5.74

Table 8. Observed and calculated elemental percentages

	Observed	Calculated for $\text{Mg}_2\text{Br}_3\text{OH}\cdot 2(\text{C}_4\text{H}_{10}\text{O})$	Calculated for $\text{Mg}_4\text{Br}_6\text{O}\cdot 4(\text{C}_4\text{H}_{10}\text{O})$
% Br	51.22	52.85	53.92
% Mg	10.76	10.72	10.94
% O	12.39 ^a	10.58	9.00
% C	21.45	21.18	21.61
% H	4.19	4.67	4.53
		M.W. = 453.64	M.W. = 889.26

^aBy difference.

Thermogravimetric analysis

A thermogravimetric analysis was also made on the material (Figure 4). The sample was at all times under a stream of nitrogen gas. The results of a chemical analysis of the residue from the thermogravimetric analysis are given in Table 9. The thermogravimetric results, while not sufficiently accurate for a quantitative treatment, do give a good qualitative picture of the thermal stability of the crystals.

Table 9. Chemical analysis following thermogravimetric analysis

	Determi- nation 1	Determi- nation 2	Determi- nation 3	Averages	Milligrams
% Br	3.01	2.78	-----	2.90	2.1
% Mg	54.79	54.69	54.72	54.73	40.2

From the time the sealed ampule containing the crystals was opened until the temperature reached 39.5° C the sample was gaining weight. This is obviously not due to a simple replacement reaction where one ether group is being replaced by one water molecule, but is probably due to increased coordination of the magnesium. The compounds $\text{MgBr}_2 \cdot \text{MgBrOH} \cdot 2\text{ether}$ and $\text{Mg}_4\text{Br}_6 \cdot 4\text{ether}$ do not have enough

Figure 4. Results of thermogravimetric analysis of $\text{Mg}_4\text{Br}_6 \cdot 0.4(\text{C}_4\text{H}_{10}\text{O})$

electron donor groups to permit even four-fold coordination of the magnesium atom without some type of bridging. Compounds such as $\text{Mg}(\text{H}_2\text{O})_6\text{Br}_2$ are quite stable and formation of this type of compound would account for the initial weight increase. The crystal begins to undergo thermal decomposition at 39.5°C . The interpretation given the results in Figure 4 was to assign the weight lost from A to B primarily to the effects of adhering solvent, ether of crystallization and water absorbed. The loss of weight from C through D is due to vaporization of the bromine, probably as HBr .

Infrared analysis

Infrared spectra taken in connection with this research problem are shown in Figures 5 through 11. The data were taken on a Perkin-Elmer model 21 infrared spectrophotometer equipped with a sodium chloride prism. The strong peaks of Figure 5 at 3 microns and 6.15 microns are typical of frequencies due to OH stretching and OH bending modes for inorganic salts containing water of hydration (50). From the thermogravimetric results and from the observation that the crystals can only be handled under extremely moisture free conditions (argon dried over two or more P_2O_5 towers), one can assume that the majority of this water of hydration is obtained during the preparation of the sample for infrared analysis. The presence of absorption peaks in the region of 4.5 microns is difficult to explain. Spectra in this range

Figure 5. Infrared spectra of $\text{Mg}_4\text{Br}_6 \cdot 4(\text{C}_4\text{H}_{10}\text{O}) + \text{H}_2\text{O} \cdot \text{KBr}$ pellet

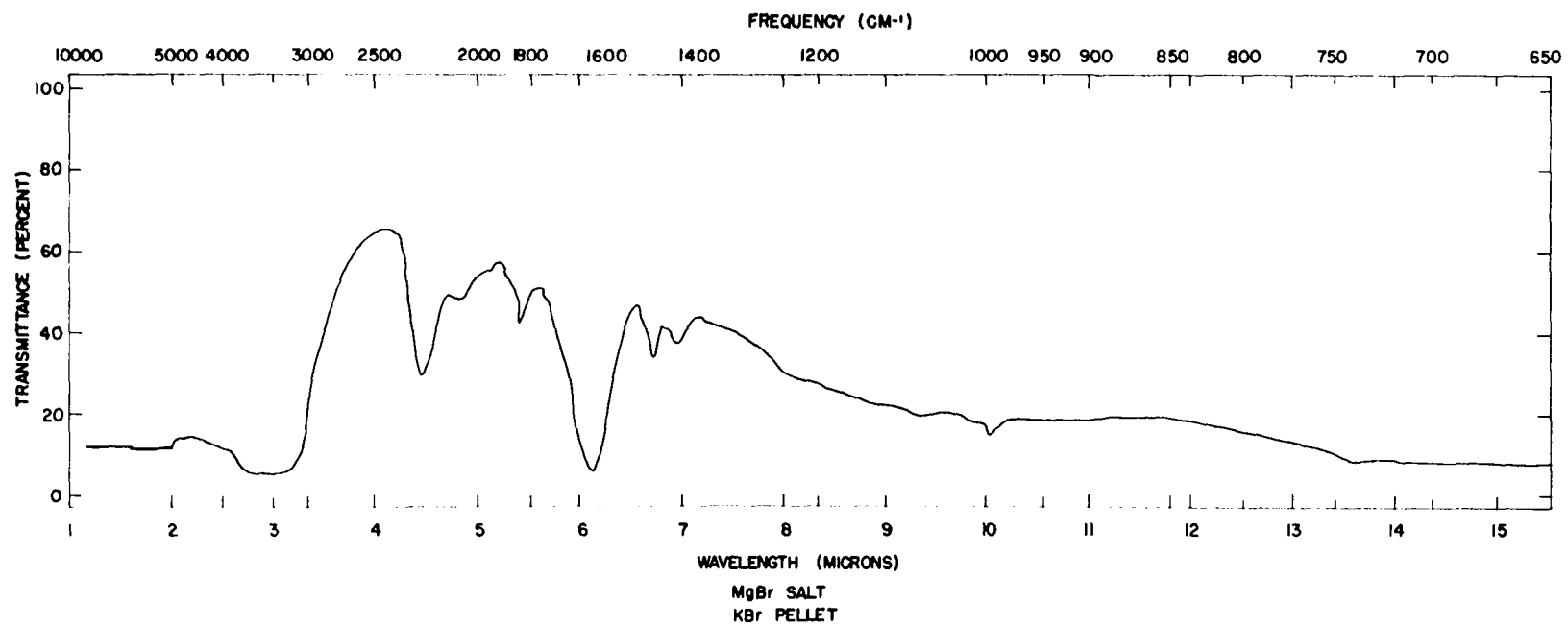
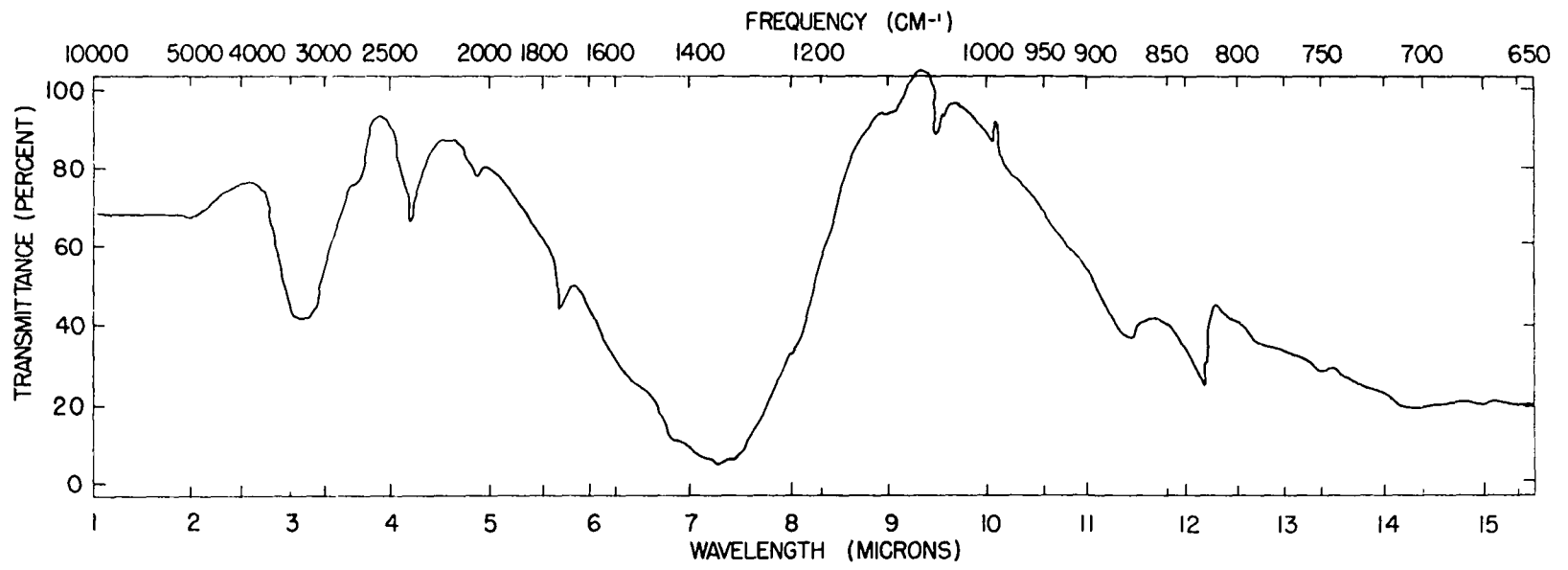
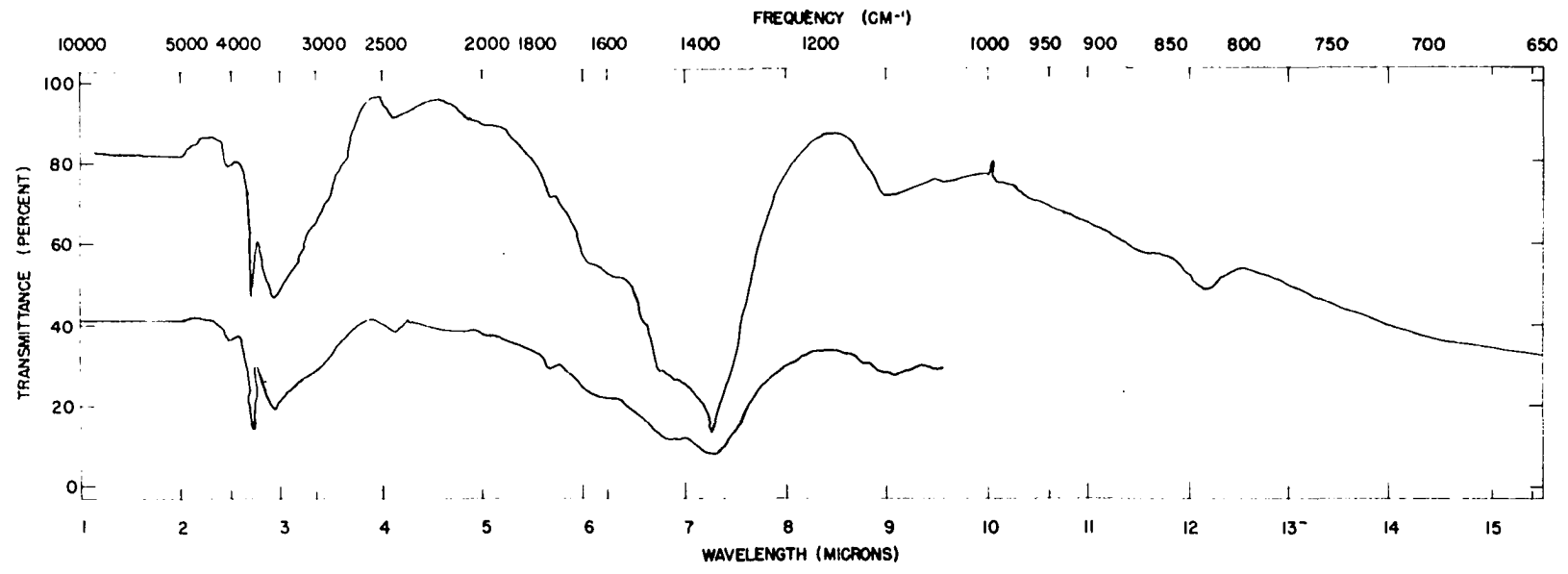


Figure 6. Infrared spectra of MgO + H₂O·KBr pellet



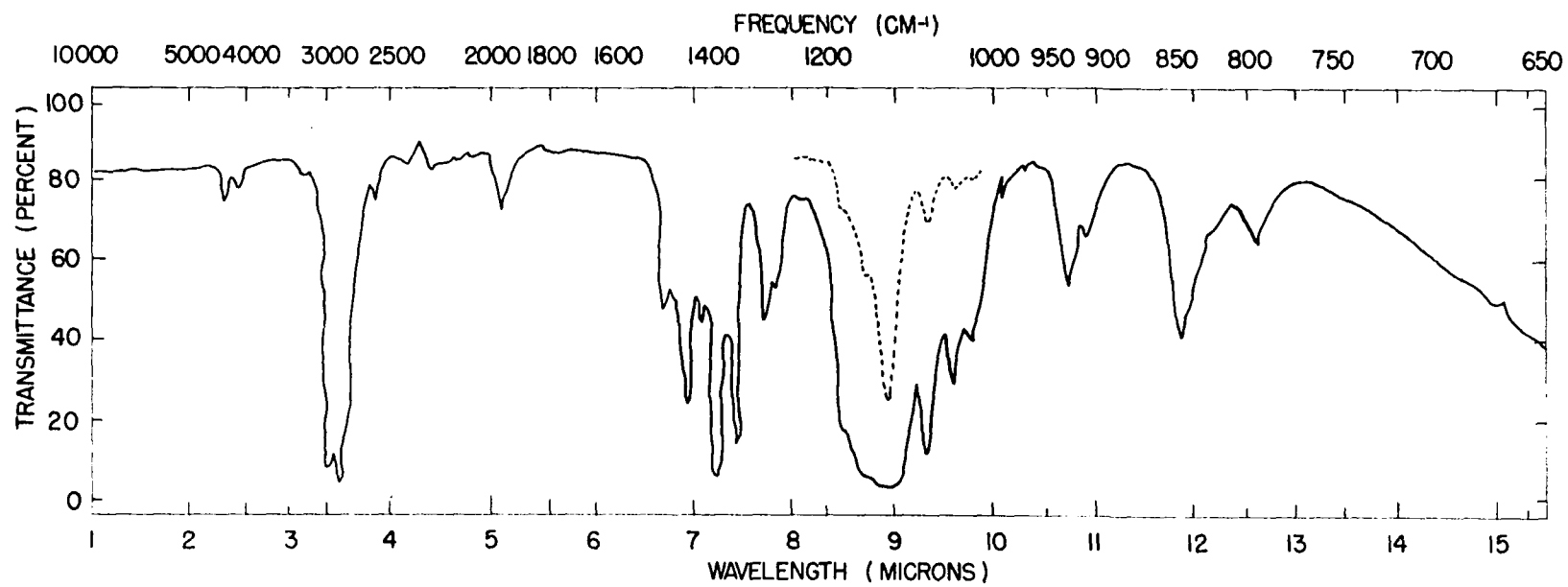
43

Figure 7. Infrared spectra of $\text{Mg(OH)}_2 \cdot n(\text{H}_2\text{O})$ KBr pellet



45

Figure 8. Infrared spectra of diethyl ether ($C_4H_{10}O$)



47

Figure 9. Infrared spectra of C_6H_5Br

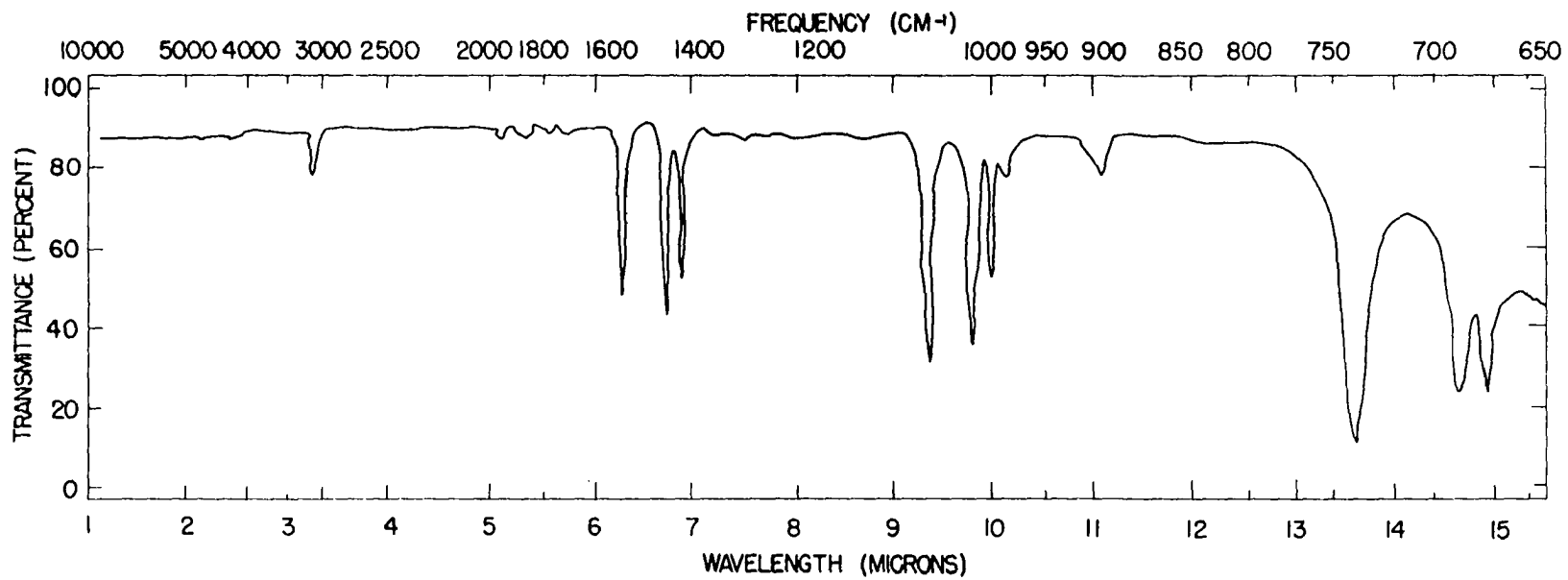


Figure 10. Infrared spectra of unsolvated $C_6H_5MgBr + H_2O$ sample

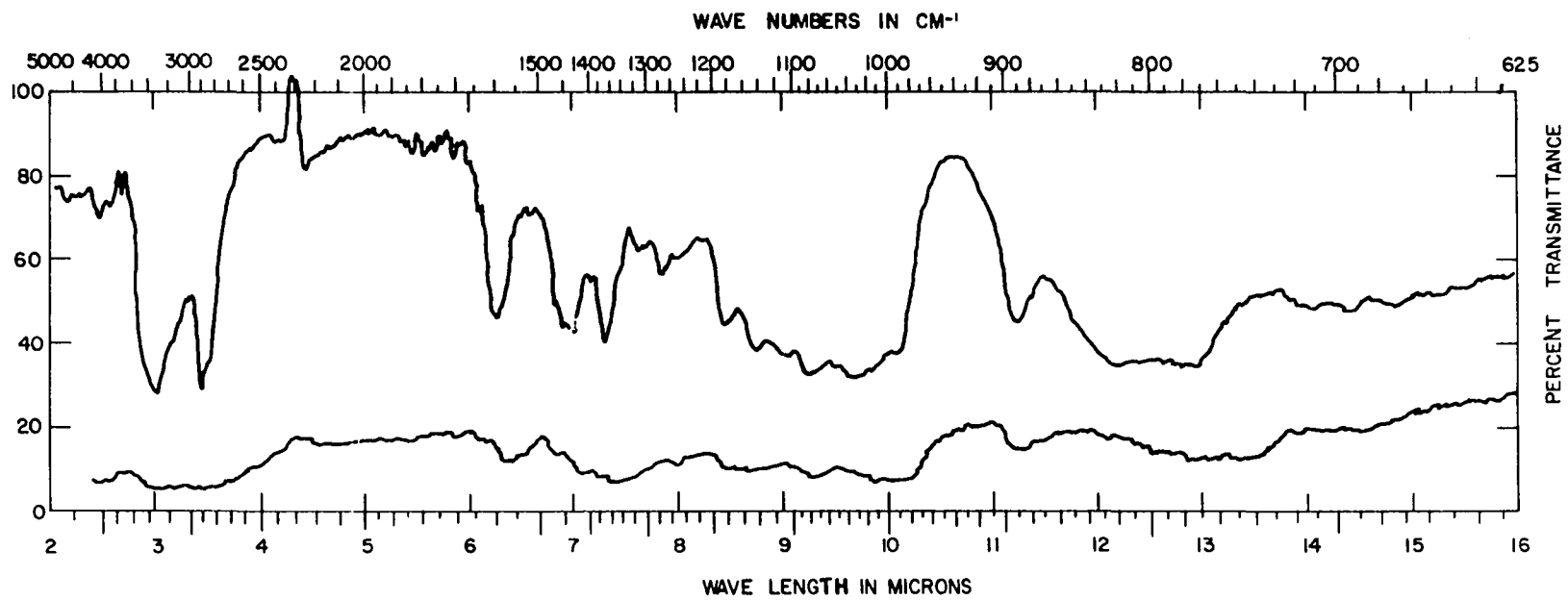
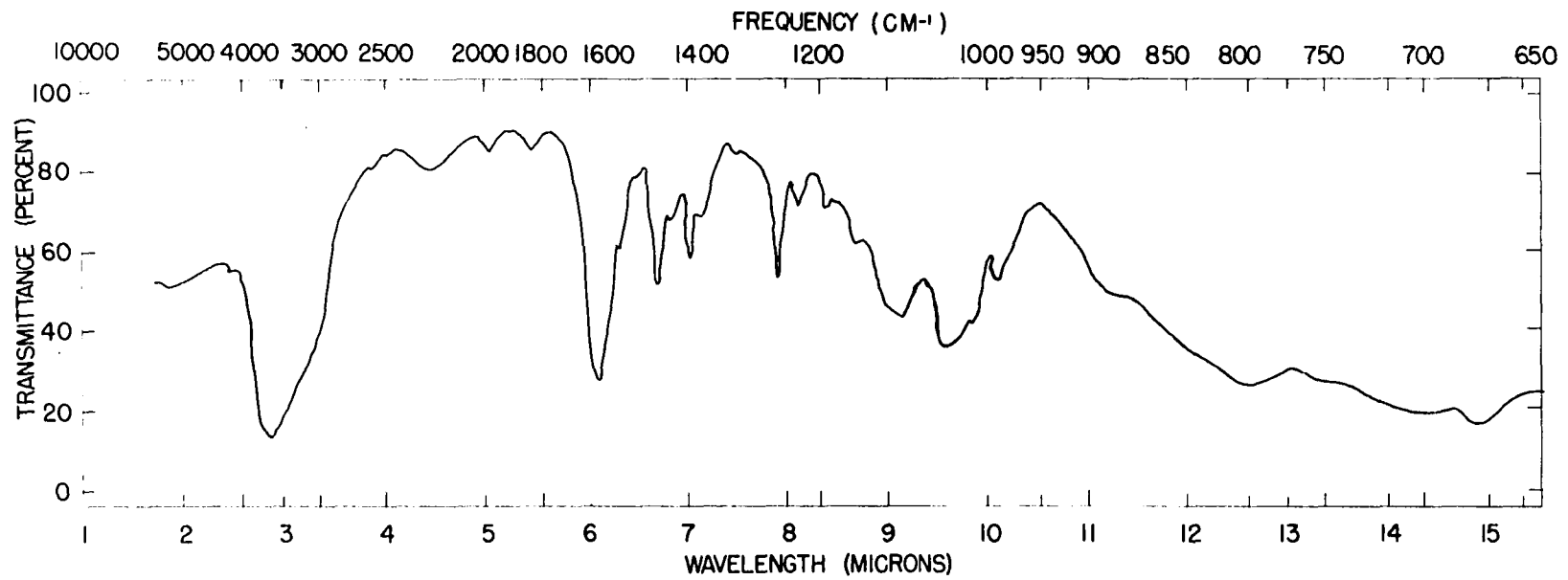


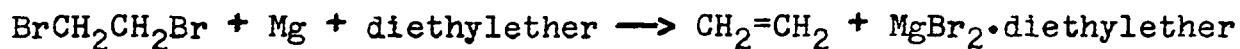
Figure 11. Infrared spectra of unsolvated $C_6H_5MgBr + H_2O$, Sample 2



derive from bonds of the type -CN, -CHS, -OCN, SiH, MgH, metal carbonyls, and multiple bonds such as -C=C=C (51, 52). A possible explanation comes from Figures 6 and 7 which show the spectra of $MgO \cdot H_2O$ and $Mg(OH)_2 \cdot n(H_2O)$. In the $MgO \cdot H_2O$ spectrum, absorption occurs at 4.2 and 4.85 microns similar to the 4.5 and 5.4 microns in the MgBr salt spectrum. It is also probably significant that these peaks are of much lower intensity in the infrared spectra of the more highly hydrated $Mg(OH)_2 \cdot n(H_2O)$. The small peaks in the region of 7 microns were attributed to the bending modes of the CH groups present as part of the ether of crystallization. Because of scattering by the magnesiumbromide content above 7.5 microns, the infrared results did not provide a basis for determining if aromatic groups were present in the crystal.

Comparison with $MgBr_2 \cdot$ diethylether

When chemical analysis first indicated a bromine to magnesium ratio of 1.90, crystals of $MgBr_2 \cdot$ diethylether were prepared to determine if this compound was the same as that prepared from the Grignard solution. The method of preparation followed that of Plum (24). The reaction



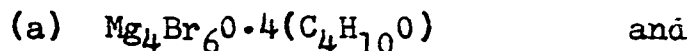
is exothermic and proceeds in a manner similar to the Grignard preparation. The method used to obtain the crystals from

solution was identical with that used to obtain the crystal from the Grignard solution.

The habit of the crystals of $\text{MgBr}_2 \cdot \text{diethylether}$ is needlelike and the external symmetry quite unlike the symmetry of the crystals obtained from the Grignard system. The density was found to be 1.99 gms/cm^3 which indicated the two crystals were not identical. This was later confirmed by the second chemical analysis. Further properties of $\text{MgBr}_2 \cdot \text{diethylether}$ are given by Menschutkin (53) and Evans and Rowley (54).

Summary of the analytical results

The empirical formula of this compound was determined almost entirely by x-ray analysis. Chemical analyses were found in the first instance to give the wrong Br/Mg ratio although later work did confirm the results which had already been found from x-ray structural analysis. None of the analytical results were of sufficient accuracy to distinguish between the formulas



The calculated density from x-ray analysis gives for the total molecular weight in the unit cell

$$\text{NM} = 1778 \text{ for (a)}$$

$$\text{NM} = 1814 \text{ for (b) } .$$

The observed total molecular weight in the crystallographic unit cell is 1802 ± 25 . Clearly both formulas fit the observed density within experimental error. Neither can one rule out either of the two formulas from electrostatic considerations. The x-ray analysis was, however, quite conclusive in distinguishing between (a) and (b). There was simply no way in which two hydroxyl groups could replace the one oxygen atom even in a disordered model. Furthermore, the oxygen temperature factors were normal, indicating that this aspect of the structure was not disordered. Finally the OH groups if present would necessarily have to lie on fourfold positions on the $\bar{4}$ axes in the space group $P\bar{4}2_1c$. With 4 bromines and two oxygen atoms already on the $\bar{4}$ axes, there is not enough room for two more hydroxyl groups or water molecules.

The conclusion was reached from x-ray analysis and was qualitatively supported by the various analytical means that the empirical formula is $Mg_4Br_6O \cdot 4(C_4H_{10}O)$.

Space Group Determination

Examination of the crystals of $Mg_4Br_6O \cdot 4(C_4H_{10}O)$ under a polarizing microscope showed that the crystals were either uniaxial or biaxial with extinctions occurring every 90° . Closer examination of several crystals seemed to indicate

that the uniaxial system was favored; however, it was difficult to ascertain this definitely as the crystals were in capillaries and were covered with either decomposition product or petroleum jelly.

A piezoelectric test for acentricity was positive indicating an acentric space group.

Initial x-ray data were taken on a precession camera. These pictures gave the Laue symmetry as $P\ 4/m\ mm$ with $a = b = 10.65\ \overset{\circ}{\text{Å}}$, and $c = 15.33\ \overset{\circ}{\text{Å}}$. The extinctions observed were $h + l = 2n + 1$, $\{h0l\}$ data; $k + l = 2n + 1$, $\{0kl\}$ data; and $l = 2n + 1$, $\{hhl\}$ data. The first two extinctions are equivalent for the tetragonal system and represent n glides in the $[010]$ and $[100]$ directions. The extinctions for $\{hhl\}$ data correspond to a c glide in the $[110]$ direction. The diffraction symbol is thus implied to be $P\text{-}nc$. The tetragonal point groups which can have $P\text{-}mm$ symmetry are $P4mm$ and $P\ 4/m\ mm$. The possible space groups are thus $P4nc$ and $P\ 4/m\ nc$.

Checking this space group determination from long exposure, Weissenberg pictures of the $\{0kl\}$ zone showed that there were some reflections with $\{0kl\}$, $k + l = 2n + 1$. This changed the observed extinctions to $\{hhl\}$, $l = 2n + 1$; $\{h00\}$, $h = 2n + 1$; and $\{0k0\}$, $k = 2n + 1$. The diffraction symbol is now $P\text{-}2_1c$. The only tetragonal point group with $P\text{-}2m$ symmetry is $P\bar{4}2m$. The probable space group is therefore

uniquely determined as $P\bar{4}2_1c$. The fact that the space group was initially determined to be $P4/mnc$ or $P4nc$ is evidence that a considerable portion of the scattering matter utilizes the symmetry of one of these space groups. Comparing the three space groups $P4/mnc$, $P4nc$, and $P\bar{4}2_1c$, it is observed that this will be the case if the positions $x, y, 0; \bar{y}, x, 0; \bar{x}, \bar{y}, 0; y, \bar{x}, 0; 1/2 + x, 1/2 - y, 1/2; 1/2 + y, 1/2 + x, 1/2; 1/2 - x, 1/2 + y, 1/2; \text{ and } 1/2 - y, 1/2 - x, 1/2$ are utilized. Special positions such as $0, 0, 0; 1/2, 1/2, 1/2$ also obviously satisfy this criteria. These conclusions were later confirmed.

A note of affirmation is given by Kitaigorodskii (55) who shows that the space group $P\bar{4}2_1c$ gives closest packing for organic structures.

Measurements made on a General Electric XRD5 diffractometer gave lattice constants of $a = b = 10.68 \pm .03 \text{ \AA}$, and $c = 15.34 \pm .02 \text{ \AA}$. These were used in the determination of the structure.

Collection and Correction of Intensity Data

Lorentz polarization

$\{hk0\}$, $\{hkl\}$, and $\{0k\}$ two-dimensional Weissenberg film data were first taken. All data were judged visually against a standard set of reflections. The data were

corrected for the polarization of the x-ray beam and the motion of the crystal (Lorentz factor) in the beam by

$$E'(hkl) = KL(hkl)p(hkl)|F(hkl)|^2 = KI'(hkl)$$

where $E'(hkl)$ = observed intensity

K = scale constant

L_p = Lorentz polarization factor

$$\frac{\sin \theta (1 + \cos^2 2\theta)}{2 \sin 2\theta (\sin^2 \theta - \sin^2 \mu)^{1/2}}$$

μ = angle of inclination of incident beam to the plane normal to the crystal rotation axis

The absorption correction is neglected in the above expression. The computer program used to make these calculations was the IBM 650 Incor I written by Zalkin and Jones* of the University of California and modified by D. E. Williams**. This program also calculates the atomic scattering factors for each reflection using a table look up.

Three sets of three-dimensional data were taken on a G.E. XRD5 diffractrometer. The first set was taken using crystals transferred under mineral oil. The crystals used to

*Zalkin, A. and Jones, R. E. Department of Chemistry, University of California, Berkeley, California. Incor I. Private communication. ca. 1958.

**Williams, D. E. Department of Chemistry, Iowa State University, Ames, Iowa. Incor IM. Private communication. ca. 1958.

take the first set of three-dimensional data had a largest radius of .3 to .35 mm., the large size being necessary to locate the transparent crystals in the mineral oil.

Absorption

The absorption of the x-ray beam by the crystals of this compound is a serious effect. If $I'(hkl)$ is the intensity of the diffracted beam corrected for Lorentz and polarization effects, the true expression for the observed intensity is

$$E(hkl) = KA(hkl)I'(hkl) = KI(hkl)$$

$$= K \left\{ \int_0^V \frac{1}{v} \exp \left[-\mu(r_\alpha + r_\beta) \right] dv \right\} I'(hkl) ,$$

where r_α = path length of the incident beam in the crystal

r_β = path length of the diffracted beam in the crystal

μ = total absorption coefficient

$$= \rho \sum_{i=1}^K g_i (\mu/\rho)_i ,$$

ρ = density of crystal

g_i = mole fraction of i th element

$(\mu/\rho)_i$ = mass absorption coefficient for i th element .

If the values of $(\mu/\rho)_i$ given in "The International Tables for

X-ray Crystallography", Volume III (56) are used for the compound $\text{Mg}_4\text{Br}_6\text{O}\cdot 4(\text{C}_4\text{H}_{10}\text{O})$, the value of μ for molybdenum radiation is 75.70 cm^{-1} and for copper is 104.02 cm^{-1} .

The two-dimensional data and the first set of three-dimensional data were corrected for absorption by assuming spherical crystals. Values for this type of absorption correction have been tabulated in Volume II of "International Tables for X-ray Crystallography" (56). Structural analysis of the two-dimensional and first three-dimensional set of data failed to locate the ether carbon atoms so it was decided that better data were needed. This was achieved in two ways: by improvement in transfer techniques which gave better and smaller crystals, and by using an absorption correction program written by W. R. Busing* of the Oak Ridge National Laboratory.

Busing's program makes use of Gauss's approximation (in 57) to evaluate the absorption integral for a crystal bounded by a set of planes. For the last two sets of three-dimensional data two crystals were used (Crystals 1 and 2) having ten and nine bounding planes respectively. The equations of the planes were determined by measuring the corners of the planes in a convenient coordinate system. Of the 19 planes observed for the two crystals, only one was

*Busing, W. R. Oak Ridge National Laboratory, Tennessee. Abcor. Private communication. 1962.

defined by only three corners so that in general it was desirable to fit the observed n points to a plane. This could have been done by least squares analysis, however, complications arise in using this method because there is a high probability that the points defining the plane face of a crystal will have n fold rotation or mirror symmetry and it is sometimes convenient to define the origin in such a way that some of the planes pass through the origin. This causes some of the terms in the least squares matrix to vanish and usually results in a singular matrix. To avoid any complications due to symmetry, the following method was used. For a set of n planar points the number of all possible planes through these points is equivalent to the number of ways of combining n objects three at a time which is

$$\frac{n!}{(n-3)!3!}$$

Tabulated this gives

no. pts.	no. planes
3	1
4	4
5	10
6	20
7	35

The best fit as determined by least squares of the coefficients of all possible planes to an "average plane" is simply the

average of the coefficients. This method needs only minor modifications to be independent of the location of the origin. A 704 program was written with R. Dillon* of the Computer Service Group of Iowa State University which

- a. scaled, inverted, and rotated the microscope coordinate system to give a coordinate system consistent with Busing's program
- b. calculated and printed out all possible planes for a set of points in terms of the direction cosines of the plane and its distance from the origin and
- c. formed an "average plane" for each set of points and the distance of each point from the average plane.

This made it convenient to determine quickly if some points were greatly in error.

A simple method for checking the absorption correction is inherent in the data collection geometry of the XRD5 diffractometer. The reciprocal space of a crystal can be defined in terms of machine coordinates χ , ϕ , and 2θ . The XRD5 is instrumented in such a way that a reflection observed at $\chi = 90^\circ$ is independent of the ϕ setting. This means that as the crystal is rotated through ϕ , the intensity of a spherical crystal should remain constant. For a non-spherical

*Dillon, R. Computer Services Group, Ames Laboratory, Atomic Energy Commission, Ames, Iowa. AVPN1. Private communication. ca. 1962.

crystal, even for very small absorption coefficients, the intensity will vary as the path length of the x-ray beam through the crystal varies. The intensity curves for crystals one and two at $\lambda = 90^\circ$ are shown in Figures 12 and 13. It is obvious from these curves that the assumption that the crystals are spherical is a very poor one. The absorption corrections and the corrected intensities at $\lambda = 90^\circ$ are also shown in these figures. Only 180° in θ are shown as the intensity and absorption curves are duplicated through 180° . The maximum intensity error for crystal one was 10.70%. The average error should be somewhat less than this. The results for crystal two were not as satisfactory as there is a maximum error in intensity of about 25%. Because of this the results from this crystal were not averaged together with those from crystal one, but were used only as a reference to check the results of crystal one.

Collection of data on the G.E. XRD5 diffractometer

This instrument is capable of giving extremely accurate intensities; however, because there are more machine parameters than for a film camera more care must be taken in collecting the data. It is extremely important that the optimum x-ray aperture widths, x-ray tube alignment, voltage settings, and peak height analyzer settings be used. The reader is referred to the General Electric Company's instruction manual (58) for making these adjustments.

Figure 12. Experimental verification of absorption correction for $\text{Mg}_4\text{Br}_6 \cdot 4(\text{C}_4\text{H}_{10}\text{O})$, Crystal 1

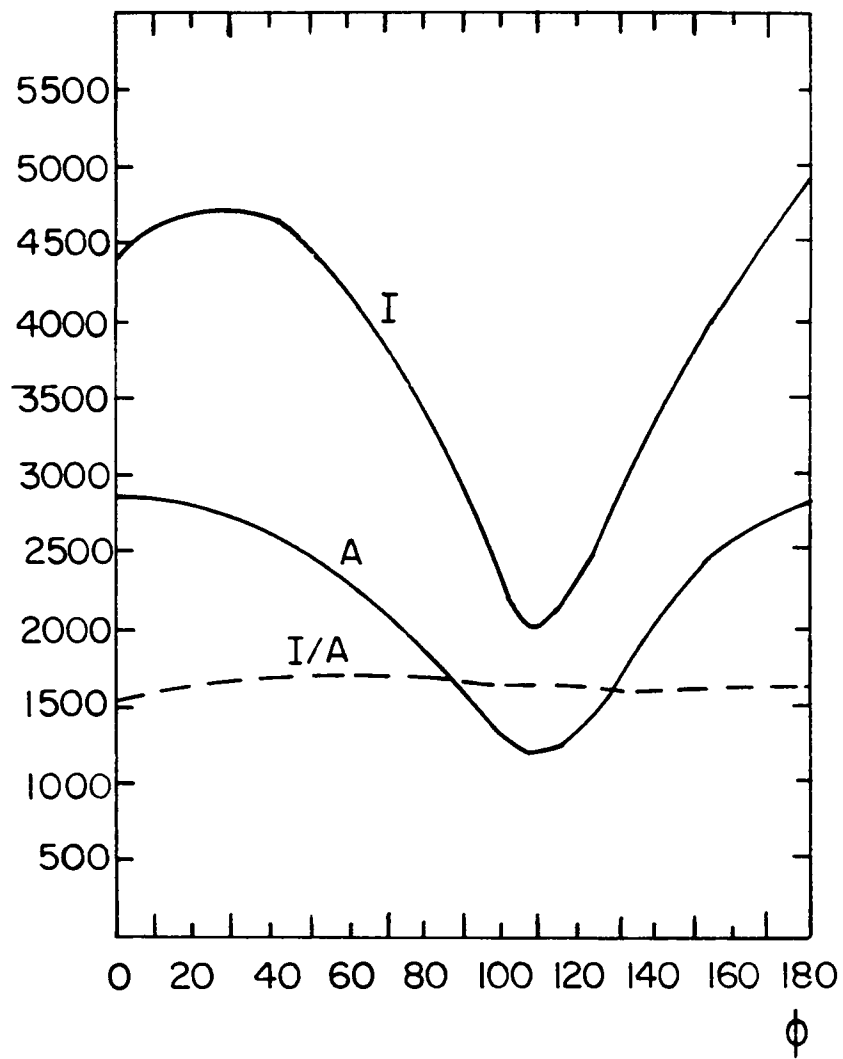
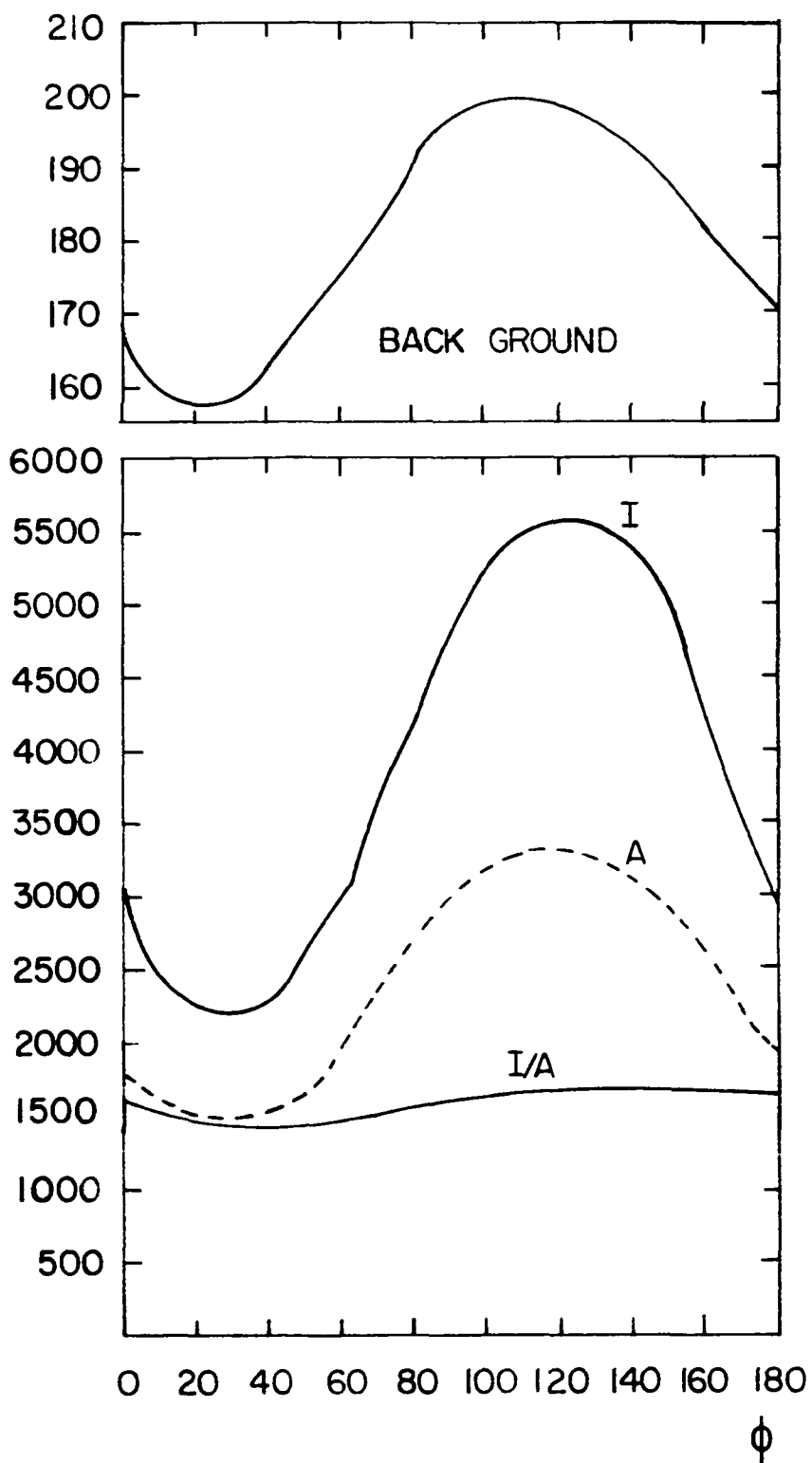


Figure 13. Variation of background intensity at $\chi = 90^\circ$
and verification of absorption correction for
 $\text{Mg}_4\text{Br}_6 \cdot 0.4(\text{C}_4\text{H}_{10}\text{O})$, Crystal 2



Decomposition

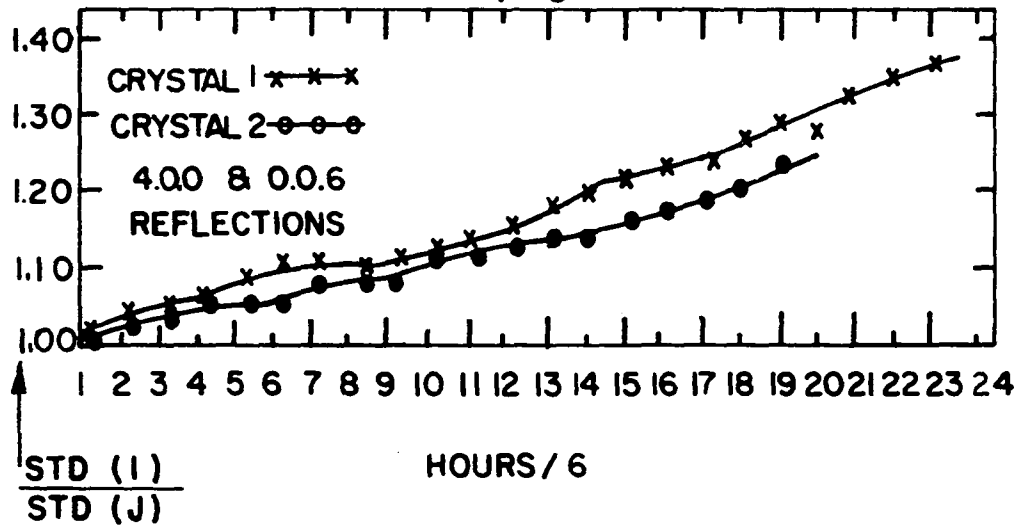
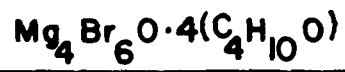
The decomposition of the crystal in the x-ray beam (Figure 14) was recorded by taking two standard reflections every six hours. Crystals exposed to the x-ray beam also changed color to a pale yellow while crystals which were transferred simultaneously but not exposed to x-rays did not show a similar change. The yellow color could be explained by decomposition with the liberation of bromine. The maximum intensity decrease desired was 25%. It was possible to take an average of 150 reflections a day using a 200 second scan and a 100 second scan for the background associated with each reflection. A total of about 900 reflections were taken so that it was possible to get a complete data set, including streak corrections and machine checks, in seven days. The decrease in intensity over this period of time was not greater than 25%. The effect of decomposition was corrected by interpolation for each reflection between the points in the curve in Figure 14.

Streak

The x-ray tube does not emit pure monochromatic radiation and this results in a significant portion of the diffracted energy from a given reflection having a non-Laue contribution. This "streak intensity" must be subtracted from the total peak intensity. Necessary equations for this

Figure 14. Rate of photochemical decomposition of
 $\text{Mg}_4\text{Br}_6\text{O} \cdot 4(\text{C}_4\text{H}_{10}\text{O})$, molybdenum K α radiation

DECOMPOSITION OF



correction have been independently derived by Dr. D. R. Fitzwater* and D. E. Williams**. The form of this correction is given by the following. If an effective wave length of λ_k is being used, an absorption edge filter will remove all radiation with $\lambda < \lambda_a$. For example for molybdenum radiation $\lambda_k = .7107 \text{ \AA}$ so that a zirconium filter with an absorption edge, $\lambda_a = .6888 \text{ \AA}$, will remove all radiation with $\lambda < .6888 \text{ \AA}$. The intensity of the nth reflection will have a streak contribution from the reflections which lie on a line toward the origin of the reciprocal lattice. The corrected intensity for the nth reflection is then given by

$$I_k^n \text{ (streak corrected)} = I_k^n \text{ (uncorrected)} - \sum_m I_s^m$$

where
$$I_s^m = \frac{I_k(Lp)_n \ 2d_m \ \cos \theta_n \ \sin(\Delta\theta)_s \ \hat{F}_s^2}{(Lp)_m \ \Delta\lambda_k}$$

and
$$\hat{F}_s^2 = \frac{I_s(Lp)_k \ \Delta\lambda_k}{I_k(Lp)_s \ 2d_r \ \cos \theta_r \ \sin(\Delta\theta)_s}$$

\hat{F}_s^2 is evaluated at $\lambda_m/\lambda_k = d_m/d_n$. The factor $\Delta\lambda_k/\sin(\Delta\theta)_s$ in \hat{F}_s^2 need not be evaluated since its reciprocal appears in

*Fitzwater, D. R. Department of Chemistry, Iowa State University, Ames, Iowa. Streak correction. Private communication.

**Williams, D. E. Department of Chemistry, Iowa State University, Ames, Iowa. Streak correction. Private communication. 1962.

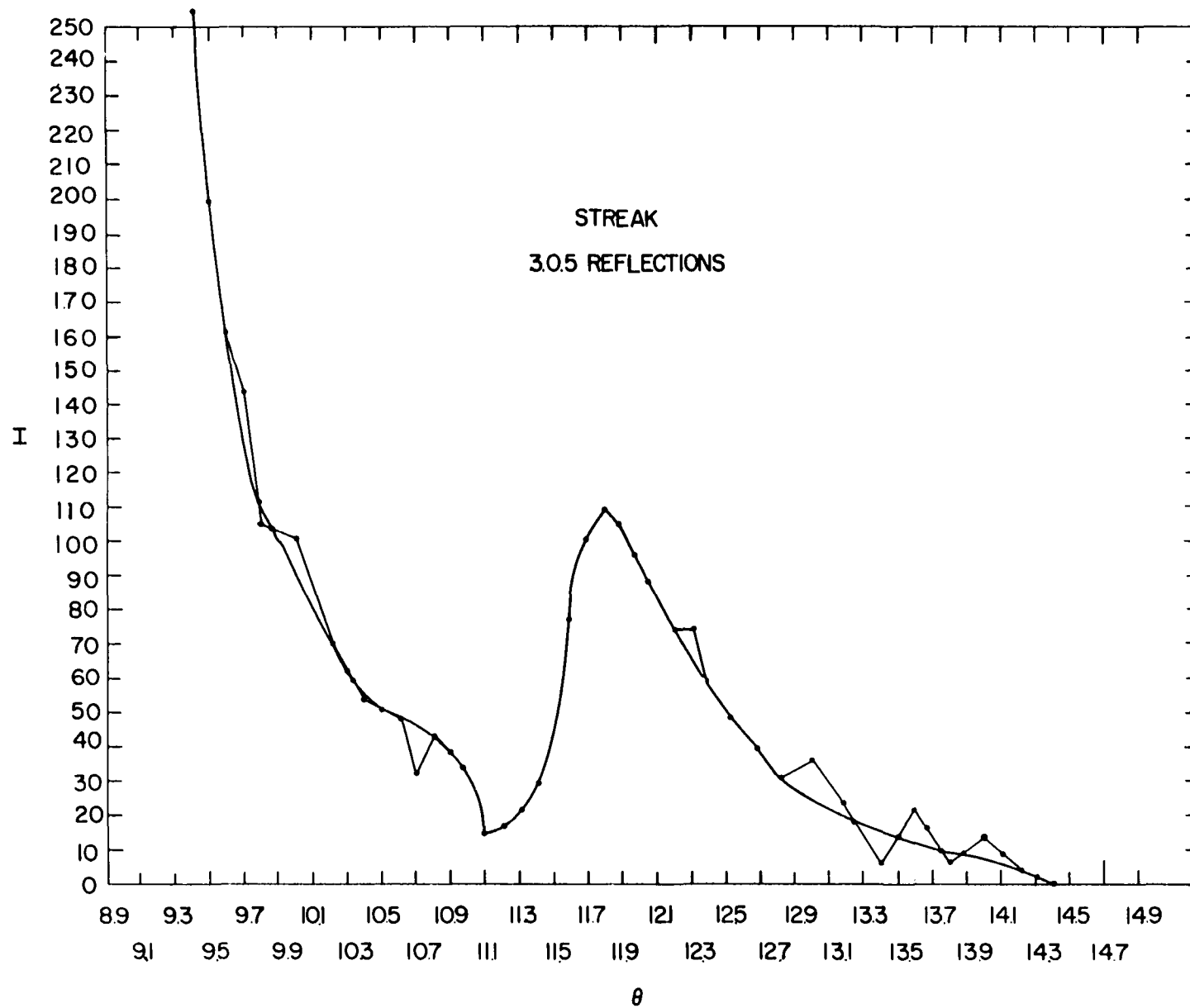
I_s^m . In practice a table of the \hat{F}_s^2 is made up and a table interpolation made. The streak correction calculation was carried out on the 704 computer using a program written by D. R. Fitzwater* and modified by R. D. Willett**. The (305) reflection streak was used to make up the streak table since it is a strong prime reflection at a comparatively high 2θ value (17.87°).

Since molybdenum radiation gives a lower absorption coefficient (75.70 cm^{-1}) than copper radiation (104.02 cm^{-1}), it was used to collect the intensity data. Generally there is a great deal of difference between the total absorption coefficient for molybdenum radiation and that for copper. The reason there is not in this case is that the bromine K α absorption edge is at 0.92 \AA which is fairly close to the wavelength for the molybdenum radiation mean K α wavelength of 0.7107 \AA . This greatly complicates the streak correction curve (Figure 15). The large peak observed in the middle of this curve results because white radiation with a wavelength less than $.9200 \text{ \AA}$ is highly absorbed by the bromine atoms while all radiation with wavelengths longer than this are much less

*Fitzwater, D. R. Department of Chemistry, Iowa State University, Ames, Iowa. 704 streak. Private communication. 1961.

**Willett, R. D. Department of Chemistry, Washington State University, Pullman, Washington. 704 streak M. Private communication. 1961.

Figure 15. Streak curve for $\text{Mg}_4\text{Br}_6\text{O}\cdot 4(\text{C}_4\text{H}_{10}\text{O})$ Molybdenum K α radiation



absorbed. The ideal situation would have been to collect the data using radiation of .93 or .94 Å; however the means for this were not available. This effect results in less accurate intensity measurements for very low order reflections. The wave length range covered by the fixed scan $\Delta\theta_s$ is given by

$$\Delta\lambda_r = 2d_r \cos \theta_r \sin (\Delta\theta_s)$$

for the rth reflection. The intensity data were taken with a fixed $\Delta\theta$ scan, so that for low order reflections a much larger $\Delta\lambda$ range is covered and the absorption edge is included in the $\Delta\theta_s$ scan. The streak correction is also not as accurate for this type of curve.

Anomalous dispersion

One final consideration arises from the use of radiation only .21 Å less than bromine absorption edge. This is the effect of anomalous dispersion. The radiation scattered from the bromine atom has an anomalous phase shift because of the K α absorption edge. The atomic scattering factor for the bromine atom is therefore represented by

$$f = f_0 + f' + if'' \cong f_0 - .3 + i \quad (2.6)$$

Experimentally this means that Friedel's law does not hold and it is no longer true that

$$E(hk\ell) = E(\bar{h} \bar{k} \bar{\ell}) .$$

This effect can be used quite effectively (59) for determining the phases of a non-centrosymmetric structure if f'' is large enough. For film data f'' should be 3.0 or greater, but for counter data Pepinsky claims structures with f'' as low as .5 may be determined by this method. Because of the problems of decomposition and high absorption, this method was not applied to this structure; however the real part of the correction to the scattering factor was used.

Background

In addition to the Bragg scattering, crystals scatter radiation incoherently due to thermal vibrations, the influence of strains and deformations, the Compton effect, and similar phenomena. It is necessary to subtract out the contribution of the incoherent scattering from the total intensity. To do this the assumption is made that the total intensity may be represented by

$$I_T = I_B + I_{PK}$$

where I is the total intensity, I_B is the background or diffuse scattering contribution and I_{PK} is the Bragg intensity. For $Mg_4Br_6O \cdot 4(C_4H_{10}O)$ counter data this correction was realized by the following method. The intensity data were taken by using a constant 200 second $\Delta\theta$ scan through a reflection peak. The crystal was then effectively rotated

to a point where it was just offset from the Bragg reflection position. The diffuse scattering was measured using a constant 100 second $\Delta\theta$ scan. This measurement was made for all reflections. The backgrounds thus observed were separated into small groups of $\sin \theta$, the grouping being also a function of the order in which the reflections were measured. Plots were made of the backgrounds in a group versus the 2θ values for the backgrounds. Points lying off the resulting curves were rechecked for recording errors and were weighted toward the background curve. These corrected and checked background values were then used to determine the Bragg intensities.

Computer programming for correction of raw data

For the first set of counter data, a 704 master program was written which corrected the data for the above effects excluding the streak correction and assuming a spherical absorption correction. For the second two sets of data, a program written by G. E. Engebretson* was modified to permit correction for decomposition and all of the above effects were taken into account, including the absorption correction for a crystal bounded by n planes. This latter calculation was performed first by Busing's Abcor program**.

*Engebretson, G. E. Department of Chemistry, Iowa State University, Ames, Iowa. Private communication. Counter workup. 1961.

**Busing, W. R. Oak Ridge National Laboratory, Tennessee. Private communication. Abcor. 1962.

Solution of Structure

Because the identity of the compound was not definitely known at the start of this problem, solution of the structure was by a trial and error procedure. It was soon apparent from the two-dimensional data that the chemical analysis giving a ratio of bromine to magnesium of 2 to 1 was untenable from the crystallographic standpoint.

The procedure employed in the determination of the structure was to calculate the Patterson projection, establish the atomic parameters, and confirm these by electron density maps and least squares refinement.

The Patterson function for the space group $P\bar{4}2_1c$ has the symmetry of the Laue Group $P 4/m mm$. The general vector positions for $P 4/m mm$ are given in Table 10. The reader is referred to the "International Tables for X-ray Crystallography", Volume I (56), for the special positions.

The Patterson function for the general case is

$$P(uvw) = \frac{1}{v_c} \sum_{h=-\infty}^{\infty} \sum_{k=-\infty}^{\infty} \sum_{l=-\infty}^{\infty} |F(hkl)|^2 \cos 2\pi(hu + kv + lw)$$

For D_{2h} symmetry this reduces to

$$P(uvw) = \frac{8}{v_c} \sum_{h=0}^{\infty} \sum_{k=0}^{\infty} \sum_{l=0}^{\infty} |F(hkl)|^2 \cos 2\pi hu \cos 2\pi kv \cos 2\pi lw$$

Table 10. Vector space symmetry (P 4/m mm) for the space group $P\bar{4}2_1c$

Wyckoff notation	No. of positions	Point symmetry	Positions			
u	16	1	u v w	\bar{u} \bar{v} w	u v \bar{w}	\bar{u} \bar{v} \bar{w}
			\bar{u} v w	u \bar{v} w	\bar{u} v \bar{w}	u \bar{v} \bar{w}
			\bar{v} u w	v \bar{u} w	\bar{v} u \bar{w}	v \bar{u} \bar{w}
			v u w	\bar{v} \bar{u} w	v u \bar{w}	\bar{v} \bar{u} \bar{w}

The full expression to be calculated for D_{4h} (P 4/m mm) can be shown to be

$$P(uvw) = \frac{8}{v_c} \sum_{h=k}^{\infty} \sum_{k=0}^{\infty} \sum_{l=0}^{\infty} |F(hkl)|^2 \{ \cos 2\pi hu \cos 2\pi kv$$

$$+ \cos 2\pi ku \cos 2\pi hv \} \cos 2\pi lw$$

For computing purposes however, it is more convenient to use the function for D_{2h} and to supply the redundant intensities $|F(hkl)|^2$, $h < k$. Since $|F(hkl)|^2 = |F(khl)|^2$ for D_{4h} , the correct symmetry is obtained by this procedure.

Because of the high symmetry of the tetragonal system, a simplification is obtained in the interpretation of the vectors for $P\bar{4}2_1c$ if the principles of group theory are applied. The analysis of coordinates and vector distances for the space group $P\bar{4}2_1c$ is given in Table 11.

Table 11. Analysis of coordinates and vector distances for $\overline{P4}_2c$

Operation	Axis	Location	Coordinates			General vectors $P \frac{4}{m} \text{mmm}:16(u)$		
1	-		x	y	z	$x_1 - x_2$	$y_1 - y_2$	$z_1 - z_2$
2	001	000	\overline{x}	\overline{y}	z	$x_1 + x_2$	$y_1 + y_2$	$z_1 - z_2$
$\overline{4}^{-1}$	001	000	\overline{y}	\overline{x}	\overline{z}	$x_1 - y_2$	$y_1 - x_2$	$z_1 + z_2$
$\overline{4}$	001	000	y	\overline{x}	\overline{z}	$x_1 - y_2$	$y_1 + x_2$	$z_1 + z_2$
2_1	010	$\frac{1}{2}0\frac{1}{2}$	$\frac{1}{2} - x$	$\frac{1}{2} + y$	$\frac{1}{2} - z$	$\frac{1}{2} + x_1 + x_2$	$\frac{1}{2} + y_1 - y_2$	$\frac{1}{2} + z_1 + z_2$
2_1	100	$0\frac{1}{2}\frac{1}{2}$	$\frac{1}{2} + x$	$\frac{1}{2} - y$	$\frac{1}{2} - z$	$\frac{1}{2} + x_1 - x_2$	$\frac{1}{2} + y_1 + y_2$	$\frac{1}{2} + z_1 + z_2$
n	-	110	$\frac{1}{2} + y$	$\frac{1}{2} + x$	$\frac{1}{2} + z$	$\frac{1}{2} + z_1 - y_2$	$\frac{1}{2} + y_1 - x_2$	$\frac{1}{2} + z_1 - z_2$
c	-	110	$\frac{1}{2} - y$	$\frac{1}{2} - x$	$\frac{1}{2} + z$	$\frac{1}{2} + x_1 + y_2$	$\frac{1}{2} + y_1 + x_2$	$\frac{1}{2} + z_1 - z_2$

ances for $\overline{P4}_1c$

General vectors $P \frac{4}{m} \text{mmm}: 16(u)$			Special vectors $P \frac{4}{m} \text{mmm}$			
$x_1 - x_2$	$y_1 - y_2$	$z_1 - z_2$	8(e)	0	0	0
$x_1 + x_2$	$y_1 + y_2$	$z_1 - z_2$	8(f)	2x	2y	0
$x_1 - y_2$	$y_1 - x_2$	$z_1 + z_2$	16(u)	x + y	y - x	2z
$x_1 - y_2$	$y_1 + x_2$	$z_1 + z_2$	16(u)	x - y	y + x	2z
$\frac{1}{2} + x_1 + x_2$	$\frac{1}{2} + y_1 - y_2$	$\frac{1}{2} + z_1 + z_2$	8(t)	$\frac{1}{2}$	$\frac{1}{2} + 2z$	$\frac{1}{2} + 2z$
$\frac{1}{2} + x_1 - x_2$	$\frac{1}{2} + y_1 + y_2$	$\frac{1}{2} + z_1 + z_2$	8(t)	$\frac{1}{2}$	$\frac{1}{2} + 2y$	$\frac{1}{2} + 2z$
$\frac{1}{2} + z_1 - y_2$	$\frac{1}{2} + y_1 - x_2$	$\frac{1}{2} + z_1 - z_2$	4(r)	$\frac{1}{2} + x - y$	$\frac{1}{2} + y - x$	$\frac{1}{2}$
$\frac{1}{2} + x_1 + y_2$	$\frac{1}{2} + y_1 + x_2$	$\frac{1}{2} + z_1 - z_2$	4(k)	$\frac{1}{2} + x + y$	$\frac{1}{2} + y - x$	$\frac{1}{2}$

Table 10 and Table 11 are all that are needed for the complete analysis of a three-dimensional Patterson. Any two-dimensional Patterson will be a special case of the above tables. The multiplicity of the vectors is very important as it determines the integrated peak intensities in vector space which in turn indicate the type of atoms for which the interactions are occurring. For the general vectors the multiplicity is 1, that is, they are in 16 fold positions. The "special positions" represent the vectors for atoms in equivalent positions in the space group $P\bar{4}2_1c$. Since there are 8 equivalent positions, there will be an 8 fold multiplicity for the vector at the origin of vector space for each atom in a general position in real space. The special vector $2x\ 2y\ 0$ will have a multiplicity of 2 because the vectors $u\ v\ w$ and $u\ v\ \bar{w}$ of $P\ 4/m\ mm$ have degenerated into the special set $8(p)$ which has mirror point symmetry.

Two-dimensional Patterson

The two-dimensional Patterson functions for $\{hk0\}$, $\{hkl\}$, $\{0kl\}$ data are shown in Figures 16, 17, and 18. The $\{hkl\}$ Patterson is a "generalized" Patterson, and is given by

$$P_1(uv) = \sum_h \sum_k |F(hkl)|^2 \cos 2\pi hu \cos \pi kv .$$

The results of this can be interpreted as if the peaks of the $\{hk0\}$ Patterson projection were weighted by the function

Figure 16. Patterson (001) projection for
 $\text{Mg}_4\text{Br}_6^{0.4}(\text{C}_4\text{H}_{10}\text{O})$

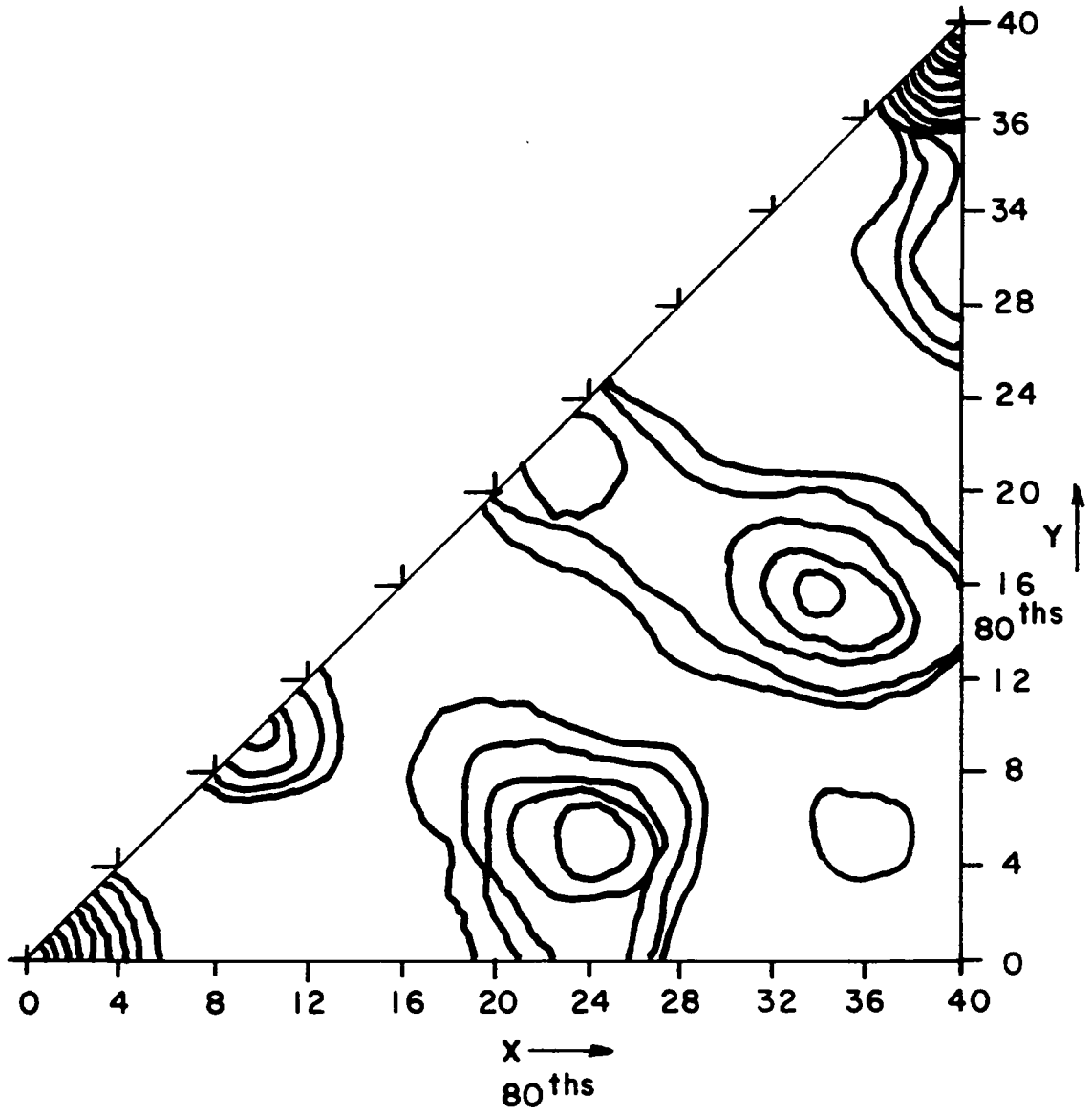


Figure 17. Generalized Patterson ({hkl} data) for
 $\text{Mg}_4\text{Br}_6^{0.4}(\text{C}_4\text{H}_{10}\text{O})$

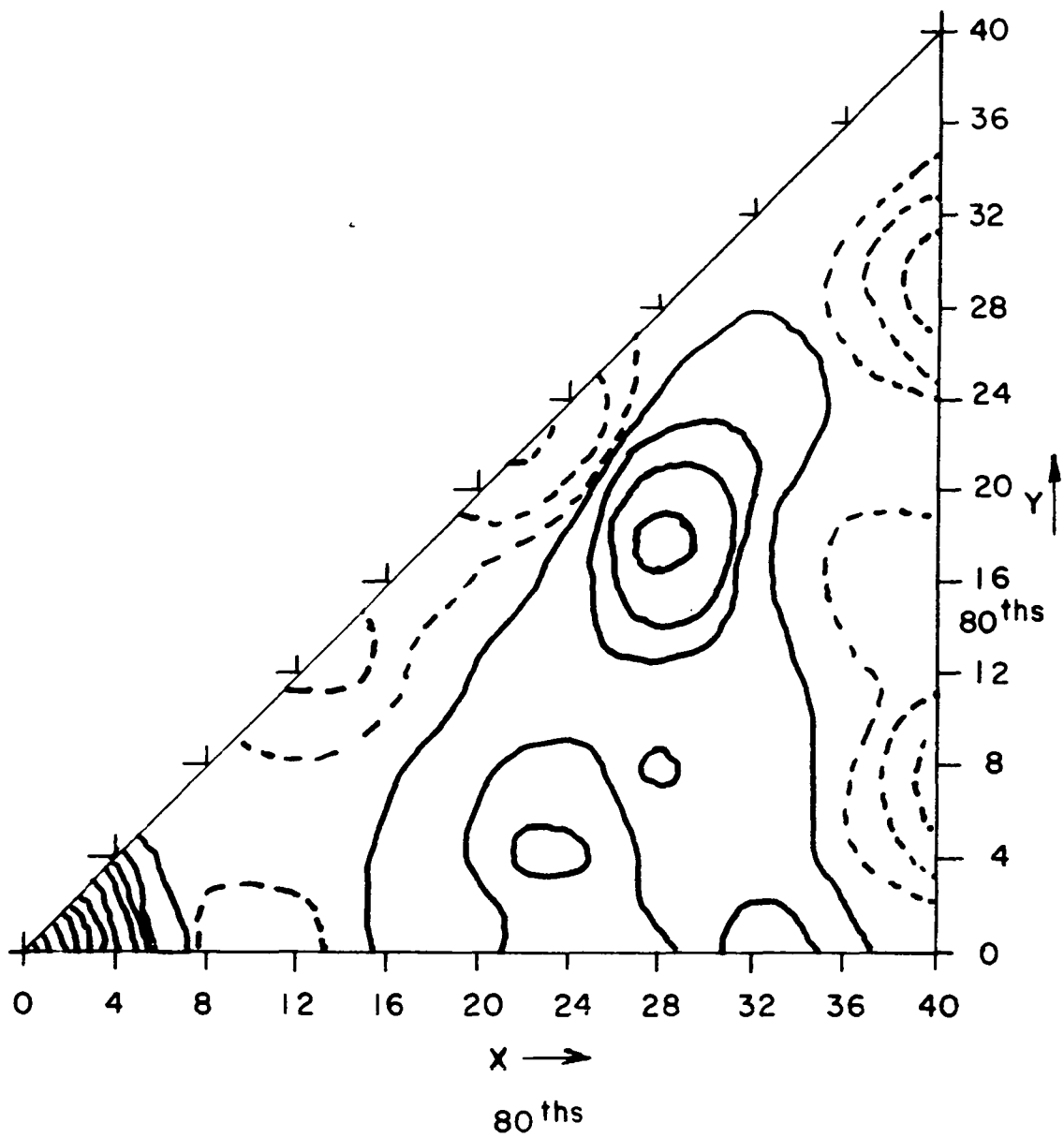
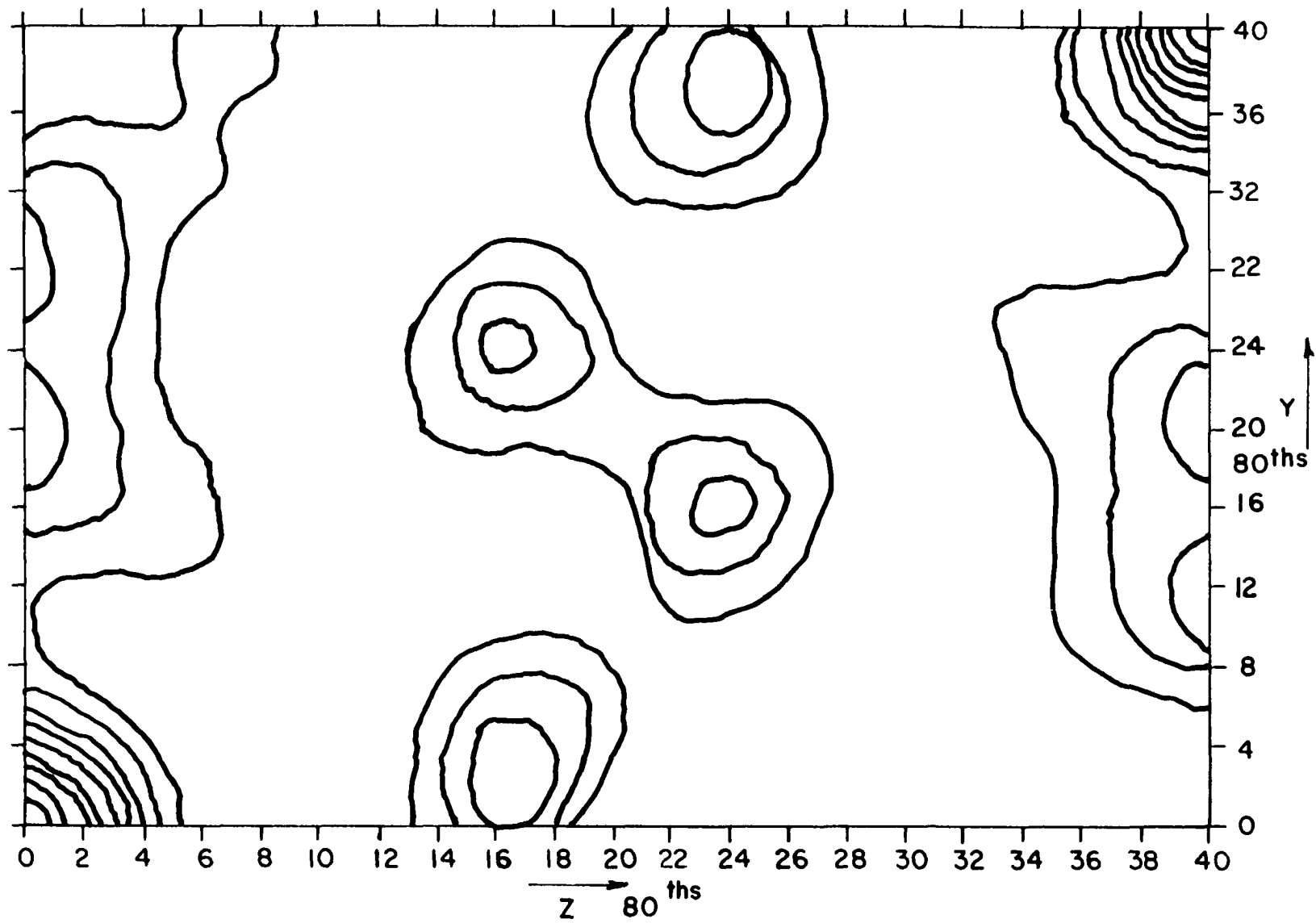


Figure 18. Patterson (100) projection for $\text{Mg}_4\text{Br}_6 \cdot 0.4(\text{C}_4\text{H}_{10}\text{O})$



$\cos 2\pi w$. The peaks at $w = 1/2$ should have the same modulus as the Patterson projection onto (001) but should be negative in sign. The peaks at $w = 1/4$ should vanish and those at $w = 0$ should have the maximum algebraic value.

From the $\{hkl\}$ projection it is observed there are two large negative peaks at $12.5/80, 12.5/80, 1/2$ and $23.5/80, 23.5/80, 1/2$. Referring to Table 11, special vectors are expected $1/2 + x - y, 1/2 + y - x, 1/2$ and $1/2 + x + y, 1/2 + y + x, 1/2$. The first of these using the results in Table 10 can be written $1/2 + x - y, 1/2 + x - y, 1/2$. Assuming the large observed peaks are bromine-bromine interactions for the equivalent set it is found that

$$x = 23/80, \quad y = 4.5/80$$

satisfy the above Patterson vectors. These peaks have a multiplicity of 4. The above values predict a vector at $x + y + 27.5/80$ $x - y = 18.5/80$. The $\{hkl\}$ Patterson shows there is a very strong peak at $w = 0$ corresponding to this vector. This implies $2z = 0$ so that $z = 1/2$ or 0 . There is no way to distinguish between these two values of z , hence the bromine positions to a first approximation are given by $x = 23/80, y = 4.5/80, z = 0$ or $1/2$. The results for the remainder of the special vectors are given in Table 12. Agreement is good with the exception of the $2x, 2y, 0$ peak which has a multiplicity of only 2 and is not as obvious.

Table 12. Vector distances for bromine atoms at (23, 4.5, 0 or 1/2)

Special vectors			<u>Positions in 80ths</u>			Multiplicity
			x	y	z	
0	0	0	0	0	0	8
2x	2y	0	-34	9	0	2
x + y	y - x	2z	27.5	-18.5	0	4
x - y	y + x	2z	18.5	27.5	0	4
$\frac{1}{2} + 2x$	$\frac{1}{2}$	$\frac{1}{2} + 2z$	6	$\frac{1}{2}$	$\frac{1}{2}$	4
$\frac{1}{2}$	$\frac{1}{2} + 2y$	$\frac{1}{2} + 2z$	$\frac{1}{2}$	-31	$\frac{1}{2}$	4
$\frac{1}{2} + x - y$	$\frac{1}{2} + y - x$	$\frac{1}{2}$	-21.5	21.5	$\frac{1}{2}$	4
$\frac{1}{2} + x + y$	$\frac{1}{2} + y + x$	$\frac{1}{2}$	-12.5	-12.5	$\frac{1}{2}$	4

Table 13. Vector distances for bromine atoms at (0, 0, 17)

Special vectors			Positions in 80ths			Multiplicity
			x	y	z	
0	0	0	0	0	0	4
0	0	2z	0	0	34	2
$\frac{1}{2}$	$\frac{1}{2}$	$\frac{1}{2} + 2z$	$\frac{1}{2}$	$\frac{1}{2}$	6	2
$\frac{1}{2}$	$\frac{1}{2}$	$\frac{1}{2}$	$\frac{1}{2}$	$\frac{1}{2}$	$\frac{1}{2}$	4

Table 14. Vector distances for bromine atoms at (0, 0, 17) and (23, 4.5, 0)
(non-equivalent interactions)

Vectors			Positions in 80ths			Multiplicity
			x	y	z	
x_1	y_1	$-z_2$	23	4.5	-17	4
x_1	y_1	z_2	23	4.5	17	
$\frac{1}{2} + x_1$	$\frac{1}{2} + y_1$	$\frac{1}{2} + z_2$	-17	-35.5	-23	4
$\frac{1}{2} + x_1$	$\frac{1}{2} + y_1$	$\frac{1}{2} - z_2$	-17	-35.5	23	

The vector peak at $x = 23.0/80$, $y = 4.5/80$ on the $\{hk0\}$, $\{hkl\}$, and $\{0k\ell\}$ Patterson projections all imply a second bromine atom at $0, 0, z$. This is checked as above, the results being given in Table 13. Again, the bromine-bromine interactions along z have a multiplicity of only two and are difficult to distinguish. The question as to whether to assign the value of $z = 0$ or $z = 1/2$ to the first bromine is now settled as indicated in Table 14. If z were $1/2$ the z parameters of the first two and last two entries would be interchanged, but the resulting positions are not observed on the $\{0k\ell\}$ projection.

There are several observations to be made at this point. First, all of the obvious peaks were explained by the two sets of bromine atoms. This was disappointing since it implied that the lighter atoms would be difficult to locate from these data. Actually, this difficulty is not so much inherent in the data as in the problem itself. Since on the average the contribution of any one atom to the diffracted intensity is

$$\langle I(hkl) \rangle = \sum_j f_j^2 ,$$

it can be shown that the contribution of the bromine atoms for $Mg_4Br_6O \cdot 4(C_4H_{10}O)$ will be about $3/4$ of the total contribution. In effect the contribution of the remaining atoms is

"swamped" by the bromine scattering.

Second, the previous note that the extinctions $k + l = 2m + 1$ implied a large amount of scattering matter with the symmetry of the space group $P 4/m nc$ is confirmed. The near 2 fold symmetry at $1/4, 1/4$ is not a property of $P\bar{4}2_1c$ but of $P 4/m nc$. The bromine atoms are in fact centrosymmetric and do not contribute to the determination of any of the phases of the acentric structure.

The bromine positions above will then give two structures, that is, each acentric position will have a centric counterpart if an electron density map is computed on the basis of the bromine positions. While it simplifies the solution to have a heavy atom which determines the phases of diffracted intensities, the problem becomes more difficult if the heavy atom contributes so much that the light atoms are difficult to find. It is even more difficult to locate light atoms when the heavy atoms are in special positions.

Even though the first set of three-dimensional counter data were poorly corrected for absorption, the crystallographic results obtained from these data did not differ significantly from that obtained from the last two sets of counter data. However, since it is believed that the last counter data were better than the first set, the treatment and results will be given in reference to the final two sets of data.

Three-dimensional Patterson

Because there is a good possibility that independent vectors of a Patterson map may overlap, it is important that the individual peaks be resolved as much as possible. If it is assumed the scattering factors of the structure can be written

$$f_n = \hat{f} \cdot z_n$$

where \hat{f} , the unitary scattering factor, is the atomic scattering factor normalized to 1 at $\sin \theta = 0$, one can write

$$\frac{F}{\hat{f}}(hkl) = \sum z_n \exp 2\pi i(hx + ky + lz) .$$

$F(hkl)/\hat{f}$ are the structure factors of a set of point atoms, and if

$$\frac{|F(hkl)|^2}{|\hat{f}|^2}$$

are used in computing the Patterson function, better resolution of the peaks is obtained. The coefficients

$$\frac{|F(hkl)|^2}{\hat{f}^2}$$

need, however, to be infinite in number so that the Patterson

function will converge. To circumvent this requirement, Jacobson et al. (60) and Donohue and Trueblood (61) have considered convergence functions of the form

$$\frac{A + B \sin^n \theta}{\lambda^n} \exp \frac{-c^2 \sin^2 \theta}{\lambda^2} .$$

The sharpened coefficients can be written

$$|S_F(hk\ell)|^2 = \left(\frac{\Sigma z_n}{\Sigma f_n^0} \right)^2 |F(hk\ell)|^2 \exp 2B \frac{\sin^2 \theta}{\lambda^2}$$

The application of the convergence function gives

$$|S_F(hk\ell)|^2 = \left(\frac{\Sigma z_n}{\Sigma f_n^0} \right)^2 |F(hk\ell)|^2 (A + B \frac{\sin^P \theta}{\lambda^P}) \exp(2B - c^2) \frac{\sin^2 \theta}{\lambda^2}$$

Typical values used by Donohue are

$$B = 16, \quad P = 4, \quad A = 0, \quad c^2 = 18.66 .$$

Jacobson et al. (60) derive their sharpening function by defining a gradient Patterson function.

$$\begin{aligned} Q(u,v,w) &= v \int_0^1 \int_0^1 \int_0^1 \nabla \rho(x,y,z) \cdot \nabla \rho(x+u, y+v, z+w) \, dx dy dz \\ &= \frac{16\pi^2}{v} \sum_{-\infty}^{\infty} \sum_{-\infty}^{\infty} \sum_{-\infty}^{\infty} \frac{(\sin \theta)^2}{\lambda} |F(hk\ell)|^2 \exp 2\pi i (hu + kv + \ell w) . \end{aligned}$$

This function gives a highly peaked maximum in vector space

with minima surrounding it. The minima can be reduced by adding in some of the original Patterson function so that the total function computed is

$$AP(u, v, w) + BQ(u, v, w)$$

or

$$\frac{16\pi^2}{v} \sum_{hkl}^{\infty} |F(hkl)|^2 \left(A' + \frac{\sin^2 \theta}{\lambda^2} \right) \exp\left((2B - c^2) \frac{\sin^2 \theta}{\lambda^2} \right) \exp 2\pi i (hu + kv + lw)$$

where c^2 is $4\pi^2/p$ (62). The values for the parameters are usually taken as $A' \cong 1/6$ and $c^2 = 5.5$.

Figures 19 and 20 give the level $w = 0$ for Lipscomb's sharpening. In Figure 19 the value of $2B - c^2$ was taken as 3.5 and in Figure 20 the value of $2B - c^2$ was -5.5. Donohue's function for $w = 0$ is shown in Figure 21. The point is well illustrated here that while there is no ambiguity in interpreting the largest peaks, the smaller peaks must be assigned with care. This is particularly true around the origin or large peaks where "ripple" effects are more noticeable.

From the first chemical analysis, it was expected that there would be six magnesium atoms. From Figure 22 and Table 15 which give the space group diagrams and positions

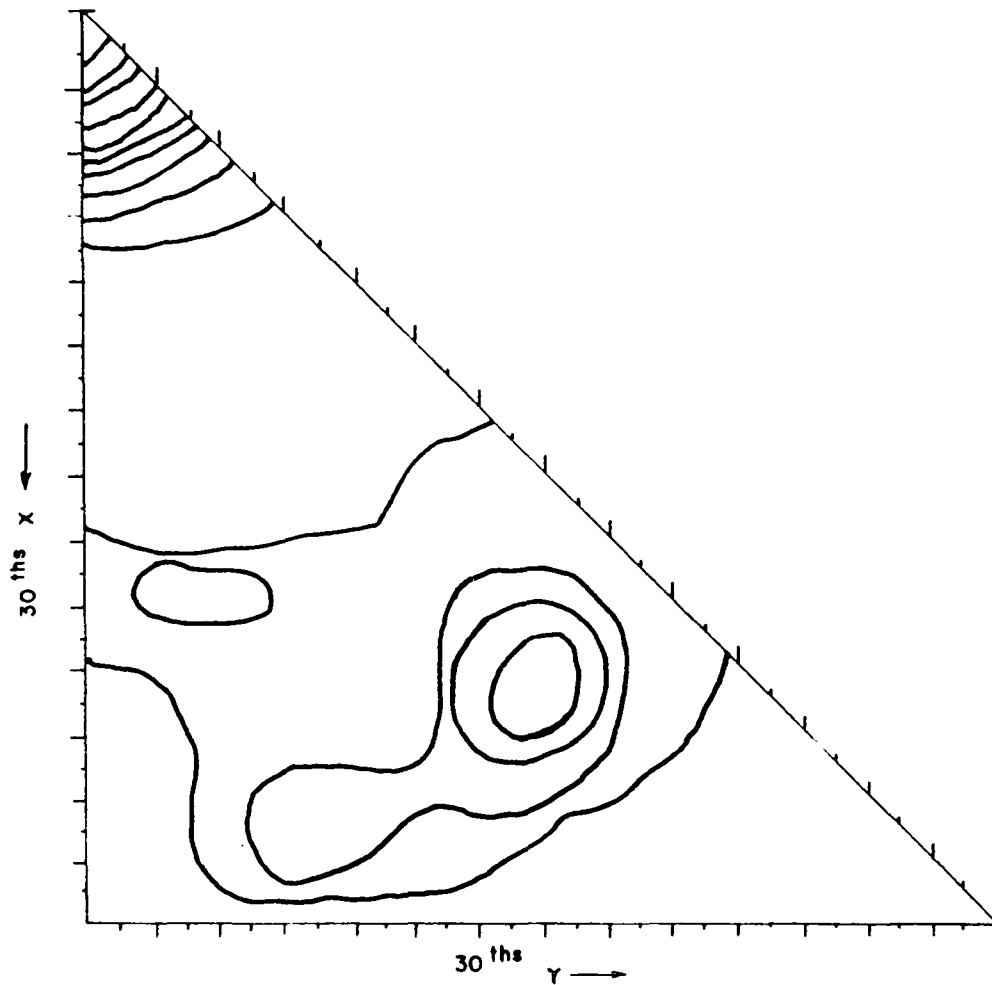


Figure 19. Sharpened Patterson section, $w = 0$, for $\text{Mg}_4\text{Br}_6 \cdot 0.4(\text{C}_4\text{H}_{10}\text{O})$. $2B - c^2 = 3.5$. Sharpened according to Jacobson *et al.* (60)

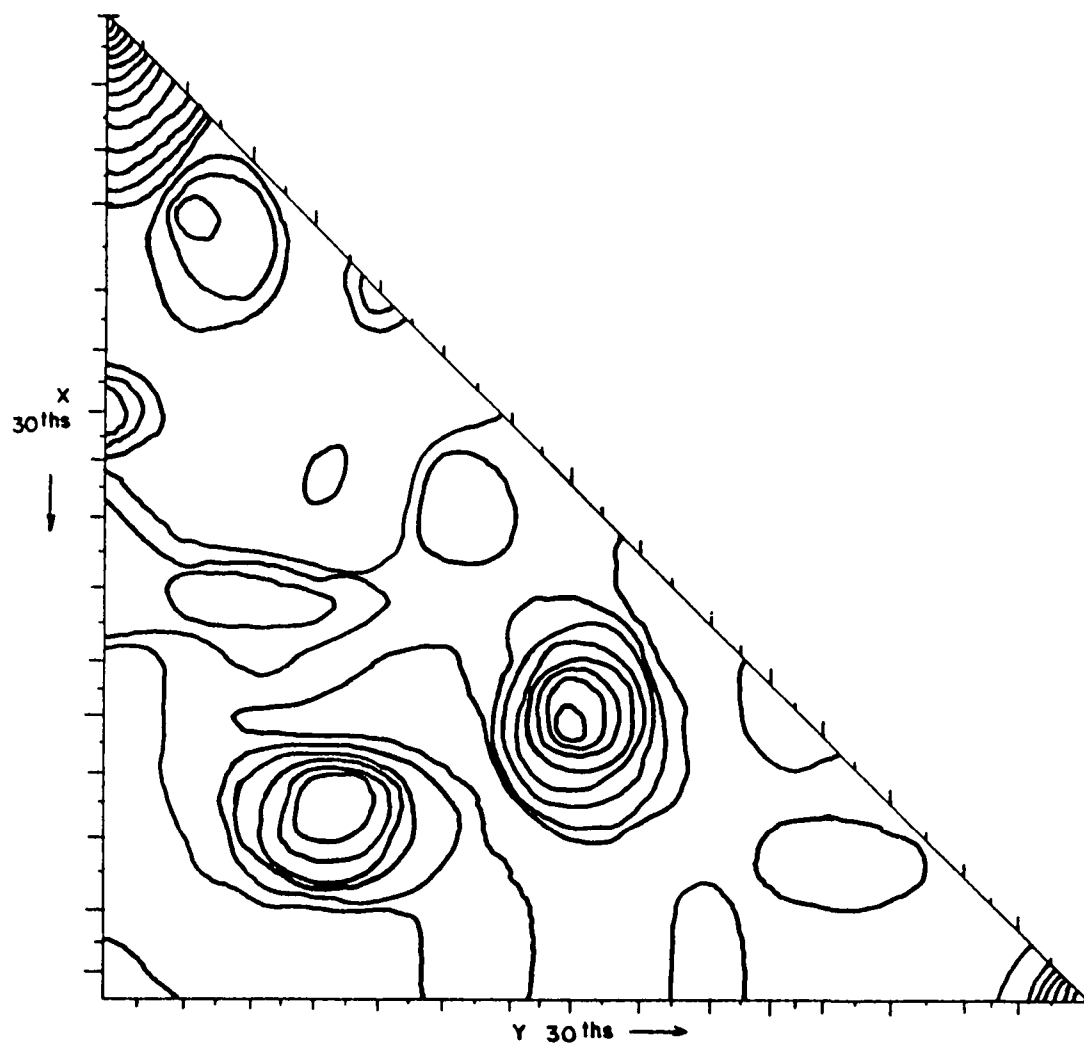


Figure 20. Sharpened Patterson section, $w = 0$, for $\text{Mg}_4\text{Br}_6\text{O} \cdot 4(\text{C}_4\text{H}_{10}\text{O})$. $2B - c^2 = -5.5$. Sharpened according to Jacobson et al. (60)

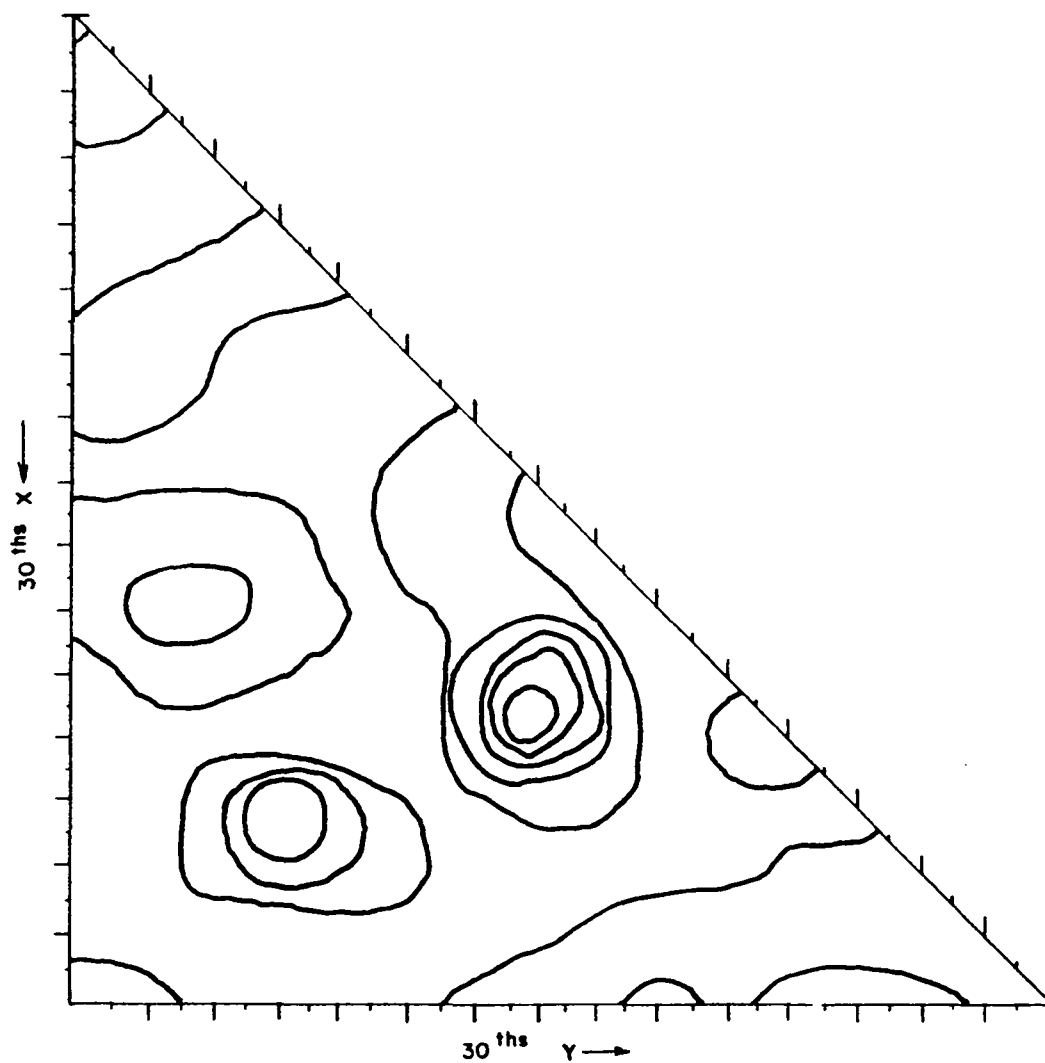


Figure 21. Sharpened Patterson section, $w = 0$ for $\text{Mg}_4\text{Br}_6\text{O} \cdot 4(\text{C}_4\text{H}_{10}\text{O})$. Sharpened according to Donohue and Trueblood (61)

Table 15. Positions for $P\bar{4}2_1C$ D_{2d}^4

No. positions and Wyckoff notation	Point symmetry	Coordinates of equivalent reflections			Conditions limiting possible reflections	
8e	1	x y z	$\frac{1}{2} - x$	$\frac{1}{2} + y$	$\frac{1}{2} - z$	
		$\bar{x} \bar{y} z$	$\frac{1}{2} + x$	$\frac{1}{2} - y$	$\frac{1}{2} - z$	hhl: $l=2n$
		$\bar{y} x \bar{z}$	$\frac{1}{2} + y$	$\frac{1}{2} + x$	$\frac{1}{2} + z$	h00: $h=2n$
		y $\bar{x} \bar{z}$	$\frac{1}{2} - y$	$\frac{1}{2} - x$	$\frac{1}{2} + z$	Remainder have above plus
4d	2	0 $\frac{1}{2}$ z	0	$\frac{1}{2}$	$\frac{1}{2} + z$	hkl: $l=2n$
		$\frac{1}{2}$ 0 \bar{z}	$\frac{1}{2}$	0	$\frac{1}{2} - z$	hk0: $h+k=2n$
4c	2	0 0 z	$\frac{1}{2}$	$\frac{1}{2}$	$\frac{1}{2} + z$	hkl: $h+k+l=2n$
		0 0 \bar{z}	$\frac{1}{2}$	$\frac{1}{2}$	$\frac{1}{2} - z$	

Table 15 (Continued)

No. positions and Wyckoff notation	Point symmetry	Coordinates of equivalent reflections				Conditions limiting possible reflections
2b	$\bar{4}$	0 0 $\frac{1}{2}$	$\frac{1}{2}$	$\frac{1}{2}$	0	hkl: $h+k+l=2n$
2a	$\bar{4}$	0 0 0	$\frac{1}{2}$	$\frac{1}{2}$	$\frac{1}{2}$	hkl: $h+k+l=2n$

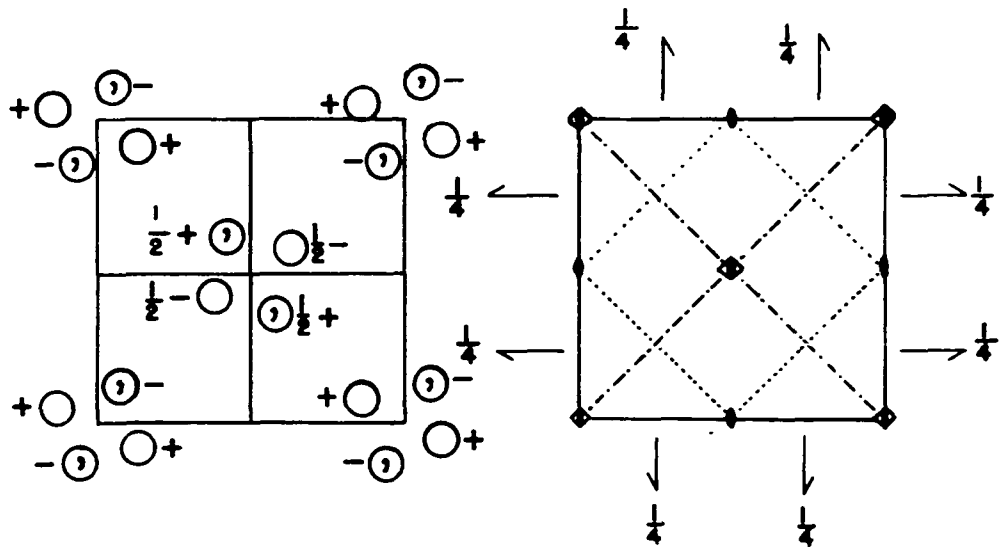


Figure 22. Space group diagram for $P\bar{4}2_1c$

for $P\bar{4}2_1c$ as given in "International Tables for X-ray Crystallography", Volume 1 (56), it can be seen that six magnesium atoms would require the use of the special positions 4d or 4c plus 2b or 2a. The magnesium atoms in 4d or 4c would be required to have two-fold symmetry while those in 2b or 2a would have to have $\bar{4}$ symmetry.

The three-dimensional Patterson indicated the utilization of the set 2a. There was the possibility of two equivalent atoms in 2b, however the 2b interactions were much less than those for 2a and were questionable. Since the distance of both sets of bromine atoms to the origin (2a) is about $3.16 \overset{\circ}{\text{Å}}$, there could be no bonding between the bromine atoms and the atom at the origin. The Patterson map then revealed the presence of Atom 2 in either the general position $x = .13 \quad y = -.08 \quad z = .07$ or $x = .13 \quad y = .08 \quad z = .07$. The reason for the two choices is that when several atoms are in centrosymmetric positions in an acentric space group, there is an arbitrary choice in locating the first atom which occupies an acentric position since the atom can be placed in a general position, (x, y, z) , or in the centrosymmetric counterpart, $(\bar{x}, \bar{y}, \bar{z})$. The choice determines uniquely the origin of the unit cell and in this case whether a "left- or right-handed" notation is to be followed.

Atom 2 was slightly less than $2.0 \overset{\circ}{\text{Å}}$ from the origin, but the most significant factor was that it was only about

2.6 Å from the bromine atoms. The approximate Van der Waal radius of bromine is 1.95 Å and of oxygen is 1.4 Å. The expected bromine-oxygen distance is therefore about 3.35 Å. The ionic radius of magnesium is .65 Å so one expects a magnesium bromide distance of 2.55 Å. These considerations strongly implied that the atom at the origin was not magnesium, but oxygen. Furthermore, Atom 3 was found from the Patterson map at $x = .26, y = .17, z = .15$ or $x = .26, y = .17, z = .15$, depending on whether Atom 2 was taken at $x = .13, y = -.08, z = .07$ or $x = .13, y = .08, z = .07$. The distance of Atom 3 to Atom 2 was close to 2.05 Å, approximately the proper distance for a magnesium-oxygen distance.

No other atoms could be definitely located from the three-dimensional Patterson function. In particular no magnesium atom interaction peaks could be found in either the set 4d or 4c.

Figure 23 shows the proposed model derived from the three-dimensional Patterson.

Least squares and Fourier analysis

The equations for the structure factors which are the coefficients of the electron density or Fourier maps of the space group $P\bar{4}2_1c$ are given in Table 16. Although the analysis of the Patterson was confirmed by successive Fouriers, the least squares calculation was used to calculate the signs and phases of the Fourier coefficients. The least squares

Figure 23. Model of $\text{Mg}_4\text{Br}_6\text{O}\cdot 4(\text{C}_4\text{H}_{10}\text{O})$ showing octahedral arrangements of bromine atoms about origin. Small spheres represent magnesium atoms, dark sphere at center of octahedron is oxygen atom. Ether oxygens are not shown.

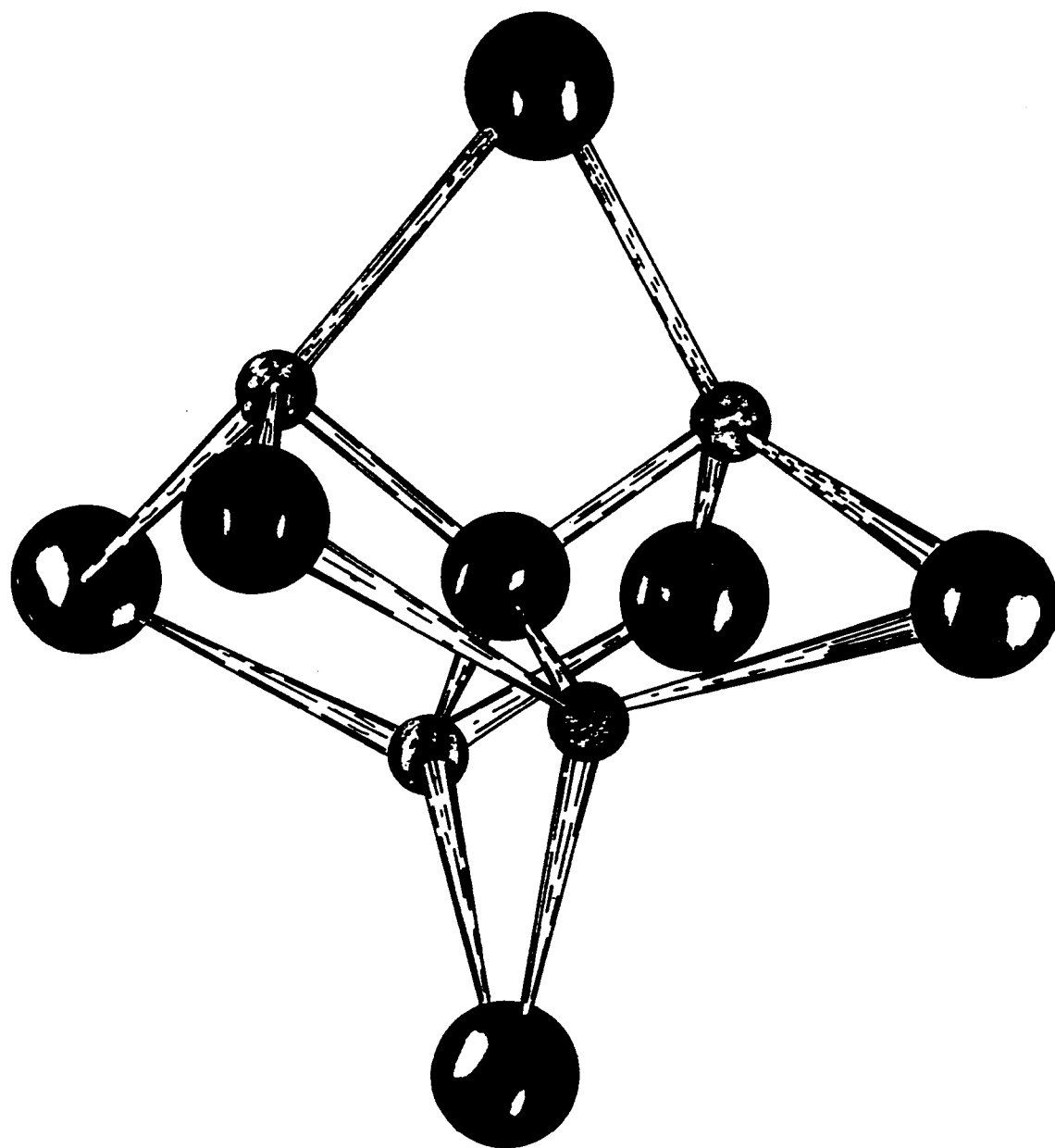


Table 16. Structure factor equations for $P\bar{4}2_1c$ D_{2d}^4

$$F(hkl) = A(hkl) + B(hkl) \quad \tan^{-1} B/A = \alpha(hkl)$$

Condition	Equations
$h + k + l = 2n$	$A(hkl) = 4 \cos 2\pi lz [\cos 2\pi hx \cos ky + \cos 2\pi kx \cos 2\pi hy]$ $B(hkl) = -4 \sin 2\pi lz [\sin 2\pi hx \sin 2\pi ky + \sin 2\pi kx \sin 2\pi hy]$ with $\alpha(hkl) = -\alpha(\bar{h} \bar{k} \bar{l}) = -\alpha(\bar{h}k\bar{l}) = -\alpha(h\bar{k}\bar{l}) = -\alpha(hk\bar{l})$
$h + k + l = 2n + 1$	$A(hkl) = 4 \cos 2\pi lz [-\sin 2\pi hx \sin 2\pi ky + \sin 2\pi kx \sin 2\pi hy]$ $B(hkl) = -4 \sin 2\pi lz [-\cos 2\pi hx \cos 2\pi ky + \cos 2\pi kx \cos 2\pi hy]$ with $\alpha(hkl) = -\alpha(\bar{h} \bar{k} \bar{l}) = \pi - \alpha(\bar{h}k\bar{l}) = \pi - \alpha(h\bar{k}\bar{l}) = -\alpha(hk\bar{l})$

comparison of the observed and calculated structure factors was then also used as an added criterion for the "correctness" of the proposed model.

Weighting of least squares The importance of weighting of the least squares equations and some of the types of weighting recently used for counter data in this laboratory have been discussed by Willett (63). Willett used a weighting scheme based on the concept of finite differences which worked satisfactorily. Another scheme which utilizes Hamilton's treatment of unobserved reflections (64) was used for this problem and is given below.

Let the observed intensity be given by

$$I(hkl) = AL_p |F(hkl)|^2$$

where A is the absorption correction, L_p the Lorentz polarization factor, and $|F(hkl)|$ the magnitude of the structure factor. The definition of the standard deviation is

$$\sigma^2(f) = \sum_{i=1}^n \left(\frac{\partial f}{\partial x_i} \right)^2 \sigma^2(x_i) + \text{covariant terms} .$$

The covariant terms may be neglected, since to a first approximation there is no interaction between A and $|F|$. Using this definition one arrives at the following expression for $\sigma(F)$:

$$\sigma^2(F) = \frac{\sigma^2(I) + (\sigma^2(A)/A^2) I^2}{4 IALp}$$

The weighting of the least squares when refinement is carried out on $|F(hkl)|$ is $\frac{1}{\sqrt{\sigma(F)}}$ so that if expressions can be found in terms of observables for $\sigma(I)$ and $\sigma(A)$, the desired function will be obtained.

$\sigma^2(I)$ is a function of both systematic and statistical errors.

$$\sigma^2(I) = \sigma_{sy}^2(I) + \sigma_{st}^2(I)$$

The statistical variations of counter data are given by a Poisson distribution. Since

$$I = \text{Total counts} - \text{Background counts} - \text{Streak counts}$$

$$I = T - B - S$$

$$\sigma_{st}^2(I) = T + B + S$$

The systematic errors to be included are extinction, small variations in circuit voltage because of electronic tubes going "bad", the readjustments of the voltage to compensate for this, and any other non-random errors. A good assumption regarding these errors is that they are a function of the intensity measured, that is

$$\sigma_{sy}^2(I) = (P_T T)^2 + (P_B B)^2 + (P_S S)^2$$

where P_T , P_B , and P_S are the estimated percentage systematic errors in the recording of the intensity for total, background, and streak counts respectively. The same assumption is made for $\sigma(A)$,

$$\sigma^2(A) = (P_A A)^2 .$$

The particular problem under consideration is the case when the measured intensity, I , is small. In this instance the statistical standard deviation $\sigma_{st}^2(I)$ is greater than the measurement, I , and no meaningful measurement can be given for the value of I .

Hamilton (64) has considered this problem and has derived the equations for the most probable intensity and the statistical standard deviations for these reflections for both acentric and centric space groups.

$$\mu = \text{most probable intensity} = \frac{I_{\min}}{2} \text{ (acentric)}$$

$$= \frac{I_{\min}}{3} \text{ (centric)}$$

$$\text{Centric: } \sigma_{st}^2(I) = \frac{4 I_{\min}^2}{45} \qquad \sigma_{st}(I) = \frac{2 I_{\min}}{3 \sqrt{5}}$$

$$\text{Acentric: } \sigma_{st}^2(I) = \frac{I_{\min}^2}{12} \qquad \sigma_{st}(I) = \frac{I_{\min}}{2 \sqrt{3}}$$

Hamilton left the definition of I_{\min} to the reader.

D. R. Fitzwater* has defined I_{\min} as "that intensity which would have to be measured to be statistically significant."

In making the decision as to what this value must be, the observation is first made that the systematic errors previously described do not contribute to determining whether a reflection is to have a statistically significant value. Using a 99.7% confidence limit, I will be statistically significant

$$\text{if } I > 3 \sigma_{\text{st}}(I) = 3 [T + B + S]^{1/2} .$$

If, however, $I \leq 3 \sigma_{\text{st}}(I)$ then

$$I_{\min} = 3 \sigma_{\text{st}}(I) .$$

Using Hamilton's results (64), $\sigma'_{\text{st}}(I) = a I_{\min}$ where

$$a = \frac{2}{3\sqrt{5}} \text{ for centric structures, and } \frac{1}{2\sqrt{3}} \text{ for acentric}$$

structures. The intensity for the reflection is given by

$$\mu = \frac{I_{\min}}{b} \quad \begin{array}{l} b = 3 \text{ for centric structures} \\ = 2 \text{ for acentric structures} . \end{array}$$

The procedure is now the same for both groups of reflections

*Fitzwater, D. R. Department of Chemistry, Iowa State University, Ames, Iowa. Disc. 1001. Private communication. 1962.

$$\sigma^2(I) = \sigma_{st}^2(I) + \sigma_{sy}^2(I)$$

$$\begin{aligned} \sigma_{st}(I) &= \sigma'_{st}(I) \text{ if } I < 3 \sigma_{st}(I) \\ &= \sigma_{st}(I) \text{ if } I > 3 \sigma_{st}(I) . \end{aligned}$$

Refinement Structure factor calculations were first made for bromine atoms only. Temperature factors were not varied, but were set equal to 3.00. The scale factor between observed and calculated data was found by carrying out some trial two-dimensional calculations on an IBM 650.

The bromine positions found from Patterson analysis were used as input. After three cycles of least squares, the positions were Br (0, 0, .206) and Br (.293, .061, -.010). The agreement factor

$$R = \frac{\Sigma ||F_o| - |F_c||}{\Sigma |F_o|}$$

for the observed reflections was 30.7%. The weighted agreement factor

$$R_w = \frac{\Sigma w(|F_o| - |F_c|)^2}{\Sigma w|F_o|^2}$$

was 34.5% for observed reflections.

The expression for the calculation of the Fourier electron density map for $P\bar{4}2_1c$ which is suitable for computa-

tion on a computer is

$$\rho(xyz) = \frac{8}{v_c} \left\{ \sum_{\substack{h \\ 0}}^{\infty} \sum_{\substack{k \\ 0}}^{\infty} \sum_{\substack{l \\ 0}}^{\infty} (A(hkl) \cos 2\pi hx \cos 2\pi ky \cos 2\pi lz \right. \\ \left. - B(hkl) \sin 2\pi hx \sin 2\pi ky \sin 2\pi lz \right. \\ \left. + \sum_{\substack{h \\ 0}}^{\infty} \sum_{\substack{k \\ 0}}^{\infty} \sum_{\substack{l \\ 0}}^{\infty} (B(hkl) \cos 2\pi hx \cos 2\pi ky \sin 2\pi lz \right. \\ \left. - A(hkl) \sin 2\pi hx \sin 2\pi ky \cos 2\pi lz) \right\} .$$

As for the Patterson function, redundant terms have been added to give the correct symmetry. The calculated phase angle is given by

$$\tan^{-1} B_c/A_c = \alpha .$$

The observed A_o and B_o are given by

$$A_o = |F_o| \cos \alpha, \quad \text{and} \quad B_o = |F_o| \sin \alpha .$$

The Fourier is calculated using these coefficients. The difference Fourier is given by coefficients $A_o - A_c$ and $B_o - B_c$.

A three-dimensional Fourier and a difference Fourier map for the bromine atoms were calculated using the IBM 704. Taking the largest peak which matched on both the Fourier and

difference Fourier gave the same magnesium position as found previously. The resolution of the Fourier was disappointing. This was probably due to the bromine atoms contributing only to the real part of the structure factor so that the Fourier shows all acentric atoms as being centric and having half weight.

The magnesium atom was next inserted at $x = .076$, $y = -.14$, $z = .078$ with an isotropic temperature factor of 4.0. Least squares refinement gave the shifts and results in Table 17 after three cycles.

Table 17. Shifts and results of least squares refinement including bromine and magnesium atoms

Atom	<u>Original position</u>			<u>Shifted position</u>		
	x	y	z	x	y	z
Br	0	0	.2078	0	0	.2075
Br	.2938	.0619	-.0065	.2941	.0597	-.0092
Mg	.0762	-.1407	.0778	.0847	-.1243	.0730
Agreement factor:	observed reflections			R = 26.3	$R_w = 28.4$	
	all reflections			R = 31.7	$R_w = 28.7$	

From the Fourier calculated using the magnesium atom both oxygen atoms were discernable. The peak height of the oxygen atom at the origin was about 9 electrons/ \AA^3 . The

bromine peak height was 51 electrons/ \AA^3 . The peak height of the oxygen atom in the general position $x = .178$, $y = -.252$, $z = .144$ was 5 electrons/ \AA^3 . The magnesium peak height was about 18 electrons/ \AA^3 . The difference Fourier showed positive peaks in the bromine and magnesium positions. This indicated the scale factor was still low since Busing scales $F(\text{calculated})$ to $F(\text{observed})$ and the coefficients $|F_o| - k|F_c|$ were too large.

Putting oxygen atoms in two fold positions at the origin and in eight fold positions at $x = .178$, $y = -.252$, and $z = .144$ gave $R = 23.1$ and $R_w = 23.9$ for observed data. The temperature factors were isotropic and not varied.

At this point a comparison was made with the least squares results from two-dimensional film data. The $\{hk0\}$ film data were not of sufficient quality that an analysis was possible. This was determined by an examination of equivalent reflections. The $\{hkl\}$ and $\{0kl\}$ data, however, were refined using least squares methods. These data were taken on different crystals and with different transfers and were completely independent of the counter data and each other. The result was an R factor of 15.7% for observed data for both $\{hkl\}$ and $\{0kl\}$ data. The refined positions and temperature factors of the two-dimensional data are compared with the refined positions of the counter data in Table 18. The temperature factors of the three-dimensional counter data

Table 18. Comparison of results of refinement of 2d and 3d data--5 atoms

Atom	Counter parameters				{hkl} and {0k ℓ } parameters			
	x	y	z	B	x	y	z	B
Br	.0	.0	.2071	3.0	0	0	.2061	4.67
Br	.2938	.0594	-.0092	3.0	.2932	.0576	-.0060	6.10
Mg	.0813	-.1241	.0730	4.0	.0840	-.1239	.0684	2.86
0	.1775	-.2524	.1440	4.0	.1754	.2703	.1625	2.60
0	0	0	0	4.0	.0	.0	.0	7.03

had not been varied for this model.

The Fourier maps from the 3-d data 5 atom model indicated possible carbon atom parameters for the two atoms close to the oxygen atom. When these were included and the temperature factors of all the atoms refined it was possible to postulate the remaining ether carbon positions from the resulting Fourier.

The ether carbon positions were not at all clear on the Fourier maps. The peaks which were chosen to represent the atoms were in approximately the right positions but very weak. That these positions were highly dubious was revealed by the refinement of the model with the ether carbons included. The R factor for this model was 15.7% for observed reflections. The weighted R factor for all data was 14.2% and for observed reflections only was 13.5%. The temperature factors of the carbon atoms had, however, gone up to the extent that their contribution was nearly negligible. It was also observed that the temperature factors of the bromine atoms were relatively high. The values for the bromine atoms were 5.39 and 6.41. The value for the magnesium atom was 3.29. The oxygen temperature factors were 7.67 for the atom in the general position and 4.15 for the atom at the origin. The carbon temperature factors ranged from 17 to 25.

Since the thermal motion of the bromine atoms was high and also, as indicated by a difference Fourier map,

quite anisotropic; it was decided to use anisotropic temperature factors for the atoms and to continue the refinement. All of the information obtained prior to this point was reanalyzed in an attempt to find better carbon atom positions. When it was felt that this had been done, refinement was continued. After four cycles the R value had dropped to 9.4% for observed reflections. The weighted R value for all data was 9.4% and for observed reflections was 8.6%. The ether carbon shifts, however, were still as much as .1 of an angstrom which is surprisingly high at this stage of a structure determination.

Although little has been said in regard to packing considerations, these were used at all stages of the determination as guides and aids toward finding the correct structure. The basic structure at this last stage is still that in Figure 23. The bromine atoms form an octahedron about the origin of the unit cell. The distance from the origin oxygen to the bromine atoms along 00z is $3.17 \overset{\circ}{\text{Å}}$. The distance of the remaining four bromine atoms to the origin is $3.19 \overset{\circ}{\text{Å}}$. These latter bromine atoms were $.08 \overset{\circ}{\text{Å}}$ off the plane $z = 0$. The bromine-magnesium distances were equal for both sets of bromine atoms and were $2.62 \overset{\circ}{\text{Å}}$. The magnesium-origin oxygen distance was $1.95 \overset{\circ}{\text{Å}}$ and the magnesium-ether oxygen distance was $2.11 \overset{\circ}{\text{Å}}$.

Discussion of Structure

The final observed and calculated structure factors are given in Figure 24. The weighted discrepancy factor including unobserved reflections was 9.4%. The weighted discrepancy factor omitting unobserved was 8.3% while the unweighted discrepancy factor omitting unobserved reflections was 9.4%. The final parameters obtained from least squares are given in Tables 19 and 20. Table 21 gives bond angles and distances for these parameters and Figure 25 illustrates the thermal ellipsoids described by the atoms by means of stereograms projected along the z axis of the unit cell. The magnitudes of the displacements along the axes of the ellipsoids are given in angstroms.

Although the observed density, 1.73 gms/cm^3 , agreed with the calculated density for $\text{Mg}_4\text{Br}_6\text{O}\cdot 4(\text{C}_4\text{H}_{10}\text{O})$, 1.69 gms/cm^3 ; a styrofoam Van der Waal packing model of the unit cell showed that the atoms were not closest packed. This was particularly true in the region about $1/2, 1/2, 0$ in the unit cell. This could be explained if

- (a) the model were incorrect or
- (b) the ether molecules were disordered.

(a) was unlikely because of the very good agreement between observed and calculated structure factors (9.4%). (b) on the other hand was highly probable for several reasons.

Figure 24. Comparison of observed and calculated structure factors for $\text{Mg}_4\text{Br}_6\text{O}\cdot 4(\text{C}_4\text{H}_{10}\text{O})$. Columns are for constant h and k miller and are F_{obs} F_{calc} A_{calc} B_{calc} . Asterisks indicate unobserved reflections.

17*	13	15	-14	6	15*	13	1	1	1	7*	13	12	-12	1	12	30	27	-26	-8	12*	12	8	-7	-4	
F= 5 K= 1				F= 8 K= 1						8*	13	1	1	0	13	25	19	-19	-3	13*	12	7	7	-2	
C	20	28	-28	-0	0*	11	1	-1	0	9*	13	9	-8	4	14*	13	20	20	2	14*	13	3	-3	-2	
1	45	42	41	7	1*	12	2	1	2	10*	13	20	-2	20	15*	13	17	-11	-5	15*	23	19	18	-5	
2	129	135	-135	3	2	21	20	-2	20	11*	14	14	-14	-1	16*	13	5	-3	4	16*	13	5	-3	4	
3	24	32	32	3	3	35	36	-36	1	17*	13	5	-4	-3	17*	13	6	-5	-3	17*	13	6	-5	-3	
4*	11	15	-11	10	4	21	20	-10	18	2*	13	5	-4	-3	F= 5 K= 2				0	41	44	44	0		
5	43	49	48	12	5	18	15	14	-6	3*	13	20	-20	-0	C	67	67	-62	0	1*	11	17	-16	3	
6	18	17	-13	10	6*	12	21	-16	14	4*	13	7	-4	-6	1	28	29	-29	-4	2*	12	18	-16	-9	
7	55	55	54	11	7	33	35	-35	14	5*	13	4	-4	-1	2	61	61	-61	-3	3*	26	27	-26	8	
8	37	40	-40	8	8*	12	10	-10	14	6*	12	15	5	0	3	71	69	-69	0	5	35	35	-31	17	
9	22	21	19	8	9*	12	15	5	10	7*	12	15	5	-4	4	35	37	-38	-8	6*	12	8	2	-8	
10	18	21	19	7	10*	12	8	-7	-4	8	9*	12	15	5	5	43	43	40	-10	7	21	24	-23	6	
11*	12	12	9	8	11*	12	6	-4	5	C	35	11	31	0	6*	12	6	-6	1	8*	12	14	-12	7	
12	44	46	-46	6	12*	12	3	-3	-1	2	255	247	-246	18	7	52	58	-57	-8	9*	12	18	-18	-0	
13*	12	7	6	4	13*	12	4	-3	3	4	91	90	-60	66	8*	12	14	-5	13	10*	12	20	19	5	
14*	13	7	5	5	14*	13	4	1	3	6	59	57	-57	6	9*	12	19	19	7	11	18	17	-10	5	
15*	13	2	-0	2					8	8	81	87	-85	-21	10	17	17	-13	11	12*	12	9	-9	0	
16*	13	9*	-4	2	F= 9 K= 1				10	10	40	39	13	-37	11*	12	14	-11	-8	13*	12	3	-1	3	
H= 6 K= 1				C	19	14	14	-0	12	12	62	61	-59	-17	12*	12	13	-13	4						
C	49	53	53	0	1	21	18	17	-5	14	20	19	19	-1	13*	12	16	-16	-0	F= 9 K= 2					
1	15	17	17	-2	2	34	31	-31	-4	16*	14	15	-14	3	14*	13	12	-11	2	C	35	37	37	0	
2	54	54	53	7	3*	13	9	7	6	F= 3 K= 2				6	15*	13	15	15	-0	1*	12	15	14	-5	
3	19	21	-20	-3	4*	13	5	-4	-2	C	27	24	-24	0	H= 6 K= 2				2	2	29	28	27	5	
4	59	58	57	11	5*	12	8	-1	8	1	48	48	47	11	0	90	88	88	-0	3*	12	19	-18	-5	
5	67	69	69	-1	6*	12	14	-14	0	1	48	48	47	11	-40	1	17	11	3	4*	13	13	11	7	
6	44	48	48	-1	7*	12	4	-4	2	2	34	41	-11	-40	U	17	11	3	11	5*	13	19	17	-7	
7	22	23	-22	7	8	19	21	-20	5	3	76	72	-50	52	1	19	24	-6	-23	6*	13	7	7	7	
8	34	34	33	-9	9	10*	12	9	-9	4	36	31	23	-20	2	19	24	-6	4	7	21	15	-15	-2	
9	36	34	32	11	10*	12	9	-9	1	5	108	114	110	29	3	19	16	15	4	8*	12	2	-2	-0	
10	22	25	23	-8	11	11*	12	1	1	6*	11	9	4	-8	4	56	60	57	-19	9*	12	9	9	-0	
11*	12	8	-1	B	12	19	11	-11	1	7	37	36	-32	-16	5	32	33	30	-12	10*	12	4	2	3	
12*	12	12	10	-6	H= 10 K= 1				1	8	31	28	7	-27	6	24	30	25	-16	11*	12	5	-0	-5	
13*	12	13	-11	7	0	21	11	11	-0	9	51	57	47	-32	7*	12	24	24	1	12*	13	9	9	3	
14*	12	5	2	-4	1	41	38	37	-4	10*	12	13	10	-8	8*	12	5	-5	-1						
15	18	14	14	1	1	1	41	38	37	-4	12*	12	4	-3	9*	12	16	16	1	F= 10 K= 2					
16*	13	3	2	1	2*	13	7	6	-3	13	20	9	-6	-7	10	36	40	40	-2	0	49	46	46	0	
16*	13	3	2	1	3*	12	16	16	-8	14*	13	9	-3	-8	11*	12	7	6	-5	1	27	25	25	0	
F= 7 K= 1					4*	13	9	-4	-8	15*	13	20	20	-0	12*	12	16	-16	-3	2	18	15	15	-2	
C	106	109	109	0	5	41	36	36	-5	16*	13	6	-0	-6	14	24	20	19	-2	3	18	15	15	-3	
1*	11	13	5	11	6*	13	9	-7	-5	17	20	17	-16	5	15*	13	2	-2	1	4	33	32	32	2	
2	23	28	26	-8	7*	13	5	5	0											5*	13	2	2	-1	
3	31	30	24	17	8*	13	9	-7	-6	H= 4 K= 2				0	C	29	28	-28	-0	6*	13	23	22	-2	
4	71	70	70	-3	9*	22	21	21	-0	0	102	98	98	0	1	82	84	82	-11	7*	13	4	-4	-2	
5*	12	15	12	9	10*	12	2	-2	-1	1	112	114	-113	-14	1	18	19	-18	-6	8*	13	9	9	-0	
6	42	45	45	3	11*	13	9	9	1	2	35	39	-32	22	2	42	41	38	-15	9*	12	3	1	-3	
7*	12	6	C	-6	F= 11 K= 1				1	3	82	89	-87	-19	3	42	41	38	-15	6	10	25	20	20	-2
8	22	20	15	-14	0*	13	17	17	0	4	60	58	55	-19	4	18	12	-12	-3	10*	12	5	-2	-2	
9	23	17	8	-15	1*	13	10	-10	-1	5	53	51	-50	-11	5	84	85	85	-8	7*	13	4	-4	-2	
10	40	44	42	-13	2*	13	4	-4	-1	6	34	36	36	-2	6	22	14	-14	-0	8*	13	9	9	-0	
11*	12	14	3	-13	3*	13	16	-14	-7	7	37	35	-32	-14	7*	12	6	5	-2	9*	12	3	1	-3	
12*	12	10	-6	-13	4*	13	10	10	-7	8*	12	7	-4	-5	8*	12	10	-8	-7	10*	12	3	-2	2	
13*	12	9	-2	-4	5*	13	14	-14	-4	9	24	25	-24	-6	9	43	43	42	8	3*	13	3	-2	2	
14	22	21	21	3	6*	13	6	6	0	10	48	52	51	-10	10*	12	10	-6	-8	4*	13	12	-12	-2	
									0	11	23	23	-23	3	11*	12	18	17	5	5*	13	15	15	1	

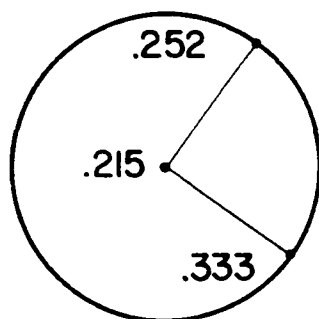
Figure 24 (Continued)

6*	13	14	-14	2	13	22	17	-16	6	0*	11	5	5	-0	H=	5	K=	4	2	30	33	-33	-1																		
7*	13	2	-2	-0	14	19	19	18	2	1	36	37	37	-4	0	14	13	13	-0	3	23	20	-18	-9																	
8*	13	10	-9	3	15*	13	10	-9	3	2	38	34	-34	-3	1	34	37	31	-19	4*	12	11	0	11																	
				H=	12	K=	2					3	32	27	27	0	2	27	26	25	-3	6*	12	12	-10	6															
								H=	6	K=	3					4*	12	7	-7	1	3	40	46	-46	-7	7	20	18	-18	1											
												5	19	12	12	-10	-6	5	27	19	19	2	9	18	15	-12	8														
												6*	12	12	-10	-6	5	27	19	19	2	9	18	15	-12	8															
												7*	13	3	3	-1	6	29	26	26	3	10	19	12	12	4															
												8*	13	16	-16	-2	7	57	55	-54	5	11*	13	9	-6	6															
												9*	12	5	5	1	6	25	24	23	6	12	24	14	-14	2															
												10*	12	8	5	-6	9	19	15	10	11					11															
												11*	12	9	9	0	10*	13	17	13	11					11															
												12	25	14	-13	-5	11	22	11	-4	11					11															
																12*	12	H	1	8	C	21	24	24	-0																
																13	20	12	1	12	1*	11	3	-1	-3																
																14*	13	2	-C	2	2	23	24	24	0																
																15*	13	17	17	-1	3*	12	16	-14	9																
																				0	26	26	26	0	4	21	18	16	-7												
																1*	12	8	8	-0	5	20	16	16	4																
																2	24	24	24	2	H=	6	K=	4	6*	13	6	6	-0												
																3	2	24	24	24	2	H=	6	K=	4	7*	13	14	-14	-2											
																4	12	7	-5	5	0	62	62	62	0	8*	13	7	6	3											
																5*	13	13	12	-4	1	66	68	67	-11	9*	13	8	8	-1											
																6*	13	3	1	-3	2	35	36	-33	-16	10*	13	6	6	2											
																7*	13	5	-5	-1	3	69	71	68	-22	11*	13	7	-2	-6											
																8*	13	6	2	-5	4*	11	5	2	-5	11*	13	7	-2	-6											
																9*	13	9	9	1	5	68	66	65	-10																
																10*	13	9	6	-6	6*	11	12	-6	-10																
																				7	59	58	58	-1																	
																				8	28	28	-27	8																	
																				9	36	37	37	5																	
																				10	19	18	16	9																	
																				11*	12	19	17	8																	
																				12*	12	13	-12	3																	
																				13*	13	10	-10	1																	
																				14*	13	6	3	5																	
																				15	21	16	-16	2																	
																				16*	13	1	1	-1																	
																				7	20	13	-13	0																	
																				8*	13	4	-3	3																	
																								H=	7	K=	4														
																												C*	10	2	-2	0									
																												1*	11	8	7	-4									
																												2*	11	20	-4	-19									
																												3	26	29	-28	5									
																												4*	11	17	2	-17									
																												5	23	19	19	-2									
																												6*	12	15	13	-7									
																												7	35	36	-35	9									
																												8*	12	6	5	-2									
																												9*	13	21	7	19									
																												10*	13	6	-1	6									
																												11*	12	5	-2	4									
																												12*	12	4	-1	4									
																												13*	13	7	-5	6									
																												14*	13	3	-2	-2									
																																H=	8	K=	4						
																																0	11	9	9	0					
																																1	26	26	-26	-2					
																																0	94	93	93	0					
																																2	23	25	-1	-25					

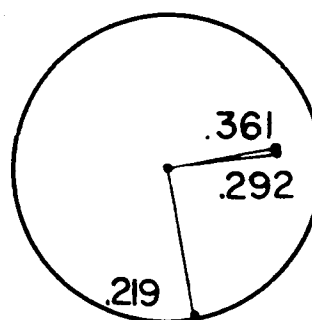
Figure 24 (Continued)

4	34	33	33	3	0	31	36	36	-0	0	18	19	19	0	4*	12	5	-1	-5	
6*	11	11	10	-6	1*	11	12	12	-2	1*	11	12	12	-2	5	17	14	14	3	
8	18	13	-13	2	2*	12	7	7	1	1	26	23	-23	-4	6*	12	5	4	-3	
10	30	36	35	7	3*	12	14	13	-5	2	17	16	-16	1	7*	12	9	-9	-0	
12*	13	7	-2	7	4	31	30	28	10	3	20	21	-18	-10	8*	13	2	2	-1	
14	19	21	21	1	5*	12	11	11	2	4	21	19	13	13	9*	13	9	7	5	
H= 6 K= 5					6	21	21	21	-4	5*	12	11	-11	-4	H= 9 K= 7					
0	39	37	37	0	7*	13	13	12	6	6	19	16	16	-3	0*	11	7	7	0	
1	43	42	41	-9	8*	13	8	8	-3	7*	12	3	2	2	1*	12	5	5	-2	
2	36	37	35	-11	9*	13	8	7	4	8*	13	2	2	-0	2*	12	10	-10	-1	
3*	11	7	7	-2	10	22	19	17	-8	9*	13	5	-3	4	3*	12	10	8	-5	
4	36	36	35	-9	H= 10 K= 5					10*	13	13	17	-5	4*	12	8	8	3	
5	49	52	49	-15	0*	12	5	5	0	11*	13	7	-6	4	5*	12	13	12	-5	
6	33	35	35	-5	1*	12	10	9	-2	H= 9 K= 6				0*	12	7	4	-6		
7*	12	21	-18	-10	2*	12	4	3	2	0*	11	9	9	-0	7*	13	10	10	-2	
8	19	26	26	0	3*	12	9	-1	9	1*	12	11	11	-3	H*	13	2	-2	1	
9	22	27	27	6	4*	12	4	2	3	2*	12	12	10	-6	H= 10 K= 7					
10*	13	15	14	6	5	21	17	16	4	3*	12	6	-0	6	0*	12	6	-6	-0	
11*	13	15	13	-5	6*	13	6	5	4	4	18	15	14	-3	1	24	10	-9	-3	
12*	13	7	6	3	7*	13	4	-4	-1	5	18	24	23	-2	2*	12	2	-2	-1	
13*	13	3	3	-1	8*	13	3	3	-0	6	18	18	18	1	3*	12	16	-16	3	
14*	13	4	4	-1	H= 11 K= 5					7*	13	7	-0	-7	4*	13	4	3	-3	
H= 7 K= 5					0*	12	10	10	-0	8*	13	12	12	-0	5*	13	3	-3	-1	
0	39	42	42	-0	1	22	16	-16	4	H= 10 K= 6				-5	H= 8 K= 8					
1	20	23	-22	-5	2*	13	5	-5	2	0*	12	3	3	-0	0	26	18	18	-0	
2*	11	9	-8	2	3	22	17	-16	6	1*	12	3	3	-0	2*	12	1	1	-0	
3	19	17	-11	-13	4*	13	9	5	8	2	19	14	-14	2	4	21	20	19	4	
4	26	25	24	3	5	22	14	-13	6	3*	12	7	7	-1	6*	12	14	14	-3	
5*	11	13	-1	-13	H= 6 K= 6					4*	12	7	-1	7	8*	13	10	8	6	
6	17	10	9	-3	0	24	31	31	-0	5*	13	9	9	0	H= 9 K= 8					
7*	12	2	-1	-2	2*	10	15	-13	-8	6*	13	5	-4	-3	0*	12	2	-2	0	
8*	12	14	-1	14	4	26	25	23	-8	7	19	7	7	0	1*	12	15	14	-5	
9*	13	9	-2	8	6	20	19	0	-19	H= 11 K= 6				0	2*	12	1	-1	-1	
10	31	24	24	0	8*	12	6	-5	-4	0*	12	9	-9	0	3*	12	7	7	-1	
11*	13	8	-3	7	10	22	30	27	-12	1*	13	1	1	-1	4*	12	2	1	-2	
12*	13	9	-9	-1	12*	13	14	-11	-8	2*	13	7	-6	4	5*	13	20	20	-4	
13*	13	4	-4	1	H= 7 K= 6					3*	13	9	-7	6						
H= 8 K= 5					0	30	29	-29	-0	H= 7 K= 7										
0	39	35	-35	0	1	17	15	-12	-8	0	19	24	-24	0						
1	26	25	24	-2	2	26	24	-24	-4	2	58	56	-56	-1						
2	24	26	-25	-6	3	37	33	-33	5	4	27	26	-20	17						
3*	11	12	2	12	4	17	20	-17	-9	6*	12	11	-11	-0						
4	17	21	-17	-12	5*	11	11	10	3	8*	12	17	-17	1						
5	40	39	38	8	6*	12	12	-12	-4	10*	13	1	-1	-0						
6	19	16	-16	0	7*	12	16	-16	-2	H= 8 K= 7										
7*	12	6	4	4	8*	12	7	-6	4	0*	12	5	-5	-0						
8*	13	13	-9	9	9*	12	11	10	-3	1*	11	12	-11	-3						
9	21	22	21	4	10*	13	7	-6	4	2*	11	6	-5	-4						
10*	13	11	-6	9	11*	13	9	-6	-7	3	19	20	-17	10						
11*	13	6	5	-4	12*	13	6	-6	1											
12	19	9	-7	5	H= 8 K= 6															
H= 9 K= 5																				

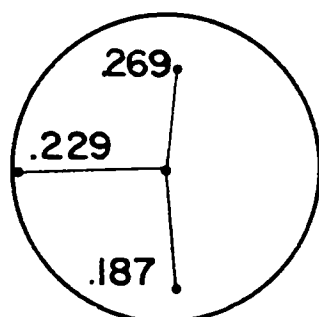
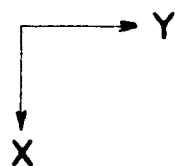
Figure 24 (Continued)



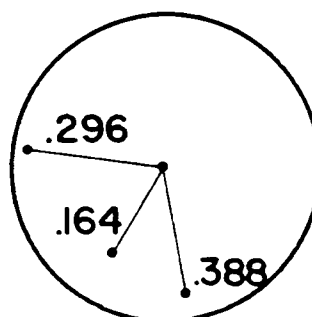
Br (0,0,Z)



Br (X,Y,Z)



Mg (X,Y,Z)



O (X,Y,Z)

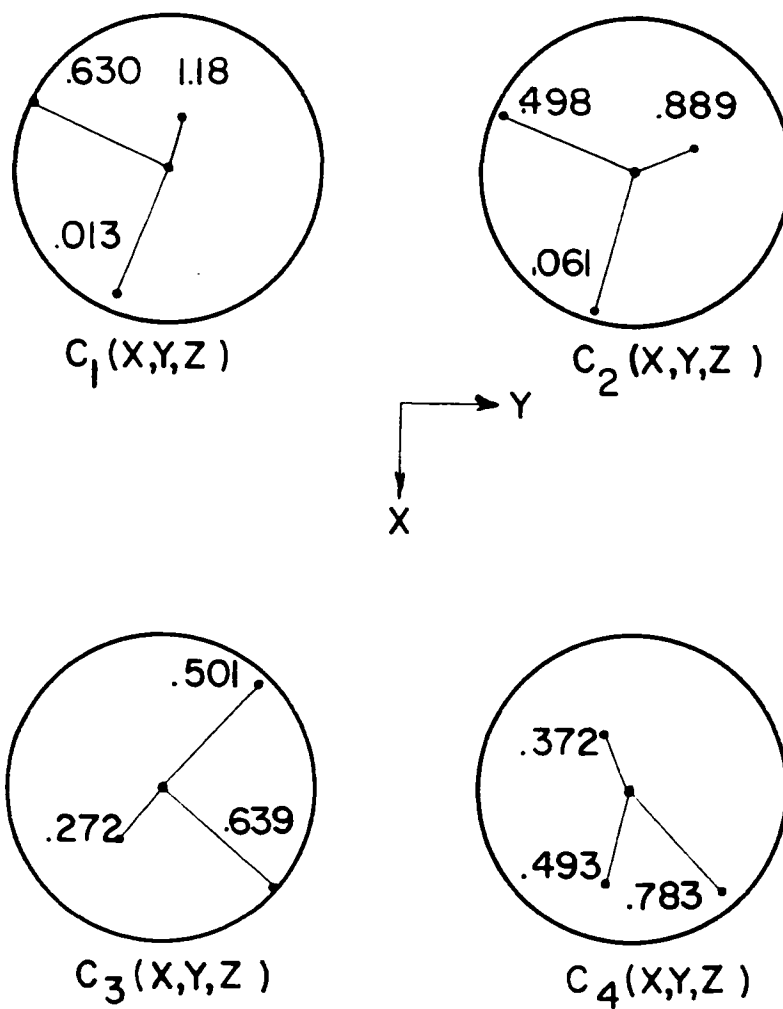


Figure 25 (Continued)

Table 19. Final positional parameters and standard errors obtained from least squares refinement for $\text{Mg}_4\text{Br}_6\text{O}\cdot 4(\text{C}_4\text{H}_{10}\text{O})$

Atom	x	y	z	$\sigma(x)$	$\sigma(y)$	$\sigma(z)$
Br ₁	.0000	.0000	.2065	.0000	.0000	.0002
Br ₂	.2930	.0586	-.0054	.0002	.0002	.0004
Mg	.1262	-.0821	.0722	.0007	.0007	.0005
O ₁	.2627	-.1701	.1501	.0018	.0016	.0012
C ₁	.157	.241	.373	.006	.008	.011
C ₂	.099	.273	.364	.003	.007	.007
C ₃	.277	.239	.286	.007	.006	.002
C ₄	.141	.431	.293	.006	.007	.004
O ₂	.0000	.0000	.0000	.0000	.0000	.0000

Table 20. Final thermal parameters and standard errors obtained from least squares refinement for $\text{Mg}_4\text{Br}_6\text{O}\cdot 4(\text{C}_4\text{H}_{10}\text{O})$

Atom	(a) Anisotropic temperature factors					
	B ₁₁	B ₂₂	B ₃₃	B ₁₂	B ₁₃	B ₂₃
Br ₁	.0138	.0163	.0039	.0039	.0000	.0000
Br ₂	.0088	.0180	.0091	-.0022	-.0009	.0026
Mg	.0086	.0091	.0048	-.0004	-.0022	.0001
O ₁	.0198	.0140	.0059	.0029	-.0064	.0015
C ₁	.0387	.0595	.1019	-.0187	-.0526	-.0136

Table 20 (Continued)

Atom	(a) Anisotropic temperature factors					
	B_{11}	B_{22}	B_{33}	B_{12}	B_{13}	B_{23}
C ₂	.0113	.0526	.0555	-.0037	-.0196	-.0241
C ₃	.0525	.0554	.0091	-.0165	-.0070	-.0049
C ₄	.0680	.0673	.0183	-.0251	.0165	-.0133
O ₂	.0088	.0088	.0025	.0000	.0000	.0000
	(b) Standard errors of anisotropic temperature factors					
Atom	$\sigma(B_{11})$	$\sigma(B_{22})$	$\sigma(B_{33})$	$\sigma(B_{12})$	$\sigma(B_{13})$	$\sigma(B_{23})$
Br ₁	.0008	.0008	.0001	.0007	.0000	.0000
Br ₂	.0003	.0004	.0002	.0002	.0004	.0004
Mg	.0009	.0009	.0003	.0007	.0006	.0006
O ₁	.0028	.0024	.0010	.0020	.0015	.0014
C ₁	.0110	.0142	.0185	.0105	.0135	.0120
C ₂	.0048	.0112	.0090	.0057	.0058	.0084
C ₃	.0220	.0216	.0037	.0214	.0074	.0079
C ₄	.0134	.0145	.0053	.0119	.0068	.0079
O ₂	.0015	.0015	.0010	.0000	.0000	.0000

Table 21. Bond angles and interatomic distances
 $\text{Mg}_4\text{Br}_6\text{O}\cdot 4(\text{C}_4\text{H}_{10}\text{O})$

(a) Bond angles		
Atoms defining bond angle ^a	Bond angle	Error
$\text{O}_2 - \text{Mg} - \text{Br}_2$	87.36	± 0.29
$\text{O}_2 - \text{Mg} - \text{Br}_2$ (III)	88.48	± 0.28
$\text{O}_2 - \text{Mg} - \text{Br}_1$	86.61	± 0.29
$\text{O}_2 - \text{Mg} - \text{O}_1$	179.80	$\pm .65$
$\text{Br}_1 - \text{Mg} - \text{Br}_2$	121.14	$\pm .30$
$\text{Br}_1 - \text{Mg} - \text{Br}_2$ (III)	117.53	$\pm .30$
$\text{Mg} - \text{Br}_1 - \text{Mg}$ (I)	75.93	$\pm .35$
$\text{Mg} - \text{Br}_2$ (III) - Mg (III)	75.33	$\pm .34$
$\text{Mg} - \text{O}_1 - \text{C}_1$	127.85	± 6.04
$\text{Mg} - \text{O}_1 - \text{C}_3$	118.85	± 2.90
$\text{Mg} - \text{O}_1 - \text{C}_2$	136.44	± 3.63
$\text{Mg} - \text{O}_1 - \text{C}_4$	114.82	± 2.40
(b) Interatomic distances		
Atoms defining interatomic distances	Interatomic _o distances Å	Error Å
$\text{Br}_1 - \text{Br}_2$	4.555	$\pm .005$
$\text{Br}_1 - \text{Br}_2$ (II)	4.438	$\pm .005$
$\text{Br}_2 - \text{Br}_2$ (II)	4.516	$\pm .003$

^aThe subscripted atoms correspond to the positions given in Table 19. The Roman numeral suffix denotes the subscripted atom has been operated on by the following symmetry operators: (I) $\bar{x} \bar{y} \bar{z}$; (II) $\bar{y} \bar{x} \bar{z}$; (III) $\bar{y} \bar{x} \bar{z}$.

Table 21 (Continued)

Atoms defining interatomic distances	(b) Interatomic distances Interatomic distances Å	Error Å
Br ₁ - Mg	2.613	± .009
Br ₂ - Mg	2.617	± .008
Br ₁ - Mg (II)	2.578	± .008
Br ₂ - O ₂	3.192	± .002
Br ₁ - O ₂	3.168	± .003
Br ₁ - O ₁	3.45	± .02
Br ₂ - O ₁	3.43	± .02
Br ₂ - O ₁ (II)	3.38	± .02
Mg - O ₁	2.11	± .02
Mg - O ₂	1.952	± .008
O ₁ - C ₁	1.33	± .09
O ₁ - C ₂	1.61	± .06
O ₁ - C ₃	1.44	± .05
O ₁ - C ₄	.73	± .08
C ₁ - C ₂	.72	± .09
C ₃ - C ₄	2.5	± .1

First, the symmetry of the ether oxygen, with respect to the bromine atoms, is for all practical purposes trigonal. There are three possible ways which are equally suitable to

pack an ether molecule against the bromine atoms. This is illustrated in Figure 26. Second, the Fourier maps indicated small peaks with about 1/3 the expected carbon peak heights in the regions close to the ether oxygen. Finally, the anisotropic thermal parameters and coordinate shifts of the ether carbons in the final model indicated the statistical electron density in the regions close to the ether oxygen was distributed over a large area.

To determine the optimum orientations of the ether molecule it is convenient to define a new coordinate system $\vec{b}_1, \vec{b}_2, \vec{b}_3$, in terms of the old coordinate system $\vec{a}_1, \vec{a}_2, \vec{a}_3$, where the \vec{a}_i 's are orthogonal unitary vectors coincident with the \vec{a} , \vec{b} , and \vec{c} unit cell vectors. \vec{b}_3 is defined to be in the same direction as the origin magnesium - ether oxygen vector. This vector also defines the pseudo three-fold axis of the bromine atom. \vec{b}_3 defines an angle α with \vec{a}_3 (the \vec{c} axis of the unit cell). The vector produced when \vec{b}_3 is projected on the plane defined by \vec{a}_1 and \vec{a}_2 defines an angle β with \vec{a}_1 (the \vec{a} axis of the unit cell). The relation between $\vec{b}_1, \vec{b}_2, \vec{b}_3$ and $\vec{a}_1, \vec{a}_2, \vec{a}_3$ is then given by the following

$$\begin{bmatrix} \vec{b}_1 \\ \vec{b}_2 \\ \vec{b}_3 \end{bmatrix} = \begin{bmatrix} \cos \alpha \cos \beta & -\cos \alpha \sin \beta & -\sin \alpha \\ \sin \beta & \cos \beta & 0 \\ \sin \alpha \cos \beta & -\sin \alpha \sin \beta & \cos \alpha \end{bmatrix} \begin{bmatrix} \vec{a}_1 \\ \vec{a}_2 \\ \vec{a}_3 \end{bmatrix}$$

$$\begin{array}{lll} \cos \alpha = .5682 & \sin \alpha = .8229 & \alpha = 55.38^\circ \\ \cos \beta = .8393 & \sin \beta = .5438 & \beta = 32.94^\circ \end{array}$$

This reduces to:

$$\begin{bmatrix} b_1 \\ b_2 \\ b_3 \end{bmatrix} = \begin{bmatrix} .4769 & - .3090 & - .8229 \\ .5438 & .8393 & 0 \\ .6907 & - .4775 & .5682 \end{bmatrix} \begin{bmatrix} a_1 \\ a_2 \\ a_3 \end{bmatrix}$$

Figure 26 represents a projection in the direction of $-\vec{b}_3$ of the bromine and magnesium atoms. Figure 27 shows the overlap of the methyl groups with the bromine atoms assuming the ether molecule is linear and the oxygen atom is trigonally bonded to the magnesium atom. This configuration gives a bromine - methyl carbon distance of 2.41 \AA if the C-O-C angle is trigonal and 2.54 \AA if the C-O-C angle is tetrahedral. The expected bromine-methyl Van der Waal's radius is 3.95 \AA so that this configuration is highly improbable. One can assume either that the ether groups are not planar and the methyl groups are rotated about the methylene-oxygen axis away from the bromine atoms or that the ether group is tetrahedrally coordinated to the magnesium atom. The first possibility, that the methyl groups are rotated, is explored first. Assuming an O_1-C distance of 1.45 \AA and an C-O₁-C bond angle of 108° (electron diffraction) the methylene

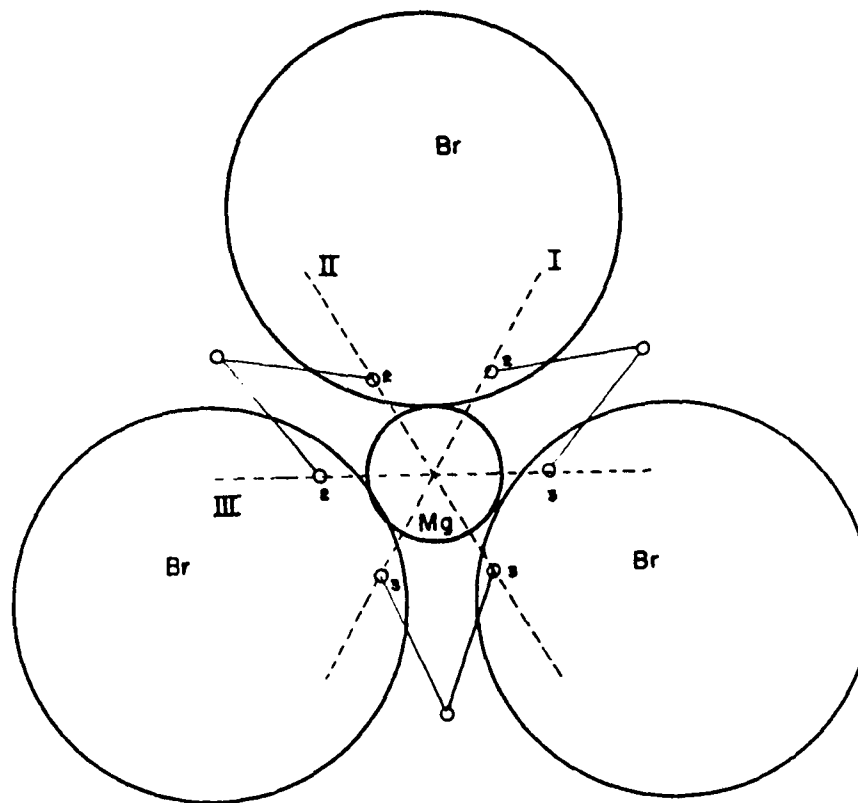


Figure 26. Projection along pseudo 3 fold axis through octahedral face of bromines in $Mg_4Br_6O \cdot 4(C_4H_{10}O)$. Dashed lines indicate planes for optimum packing of a linear ether molecule (excluding hydrogens). Trigonal coordinated to the magnesium atom.

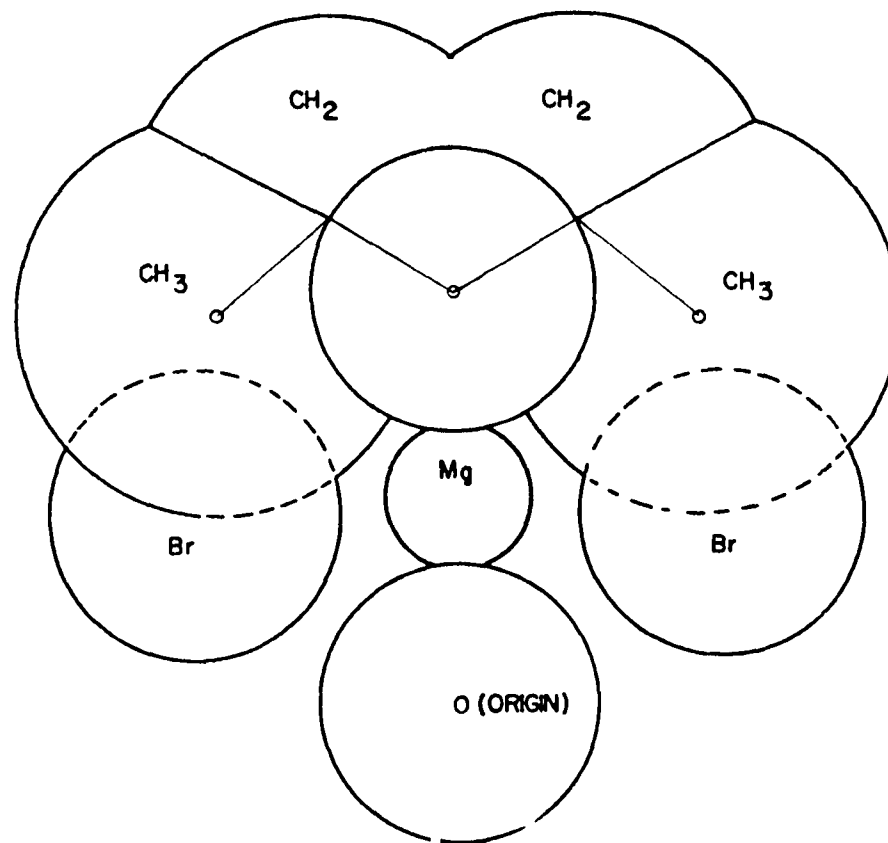


Figure 27. Overlap of bromine atoms and methyl groups for planar (excluding the hydrogen atoms) trigonally bonded ether molecule. This is a section through Plane II in Figure 26.

carbon-bromine distance for an ether molecule trigonally bonded to the magnesium atom is found to be 3.44 \AA . The distance of the methyl carbon from the bromine atom as a function of the rotation angle about the methylene carbon - ether oxygen axis is given by

$$d_{\text{CBr}}^2 = d_{\text{MBr}}^2 + d_{\text{MC}}^2 - 2d_{\text{MBr}}d_{\text{MC}} \cos (a + \phi_0)$$

where d_{MBr} is the bromine - methylene carbon distance and is equal to 3.44 \AA for C_2 of Plane I in Figure 26. d_{MC} is taken from electron diffraction values to be 1.50. a is the rotation angle measured from ϕ_0 and ϕ_0 is the angle Br-M-C for a linear ether molecule. d_{CBr} is 2.50 \AA for the linear molecule so ϕ_0 is given by

$$(2.50)^2 = (3.44)^2 + (1.50)^2 - 2(3.44)(1.50)\cos \phi_0$$

$$\cos \phi_0 = .7587, \quad \phi_0 = 40.65^\circ .$$

The amount of rotation required to give a Br-C Van der Waal's distance of 3.95° is given by

$$(3.95) = (3.44) + (1.50) - 2(3.44)(1.50)\cos (40.65 + a)$$

or $a = 57.78^\circ .$

If l_1 l_2 l_3 are the direction cosines of the oxygen-

methylene carbon vector in the coordinate system $(\vec{b}_1, \vec{b}_2, \vec{b}_3)$, then the relation between the coordinates of the rotated methyl group and the linear model methyl group is

$$\begin{bmatrix} x_n \\ y_n \\ z_n \end{bmatrix} = \begin{bmatrix} x_0 & y_0 & z_0 \end{bmatrix} \begin{bmatrix} \rho \end{bmatrix}$$

where*

$$\rho = \begin{bmatrix} \cos \alpha + t_1^2(1-\cos \alpha) & t_1 t_2(1-\cos \alpha) + t_3 \sin \alpha & t_3 t_1(1-\cos \alpha) - t_2 \sin \alpha \\ t_1 t_2(1-\cos \alpha) - t_3 \sin \alpha & \cos \alpha + t_2^2(1-\cos \alpha) & t_2 t_3(1-\cos \alpha) + t_1 \sin \alpha \\ t_3 t_1(1-\cos \alpha) + t_2 \sin \alpha & t_2 t_3(1-\cos \alpha) - t_1 \sin \alpha & \cos \alpha + t_3^2(1-\cos \alpha) \end{bmatrix}$$

Choosing the rotation axis to be the O_1-C_2 bond for the ether Plane I in Figure 26 gives

*See, for example, Volume II, page 63, of International Tables for X-ray Crystallography (56).

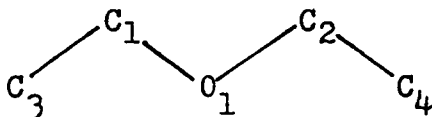
$$\rho = \begin{bmatrix} .767 & -.627 & .138 \\ .367 & .605 & .707 \\ -.525 & -.491 & .694 \end{bmatrix}$$

and new methyl coordinates of $(-1.18 \text{ \AA}, 2.02 \text{ \AA}, 4.60 \text{ \AA})$ in the coordinate system $(\vec{b}_1, \vec{b}_2, \vec{b}_3)$. It is interesting to note that these methyl positions are midway between the bromine atoms (Figure 26). The methyl coordinates for the remaining ether molecules are easily found by making use of their three fold symmetry about \vec{b}_3 and the methylene coordinates are similarly determined by using their six fold symmetry about \vec{b}_3 .

There is a strong reason for suspecting that the ether molecule does not in actuality use the orientation indicated by Plane III in Figure 26. This plane is perpendicular to the \vec{c} axis of the unit cell so that the long distance of the ether molecule is parallel to the plane defined by the \vec{a} and \vec{b} unit cell axes. Without the ether molecules the configuration of the atoms about the origin is spherical so that the closest packed structure would be a body centered cubic. Placing the ether molecules in the structure as described with the long axis of the ether molecule perpendicular to the \vec{c} axis would be expected to give if anything a lengthening of the \vec{a} and \vec{b} unit cell axes. The unit cell axes are, however, in the ratio 1:1:1.44 which indicates the closest packing of an ellipsoid of revolution which has its

long axis in the \vec{c} direction. This would only be true if the ether molecules were lying along Planes I and II in Figure 26.

The carbon positions for the disordered ether molecules are given in Table 22. Because it is unlikely that the Plane III configuration is used, these positions are indicated by an asterisk. The ether molecule is labeled



and the Roman numerals indicate the corresponding C_1-O-C_2 plane in Figure 26.

To compare the carbon positions in Table 22 with those in Table 20 it is necessary to transform the least squares carbon positions by the space group symmetry relation $1/2 - x, 1/2 + y, 1/2 - z$. Table 23 gives the transformed least squares carbon positions.

Table 24 gives some of the packing distances for the disordered ether model.

The possibility of a tetrahedrally coordinated ether oxygen is rejected for the following reasons. The methylene-carbon bromine distance for the trigonally coordinated ether oxygen is calculated to be $3.43 \overset{\circ}{\text{Å}}$. Pauling (65) assigns a Van der Waal's radius of $2.0 \overset{\circ}{\text{Å}}$ to the methylene group which gives a theoretical bromine methylene carbon distance of $3.95 \overset{\circ}{\text{Å}}$. Since the hydrogens are not pointing at the bromine

atom the $.52 \text{ \AA}$ discrepancy is probably permissible, however, if the oxygen atom is tetrahedrally coordinated, either the methylene carbons or the methyl carbons are of necessity rotated closer to the bromine atoms. In the linear ether model, the methyl groups are already too close to the bromine atom (2.50 \AA) and the methylene carbons are at the lower limit of their Van der Waal's radius from the bromine atoms (3.43 \AA) so that it is doubtful if a tetrahedral oxygen configuration could be utilized.

Table 22. Possible disordered ether carbon positions

Atom	Coordinates			Coordinates		
	in \vec{b}_1 \vec{b}_2 \vec{b}_3 (Å)			in \vec{a}_1 \vec{a}_2 \vec{a}_3 (Å)		
	x'	y'	z'	x	y	z
C ₁ (I)	1.01	- .59	4.91	3.55	-3.01	1.96
C ₃ (I), C ₃ (II)	2.34	0	4.60	4.30	-2.78	.68
C ₂ (I)	-1.01	.59	4.91	3.23	-1.39	3.62
C ₄ (I), C ₃ * (III)	-1.18	2.02	4.60	3.72	0	3.58
C ₁ (II)	1.01	.59	4.91	4.19	-2.01	1.96
C ₂ (II)	-1.01	- .59	4.91	3.07	-2.39	3.62
C ₄ (II), C ₄ * (III)	-1.18	-2.02	4.60	1.52	-3.40	3.58
C ₁ * (III)	.00	1.17	4.91	4.03	-1.22	2.79
C ₂ * (III)	.00	-1.17	4.91	2.75	-3.18	2.79

Coordinates
(\vec{a}_1 \vec{a}_2 \vec{a}_3)

in fractions of the unit cell

	x	y	z
C ₁ (I)	.332	-.282	.128
C ₃ (I), C ₃ (II)	.403	-.260	.044
C ₂ (I)	.302	-.130	.236
C ₄ (I), C ₃ (III)	.348	0	.233
C ₁ (II)	.392	-.188	.128
C ₂ (II)	.287	-.224	.236

Table 22 (Continued)

	Coordinates		
	$(\vec{a}_1 \vec{a}_2 \vec{a}_3)$		
	in fractions of the unit cell		
	x	y	z
C_4 (II), C_4 (III)	.142	-.318	.233
C_1 (III)	.377	-.114	.182
C_2 (III)	.257	-.298	.182

Table 23. Least squares carbon positions for comparison with Table 22

Atom	x	y	z
C_1	.343	-.259	.127
C_2	.401	-.227	.136
C_3	.223	-.261	.214
C_4	.359	-.069	.207

Table 24. Some packing distances^a for disordered ether model for $Mg_4Br_6O_4(C_4H_{10}O)$ as calculated by Busing's function and error, IBM 704 computer program (66)

Description of distance	Distance, Å ^o
$C_3(I)$ to $C_1(I)$ (intramolecular)	1.51
$C_2(I)$ to $O_1(I)$ (intramolecular)	1.45
$C_2(I)$ to $C_1(I)$ (intramolecular)	1.45
$C_4(I)$ to $C_2(I)$ (intramolecular)	1.45
$C_3(I)$ to $1/2, 1/2, 0$ ^b	2.85
$C_3(I)$ to $C_3(I)$ at $(\bar{4}, x, \bar{z})$	4.14
$C_2(I)$ to Br at $(x, y, 0)$	4.22
$C_2(I)$ to Br at $(0, 0, z)$	3.54
$C_4(I)$ to Br at $(0, 0, z)$ ^c	3.74

^aLabeling of carbon atoms is as described previously. The Roman numeral in parentheses denotes the C-O-C plane in Figure 26 with which the ether molecule is associated. The subscript refers to the ether carbons. 1 and 2 are methylene groups as illustrated in Figure 26 and 3 and 4 are the methyl carbons which go with 1 and 2 respectively. The intramolecular distances for ether molecules of Plane I are given for illustration.

^bThis distance together with the distances immediately following describes the packing of the proposed methyl ethers about $(1/2, 1/2, 0)$.

^cThe bromine-methyl Van der Waal radius of 3.95 Å^o was used to derive the methyl carbon positions, however, the assumption was made that the bromine atoms are planar and rotated by 3-fold symmetry which is not precisely true. Hence, as the true bromine positions were used for the function and error program there is a discrepancy between the calculated and Van der Waal's diameter. This difference is not great enough to affect the argument.

Table 24 (Continued)

Description of distance	Distance, Å ^o
O ₄ (I) to Br at (x, y, 0)	3.76
C ₁ (I) to Br at (0, 0, z)	4.81
C ₃ (I) to Br at (x, y, 0)	4.19
C ₃ (I) to Br at (x, y, 0)	3.68
C ₄ (II) to Br at (0, 0, z)	3.74
C ₄ (II) to Br at (x, y, 0)	3.61
C ₄ (I) to C ₁ (I) at (1/2 - x, 1/2 + y, 1/2 - z)	3.70
C ₁ (I) to Br at (1/2, 1/2, z)	3.88
C ₁ (I) to Br at (1/2 + x, 1/2 - y, 1/2)	3.88
C ₂ (II) to Br at (1/2 + x, 1/2 - y, 1/2)	3.88
C ₂ (III) to Br at (1/2 + x, 1/2 - y, 1/2 - z)	3.78

STRUCTURE OF $C_6H_5MgBr \cdot 2(C_4H_{10}O)$

Preparation, Purification and Properties

The Grignard reagent was prepared as described for $Mg_4Br_6O \cdot 4(C_4H_{10}O)$. The apparatus (Figure 3) was thoroughly dried by infrared light and vacuum pump. The magnesium metal was covered with ether and then 10 ml of a solution of 5 ml diethylether and 95 ml of bromobenzene added. The length of time required for the reaction to start depends on the amount of moisture present in the diethylether. Reagent grade canned anhydrous ether was used. Care must be taken not to add too much bromobenzene initially as the reaction is very exothermic and diethylether quickly volatilizes to build up excess pressure in the apparatus. It is advisable to have an ice bath available the first few times the reaction is carried out. A one molar solution was used for most preparation although more diethylether was added if needed. If an inadequate amount of ether is present or if the reaction gets so hot that the ether is evaporated out of the system, the reagent already prepared gives off a light grey smoke.

After the initial addition of the bromobenzene-ether solution, the remainder of the bromobenzene and ether is added over a period of about an hour. The solution is a dark reddish brown depending on the concentration. The

transfers to the purification apparatus were made after allowing the solution to stand for several hours or overnight.

After transferring to the right side of the apparatus in Figure 28 the solution is allowed to stand for several hours. It is then filtered into the left side and a dry ice-acetone bath placed under the left side. After several minutes the dry ice - acetone bath is removed and the solution is allowed to warm up. As the solution warms up spontaneous crystallization occurs, the crystals forming in groups which are spherical in shape. The melting point of the crystals was 15 - 20° C, however no crystallization was obtained by lowering the temperature of the solution just below the melting point for several hours. After crystallization was complete, the excess mother liquor was decanted back to the right side of the container in Figure 28. The crystals were allowed to partially melt and then the dry ice - acetone bath was placed again under the left side. This causes diethylether to thermally distill to the low temperature side. The solution is again allowed to warm up so that the crystals nearly melt and then crystallization is reinduced, only this time the temperature is lowered gradually so that the crystallization proceeds slowly. The mother liquor from the crystallization is decanted to the right side and pure ether redistilled back over. The crystals are then regrown and the process repeated until crystals of the desired purity are

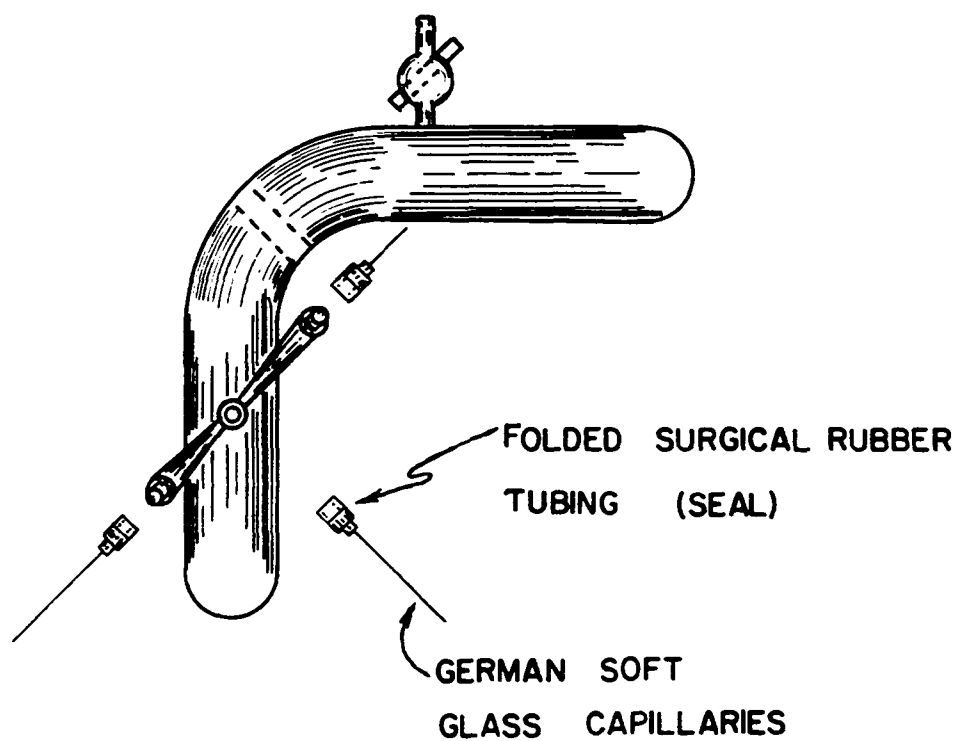


Figure 28. Apparatus for preparation of samples of $C_6H_5MgBr \cdot 2(C_4H_{10}O)$ and $(C_6H_5)_2Mg \cdot 2(C_4H_{10}O)$ for x-ray analysis

obtained. When care is taken in the preparation and purification, the crystals are white; however, more often they have a creamy or light reddish tan color which is a diluted version of the color of the phenylmagnesiumbromide solution.

The purification proceeds best when the apparatus is partially evacuated. This evacuation must not be too great or the crystals "explode" as ether of crystallization vaporizes. If too much of the ether is removed, the Grignard becomes a syrupy polymeric substance and crystallization is not possible. Once the material on the left side has been purified the container is kept sealed.

To get the purified reagent into the capillaries, the right side is frozen with a liquid nitrogen bath and the pure crystals on the left side allowed to melt. The crystalline melt is then poured into the capillary connections. A dewar filled with either liquid nitrogen or a dry ice - acetone mixture is placed beneath the capillaries to force the melt to run into the capillaries. Two considerations are important in filling the capillaries. First, only a small amount of melt can be used in the capillary in taking data. Ideally a single droplet which is 1 or 2 mm long in a .2 mm radius capillary is desired. Second, the liquid must be quickly drawn into the capillary and the capillary sealed to prevent thermal distillation of ether into the capillary, since it was found that crystallization in the capillary could

not be induced if the solution was diluted. The capillary is sealed using a liquid nitrogen dewar and a gas torch with a very fine tip, preferably a micro-burner attachment. It is then cut into lengths of about 1 cm and mounted on the x-ray camera.

Chemical analysis

The results of the chemical analysis of three samples of the crystalline melt are given in Table 25.

Table 25. Chemical analysis of $C_6H_5MgBr \cdot 2(C_4H_{10}O)$

Sample number	Run 1 % Br	Run 2 % Br	Avg. % Br	Run 1 % Mg	Run 2 % Mg	Avg. % Mg	Br/Mg
1	25.32	26.20	26.26	7.69	7.69	7.69	1.04
2	28.33	28.49	28.41	8.57	8.57	8.57	1.01
3	27.74	27.67	27.70	8.34	8.35	8.34	1.01

The calculated percentages of bromine and magnesium in $C_6H_5MgBr \cdot 2(C_4H_{10}O)$ are 26.6 and 7.33 respectively. In a qualitative chemical test the melt gave a positive result for Gilman and Schulze's test for a metal-carbon linkage (67).

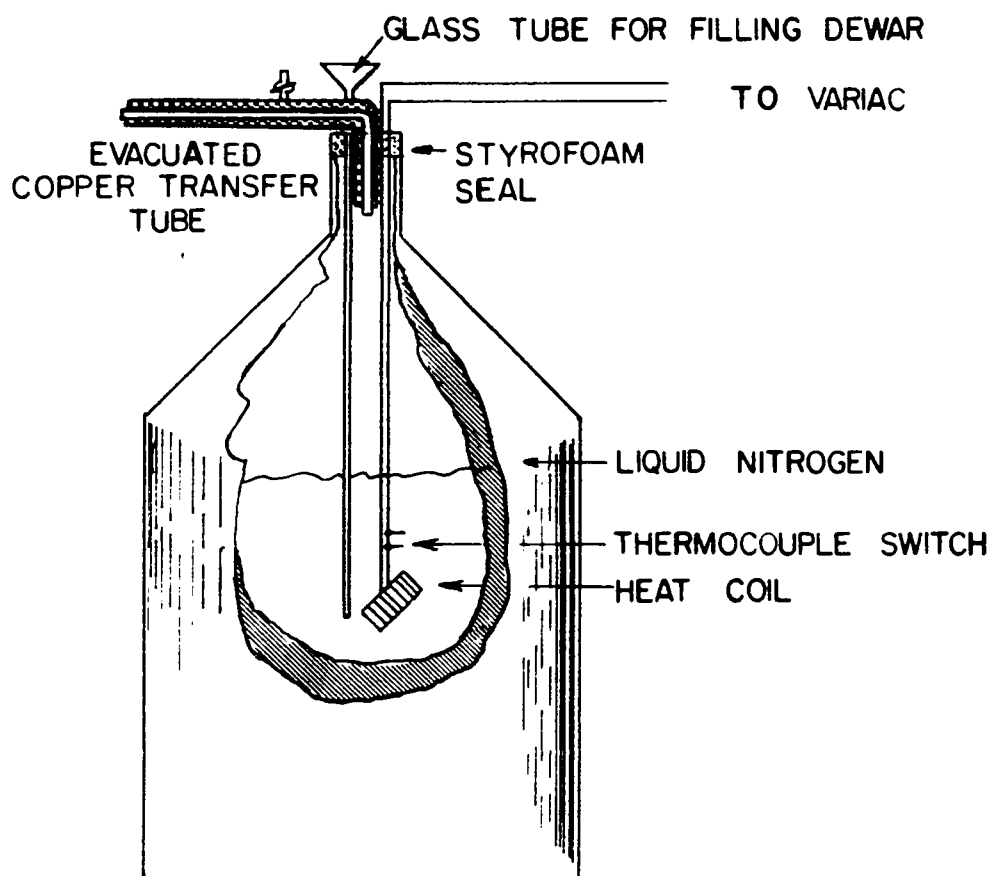
Growth of Single Crystals

Low temperature apparatus

The low temperature apparatus used to collect data for this compound is shown schematically in Figure 29. The thermocouple switch breaks the circuit to the heating element if the nitrogen level gets too low, thus preventing damage to the glass lined liquid nitrogen dewar. This apparatus was later modified as indicated in the experimental discussion for $(C_6H_5)_2Mg \cdot 2(C_4H_{10}O)$.

Experimental techniques for growing single crystals

Crystallization was induced in the capillary by first putting a small drop of liquid nitrogen on the capillary and then allowing the temperature to increase to near room temperature. A polarized light source was placed on one side of the capillary and an analyzer (polarizing) lens inserted in a microscope on the other side. The poly-crystalline mass first grown was allowed to melt fairly rapidly until a small portion of it remained, the temperature then being adjusted so that the melting of the remaining crystals was barely observable. Stroking the capillary with a hat pin which had previously been warmed to room temperature gave the desired temperature gradient. When the crystals have been regrown and melted so that only one nucleus is left, the last nucleus can be oriented by virtue of its movement due to the Brownian



LOW TEMPERATURE APPARATUS
USED FOR $C_6H_5MgBr \cdot 2 C_4H_{10}O$

Figure 29. Low temperature apparatus for
 $C_6H_5MgBr \cdot 2(C_4H_{10}O)$

motion of the liquid. Although this movement is quite rapid when the nucleus is small, it decreases as the crystal increases in size and with a little patience the desired orientation can be obtained. The needle crystals had a decided tendency to be dendritic in directions close to the needle axis and once grown also thermally distilled along this axis so that the preferred orientation was to have the needle axis of the crystal perpendicular to the direction of the greatest thermal gradient of the cold stream of nitrogen.

Space Group and Lattice Constants

The space group determination was made with a precession camera using a crystal grown with the needle axis perpendicular to the capillary walls.

The Laue symmetry was Pmmm and the crystal class was orthorhombic with

$$a = 12.25 \pm .04 \text{ \AA}$$

$$b = 12.81 \pm .04 \text{ \AA}$$

$$c = 11.02 \pm .04 \text{ \AA}$$

The precession axis, using this assignment of axes, was b. To confirm the space group $\{0kl\}$, $\{1kl\}$, $\{2kl\}$, $\{hk0\}$, $\{hkl\}$, and $\{hk2\}$ data were collected. The following extinctions were noted:

$$\begin{aligned} \{h00\} & \quad h = 2n + 1 \\ \{0k0\} & \quad k = 2n + 1 \\ \{00l\} & \quad l = 2n + 1 \end{aligned}$$

In addition $\{hk0\}$ with $k = 2n + 1$ and $\{h0l\}$ with $h + l = 2n + 1$ were weak or missing. The space group was uniquely determined to be $P2_12_12_1$. It can be shown that the two-fold screw axes in this space group do not intersect, so that the origin of the unit cell is conveniently chosen to be midway between the three pairs of non-intersecting screw axes. There are two ways to do this, with the alternative origins $1/4, 1/4, 1/4$ from each other. The convention used in the "International Tables for X-ray Crystallography", Vol. I (56) was followed. The space group diagram is given in Figure 30, and Table 26 gives the equivalent positions for $P2_12_12_1$.

Table 26. Equivalent positions $P2_12_12_1$

No. of positions and Wyckoff notation	Point symmetry	Equivalent positions
4a	1	$x, y, z;$ $1/2 - x, \bar{y}, 1/2 + z;$ $1/2 + x, 1/2 - y, \bar{z};$ $\bar{x}, 1/2 + y, 1/2 - z$

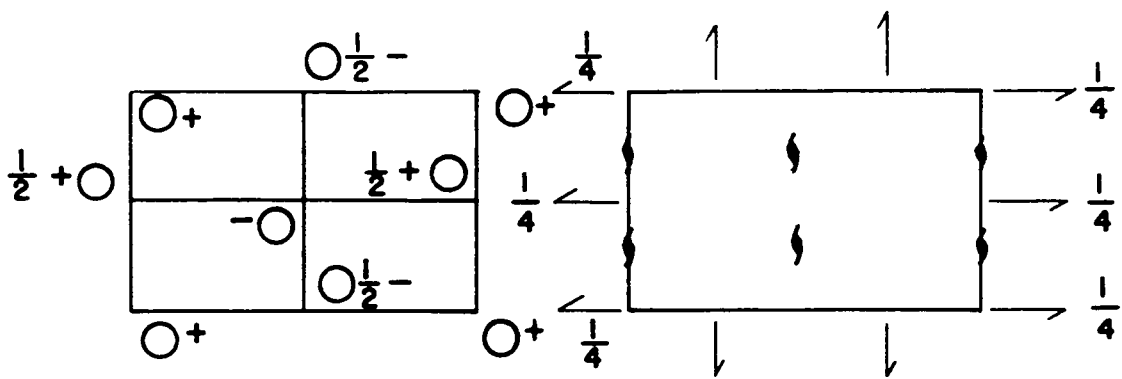


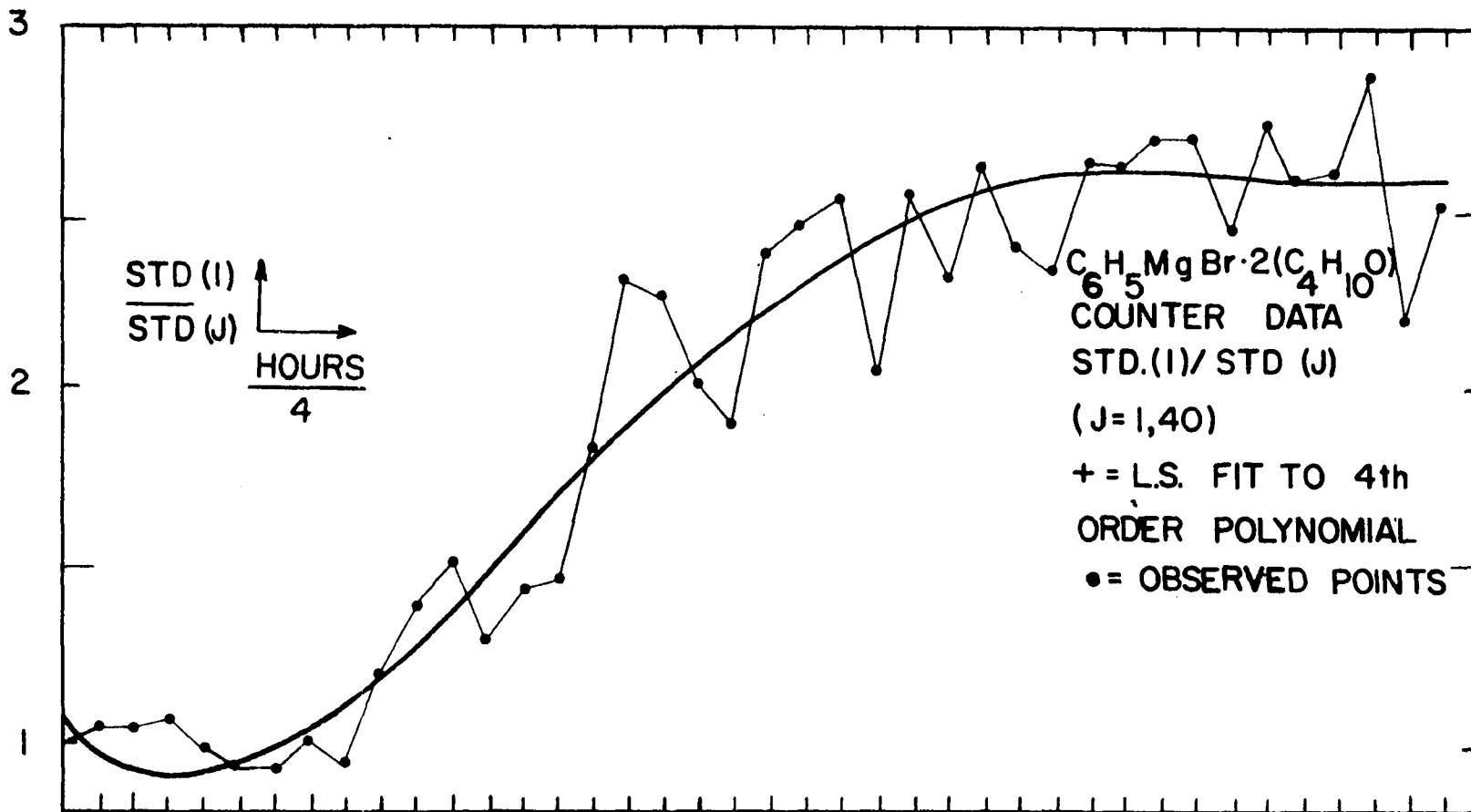
Figure 30. Space group diagrams of $P2_12_12_1$

Collection of Data

Two-dimensional $\{hk0\}$ data were collected with a precession camera using molybdenum $K\alpha$ radiation at about -50° C. Three-dimensional data were taken on the G.E. XRD5 diffractometer, also with molybdenum radiation, at the same temperature. All data were collected on a twenty-four hour basis because of difficulty in preserving the crystal.

The total number of three-dimensional intensities was 895. Since the planned method of attack for this structure was to solve two-dimensional projections, $\{h0l\}$, $\{0kl\}$, and $\{hk0\}$ data were taken before the rest of the three-dimensional data. The three-dimensional $\{hk0\}$, $\{hkl\}$, $\{hk2\}$, $\{0kl\}$, $\{lkl\}$, and $\{2kl\}$ counter data were qualitatively checked against film exposures of these reflections.

While taking the three-dimensional data, standard intensities were taken periodically and the experimental results are shown in Figure 31. The dotted curve is the least squares fit of the points to a fourth order polynomial. The variation of intensity with time was primarily due to the thermal distillation of the crystal in the capillary, although there was some evidence that the reagent was also sensitive to x-rays, and this may have made a contribution to the intensity drop. However, this latter effect was probably a minor one.



Correction of Data

The two-dimensional $\{hk0\}$ precession data were judged against internal standard reflections by two observers. The equivalent sets of reflections $\{hk0\}$, $\{\bar{h}k0\}$, $\{\bar{h} \bar{k} 0\}$ and $\{h\bar{k}0\}$ were averaged together.

The Lorentz polarization correction for the precession camera has been derived by Waser (68). The function is quite a cumbersome one and will not be repeated here. An IBM 704 program was written to make the Lorentz polarization correction for an arbitrary precession angle.

The three-dimensional data were corrected for the Lorentz polarization effect, the variation of intensity with time, and the anomalous scattering of the bromine atoms as previously described for $Mg_4Br_6O \cdot 4(C_4H_{10}O)$.

Solution of Structure

General procedure

The space group $P2_12_12_1$ is acentric so that the structure factors are complex and of the form

$$F(hkl) = |F(hkl)| \exp i \phi (hkl)$$

To avoid the necessity of determining the phase $\phi (hkl)$, it is better to do the preliminary structural work in two

dimensions since all of the pinacoidal projections for $P2_1^2 2_1^2 2_1$ are centrosymmetric. The procedure that was followed was to first calculate the three-dimensional Patterson and then to confirm the interpretation of this in the two-dimensional projections. The final least squares and Fourier analyses were then carried out in three dimensions. As a check, the two-dimensional precession data were used to calculate a two-dimensional Patterson. All features derived from the three-dimensional counter data were checked with the least squares and Fourier analysis of the two-dimensional $\{hk0\}$ precession data.

Initial considerations

The weighted reciprocal lattice gave two clues as to the nature of the packing in the crystal. For the $\{hk0\}$ reflections, it was observed that the $\{hk0\}$, k odd reflections were weak or missing and that the $\{h00\}$ reflections were relatively strong. In addition the $\{h0l\}$, $h + l$ odd reflections were generally weak. Both of the pseudo extinctions can be explained if a majority of the scattering in the crystal has near mirror symmetry at $x = 0$. It is not difficult to show that a mirror at $x = 0$ generates the additional symmetry elements $\bar{1}$, n , and b ; and that by interchanging the labels of the axis, the space group $Pnma$ is obtained. That $Pnma$ is not the true space group indicates only that there is not a true mirror at $x = 0$. Finally, the observation that the $\{h00\}$

reflections be strong requires that the following function has a large algebraic value:

$$F(h00) = \sum_{j=1}^N f_j A_j(h00)$$

$$F(h00) = 4 \sum_{j=1}^N f_j \cos 2\pi h x_j$$

Now if the $x_j = 1/8$, $F(200) = 0$; but $F(200)$ is quite large so that scattering must result from atoms at $x = 0, 1/4$, or $1/2$. This information was utilized in interpreting the Patterson vector map.

As mentioned previously the observed density is 1.17 gms/cm^3 which compares fairly well with the calculated density of 1.27 gms/cm^3 for four molecules of $\text{C}_6\text{H}_5\text{MgBr} \cdot 2(\text{C}_4\text{H}_{10}\text{O})$ per unit cell. The packing coefficient

$$k = \frac{ZV_0}{V}$$

is .64 for four molecules of phenylmagnesiumbromidedietherate using the values in Table 27 to determine V_0 . V_0 is the molecular volume, Z is the number of molecules in the unit cell, and V is the volume of the unit cell. This is in the range of the expected values for k for organic crystals as determined by Kitaigorodskii (55).

Table 27. Volume increments for determination of Kitaigorodskii's packing coefficient (55)

Group	Volume increment		Remark
Br	31.05	$r = 1.95 \text{ \AA}$	Ionic and Van der waal
Mg	11.48	$r = 1.4 \text{ \AA}$	Tetrahedral covalent
Mg	1.13	$r = .65 \text{ \AA}$	Ionic
O	5.09	$r = 1.36 \text{ \AA}$	Ionic and Van der waal
O	1.21	$r = .66 \text{ \AA}$	Covalent
Aromatic CH	13.9		Kitaigorodskii
CH ₂	16.6		Kitaigorodskii
CH ₃	22.1		Kitaigorodskii
Aromatic carbon	~8		Kitaigorodskii
OH	12.8		

Patterson calculations

The Patterson function for orthorhombic space groups is

$$P(UVW) = \frac{8}{V_c} \sum_h \sum_k \sum_l |F(hkl)|^2 \cos 2\pi hU \cos 2\pi kV \cos 2\pi lW$$

The analysis of vectors for the space group $P2_12_12_1$ is given in Table 28.

Table 28. Analysis of coordinates and vector distances for the space group $P2_12_12_1$

Operation	Axis	Location	Coordinates	General vectors $Pmmm:8(\alpha)$	Special vectors $Pmmm$
1	-	-	x, y, z	$x_1 - x_2, y_1 - y_2, z_1 - z_2$	4(a) 0, 0, 0
2_1	100	$0\frac{1}{2}0$	$\frac{1}{2} + x, \frac{1}{2} - y, \bar{z}$	$\frac{1}{2} + x_1 - x_2, \frac{1}{2} + y_1 + y_2, z_1 + z_2$	4(v) $\frac{1}{2}, \frac{1}{2} + 2y, 2z$
2_1	010	$00\frac{1}{2}$	$\bar{x}, \frac{1}{2} + y, \frac{1}{2} - z$	$x_1 + x_2, \frac{1}{2} + y_1 - y_2, \frac{1}{2} + z_1 + z_2$	4(x) $2x, \frac{1}{2}, \frac{1}{2} + 2z$
2_1	001	$\frac{1}{2}00$	$\frac{1}{2} - x, \bar{y}, \frac{1}{2} + z$	$\frac{1}{2} + x_1 + x_2, y_1 + y_2, \frac{1}{2} + z_1 - z_2$	4(z) $\frac{1}{2} + 2x, 2y, \frac{1}{2}$

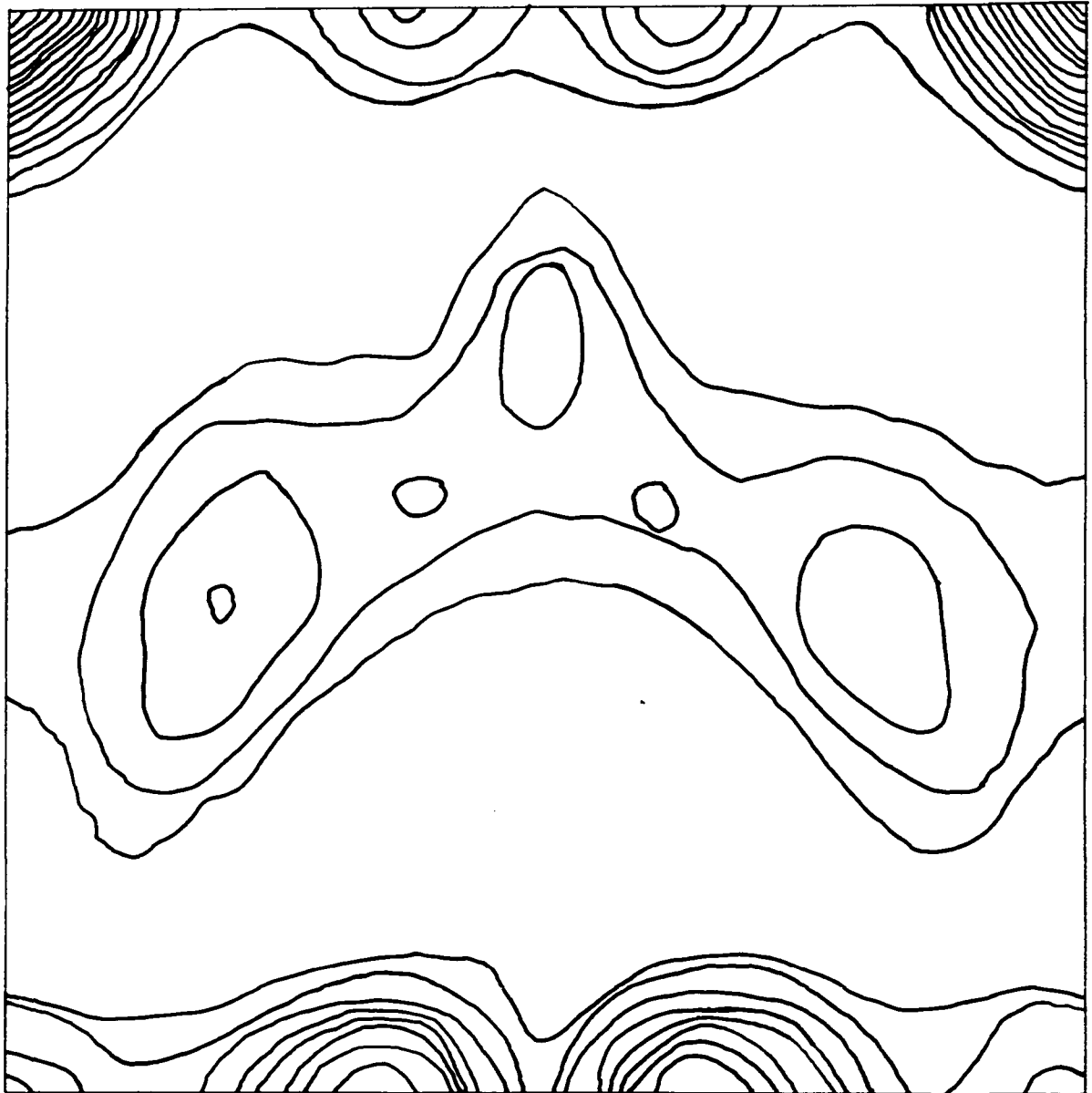
Table 29. Analysis of coordinates and vector distances for the plane group pgg

Operation	Axis	Location	Coordinates	General vectors $pmm:4(i)$	Special vectors pmm
1	-	-	x, y	$x_1 - x_2, y_1 - y_2$	4(a) 0, 0
g	-	$0\frac{1}{2}$	$\frac{1}{2} + x, \frac{1}{2} - y$	$\frac{1}{2} + x_1 - x_2, \frac{1}{2} + y_1 + y_2$	2(h) $\frac{1}{2}, \frac{1}{2} + 2y$
g	-	$\frac{1}{2}0$	$\frac{1}{2} - x, \frac{1}{2} + y$	$\frac{1}{2} + x_1 + x_2, \frac{1}{2} + y_1 - y_2$	2(f) $\frac{1}{2} + 2x, \frac{1}{2}$
2	-	00	\bar{x}, \bar{y}	$x_1 + x_2, y_1 + y_2$	4(i) $2x, 2y$

$P2_12_12_1$ projects along all three of its axes into the centrosymmetric plane group, pgg. The analysis of the vector distances for this plane group is given in Table 29.

The $\{hk0\}$ Patterson is shown in Figure 32. The large peaks at $U = 1/2$ are what one would expect for a bromine-bromine interaction with a multiplicity of two. The pseudo mirror at $V = 1/4$ results from the pseudo b glide noted previously. There will be equivalent bromine-bromine peaks at $1/2, V$ and $1/2, 1/2 - V$ if $2x' = 1/2$ so that $x' = \pm 1/4$, the prime being used to indicate plane group coordinates. If this is the case the plane group vector $1/2 + 2x', 1/2$ degenerates into $0, 1/2$ and one expects this bromine-bromine peak to have a multiplicity of four as observed. The x' and y' coordinates of the bromine are thus found to be $x' = \pm .25$, $y' = .09$ or $.16$. The magnesium-bromine vector is found by drawing a circle of radius 2.65 Angstroms about the origin. The magnesium atom, if coordinated to the bromine, must lie inside this circle. The only peaks which satisfy this criterion are the origin peak and the peak at $U = 0, V = .19$. The latter peak is about the size expected for the magnesium-bromine interaction and is $2.35 \overset{0}{\text{Å}}$ from the origin. Since it lies at $U = 0$, the magnesium atom must have the same x' coordinates as does the bromine atom, that is $x' = \pm .25$. All of the bromine-magnesium vectors lie at $U = 0$ or $U = 1/2$ and it is possible to determine the y' coordinate of the

Figure 32. (001) Patterson projection for precession data for
 $C_6H_5MgBr \cdot 2(C_2H_{10}O)$. Coordinates are $x \leftarrow y$.
1/2 x 1/2 of the unit cell is shown.



magnesium atom similar to the manner in which the bromine y' was found. It is also possible to assign oxygen x' and y' coordinates from this Patterson, however it was decided at this stage to compare the precession $\{hk0\}$ data results with the three-dimensional Patterson obtained from counter data.

The relationship between plane and space group coordinates is given in Table 30. In particular a plane group coordinate of $x' = \pm 1/4$ for the $\{hk0\}$ projection corresponds to a space group coordinate of $x = 0$ or $1/2$.

Table 30. Relationship between space group coordinates of $P2_12_12_1$ and the coordinates of the projections of $P2_12_12_1$ on (100), (010), and (001), using projections of the 2-fold screw axes as origins

xyz from $x' y'$	$x = x' + 1/4$
	$y = y'$
xyz from $y'' z''$	$y = y'' + 1/4$
	$z = z''$
xyz from $x''' z'''$	$z = z''' + 1/4$
	$x = x'''$

The level, $U = 0$, of the three-dimensional Patterson is shown in Figure 33, and $U = 1/2$ is given in Figure 34. The peak heights and locations confirm the bromine positions found from the two-dimensional Patterson. Furthermore the

Figure 33. Three-dimensional Patterson section, $u = 0$, for $C_6H_5MgBr \cdot 2(C_4H_{10}O)$

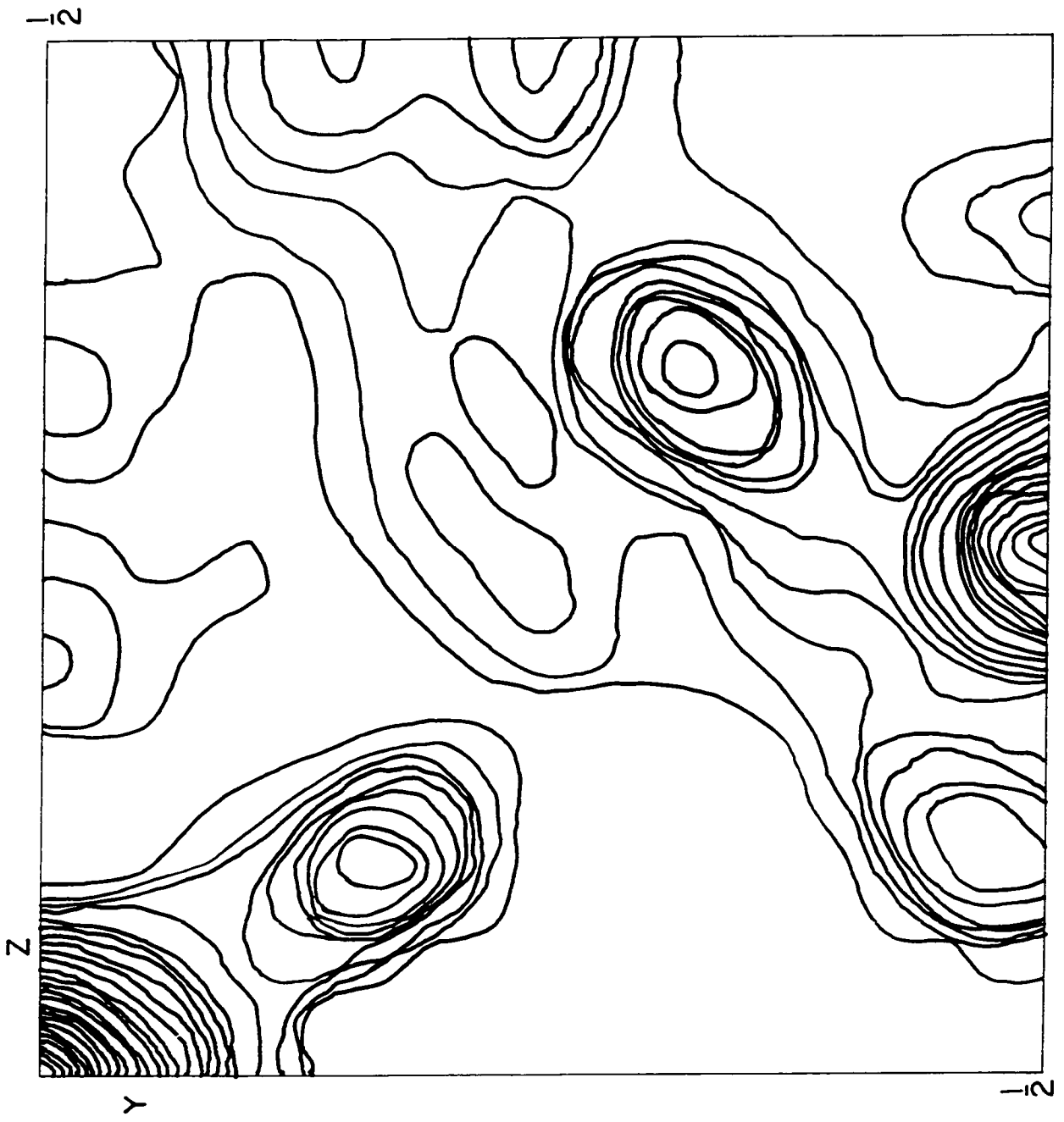
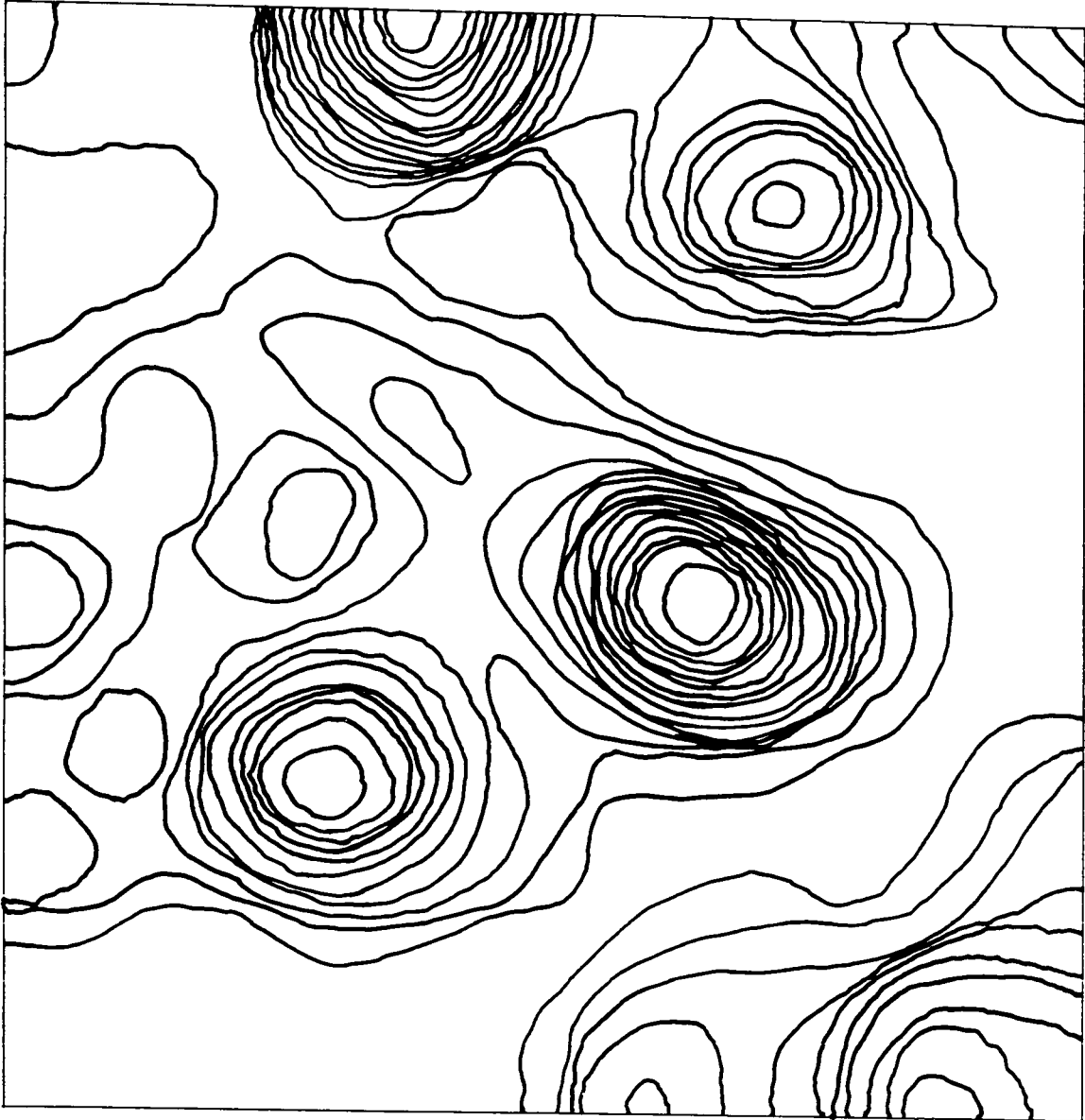


Figure 34. Three-dimensional Patterson section, $U = 1/2$, for $C_6H_5MgBr \cdot 2(C_4H_{10}O)$.
Coordinates are $\begin{matrix} z \\ y \downarrow \rightarrow \end{matrix}$.



bromine-magnesium vector is quite clear. The second largest peak at $U = 0$, $V = 1/2$, W can be explained as the overlap of the intermolecular phenyl carbon-carbon interactions if the phenyl groups are assumed to be nearly planar and lying in the same plane as the bromine and magnesium atoms at an angle of 109° to the bromine-magnesium vector. Oxygen coordinates which fit the three-dimensional Patterson were at approximately xyz and \bar{xyz} , and completed a tetrahedral arrangement about the magnesium atom. The three-dimensional Patterson was used primarily as a guide from this point, and the solution of the structure was continued by Fourier and least squares analysis.

Two-dimensional Fourier and least squares analysis

Initial two-dimensional analysis was carried out almost exclusively by the use of Fourier methods. The plane group pgg has the structure factors and electron density equations given in Table 31.

The projection of the electron density onto the (001) plane using structure factor signs for a bromine atom at $x' = 1/4$, $y' = 13/80$ is given in Figure 35. The magnesium and oxygen atoms show up in the positions predicted by the Patterson maps. The phenyl groups lie along the plane $x' = 1/4$. The bromine-magnesium distance in this projection is roughly 2.20 \AA so that the bromine-magnesium bond makes an angle of about $15^\circ - 20^\circ$ with the (001) plane.

The electron density projection onto the (010) plane

Table 31. Electron density and structure factor equations for plane group pgg

Condition	Equation
(a) Structure factors $F(hk) = A(hk)$	
$h + k = 2n$	$A = 4 \cos 2\pi hx \cos 2\pi ky$
$h + k = 2n + 1$	$A = -4 \sin 2\pi hx \sin 2\pi ky$

General structure factor equation

$$A = 4 \cos 2\pi(hx + \frac{h+k}{4}) \cos 2\pi(ky - \frac{h+k}{4})$$

(b) Electron density expression for pgg

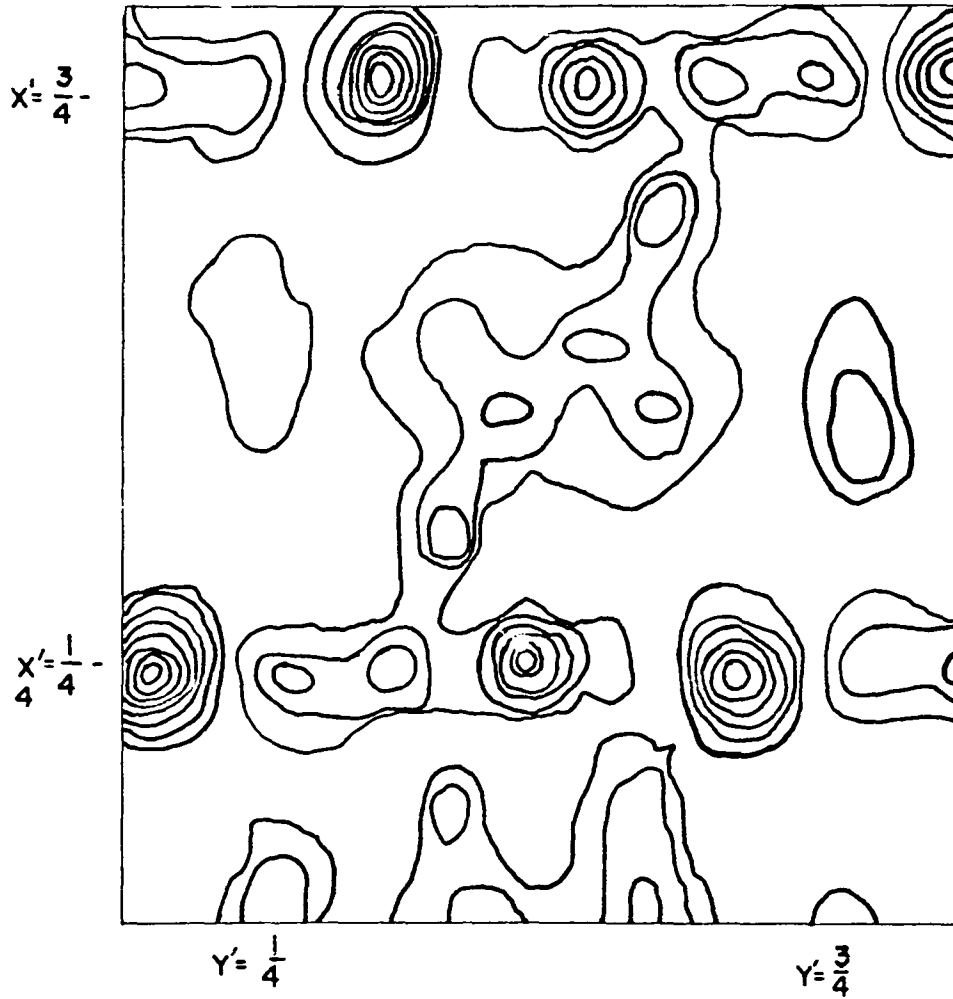
$$\rho(xy) = \frac{4}{A_c} \left\{ \sum_{\substack{h \\ h+k=2n}}^{\infty} \sum_{\substack{l \\ l+k=2n}}^{\infty} A(hk) \cos 2\pi hx \cos 2\pi ky \right.$$

$$- \sum_{\substack{h \\ h+k=2n+1}}^{\infty} \sum_{\substack{l \\ l+k=2n+1}}^{\infty} A(hk) \sin 2\pi hx \sin 2\pi ky \left. \right\}$$

$$+ \frac{2}{A_c} \left\{ \sum_{\substack{h=2n \\ h}}^{\infty} A(h0) \cos 2\pi hx + \sum_{\substack{k=2n \\ k}}^{\infty} A(0k) \cos 2\pi ky \right\}$$

$$+ \frac{1}{A_c} A(00)$$

Figure 35. (001) electron density projection for
 $C_6H_5MgBr \cdot 2(C_4H_{10}O)$



for the same model is given in Figure 36. Here the phenyl groups which are projected on edge along the plane $x = 0$ are clearly visible. The clarity is due to the fact that the two phenyl groups which lie along $x = 0$ overlap. The two overlapping positions in the space group coordinates are x, y, z and $\bar{x}, 1/2 + y, 1/2 - z$ so that these phenyl groups are $b/2$ apart. This Fourier shows that the projected magnesium-carbon distance is approximately $2.0 \overset{\circ}{\text{A}}$ so that the Mg-C bond must lie very nearly at right angles to the normal to the (010) plane. The oxygen atoms are also clearly apparent in this projection at $\pm x'$ from the bromine atom. The ether carbon positions are not definitely established but their outline is suggested. The relation between the x' and z' of the plane group and the x, z of the space group has been given in Table 30.

The electron density projected onto (100) is shown in Figure 37. This calculation was also carried out using the structure factor signs determined by the bromine atom. In this projection the magnesium atoms overlap since they have approximate space group coordinates $x, + 1/4, 0$ and $1/2 + x, + 1/4, 0$. In the plane group system these peaks show up at the origin of the projection because of the relation $y = y'' + 1/4$ given in Table 30. The oxygen atoms for a given molecule also overlap in this projection since they have approximately the same y and z coordinates and only differ in

Figure 36. (010) electron density projection for
 $\text{C}_6\text{H}_5\text{MgBr} \cdot 2(\text{C}_4\text{H}_{10}\text{O})$

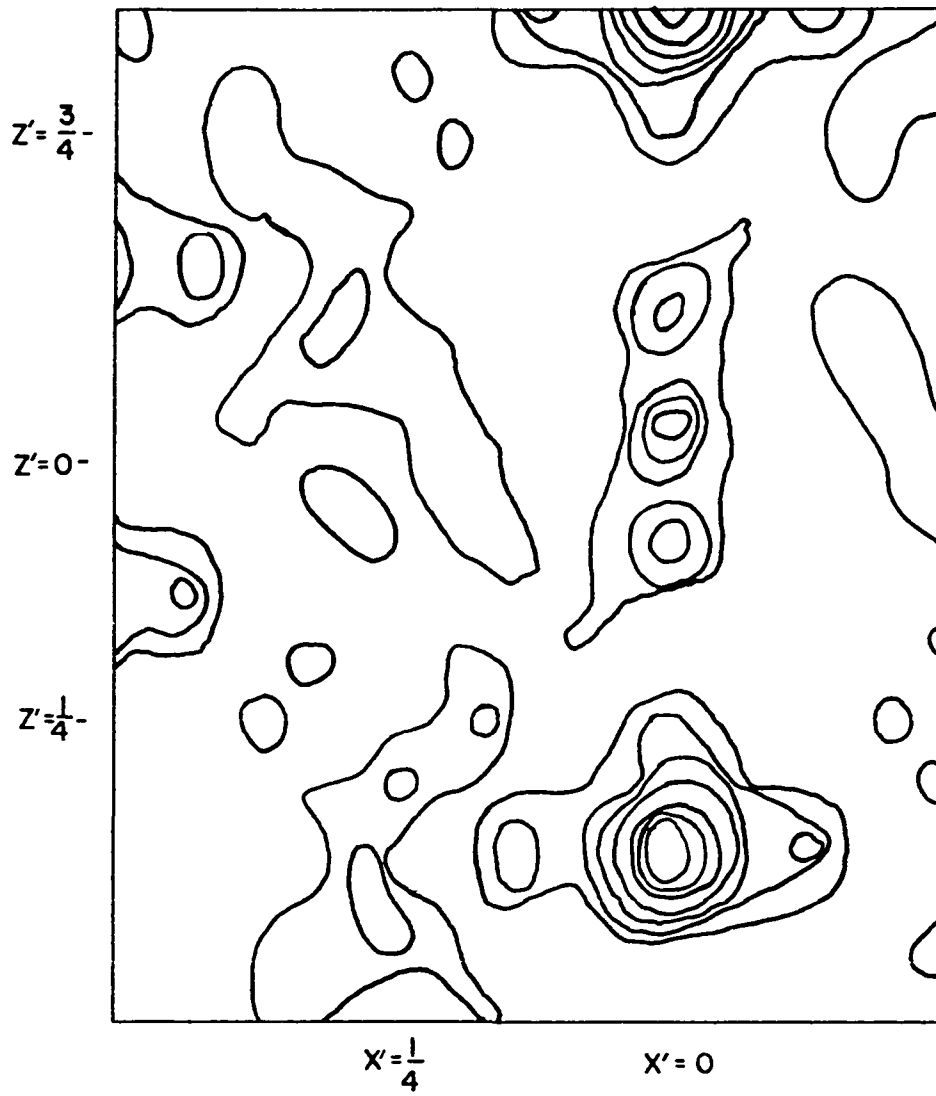
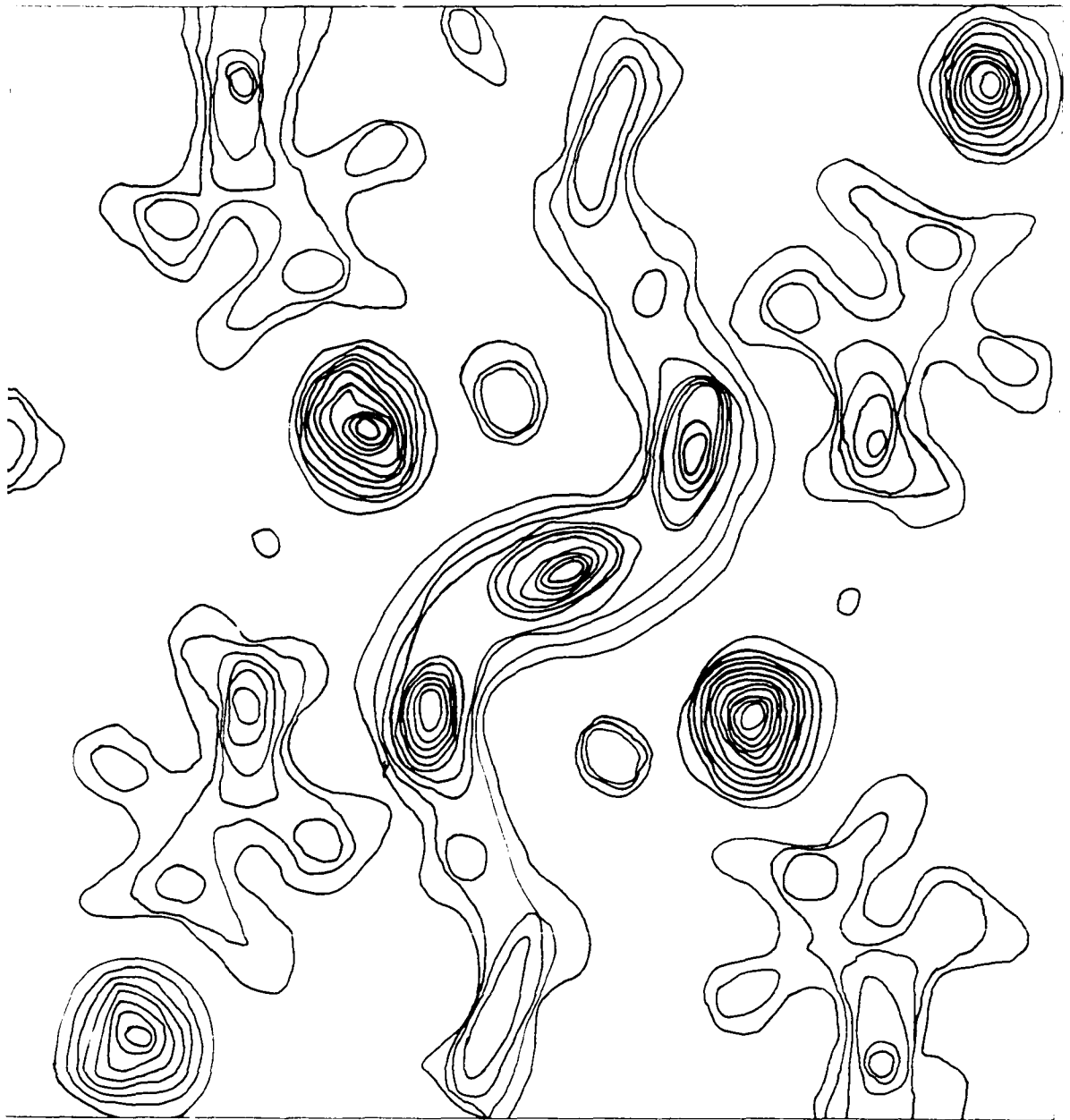


Figure 37. (100) electron density projection for $C_6H_5MgBr \cdot 2(C_4H_{10}O)$.
Coordinates are $y \uparrow$
 $z \rightarrow$.



that one is at $+x$ and the other is at $-x$. The phenyl carbons do not stand out as well as might be desired in this projection with the exception of the small peak near the origin which is correctly positioned to correspond to the carbon of the carbon-magnesium bond. Two of the remaining six carbons are probably overlapped by the bromine and the ether carbon atoms respectively. The other four phenyl carbon peaks are present but distorted.

The least squares analysis of the three projections was complicated by the overlap of atoms. The bromine atom and the two oxygen atoms in the (001) projection, the ether oxygens and some of the ether carbons in the (010) projection, and the bromine atom and four of the phenyl carbons in the (100) projection did not overlap. The number of data available for the (010) and (001) projections were limited because of the pseudo mirror symmetry in the (100) plane which caused extinctions in the $\{h0l\}$ and $\{hk0\}$ data. The final agreement factors obtained for the three zones were: $\{hk0\}$ precession data, 21.6%; $\{h0l\}$ counter data, 15.8%; $\{0kl\}$ counter data, 17.1%. The coordinates obtained from these two-dimensional refinements were then used for the three-dimensional least squares and Fourier analysis. The positions used at the start of the refinement are given in Table 32. The phenyl carbon positions were assigned with the constraint that they form a benzene ring.

Table 32. Parameters obtained from two-dimensional analysis for $C_6H_5MgBr \cdot 2(C_4H_{10}O)$ and used for input parameters for three-dimensional least squares

Atom	x	y	z
Br	0	.095	-.114
Mg	0	.274	-.0246
O ₁	-.136	.354	-.096
O ₂	.136	.354	-.096
ØC ₁	0	.29	.15
ØC ₂	0	.20	.22
ØC ₃	0	.20	.37
ØC ₄	0	.30	.43
ØC ₅	0	.36	.36
ØC ₆	0	.37	.22

Three-dimensional Fourier and least squares analysis

The expression used to compute the electron density and structure factors for $P2_12_12_1$ are given in Table 33. The space group diagram is shown in Figure 30. The complete expansion of the electron density is not given; however, it can easily be obtained by the substitutions

$$A'(hkl) = \frac{1}{2^n} A(hkl)$$

$$B'(hkl) = \frac{1}{2^n} B(hkl)$$

Table 33. Electron density and structure factor equations for $P2_1^2 2_1^2 2_1$

(a) Structure factors $F = A + iB$	
Condition	Equations
$h + k = 2n$	$A = 4 \cos 2\pi hx \cos 2\pi ky \cos 2\pi lz$
$k + l = 2n$	$B = -4 \sin 2\pi hx \sin 2\pi ky \sin 2\pi lz$
$h + k = 2n$	$A = -4 \cos 2\pi hx \sin 2\pi ky \sin 2\pi lz$
$k + l = 2n + 1$	$B = 4 \sin 2\pi hx \cos 2\pi ky \cos 2\pi lz$
$h + k = 2n + 1$	$A = -4 \sin 2\pi hx \cos 2\pi ky \sin 2\pi lz$
$k + l = 2n$	$B = 4 \cos 2\pi hx \sin 2\pi ky \cos 2\pi lz$
$h + k = 2n + 1$	$A = -4 \sin 2\pi hx \sin 2\pi ky \cos 2\pi lz$
$k + l = 2n + 1$	$B = 4 \cos 2\pi hx \cos 2\pi ky \sin 2\pi lz$

General equations for structure factor

$$A = 4 \cos 2\pi \left(hx - \frac{h-k}{4} \right) \cos 2\pi \left(ky - \frac{k-l}{4} \right) \cos 2\pi \left(lz - \frac{l-h}{4} \right)$$

$$B = -4 \sin 2\pi \left(hx - \frac{h-k}{4} \right) \sin 2\pi \left(ky - \frac{k-l}{4} \right) \sin 2\pi \left(lz - \frac{l-h}{4} \right)$$

(b) Electron density expression for $P2_1^2 2_1^2 2_1$

$$\rho(xyz) = \frac{8}{V_c} \sum_{\substack{k+l=2n \\ h+k=2n \\ 0 \ 0 \ 0}}^{\infty \ \infty \ \infty} [A'(hkl) \cos 2\pi hx \cos 2\pi ky \cos 2\pi lz]$$

Table 33 (Continued)

$$- B'(hkl) \sin 2\pi hx \sin 2\pi ky \sin 2\pi lz]$$

$$k+l=2n+1$$

$$h+k=2n$$

$$- \sum_{\substack{\infty \\ 0}} \sum_{\substack{\infty \\ 0}} \sum_{\substack{\infty \\ 0}} [A'(hkl) \cos 2\pi hx \sin 2\pi ky \sin 2\pi lz$$

$$- B'(hkl) \sin 2\pi hx \cos 2\pi ky \cos 2\pi lz]$$

$$k+l=2n$$

$$h+k=2n+1$$

$$- \sum_{\substack{\infty \\ 0}} \sum_{\substack{\infty \\ 0}} \sum_{\substack{\infty \\ 0}} [A'(hkl) \sin 2\pi hx \cos 2\pi ky \sin 2\pi lz$$

$$- B'(hkl) \cos 2\pi hx \sin 2\pi ky \cos 2\pi lz]$$

$$- \sum_{\substack{\infty \\ 0}} \sum_{\substack{\infty \\ 0}} \sum_{\substack{\infty \\ 0}} [A'(hkl) \sin 2\pi hx \sin 2\pi ky \cos 2\pi lz$$

$$- B'(hkl) \cos 2\pi hx \cos 2\pi ky \sin 2\pi lz}]$$

where n is the number of zero indices. The summations are then carried out from 1 to ∞ for three, two, and one dimensions.

The configuration of the molecule about the (100) plane cannot be exactly that given by the coordinates in Table 32, since if it were, the space group would be $Pnma$ rather than $P2_12_12_1$ as discussed earlier. There are six distinct

possibilities: (a) the phenyl groups are rotated about the carbon-magnesium axis off the plane; (b) the ether groups are asymmetric with respect to a mirror at (100); (c) the entire molecule is tilted off the (100) plane; (d), (e), and (f) any combinations of (a), (b), and (c). Least squares was used to try to fit the molecule on the plane with various combinations of (a) and (b), however the best agreement factor obtained was $R = 31\%$ and it was apparent that the ethyl and phenyl groups did not have sufficient freedom to give a large enough asymmetric contribution to account for discrepancies between the observed and calculated structure factors. The term "asymmetric" is used to refer to the lack of mirror symmetry at $x = 0$. The assumption was then made that the plane defined by the bromine, magnesium, and phenyl carbon 1* atoms was tilted away from the $x = 0$ plane and that the phenyl group was in the same plane as the bromine-magnesium-phenyl carbon 1 atoms. The structural problem was therefore reduced to finding the nature of the tilt of the bromine-magnesium-phenyl plane and the orientation of the diethylether molecule. The tilt of the plane is the result of the intermolecular interactions which arise when the molecules are packed together in the unit cell. The orienta-

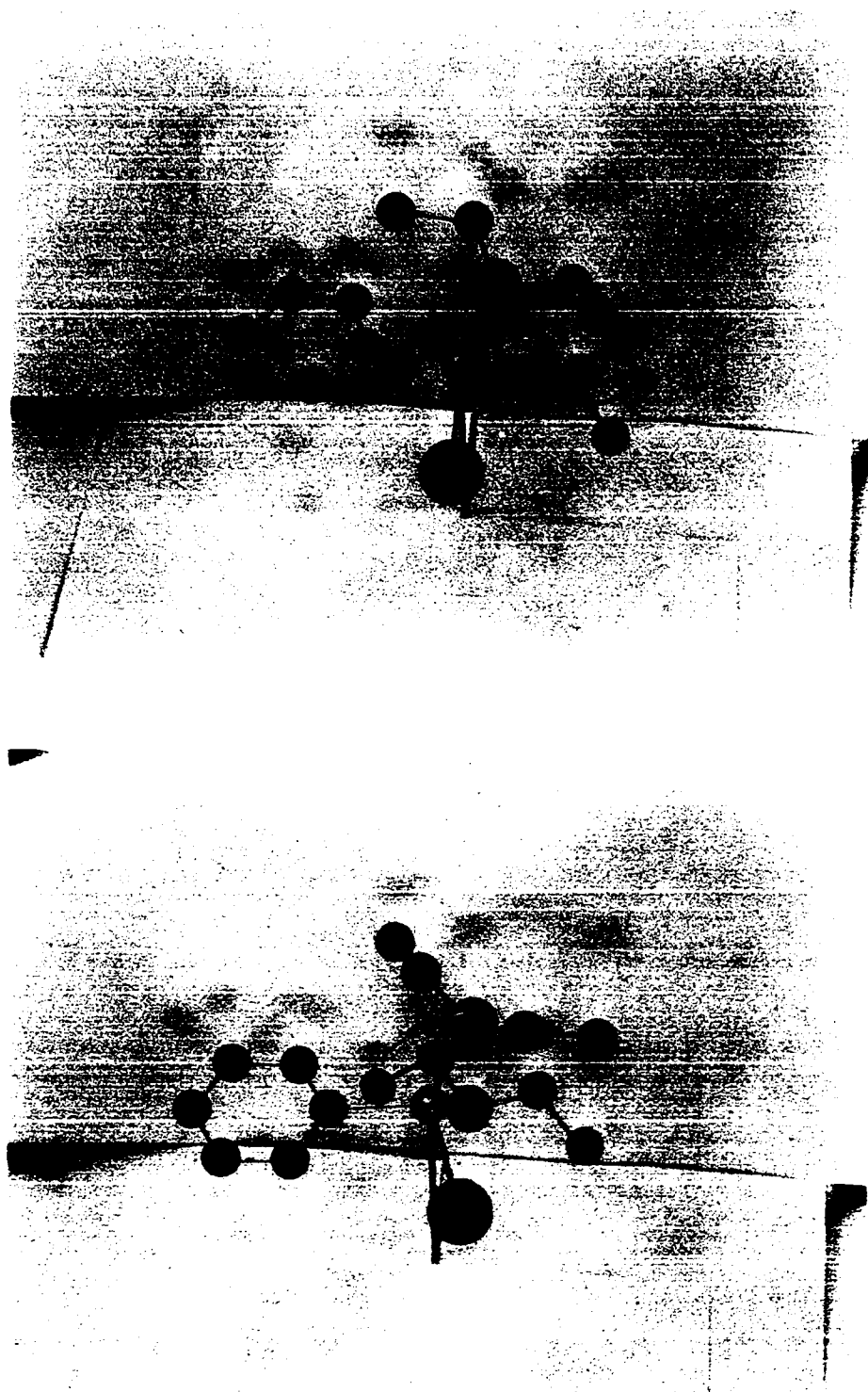
*The convention used in labeling the carbons of the phenyl group is to call the connecting carbon of the metal-carbon bond, phenyl carbon 1 (ϕC_1) and to number the remaining carbons in a clockwise direction around the ring.

tion of the diethylether molecules is more directly related to intramolecular forces although once the possible orientations are found with respect to intramolecular forces, packing considerations will place further constraints on the molecule.

There are several possible ether configurations. The ether molecule may be trigonally or tetrahedrally coordinated to the magnesium atom, and it may be planar (ignoring the hydrogen atoms) or the methyl groups may be rotated out of the plane of the methylene carbon-oxygen-methylene carbon atoms. The ether molecule can also be rotated about the oxygen-magnesium bond so that if the coordination is tetrahedral or trigonal with a non-planar molecule, the methyl groups will be pointing either away from or toward the plane defined by the phenyl group, magnesium atom and bromine atom. This is illustrated by Figures 38a and 38b which show two molecules with tetrahedral oxygen atoms. In one case the methyl groups are pointing toward the above plane, in the other they are staggered with one ether's methyl groups pointing toward the plane and the other ether's methyl groups pointing away from the plane. A third possibility, not shown, is to have all four ether methyl groups pointing away from the plane.

A three-dimensional Fourier calculated on the basis of bromine, magnesium and phenyl carbon positions indicated

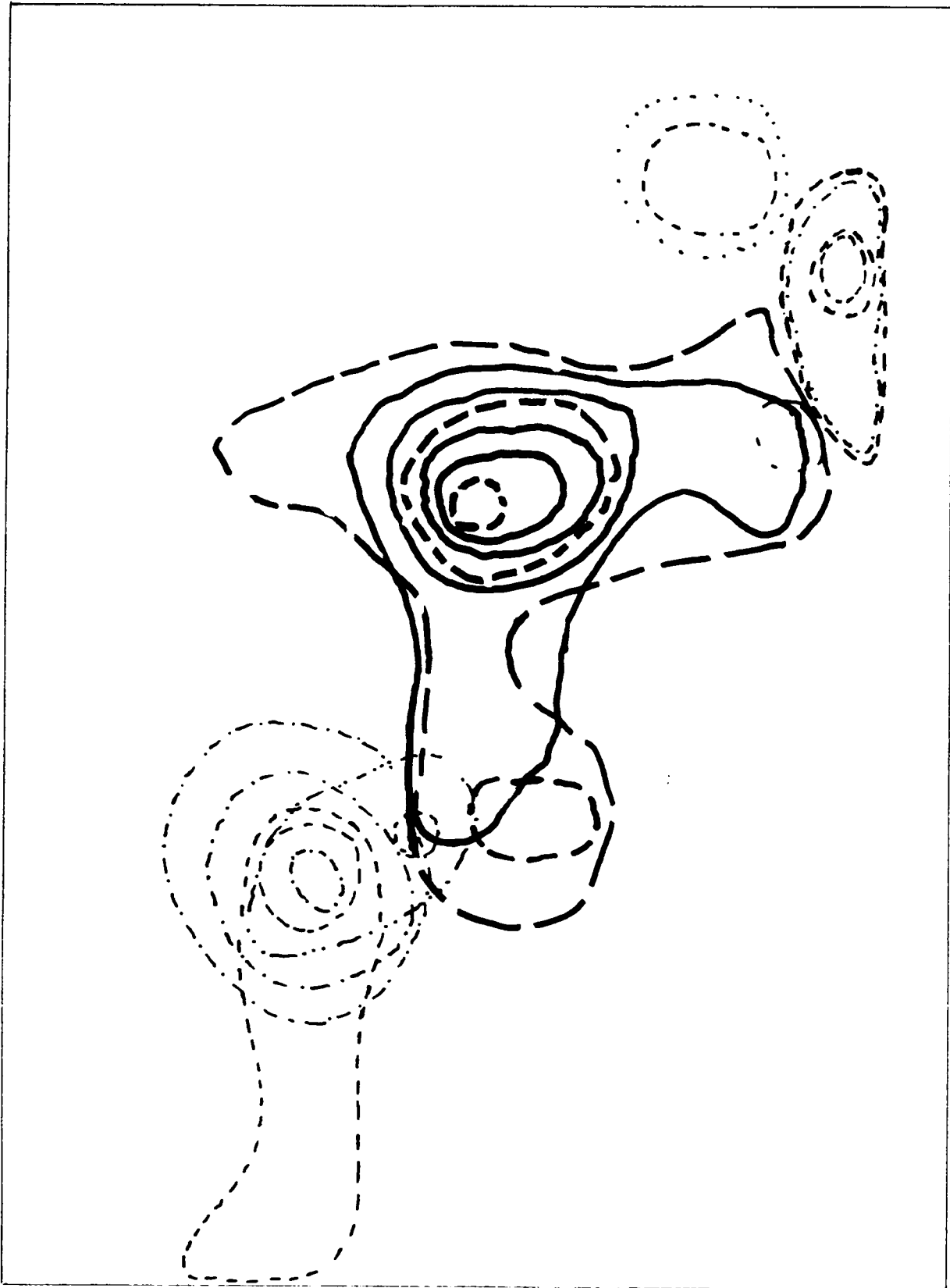
Figure 38. Models of $C_6H_5MgBr \cdot 2(C_4H_{10}O)$ indicating possible orientations of ether methyl groups



that the ether oxygens were tetrahedrally coordinated and that the methyl groups were pointed toward the bromine-magnesium-phenyl plane. In addition the methyls appeared to be rotated about the oxygen carbon bond so that the distance between the methyl groups and bromine atom and phenyl carbons was increased. The two ether molecules were for all practical purposes mirror images of each other. Figure 39 shows one of the ether groups as taken from the three-dimensional Fourier.

Unfortunately the quality of the data was not sufficient to permit refinement of the carbon positions. The probable reason for this was the thermal distillation of the crystal in the capillary while collecting the x-ray data. This distillation proceeded at a rate such that realignment of the crystal was necessary every two or three hours. This meant that the crystal size also changed and as the diffracting power of a crystal is proportional to the volume of the crystal (for a cylindrical crystal $4\pi r^2$), the scale factor correlating the observed to calculated intensities was also continually changing. The absorption of the crystal also changed continuously and although the maximum absorption coefficient was small ($\mu_r = .70$), the relative absorption error could be quite significant. The best discrepancy factor obtained after three-dimensional refinement was 17.8% for unobserved reflections only and 25.4% for all data.

Figure 39. Three-dimensional Fourier results showing probable ether carbon positions for $C_6H_5MgBr \cdot 2(C_4H_{10}O)$



Discussion of Structure

The observed and calculated structure factors are given in Figure 40 and the difference between the least squares phenyl carbon y and z coordinates and those predicted is illustrated in Figure 41. The least squares coordinates and standard errors are given in Tables 34 and 35. The bromine, magnesium and oxygen bond distances and angles are given in Table 36.

Table 34. Positional and isotropic temperature parameters obtained from least squares refinement for $C_6H_5MgBr \cdot 2(C_4H_{10}O)$

Atom	x	y	z	B
Br	-.0158	.0924	-.1169	2.88
Mg	-.0006	.2667	-.0309	3.95
O ₁	-.112	.349	-.125	5.22
O ₂	.136	.340	-.098	4.91
ØC ₁ ^a	-.001	.294	.175	6.85
ØC ₂	-.017	.219	.217	5.67
ØC ₃	.022	.188	.370	10.16
ØC ₄	-.003	.291	.414	10.06

^aCarbon positions are included although they do not give correct bond distances. For a comparison of the refined phenyl carbon positions and the proposed model see Figure 41.

Table 34 (Continued)

Atom	x	y	z	B
$\emptyset C_5$.015	.369	.371	11.08
$\emptyset C_6$	-.020	.372	.239	8.85
C_{11}^b	-.123	.348	-.283	2.64
C_{12}	-.221	.429	-.029	---- ^c
C_{13}	-.188	.312	-.269	6.18
C_{14}	-.175	.502	-.082	5.61
C_{21}	.165	.279	-.323	10.70
C_{22}	.096	.449	-.098	9.83
C_{23}	.221	.253	-.315	3.06
C_{24}	.214	.488	-.025	6.14

^bThe notation followed for the carbons is C_{ij} where i denotes the ether molecule and j the particular carbon atom. The odd j 's (1,3) are bonded carbons and the even j 's (2,4) denote the other two carbon atoms of the ether molecule. The lower values of j (1,2) are reserved for the methylene carbons.

^cTemperature factor greater than 15.

Table 35. Standard errors of positional parameters of heavy atoms of $C_6H_5MgBr \cdot 2(C_4H_{10}O)$

Atom	$\sigma(x)$	$\sigma(y)$	$\sigma(z)$
Br	.0005	.0004	.0005
Mg	.0022	.0017	.0018
O ₁	.004	.004	.005
O ₂	.004	.004	.005

Figure 40. Comparison of observed and calculated structure factors for $C_6H_5MgBr \cdot 2(C_4H_{10}O)$. Columns are for constant k and l miller indices and are

h	F_{obs}	F_{calc}	A_{calc}	B_{calc}
-----	-----------	------------	------------	------------

Asterisks indicate unobserved reflections.

4	202	159	159	0	1	18	7	-6	0	8	24	20	-20	-10	0	83	107	0	107	25	27	10	-25
5	126	137	117	0	2	24	26	-26	0	1	31	32	32	0	1	30	31	-3	-31	25	19	-6	1c
6	191	94	94	-1	3	23	31	0	-26	1	45	47	47	0	2	22	31	-16	27				
10	45	54	54	0	4	24	10	10	0	3	41	42	42	0	5	42	47	-9	38	0	57	5	0
12	23	16	16	0	5	28	27	0	0	7	6	26	26	13	6	26	23	13	17	2	36	43	-6
K = 1 L = 0																							
1	15	8	0	0	6	31	14	16	0	4	44	48	48	0	10	8	23	15	17	4	23	19	1
2	15	16	16	0	7	27	46	0	0	6	26	40	40	0	10	8	23	15	17	4	23	19	1
3	19	32	0	-12	8	24	32	-6	0	4	28	35	35	-6	9	25	23	31	3	5	25	24	4
4	33	38	38	-0	9	24	32	-6	0	3	28	35	35	-6	9	25	23	31	3	7	25	24	4
5	21	44	0	-64	0	46	64	-64	0	1	33	34	40	0	1	43	51	-1	51	8	29	26	-1
6	24	22	22	0	1	34	32	0	0	2	23	21	21	0	2	42	39	19	4	0	29	26	-1
7	25	36	0	-36	0	3	96	95	-95	0	3	23	26	0	3	38	45	24	37	0	27	26	0
8	26	24	24	0	4	27	27	0	0	4	18	22	22	0	4	40	37	22	30	1	23	19	0
9	25	30	0	-30	0	5	27	27	0	5	33	21	21	0	5	33	21	21	4	2	26	27	0
10	18	24	24	0	6	22	19	19	0	6	47	46	46	0	6	47	46	46	7	3	24	24	0
K = 2 L = 0																							
0	65	75	-75	0	7	20	14	-54	0	7	21	27	-0	8	25	27	24	16	10	6	24	22	0
1	17	4	0	-4	8	23	38	-38	0	8	17	19	19	0	9	26	24	16	10	7	24	22	0
2	39	49	-49	0	9	25	13	0	-13	1	79	74	-0	10	27	24	16	10	10	8	24	22	0
3	138	129	-129	0	10	24	26	-26	0	2	65	77	-0	11	24	26	24	16	10	9	24	22	0
4	30	16	-16	0	11	20	11	0	0	3	74	76	-0	12	24	26	24	16	10	11	24	22	0
5	75	75	0	75	12	20	12	-12	0	4	74	76	-0	13	24	26	24	16	10	12	24	22	0
6	27	23	-23	0	13	23	33	-33	0	5	20	19	-0	14	23	33	33	33	11	13	23	33	0
7	31	30	-30	0	14	24	30	-30	0	6	16	26	0	15	23	33	33	33	12	14	23	33	0
8	21	18	-18	0	15	24	10	-10	0	7	24	37	-0	16	24	30	37	37	13	15	24	30	0
9	26	13	-13	0	16	25	22	-22	0	8	21	30	-0	17	25	37	37	37	14	16	25	30	0
10	25	5	-5	0	17	26	17	-17	0	9	21	30	-0	18	26	37	37	37	15	17	26	30	0
11	24	19	-19	0	18	24	33	-33	0	10	17	30	-0	19	26	37	37	37	16	18	26	30	0
K = 3 L = 0																							
1	19	18	0	-18	1	42	38	38	0	11	126	100	-0	20	38	100	100	100	17	19	31	28	0
2	41	33	33	0	2	50	72	-72	0	2	62	72	-72	22	38	100	100	100	18	20	31	28	0
3	23	11	0	-11	3	123	117	114	-20	3	72	117	114	22	38	100	100	100	19	21	31	28	0
4	22	18	18	0	4	33	50	-34	0	4	72	117	114	22	38	100	100	100	20	22	31	28	0
5	22	7	-7	0	5	57	46	45	-7	5	72	117	114	22	38	100	100	100	21	23	31	28	0
6	21	68	48	0	6	49	53	-31	0	6	72	117	114	22	38	100	100	100	22	24	31	28	0
7	39	21	0	-21	7	38	41	40	-9	7	72	117	114	22	38	100	100	100	23	25	31	28	0
8	19	36	36	-0	8	37	52	-28	0	8	72	117	114	22	38	100	100	100	24	26	31	28	0
9	25	12	0	-12	9	23	19	15	-11	9	72	117	114	22	38	100	100	100	25	27	31	28	0
K = 4 L = 0																							
0	34	36	-36	0	10	14	23	23	0	10	14	23	23	23	6	25	21	-10	19	0	14	8	0
1	116	121	-121	0	11	53	60	58	-60	1	53	60	60	60	7	25	21	-10	19	1	18	28	-0
2	82	76	-76	0	12	122	107	107	0	2	122	107	107	107	8	25	21	-10	19	2	21	5	0
3	42	53	-53	0	13	104	95	95	-88	3	104	95	95	95	9	25	21	-10	19	3	21	5	0
4	23	4	4	0	14	111	110	110	-31	4	111	110	110	110	10	25	21	-10	19	4	21	5	0
5	57	59	-59	0	15	31	36	48	-5	5	31	36	48	48	11	25	21	-10	19	5	21	5	0
6	23	15	-15	0	16	38	41	34	-23	6	38	41	34	34	12	25	21	-10	19	6	21	5	0
7	48	64	-64	0	17	24	34	20	-22	7	24	34	20	20	13	25	21	-10	19	7	21	5	0
8	27	29	-29	0	18	25	11	0	-11	8	25	11	0	0	14	25	21	-10	19	8	21	5	0

3	12	10	-8	7	0*	23	12	12	0	55	17	30	22	3*	25	22	24	0	0	21	24	-24	0					
4	98	27	-27	0	1	23	67	5	67	7*	25	52	-32	26	4	46	41	-7	60	1*	22	11	5	-10				
5*	24	20	-11	5	2*	20	1	12	0	8*	25	23	-15	19	5*	25	21	0	0	2*	22	14	-14	1				
6	40	38	-37	-3	3	27	53	-7	52	9*	24	32	-29	12	6*	24	23	-12	23	3	26	21	-7	-27				
7*	24	14	-4	-16	4*	26	13	12	5	7*	24	16	-21	-13	7*	24	16	21	-13	4	34	25	-15	21				
8*	24	40	-19	-12	5	39	61	7	61	8*	24	16	-21	12	8*	24	16	-21	12	5	32	25	-14	-21				
9*	25	10	-5	0	6	42	0	7	0	9*	24	16	-21	0	9*	24	16	-21	12	6	21	37	-12	35				
K= 4 L= 4																												
0	88	87	37	0	7*	24	36	-1	37	0	81	83	-9	-8	K= 4 L= 5	0	43	38	38	0	21	24	-24	0				
1	56	63	19	62	0*	23	1	-5	1	1*	21	11	2	11	1*	23	11	2	11	0*	22	11	5	-10				
2	67	70	70	1	1*	23	6	-3	-5	2	115	106	-1	106	2	34	33	13	0	2*	22	14	-14	1				
3	36	47	-6	-40	2*	24	7	7	-6	3	43	41	5	12	3	43	41	5	12	3	26	21	-7	-27				
4	44	56	56	-7	3*	24	12	11	7	4	72	61	6	-61	4	72	61	6	-61	4	34	25	-15	21				
5	48	39	12	30	4*	24	19	18	7	5	41	27	23	15	5	41	27	23	15	5	26	21	-7	-27				
6	27	43	63	6	5*	24	14	5	13	6	52	56	-2	-56	6	52	56	-2	-56	6	26	21	-7	-27				
7*	24	32	-2	-32	6*	23	17	17	5	7*	24	16	-21	16	7*	24	16	-21	16	7*	24	16	-21	16				
8	33	36	36	0	K= 4 L= 5																							
9*	24	22	6	-23	K= 4 L= 5																							
K= 5 L= 4																												
0	39	49	0	49	0	31	33	-33	-33	0	23	25	-25	0	0	23	25	-25	0	0	23	25	-25	0				
1	23	23	13	12	1*	23	16	-6	15	1	50	48	-10	-47	1	50	48	-10	-47	1	31	32	-32	1				
2	33	19	5	19	2*	21	22	-18	16	2*	21	22	-18	16	2	30	30	0	0	2	30	30	0	0				
3*	23	36	22	23	3	38	41	-17	-13	3	38	41	-17	-13	3	24	20	-20	-6	3	24	20	-20	-6				
4*	23	20	-1	20	4	22	22	-17	-23	4	22	22	-17	-23	4	35	16	5	35	4	35	16	5	35				
5	33	48	28	33	5*	23	13	-6	13	5	74	58	-22	-58	5	74	58	-22	-58	5	25	16	-13	19				
6	31	26	8	25	6*	22	13	-7	-16	6*	22	13	-7	-16	6*	22	13	-7	-16	6*	22	13	-7	-16				
7*	24	36	0	36	7*	25	22	-18	-23	7*	25	22	-18	-23	7*	25	22	-18	-23	7*	25	22	-18	-23				
8*	24	17	16	10	8*	25	17	-9	-15	8*	25	17	-9	-15	8*	25	17	-9	-15	8*	25	17	-9	-15				
9*	24	35	16	33	9*	25	24	-18	-13	9*	25	24	-18	-13	9*	25	24	-18	-13	9*	25	24	-18	-13				
K= 6 L= 4																												
0	43	43	43	0	0*	24	13	0	13	0	24	13	0	13	0	24	13	0	13	0	24	13	0	13				
1	23	19	-7	16	1	58	63	62	-6	1	58	63	62	-6	1	58	63	62	-6	1	58	63	62	-6				
2	37	46	46	-6	2*	22	2	6	-7	2*	22	2	6	-7	2*	22	2	6	-7	2*	22	2	6	-7				
3*	24	25	0	24	3	31	19	39	1	3	31	19	39	1	3	31	19	39	1	3	31	19	39	1				
4	34	50	50	0	4*	24	24	-13	-21	4*	24	24	-13	-21	4*	24	24	-13	-21	4*	24	24	-13	-21				
5*	25	13	7	11	5	30	42	62	-6	5	30	42	62	-6	5	30	42	62	-6	5	30	42	62	-6				
6	33	32	32	0	6*	25	12	-12	7	6*	25	12	-12	7	6*	25	12	-12	7	6*	25	12	-12	7				
7*	24	12	5	11	7*	21	31	31	5	7*	21	31	31	5	7*	21	31	31	5	7*	21	31	31	5				
8	47	18	18	0	8*	24	13	-10	8	8*	24	13	-10	8	8*	24	13	-10	8	8*	24	13	-10	8				
9*	25	9	0	5	9*	24	16	15	3	9*	24	16	15	3	9*	24	16	15	3	9*	24	16	15	3				
K= 7 L= 4																												
0*	22	5	-0	0	0	59	47	-0	-47	0	21	6	-6	0	0	21	6	-6	0	0	21	6	-6	0				
1*	22	13	-15	-12	1	67	48	-48	-9	1*	23	25	-3	-24	1	67	48	-48	-9	1	67	48	-48	-9				
2*	26	17	14	-4	2	17	15	8	12	2	26	3	1	2	2	26	3	1	2	2	26	3	1	2				
3*	23	21	-20	-5	3	71	64	-62	15	3*	24	12	-1	-12	3*	24	12	-1	-12	3*	24	12	-1	-12				
4*	23	18	15	-10	4*	23	25	-2	-25	4*	23	25	-2	-25	4*	23	25	-2	-25	4*	23	25	-2	-25				
5	39	25	-20	-15	5*	25	24	16	-22	5*	25	24	16	-22	5*	25	24	16	-22	5*	25	24	16	-22				
6*	24	19	19	0	6*	23	16	-0	-16	6*	23	16	-0	-16	6*	23	16	-0	-16	6*	23	16	-0	-16				
7*	24	16	-6	-15	7	34	16	13	-5	7	34	16	13	-5	7	34	16	13	-5	7	34	16	13	-5				
8*	24	24	24	1	8*	24	30	-0	-30	8*	24	30	-0	-30	8*	24	30	-0	-30	8*	24	30	-0	-30				
K= 8 L= 4																												
0	31	30	0	30	0	41	49	-48	0	0	31	30	0	30	0	41	49	-48	0	0	31	30	0	30				
1	35	45	45	0	1	37	35	-8	34	1	35	45	45	0	1	35	45	45	0	1	35	45	45	0				
2	28	30	-9	28	2	51	35	-32	14	2	28	30	-9	28	2	51	35	-32	14	2	28	30	-9	28				
3	49	49	-15	47	3	49	49	-15	47	3	49	49	-15	47	3	49	49	-15	47	3	49	49	-15	47				
4	34	41	-40	-5	4	34	41	-40	-5	4	34	41	-40	-5	4	34	41	-40	-5	4	34	41	-40	-5				
5	42	35	-26	23	5	42	35	-26	23	5	42	35	-26	23	5	42	35	-26	23	5	42	35	-26	23				

Figure 40 (Continued)

K= 7 L= 6				6= 22 38 -37 -7				1= 23 14 -7 -12				K= 5 L= 8				C 4C 45 C 45							
0	48	55	-0	7= 24 20 17 26	7= 24 22 -22 -4	2= 34 43 43 4	3= 24 13 -10 -7	3= 24 13 32 32	4= 23 32 32 -4	0	20	20	-0	-20	1= 23 10 -10 1	2= 43 46 -7 46	3= 24 12 -9 -7	4= 24 37 6 36	5= 24 10 -7 -4				
1	25	27	27	K= 3 L= 7				K= C L= 6				K= 6 L= 8				K= 4 L= 9							
2	42	45	7	0= 23 24 -0 24	1= 23 12 10 -6	0	51	51	59	0	0	23	31	-31	0	27	14	14	-0				
3= 24 31 11 -2	4= 23 27 4 -27	5= 24 29 28 -7	6= 25 27 5 -26	2= 27 23 -2 23	3= 24 23 -9 21	4= 25 16 -0 16	5= 25 20 -4 20	6= 28 15 -6 15	7= 24 25 2 25	8= 24 14 -7 14	0	23	31	-31	1= 23 2 2 -1	2= 23 19 18 4	3= 24 9 8 -5	4= 24 16 13 3	5= 24 15 15 -0				
7= 23 14 12 -6	K= 4 L= 7				K= 1 L= 8				K= 7 L= 8				K= 5 L= 9										
K= 8 L= 6				0	34	48	-48	0	0= 22 21 -0 21	1= 23 6 4 -5	2= 23 29 13 15	3= 19 10 4 -9	4= 25 22 5 21	5= 25 18 4 -17	6= 26 18 14 16	7= 24 22 1 -2	8= 24 13 8 10	0	22	11	-0	11	
0= 23 7 7 0	1= 23 24 0 24	2= 24 17 -1 -17	3= 25 14 5 13	4= 23 10 4 -17	5= 25 12 -2 12	1	58	56	16	-55	1= 23 6 4 -5	2= 23 29 13 15	3= 19 10 4 -9	4= 25 22 5 21	5= 25 18 4 -17	6= 26 18 14 16	7= 24 22 1 -2	8= 24 13 8 10	0= 22 11 -0 11	1= 23 15 -35 -1	2= 24 6 1 6	3= 25 32 -32 3	
7= 24 19 5 18	K= 3 L= 6				K= 2 L= 7				K= 6 L= 8				K= 4 L= 9										
0	48	37	0	0	45	50	0	0	25	25	25	-0	0	22	21	-0	0	22	26	26	-0		
1	31	36	37	1	23	21	0	1	35	43	12	41	1	28	31	4	1	24	25	-0	1	23 4 4 -0	
2	29	28	2	2	27	30	0	2	25 25 17 16	3	25 47 2 47	4	19 30 0 -30	5	24 21 -0 -21	6	25 23 -0 -23	0	27 29 -0 -29	1	23 15 15 -0	2	24 14 -14 0
3	27	42	42	3	26	14	-0	4	25 24 24 4	5	45 38 0 38	6	24 21 -0 -21	7	25 23 -0 -23	1	22 29 29 -5	2	23 29 29 -1	3	24 10 10 0	4	24 10 10 0
4= 24 19 5 18	K= 0 L= 7				K= 5 L= 7				K= 2 L= 8				K= 8 L= 8				K= C L= 10						
1	45	50	0	0	22	3	0	0	25	25	25	-0	0	25	25	25	-0	0	23	5	-5	0	
2= 23 21 0 -21	1	45	33	-32	0	1	45	33	-32	0	0	28	31	4	-19	0	22	26	26	-0	1	23 4 4 -0	
3	27	30	0	2= 23 15 -14 0	2= 24 30 -30 -3	3= 24 30 -30 -3	4= 24 19 -11 16	5= 31 24 -23 4	6= 25 27 -26 7	7= 24 16 -14 7	0	24 25 -0 -25	1	24 1 -0 -1	2	19 30 -0 -30	3	24 14 -14 0	4	24 10 10 0			
4= 23 14 -0 -14	5= 26 14 0 14	6= 25 1 -0 1	7= 28 32 0 3	7= 24 11 0 -11	8= 24 11 -0 11	K= 6 L= 7				K= 3 L= 8				K= 1 L= 10									
9= 24 11 -0 11	K= 1 L= 7				K= 7 L= 7				K= 3 L= 9				K= 2 L= 10										
0= 24 25 -0 25	1	35	24	20	12	0	23	9	9	0	0	21	6	-0	-0	0	31	28	0	28			
1	35	24	20	12	1	30	27	1	-27	1	26	15	-15	-7	1	24	40	39	-11				
2= 23 13 9 8	3= 24 22 22 4	4= 24 23 22 7	5= 24 25 20 16	6= 25 21 20 8	7= 24 19 13 14	8= 24 26 24 10	9= 25 11 3 11	0	23	12	12	0	23	12	10	0	21	8	8	0			
7= 24 19 13 14	K= 2 L= 7				K= 8 L= 7				K= 4 L= 8				K= 2 L= 9				K= 3 L= 10						
0	34	48	-48	0	0	24	14	0	-14	0	39	49	-49	0	0	23	12	12	0				
1	49	42	-12	41	1= 24 11 -8 -7	1= 24 11 -8 -7	2= 24 18 -7 -17	3= 24 9 -4 -0	4= 23 18 -9 -16	5= 24 14 2 -14	0	23	35	8	34	1= 23 12 10 7	2= 22 4 4 0	3= 23 14 13 -6	4= 24 16 14 8	5= 24 13 8 -2	6= 24 12 13 3		
2	48	56	-55	8	2= 24 18 -7 -17	2= 24 18 -7 -17	3= 24 9 -4 -0	4= 23 18 -9 -16	5= 24 14 2 -14	0	19	30	-28	9	3= 24 16 14 8	4= 26 8 8 -2	5= 24 13 13 3	6= 24 12 9 -8	0	24	14	-14	0
3	34	38	-3	38	K= 7 L= 7				K= 4 L= 8				K= 2 L= 9				K= 5 L= 10						
4	66	63	-62	-10	0	40	53	53	-0	0	23	25	-11	22	0	23	12	12	0				
5	47	36	17	32	K= 8 L= 7				K= 3 L= 9				K= 3 L= 10										

Figure 40 (Continued)

U• 22 36 40 44
K• 0 1 11
L 92 99 5 54
K 0 1 14
G• 23 27 30

Figure 40 (Continued)

Figure 41. Difference between proposed y and z phenyl carbon coordinates and those given by least squares results. Distances are in Angstroms.

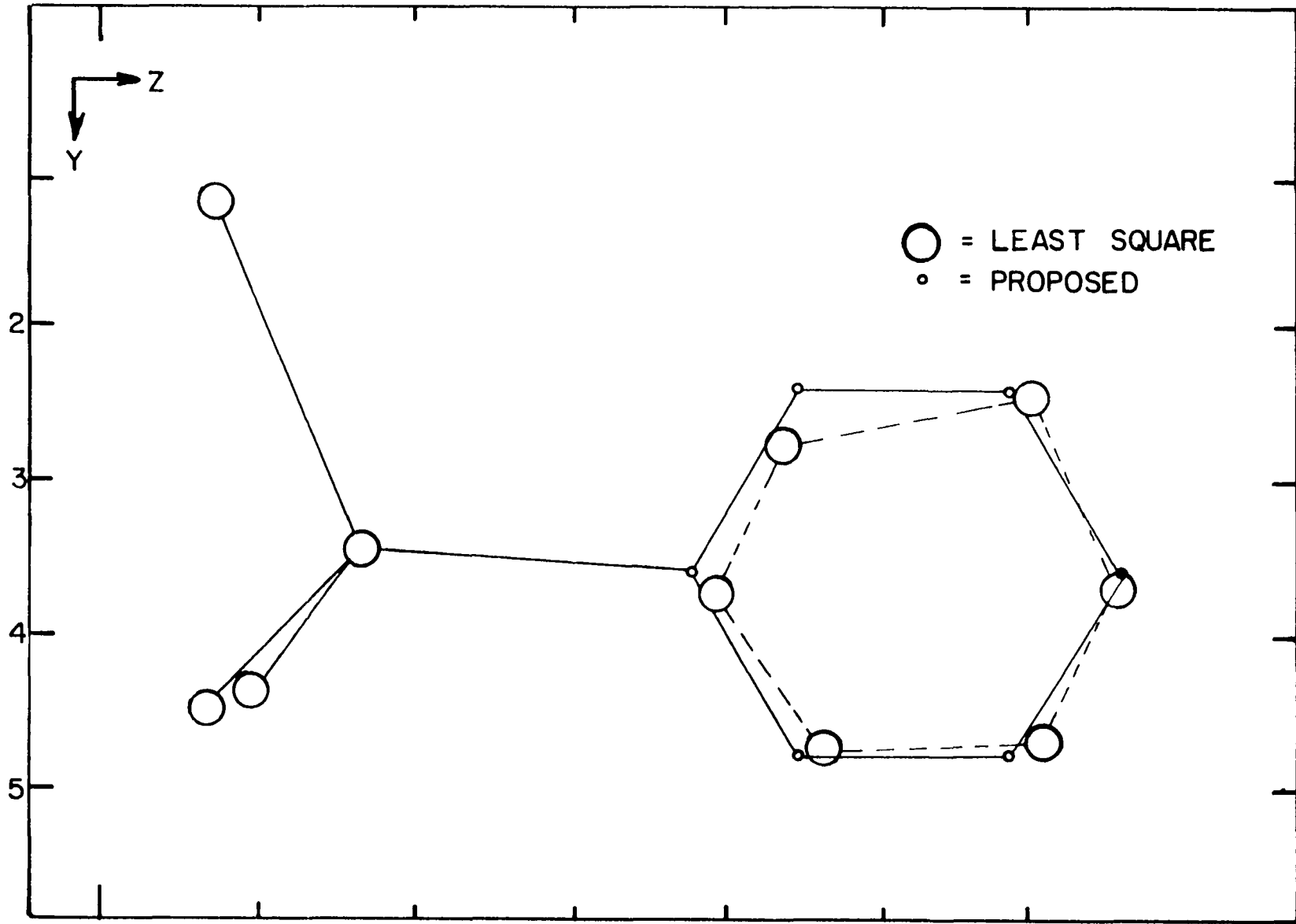
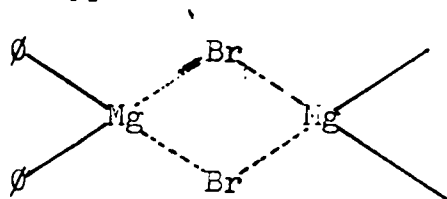


Table 36. Bond distances and angles for $C_6H_5MgBr \cdot 2(C_4H_{10}O)$
Br, Mg, and O atoms

Description of distance <u>or</u> angle	Distance <u>or</u> angle
Br-Mg	2.44 \pm .02
Mg-O ₁	2.01 \pm .04
Mg-O ₂	2.06 \pm .04
< Br-Mg-O ₁	103.26 \pm 1.57°
< Br-Mg-O ₂	109.84 \pm 1.38°

The structure can be considered as a layer of bromine, magnesium, and phenyl carbon atoms (hereafter referred to as the phenyl layer) alternating with a layer of ether molecules (the ether layer) (Figure 42). The Van der Waal packing of the phenyl layer is shown in Figure 43. The oxygen, bromine, and magnesium x parameters indicate the bromine-magnesium- \emptyset carbon plane is tilted about 7° from the $x = 0$ plane.

In spite of the fact that the carbon positions were not confirmed by least squares analysis, the bromine and magnesium positions alone preclude the possibility of a structure of the type



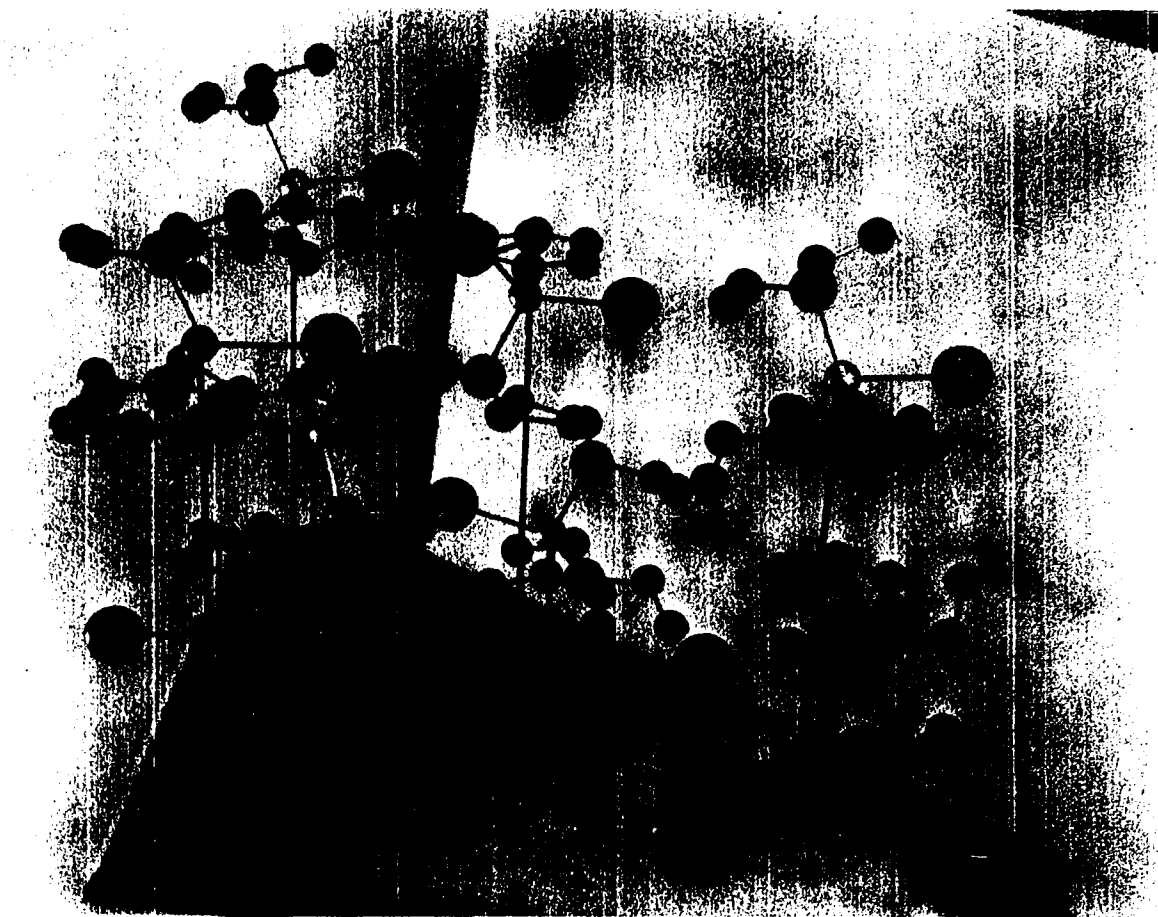
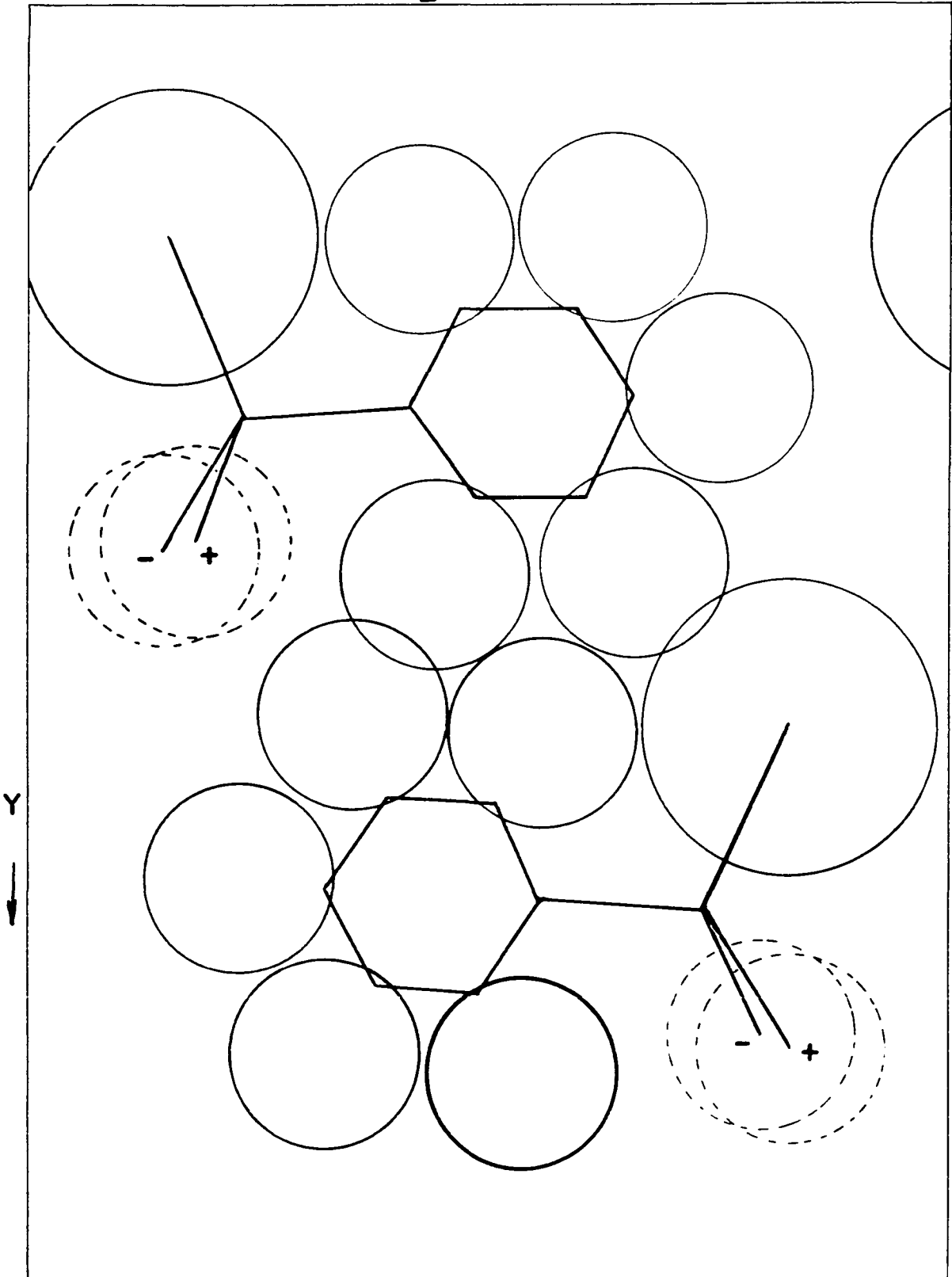


Figure 42. Model of $C_6H_5MgBr \cdot 2(C_4H_{10}O)$ showing alternating phenyl-bromine-magnesium and ether layers. Ether carbon positions are only approximate.

Figure 43. Van der Waal diagram of packing of atoms in "phenyl layer" for $C_6H_5MgBr \cdot 2(C_4H_{10}O)$. Oxygens are represented by dashed lines. Ether carbons are not shown.

Z →



Assuming Mg-Br distances of $2.45 \overset{\circ}{\text{Å}}$ and tetrahedral magnesium coordination, the bromine-bromine distance is found to be in the neighborhood of 4 angstroms for the above model, however the observed bromine-bromine distance between bromines in adjacent phenyl layers is greater than 6.1 angstroms and the closest approach between bromine atoms within a phenyl layer is more than 6.40 angstroms. Similarly the closest magnesium-magnesium distance is about 6.1 angstroms. These distances are only consistent with a monomeric rather than any polymeric structure. The structure is consistent with the fact that the crystal growth was in the x direction which is the direction along which the molecules are stacked about the two fold screw axes at $(x, 1/4, 0)$, etc. There is no indication of intermolecular interactions since the closest oxygen magnesium approach is about 4.8 angstroms, and the closest oxygen phenyl approach is about 4.5 angstroms. The bromine atoms lie very nearly in the same plane as the phenyl group and have a closest approach of about 4.20 angstroms from the phenyl groups which is nearly the expected Van der Waal distance ($4.40 \overset{\circ}{\text{Å}}$), so that the proposed model in Figure 1a is not found in the solid state. There is, of course, a very good possibility that if less than two moles of ether per gram-atom of magnesium are available, RMgBr may be coordinated either as $\text{R}_2\text{MgBr}_2\text{Mg}$ or $\text{Br}_2\text{MgR}_2\text{Mg}$. The polymeric gross properties of the liquid, when there are less than two

molecules of ether present, and the polymeric features of the unsolvated solid support this hypothesis.

The Fourier results indicated that the ethers were tetrahedrally coordinated. Intermolecular packing considerations seem to support this in a qualitative way inasmuch as there are more stringent requirements on the rotation of the methyl groups away from the phenyl bromine and magnesium atoms for the trigonally coordinated ether group. Confirmation of this must wait more accurate data.

DIPHENYLMAGNESIUMDIETHERATE

In order to study the bonding in aryl organometallics numerous attempts were made to obtain crystals of unsolvated diphenylmagnesium.

The unsolvated diphenylmagnesium is readily prepared as a powder by heating diphenylmercury with magnesium powder in an evacuated bomb tube at a temperature of 200 - 210 °C for five to six hours (31). If there is a temperature gradient in the tube, excess diphenylmercury sublimes to the cool end of the tube. Unreacted diphenylmercury is removed by the process described by Gilman (31) by leaching with benzene. Excess magnesium is removed by filtration. An alternative preparation is by the addition of dioxane to a phenylmagnesium bromide ether solution (29). The diphenylmagnesium stays in solution while magnesiumbromidedioxanate precipitates out. The former method of preparation was used in this research as it eliminates the possibility of the presence of trace amounts of bromine. If care is used in preparation, the unsolvated diphenylmagnesium is a creamy, white, infusible material with polymeric characteristics.

The problem in growing unsolvated crystals from solution is threefold. The solvent must be inert, it must not coordinate with the magnesium, and the reagent must be soluble in the solvent. Diphenylmagnesium has been reported

insoluble in diethylether and in benzene (31). It was found however that sufficient unsolvated diphenylmagnesium dissolved in benzene upon heating gives a positive Gilman's Test (67) for metal-carbon linkage. The solubility is however nearly negligible as found by Strohmeier (34) in Table 4. The solubility in diethylether was also found qualitatively to agree with Strohmeier's work. The only solvent found which satisfied all three requirements for crystallization to any extent was benzene; however, attempts to grow crystals from this solvent were unsuccessful.*

A second possible method of obtaining unsolvated crystals is by sublimation. The method of preparation from diphenylmercury indicates the compounds are thermally stable to temperatures of 200 - 210 °C. It was observed that charring and decomposition sometimes occurred if the temperatures were much higher than this or if the reactants were left in the tube for longer periods of time.

*While this thesis was being written crystals were found growing in an ether solution of diphenylmagnesium dietherate under rather unusual circumstances. A sample of $(C_6H_5)_2Mg \cdot 2(C_4H_{10}O)$ was sealed in an NMR sample tube and about six months later the spectra were rechecked against previous spectra with no observable change. A few days later large transparent crystals were found in the NMR tube. The concentration of diethylether in the solution was 2.47 moles per mole of $(C_6H_5)_2Mg$.

Coates (4) reports decomposition at 280 °C with the formation of biphenyl and magnesium. Rochow, Hurd, and Lewis (3) state that decomposition occurs from 170° to 210° with the formation of biphenyl, benzene, and ethylene. Dimethylmagnesium has been sublimed only with difficulty in a good vacuum (69) and the higher alkyl homologs through dinormalbutylmagnesium with even less facility. No report was found in the literature of the successful sublimation of diphenylmagnesium.

In this research, two methods were used in attempts to sublime diphenylmagnesium. The first was to heat the sample in a vacuum line with one or two liquid nitrogen traps placed between the sample and the pump. The second method was to place the material in an evacuated, long, cylindrical container. The container was then placed in an open-end furnace in such a manner that there was a temperature gradient along the cylinder. Both methods produced crystals, but melting point determinations and their general unreactivity indicated they were biphenyl.

Preparation and Purification

Etherated diphenylmagnesium is prepared first as indicated above from $(C_6H_5)_2Hg$ and Mg, then by leeching with benzene, washing with diethylether, and finally collecting

the pure ether solution in a suitable container. Both the unsolvated and etherated diphenylmagnesium are extremely reactive and reasonable care is necessary in handling them. Both are spontaneously inflammable in air if the ether solution of the etherated diphenylmagnesium is sufficiently concentrated. The reagent reacts with oxygen, carbon dioxide, water, any compound with an active hydrogen, carbon tetrachloride, carbon disulfide, and in general undergoes the same reactions as do the organomagnesium halides.

The method of purification and isolation follows that used for the phenylmagnesiumbromidedietherate crystals. The apparatus used is shown in Figure 28. Crystallization is obtained by supercooling the liquid to dry ice-acetone temperatures and then allowing the liquid to warm up slowly. The melting point of the crystals is about 20 - 25 °C.

The density of the crystalline material was obtained from the material used in the nuclear magnetic resonance experiments so that the ether concentration was precisely known. The volume of the NMR capillary was found by weighing an equal volume of mercury. The density of the solid was calculated to be $1.09 \pm .07$ gms/cm³. The density of the liquid diphenylmagnesium dietherate was $.97 \pm .07$ gms/cm³.

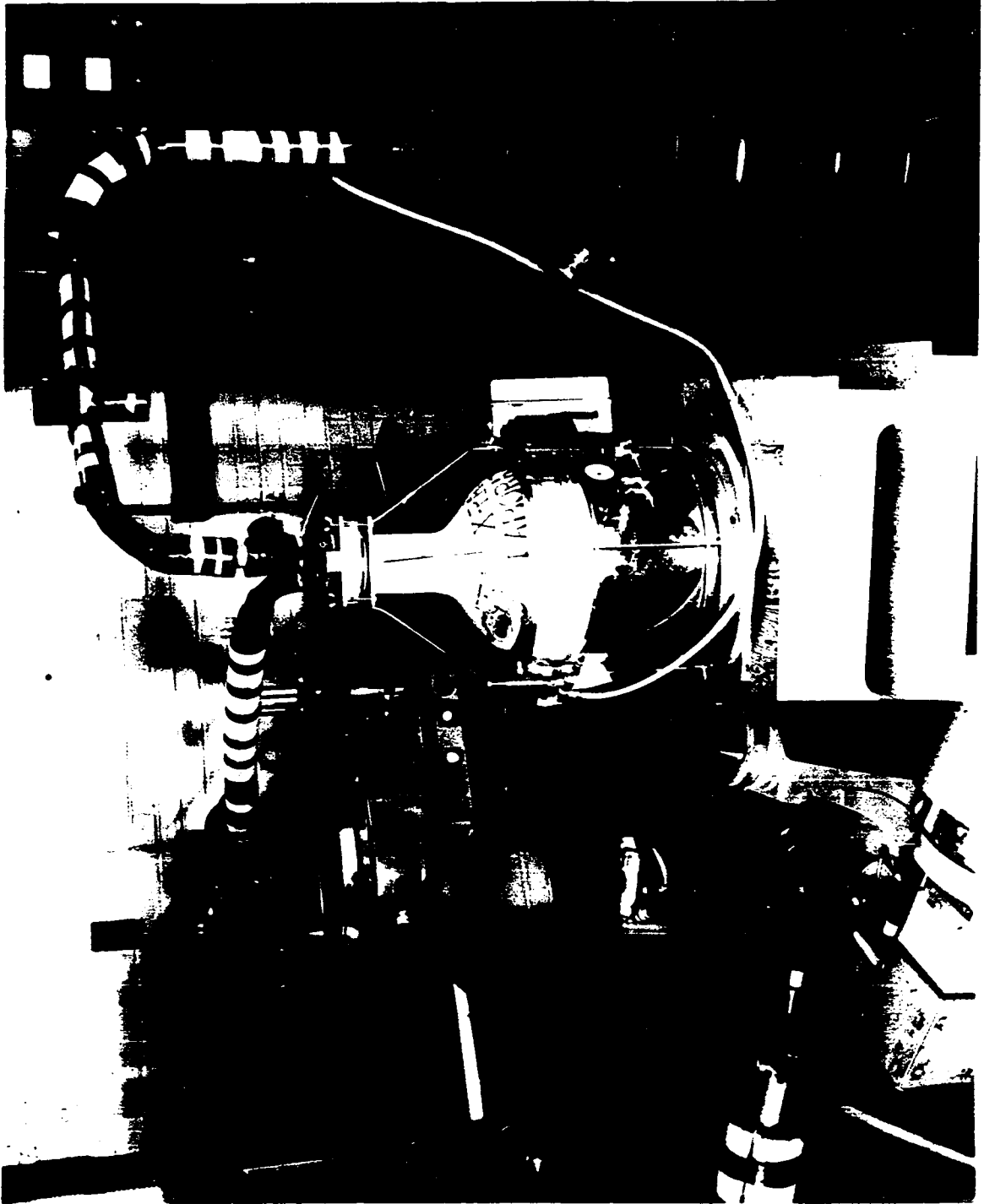
Properties and Collection of Data

German capillaries with a radius of .2 mm were loaded with a suitable amount of diphenylmagnesium etherate and mounted on a x-ray precession camera. The low temperature apparatus used was that used for phenylmagnesiumbromide. This apparatus was later modified to that shown in Figure 44. The twelve liter working dewar is filled automatically from a fifty liter auxiliary dewar by a timer and pressuretrol switch. The liquid nitrogen level can be kept nearly constant in the twelve liter dewar and by careful adjustment of a transfer valve so that transfer is essentially continuous, the variation of temperature kept to a minimum. Capillary frost is prevented by a coaxial stream of dry nitrogen around the cold air stream. Temperatures close to the boiling point of liquid nitrogen (-195°C) can be obtained, however it is more adaptable for use between -10° and -150°C .

Zero level pictures were taken of the $\{hkl\}$ and $\{hk0\}$ reflections. Intensity pictures were taken of the first and second layers of the (001) projection. The Laue symmetry was found to be $2/m$ so that the crystal system is monoclinic. The first setting given in the "International Tables for X-ray Crystallography", Volume I (56), was taken as the basis for indexing. The lattice constants were determined to be

Figure 44. Redesigned low temperature apparatus

11
12
13



$$\begin{array}{rcl}
 a & = & 14.21 \text{ \AA} \\
 b & = & 17.69 \text{ \AA} \\
 c & = & 7.87 \text{ \AA}
 \end{array}
 \qquad
 \gamma = 91.40^\circ$$

The observed extinctions were

$$\{hkl\} \quad h + l = 2n + 1 \quad .$$

Space Group Determination

The above extinctions correspond to a B centered lattice so that the diffraction symbol is $2/m B-$. There are three possible point groups in the monoclinic system; c_2 , c_s , and c_{2h} . The corresponding space groups with diffraction symmetry $2/m B-$ are B_2 , B_m , and $B \alpha/m$. Since they all have the same diffraction symbol it is not possible to distinguish between them by diffraction techniques. Although the final test for the space group is the solution of the structure, it is possible to use the intensity distribution of the diffraction pattern as an aid in determining the space group. For three-dimensional data a three-dimensional vector map calculated from the relative intensities will often limit the choice of space group (70). A second approach is through a statistical study of the relative intensities.

The statistical method is completely valid only when all points of the reciprocal lattice are used; however,

satisfactory results can be obtained using only certain zones in reciprocal space (71). It is necessary, however, that (a) the number of crystallographically independent atoms is large, (b) there is no "heavy" atom, and (c) the distribution of atoms is random.

The distribution laws are (72)

$$\bar{1} P(z)dz = (2\pi z)^{1/2} \exp(-\frac{z}{2}) dz$$

$$1 P(z)dz = \exp(-z) dz$$

where z is the intensity of each reflection divided by the local average intensity. $P(z)dz$ is the probability that z lies between z and $z + dz$. $\bar{1} P(z)dz$ is the probability function for centric distributions and $1 P(z)dz$ is the probability function for acentric distributions. The most common application of these functions is to plot the fraction $N(z)$ of reciprocal lattice points for which the normalized intensity is less than z . The functions for this method have been derived by Howell, Phillips and Rogers (71) and are

$$\bar{1} N(z) = \text{erf} (1/2 z)^{1/2}$$

$$1 N(z) = 1 - \exp(-z) .$$

These two functions are shown as the curves $\bar{1}P$ and $1P$ in Figure 45a. This is the zero moment test.

More recently Ramachandran and Srinivason (73) and

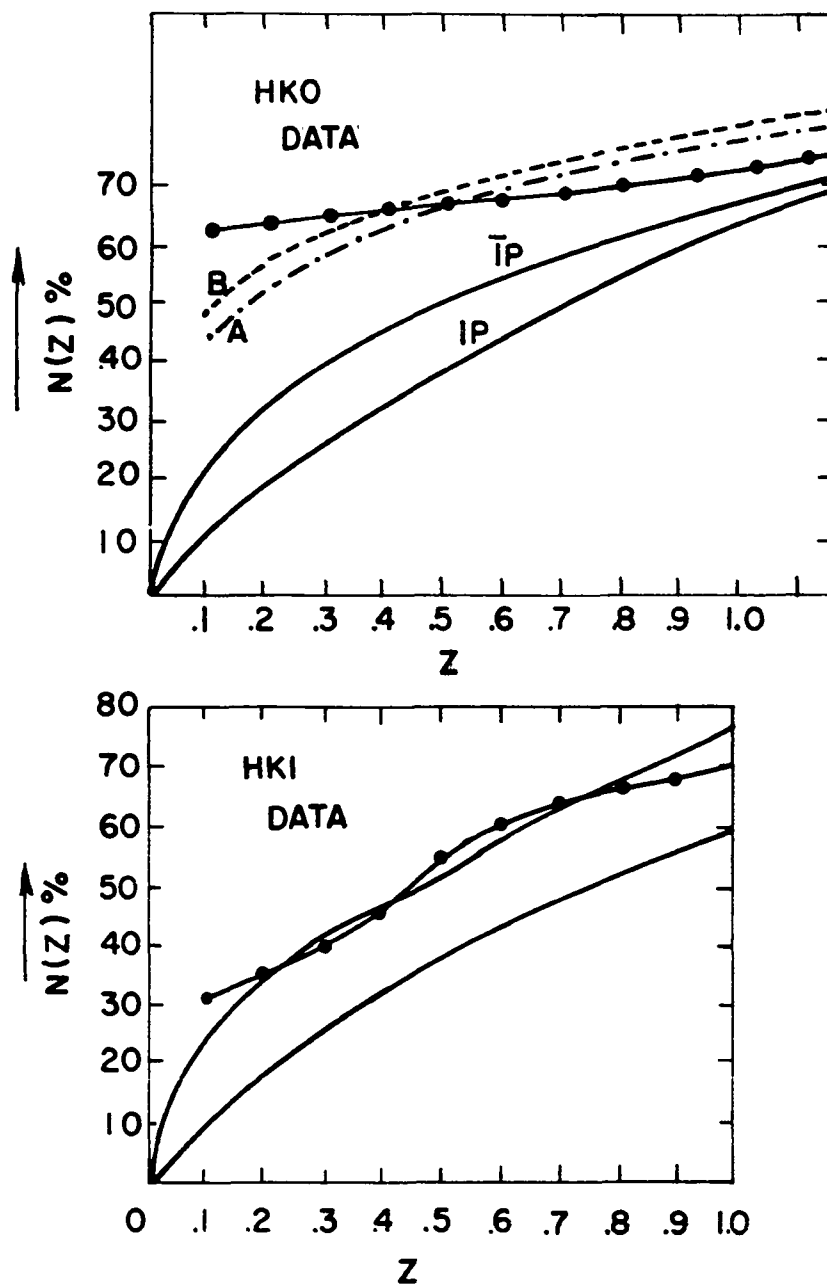


Figure 45. Results of zero-moment test for statistical determination of the space group of $(C_6H_5)_2Mg \cdot 2(C_4H_{10}O)$

Srinivason (74) have suggested using the probability function with the argument $y = z^{1/2}$. In this case the probability distributions are

$$\bar{I} P(y)dy = (2/\pi)^{1/2} \exp(-y^2/2)dy$$

$$I P(y)dy = 2y \exp(-y^2)dy$$

where $y = z^{1/2} = |F|/\sqrt{\langle I \rangle} = F/\sigma$. A practical application of Ramachandran and Srinivason's equations is as follows. The ratio of the number of reflections having a value of y between .5 and 1 to those having a value of y between .0 and .5 can be found by considering the ratio of probability functions for these two regions. This value is $N_2/N_1 = 1.96$ for an acentric distribution and .776 for a centric distribution.

A problem not discussed by Ramachandran and Srinivason is the treatment of the unobserved reflections. In applying the zero moment test Howell, Phillips, and Rogers (75) set the value of unobserved intensities equal to zero. Wilson (76), however, has shown that for the same $\sin \theta$ regions of the film the most probable value of the structure factor is

$$\bar{F} \text{ unobs} \cong 1/2 F \text{ min centric}$$

$$\bar{F} \text{ unobs} \cong 2/3 F \text{ min acentric,}$$

where F_{\min} corresponds to smallest observable values of $|F|$. Giving the unobserved intensities a value of zero means the statistical data are weighted toward a centric distribution. The procedure used therefore was to set \bar{F}_{unobs} equal to $7/12 F_{\min}$ for the various $\sin \theta$ regions. While this is still not exact from the statistical viewpoint, the difference of this value from the most probable value will not be large and the small amount of weighting now present will be equal for whichever distribution is present; centric slightly to acentric and acentric to centric.

To apply these tests to distinguish between the space groups B2, Bm, and B 2/m consider first the projection along the unique axis (c). B2 and B 2/m both project into the two-dimensional plane group P2, while Bm projects into P1. The intensity distribution of the $\{hk0\}$ reflections should therefore be centric for B2 or B 2/m and acentric for Bm. The $\{hkl\}$ data would be expected to have an acentric distribution for B2 or Bm and a centric distribution for B 2/m.

The curve for the $\{hkl\}$ data for the zero moment test is shown in Figure 45b. Except for the value for $z = .1$ the zero moment test indicates a centric distribution. Furthermore the ratio of Ramachandran and Srinivasan, N_2/N_1 , was .8 which also corresponds to a centric distribution. This indicates the space group is B 2/m.

The $\{hk0\}$ data should show a centric distribution,

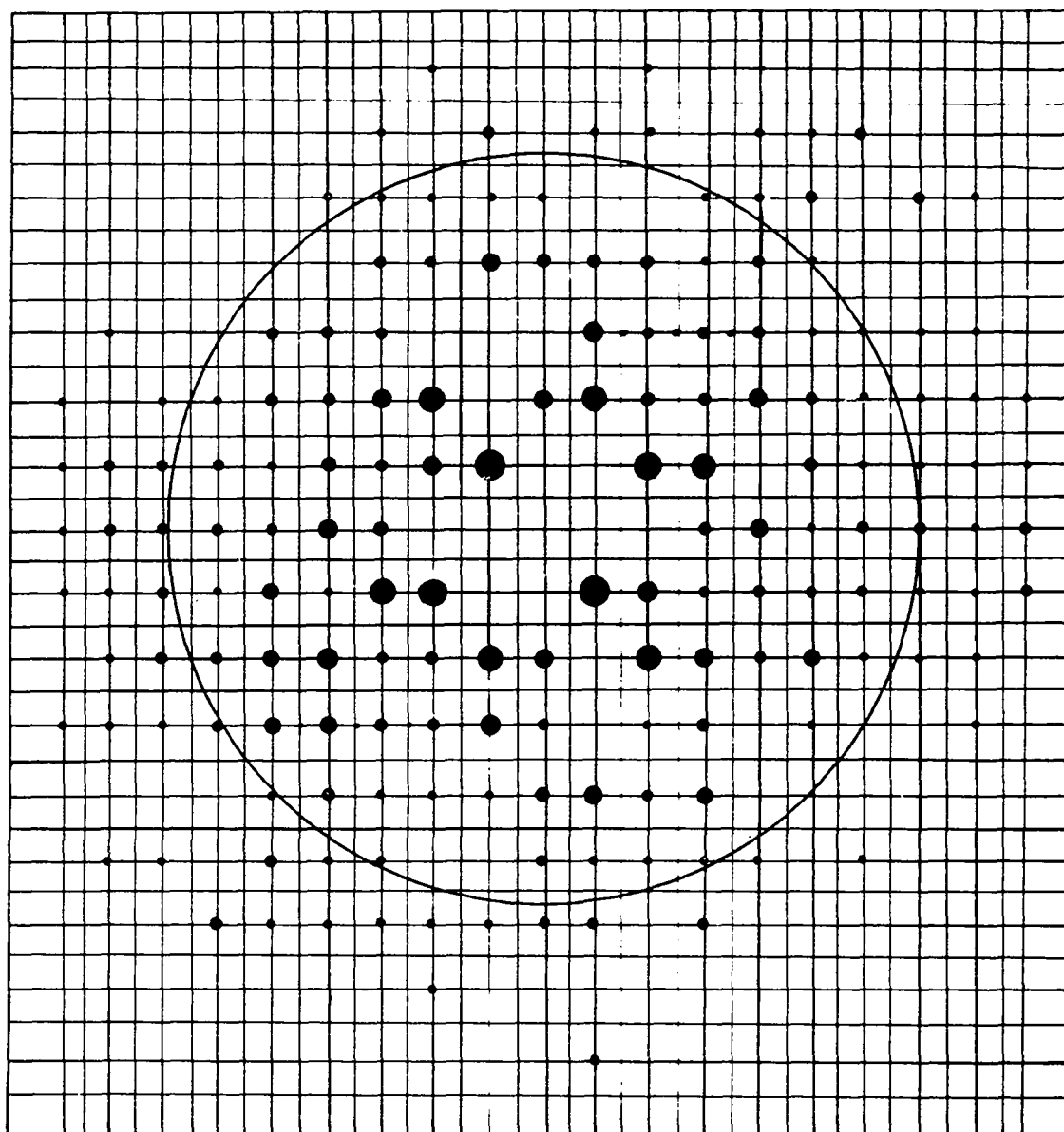
however the curve in Figure 45a for the zero moment test shows no resemblance to either an acentric or centric distribution. Ramachandran and Srinivasan's ratio (73) is .098 which does not correspond to the theoretical values of .776 (centric) and 1.96 (acentric). The difficulty can be found by an examination of the weighted reciprocal lattice (Figure 46). The majority of $\{hk0\}$, k odd reflections are weak or missing. This effect would be caused by an apparent translation of $1/2$ unit cell distance in the \vec{b} direction since the structure factor for the projection of two molecules separated by $\vec{b}/2$ is

$$\begin{aligned}
 F(hk0) &= \exp 2\pi i(hx + ky) + \exp 2\pi i(hx + k(y + 1/2)) \\
 &= \exp 2\pi i(hx + ky)[1 + \exp 2\pi i k/2] \\
 &= 0 \quad k \text{ odd} \\
 &= 2 \exp 2\pi i(hx + ky) \quad k \text{ even}
 \end{aligned}$$

It should be emphasized that the pseudosymmetry does not require that each atom in the molecule repeat itself at a distance $\vec{b}/2$. All that is required is that the projected electron density be approximately repeated.

The effects of pseudosymmetry on the statistical distribution of intensities have been considered by Rogers and Wilson (77) and by Herbstein and Schoening (78) for the

Figure 46. $\{hk0\}$ weighted reciprocal lattice for $(C_6H_5)_2Mg \cdot 2(C_4H_{10}O)$. The circle represents the distance from the origin in reciprocal space at which the benzene transformation is expected.



ρ^*

ρ^*

zero moment test. The experimental curve is not too different from the tricentric triparallel distribution, curve a, Figure 45a, or from the distribution for a centrosymmetric motif in a centrosymmetric arrangement, curve b in Figure 45a.

In summary, the statistical results imply that the space group is $B 2/m$ with a pseudo molecular translation of $b/2$ in the (001) projection.

Packing Considerations

The volume of the unit cell of diphenylmagnesiumdietherate is 1978 cubic angstroms. Using the volume increments given in Table 27, the molecular volume is 321.3 \AA^3 and the packing coefficient $k = \frac{ZV_0}{V}$ is .65 for $Z = 4$. According to Kitaigorodskii (55) this is a quite reasonable value for this type of compound.

A second indication that there are four molecules in the unit cell is from density considerations. The density measured above was $1.10 \pm .07 \text{ gms/cm}^3$. The calculated density for four molecules of diphenylmagnesiumdietherate and a unit cell volume of 1978 \AA^3 is 1.095 gms/cm^3 .

Kitaigorodskii (55) has made an analysis of the space groups allowing closest packing for organic molecules. Bm is permissible for molecules in special positions with symmetry m . $B2$ is permissible for molecules in general positions and

for molecules in special positions with symmetry 2_1 . $B 2/m$ gives limited closest packing for molecules in special positions and with symmetry $2_1/m$. From the considerations given below for the molecular configuration, it is unlikely the molecules possess m or $2_1/m$ symmetry. These results imply the space group $B2_1$.

Molecular Configuration

If a tetrahedral configuration is assumed about the magnesium atom the phenyl groups are not completely free to rotate due to steric effects from the ortho hydrogens. The covalent tetrahedral radii of the magnesium atom is 1.40 and the covalent radii for carbon is .77 so that as a first approximation one expects a Mg-C distance of 2.17 Å. The phenyl C-H distance may be taken as 1.03 Å. If tetrahedral angles are assumed, the ortho phenyl hydrogens lie on a circle as the benzene ring is rotated about the carbon-magnesium bond. The radius of the circle is

$$R = (d_{C-C} + d_{C-H}) \cos 30^\circ = 2.15 \text{ \AA} .$$

The center of the circle is at a distance ρ from the magnesium atom where

$$\begin{aligned}
 \rho &= d_{\text{C-Mg}} + d_{\text{C-C}} \cos 60^\circ - d_{\text{C-H}} \cos 60^\circ \\
 &= 2.17 + (1.4 - 1.08) \cos 60^\circ \\
 &= 2.33 \text{ \AA}
 \end{aligned}$$

When the phenyl groups lie in the plane of the C-Mg-C bond, the distance of the ortho hydrogen atom from the plane bisecting the C-Mg-C bond is given by

$$\begin{aligned}
 D &= \rho \sin 54^\circ 44' - R \cos 54^\circ 44' \\
 &= .67 \text{ \AA}
 \end{aligned}$$

The Van der Waal's radius of the hydrogen atom is 1.17 ± 0.02 (Kitaigorodskii (55)) so that there would be considerable steric interaction if the rings were planar. Let ψ be the value of the rotation angle of the phenyl groups as measured from the position in which they are mutually planar. If one assumes a two fold axis bisecting the C-Mg-C angle, one can determine the value of ψ for which the separation of the ortho-hydrogens is equal to the Van der Waal's diameter of hydrogen. It is found from

$$\begin{aligned}
 D^2 &= (\rho \sin 54^\circ 44' - R \cos \psi \cos 54^\circ 44')^2 + R^2 \sin^2 \psi \\
 (1.17)^2 &= (1.90 - 1.22 \cos \psi)^2 + 4.62 \sin^2 \psi
 \end{aligned}$$

D = distance of the ortho hydrogens from the two-fold axis through the central axis

$$\rho = 2.33 \text{ \AA} \text{ (see above)}$$

$$R = 2.15 \text{ \AA} \text{ (see above)}$$

The above reduces to a quadratic in $\cos \psi$ and gives $\psi = 24^\circ$.

If the phenyl rings are rotated 90° so that they are now perpendicular to the plane of the C-Mg bonds, the distance of the ortho hydrogen atoms from each other is given by

$$2 \rho \sin 54^\circ 44' = (4.66)(.816) = 3.80 \text{ \AA} .$$

There is therefore no reason as far as the ortho hydrogen interactions are concerned why the phenyl groups cannot be perpendicular to the C-Mg-C bond.

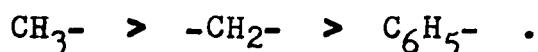
It would be necessary to know the configuration of the ether groups and the intermolecular interactions to predict even approximately the complete molecular configuration.

Nuclear Magnetic Resonance Results

Nuclear magnetic resonance studies were made on diphenylmagnesium to check the empirical ratio of one phenyl to one ether molecule and to determine if this method of analysis would give information regarding the structure of the molecular species present in solution. Since the material is a liquid at room temperature, it was possible to obtain high NMR resolution spectra (Figure 7).

Diphenylmagnesiumdietherate was prepared as described previously by heating diphenylmercury and magnesium together, washing with benzene, filtering and transferring to the container sketched in Figure 28 with the x-ray capillaries replaced by NMR sample tubes. The same difficulties in obtaining a concentration of two moles of ether per mole of diphenylmagnesium and sealing off the tubes in the presence of ether vapor were encountered and dealt with as described in the preparation of phenylmagnesiumbromide. The sample containers were commercially constructed, thin walled tubes. They were sealed off at a length of 4-1/2 to 5 inches and contained about 1-1/4 inch of reagent. The experimental runs were made by Dr. R. W. King* on a Varian HR60 spectrometer.

The chemical shift concept together with the integrated intensities (Figure 47) explains the large peaks in the spectra (Figure 48). Experimentally it is found that the resonance frequencies for the CH_3 -, $-\text{CH}_2$ -, and C_6H_5 - hydrogens generally are in the order



This is also their order of electronic shielding. An interesting exception to this is the case of the metal alkyls

*King, R. W. Department of Chemistry, Iowa State University, Ames, Iowa. $(\text{C}_6\text{H}_5)_2\text{Mg} \cdot 2(\text{C}_2\text{H}_5\text{O})$. Private communication. 1962.

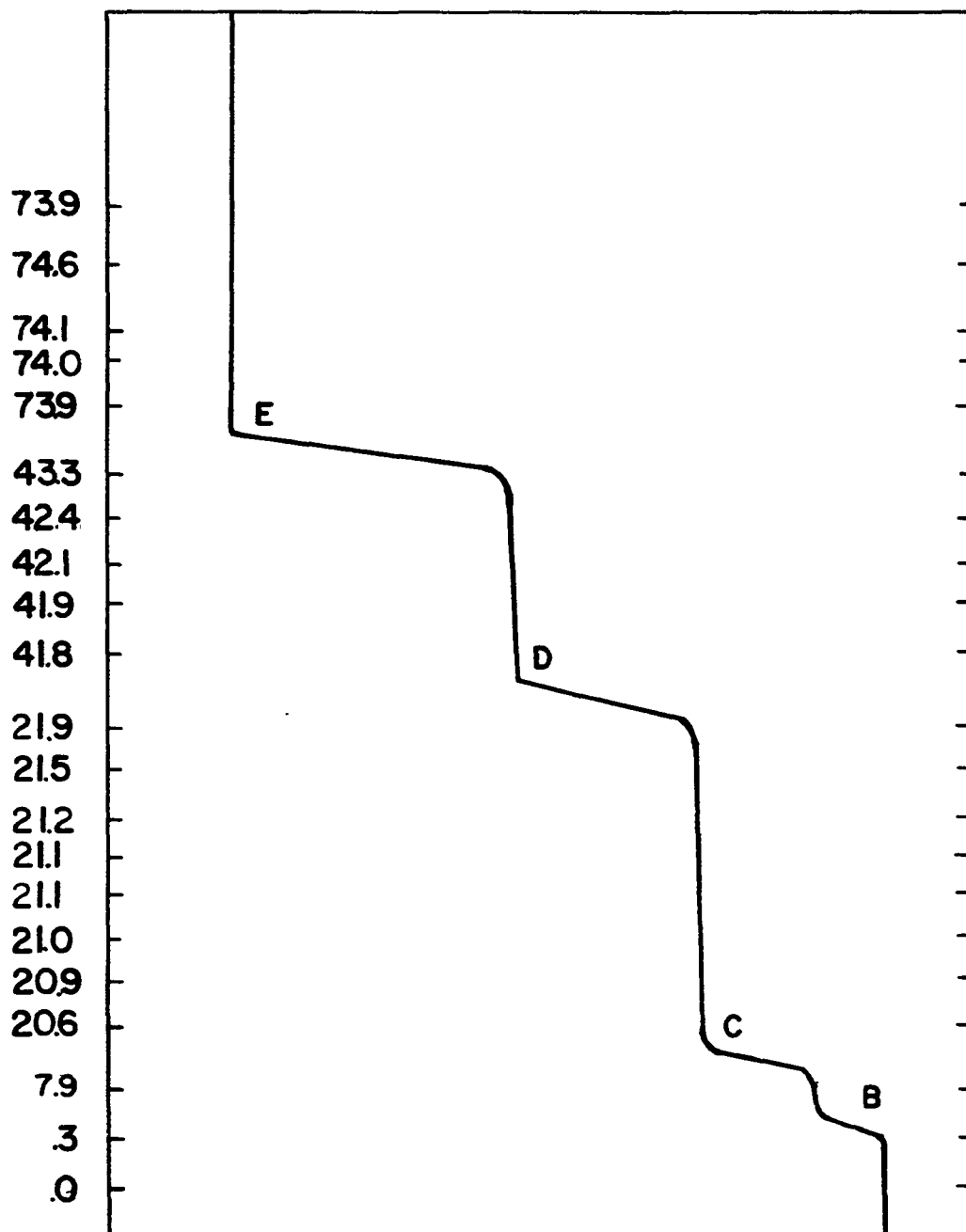


Figure 47. Integrated peak intensities of nuclear magnetic resonance spectra of $(C_6H_5)_2Mg \cdot 2(C_4H_{10}O)$. The values of the integrated intensities (horizontal axis) are indicated at the particular magnetic field value (vertical axis) the measurement was made.

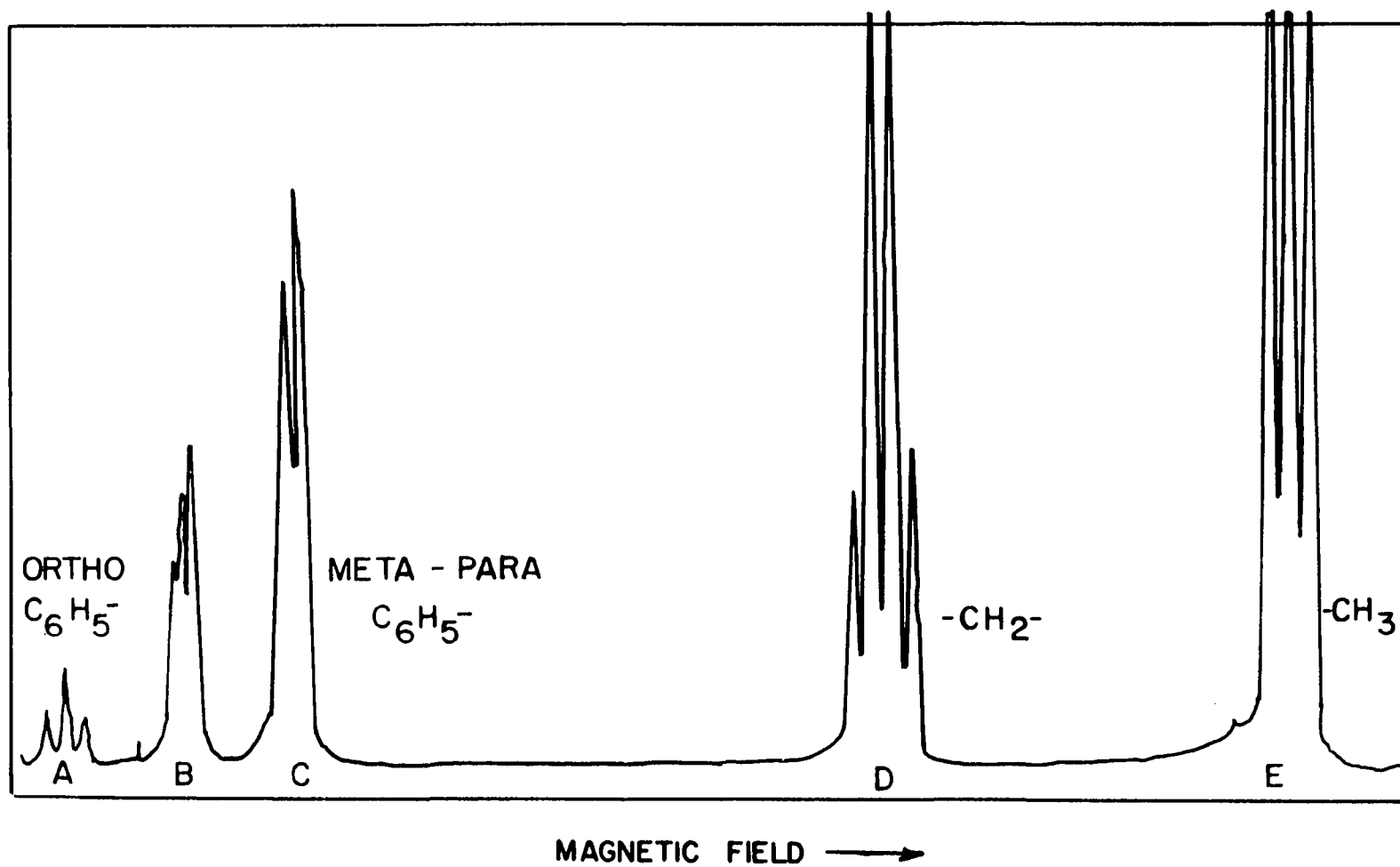


Figure 48. Nuclear magnetic resonance spectra of $(C_6H_5)Mg \cdot 2(C_4H_{10}O)$

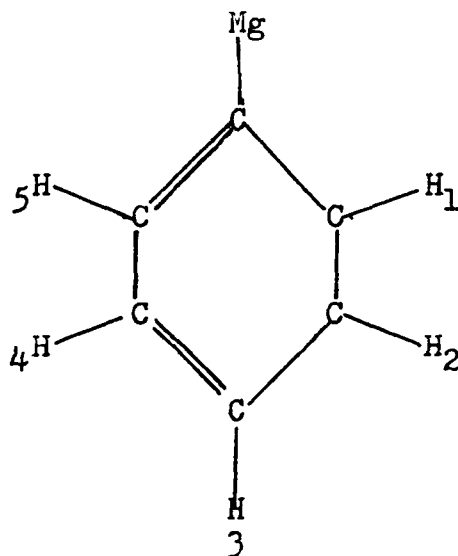
$\text{Pb}(\text{C}_2\text{H}_5)_4$ and $\text{AlCl}(\text{C}_2\text{H}_5)_2$ where the methylene shifts are equal to and greater than the methyl shifts (52). The assignment of E to CH_3^- , D to $-\text{CH}_2^-$ and B and C to C_6H_5^- is confirmed by the integrated intensities given in Figure 47. The number of the various chemically different hydrogens for $(\text{C}_6\text{H}_5)_2\text{Mg}\cdot 2(\text{C}_4\text{H}_{10}\text{O})$ is given in Table 37.

Table 37. Number of chemically different hydrogens
 $(\text{C}_6\text{H}_5)_2\text{Mg}\cdot 2(\text{C}_4\text{H}_{10}\text{O})$

Proton species	Total number
CH_3^-	12
$-\text{CH}_2^-$	8
meta + para C_6H_5^-	6
ortho C_6H_5^-	4

The ratio observed for D to E is 20.1 to 29.6 or .68. This agrees with the methylene to methyl hydrogen ratio of .67. The ratio of ether hydrogens to phenyl hydrogens is 2 to 1. The ratio of peaks B and C to D and E is 49.6 to 20.6 or 2.4 to 1. The ratio for a second sample was 2.8 to 1. The error of determination is two per cent. The results support the formula $(\text{C}_6\text{H}_5)_2\text{Mg}\cdot 2(\text{C}_4\text{H}_{10}\text{O})$ but do not exclude lesser amounts of ether. The fact that there are two types of phenyl carbons is to be expected for a strongly electropositive

substituted phenyl group

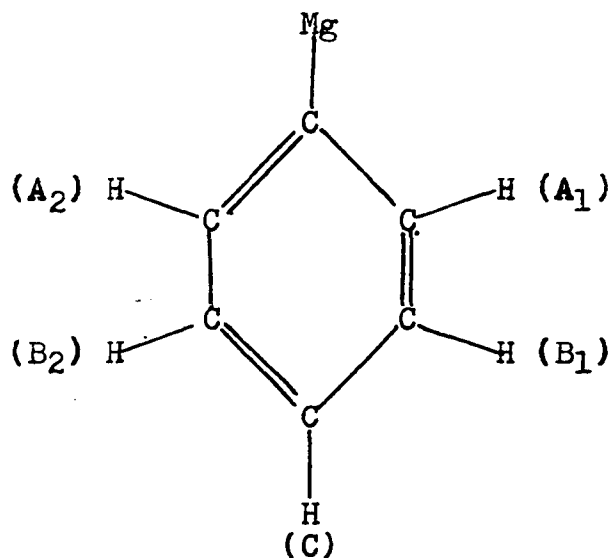


where to a first order the chemical environment of carbons 2, 3, and 4 and carbons 1 and 5 are different. Furthermore a magnesium atom would lower the shielding and hence the field for the ortho hydrogens and increase the shielding at the meta protons so that the ortho hydrogen resonance frequency is expected to be less than that of the meta or para resonance frequency. This is observed to be the case as the ratio of integrated intensities for C to B is 12.55 to 8.05 or 1.56 to 1 which compares with the theoretical 1.5 to 1 meta-para to ortho ratio.

The fine splitting of the peaks arises from the interaction of the magnetic field of one group with that in neighboring groups. The ethyl group interactions have been treated theoretically by Anderson (79) using third order

perturbation theory. To first order one predicts the methylene resonance line to be split into four peaks with intensities in the ratio 1:3:3:1 and the methyl resonance line to be split into three peaks with intensities in the ratio of 1:2:1. This agrees well with peaks d and e in Figure 48.

There are four main types of spin coupling which need to be considered for the phenyl groups: $J_{A_1B_1}$, J_{A_1C} , J_{B_1C} , and $J_{A_2B_1}$.



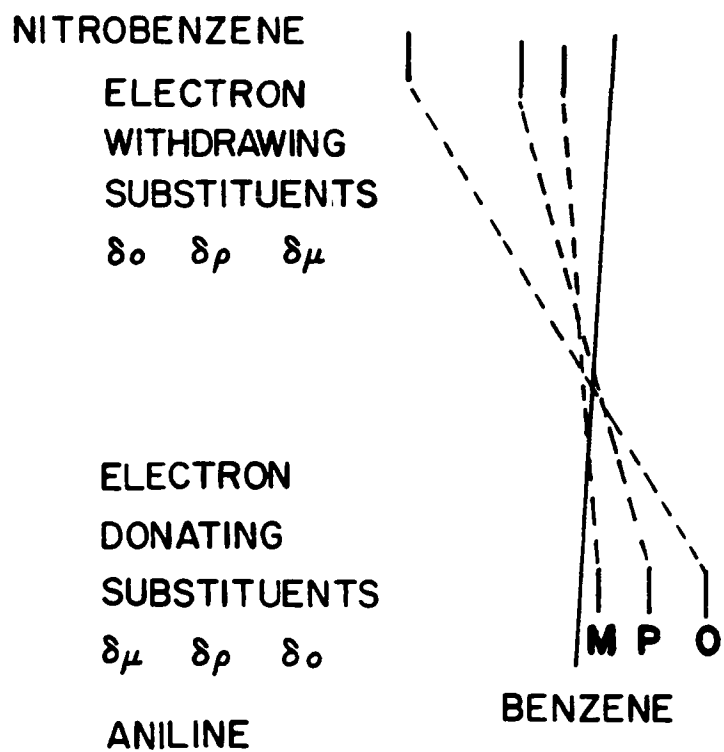
To a first order approximation $J_{A_2B_1}$ and J_{A_1C} can be neglected and $J_{A_1B_1} \cong J_{B_1C}$. This is equivalent to the assumption that the meta-para hydrogens form one equivalent group of three and the ortho hydrogens an equivalent group of two. The spectra should then be similar to that of the ethyl group with four lines for the ortho hydrogen resonance with intensi-

ties 1:2:1. This is approximately the case for the degree of resolution observed, although it is possible to detect the presence of further splitting for the meta-para hydrogen. These lines would be first the chemical shift of the meta and para protons and then the superposition of each group's interaction with the ortho protons. As for the ether molecule, all phenyl groups are equivalent on a time-average basis.

The relative positions of the meta-para and ortho peaks indicate the presence of a strong electropositive substituent. Figure 49 shows the effect of an electron withdrawing group in monosubstituted benzenes (80).

The results obtained from the NMR spectra of diphenylmagnesium can be summarized as follows:

1. The integrated intensities indicate a ratio of one phenyl to one dietherate group.
2. The phenyl group is attached to a strong electropositive atom and exists in a constant time averaged environment. The ethyl group is attached to a strongly electronegative atom and also "sees" a uniform environment. This means, for example, all the methyl protons are equivalent.
3. In spite of the fact that there is not a stoichiometric amount of ether present, all ether groups are in the same average environment. There is no way to distinguish an ether of coordination from one of solution. Chemically



(ORTHO, META, AND PARA SHIFTS
IN MONOSUBSTITUTED BENZENES)

Figure 49. Effect of electronegativity of substituent
in monosubstituted benzenes (80)

there must be a rapid exchange of ether molecules.

Data Processing

The data as collected from the precession camera were corrected for the motion of the crystal in the x-ray beam and the polarization of the diffracted beam. This correction has been discussed for the two-dimensional data for phenylmagnesium bromide. The same IBM 704 film data correction program was used as before. The unscaled observed structure factors are listed in Table 38.

The output of the above program was used as input for an IBM 704 program, Tescen, which was written to perform the calculations for statistical tests for space group determination and also to give an estimation of the scale and temperature factor to be used for the data. This latter is calculated by Wilson's method (72) from a plot of

$$\ln \frac{\langle E(hkl) \rangle}{\langle \sum (f_j^0)^2 \rangle} \text{ versus } \sin^2 \theta .$$

$\langle E(hkl) \rangle$ is the average observed intensity, $\langle \sum (f_j^0)^2 \rangle$ is the average of the sum of the squares of the atomic scattering factors, and 2θ is the Bragg diffraction angle. The averaging is over the intensities for a small range of $\sin^2 \theta$. The relation involved is

Table 38. Unscaled^a observed structure factors
 $(C_6H_5)_2Mg \cdot 2(C_4H_{10}O)$ {hk0} and {hkl} data

Reflection			F _{obs}	Reflection			F _{obs}	Reflection			F _{obs}
h	k	l		h	k	l		h	k	l	
3	0	1	22	-3	3	1	39	-3	5	1	12
4	0	0	62	3	3	1	21	3	5	1	33
5	0	1	18	-4	3	0	22	-5	5	1	38
6	0	0	17	-5	3	1	15	5	5	1	25
8	0	0	52	5	3	1	11	-6	5	0	17
9	0	1	9	-6	3	0	18	-7	5	1	17
10	0	0	19	-7	3	1	11	7	5	1	16
14	0	0	13	7	3	1	35	-9	5	1	12
-3	1	1	162	9	3	1	30	9	5	1	29
3	1	1	24	11	3	1	13	11	5	1	12
-5	1	1	45	0	4	0	13	0	6	0	53
5	1	1	17	-1	4	1	62	-1	6	1	36
-7	1	1	24	1	4	1	49	1	6	1	36
7	1	1	9	2	4	0	60	2	6	0	28
-9	1	1	13	-2	4	0	105	-2	6	0	114
9	1	1	17	-3	4	1	21	-3	6	1	32
2	2	0	171	3	4	1	30	3	6	1	24
-3	2	1	104	4	4	0	109	4	6	0	54
3	2	1	30	-4	4	0	41	-4	6	0	28
-4	2	0	103	-5	4	1	14	-5	6	1	18
-5	2	1	13	5	4	1	32	5	6	1	26
5	2	1	22	-6	4	0	31	6	6	0	26
-6	2	0	25	-7	4	1	37	-6	6	0	30
-7	2	1	13	7	4	1	10	-7	6	1	9
7	2	1	22	8	4	0	22	7	6	1	10
8	2	0	36	-8	4	0	27	8	6	0	27
-8	2	0	29	-9	4	1	13	-8	6	0	26
-9	2	1	11	9	4	1	11	10	6	0	15
10	2	0	14	10	4	0	18	-10	6	0	26
11	2	1	11	11	4	1	14	12	6	0	18
12	2	0	26	-12	4	0	10	-1	7	1	14
-12	2	0	13	14	4	0	17	1	7	1	15
16	2	0	14	-14	4	0	17	3	7	1	16
-1	3	1	108	-1	5	1	18	-5	7	1	43
1	3	1	17	1	5	1	28	5	7	1	10

^aThe scale factors for this data set ($F_{obs} = k F_{calc}$) are about 2.00 for {hk0} and 1.25 for {hkl}.

Table 38 (Continued)

Reflection				F _{obs}	Reflection				F _{obs}	Reflection				F _{obs}
h	k	l	h		k	l	h	k		l				
-6	7	0	13	-5	10	1	10	-3	15	1	12			
-7	7	1	11	6	10	0	16	0	16	0	23			
-9	7	1	15	-6	10	0	36	2	16	0	19			
0	8	0	61	-8	10	0	16	-2	16	0	14			
-1	8	1	21	-10	10	0	37	4	16	0	13			
1	8	1	24	-12	10	0	18	-4	16	0	12			
2	8	0	48	-1	11	1	10	6	16	0	14			
-2	8	0	28	1	11	1	18	-6	16	0	12			
-3	8	1	10	3	11	1	10	10	16	0	15			
3	8	1	8	5	11	1	10	0	18	0	34			
4	8	0	29	-7	11	1	17	2	18	0	20			
-4	8	0	65	-9	11	1	13	-2	18	0	14			
-5	8	1	20	0	12	0	22	4	18	0	18			
5	8	1	11	-1	12	1	9	-6	18	0	15			
-6	8	0	45	1	12	1	11	0	22	0	12			
-7	8	1	20	2	12	0	26	0	24	0	11			
-8	8	0	26	-2	12	0	22							
-9	8	1	13	4	12	0	18							
10	8	0	17	-4	12	0	20							
-10	8	0	23	-5	12	1	12							
-12	8	0	11	-6	12	0	23							
-1	9	1	17	10	12	0	18							
1	9	1	25	-12	12	0	28							
-3	9	1	14	-3	13	1	12							
-5	9	1	19	3	13	1	13							
-6	9	0	15	-5	13	1	19							
-7	9	1	12	0	14	0	25							
0	10	0	17	-1	14	1	11							
-1	10	1	11	1	14	1	10							
1	10	1	9	2	14	0	16							
2	10	0	22	-2	14	0	16							
-2	10	0	45	4	14	0	15							
-3	10	1	16	-4	14	0	21							
4	10	0	42	-6	14	0	13							
-4	10	0	51	-10	14	0	24							

$$\ln \frac{\langle E(hkl) \rangle}{\langle \Sigma(f_j^0)^2 \rangle} = (-2B/\lambda^2) \sin^2 \theta + \ln K$$

so that the slope of the resulting straight line is $-2B/\lambda^2$ and the intercept is $\ln K$. B is the Debye-Waller temperature factor, λ the wavelength of the radiation used and K the scale factor defined by

$$E(hkl) = K|F(hkl)|^2$$

The results for the $\{hk0\}$ and $\{hkl\}$ data are shown in Figure 50. The points were fitted by least squares. For $\{hk0\}$ data, $B = 3.80$, $K = .272$. For $\{hkl\}$ data, $B = 5.2$, $K = .075$.

Vector Maps

For B centered monoclinic systems the vector map has B $2/m$ symmetry. The Patterson function for the $[001]$ zone was derived to be as follows:

$$\begin{aligned} \rho(uv0) = & \frac{1}{V_c} \sum_{h=1}^{\infty} \sum_{k=1}^{\infty} \{ |F(hk0)|^2 \cos 2\pi(hu + kv) \\ & + |F(\bar{h}k0)|^2 \cos 2\pi(hu - kv) \} \\ & + \frac{1}{V_c} \sum_{h=1}^{\infty} |F(h00)|^2 \cos 2\pi hu \end{aligned}$$

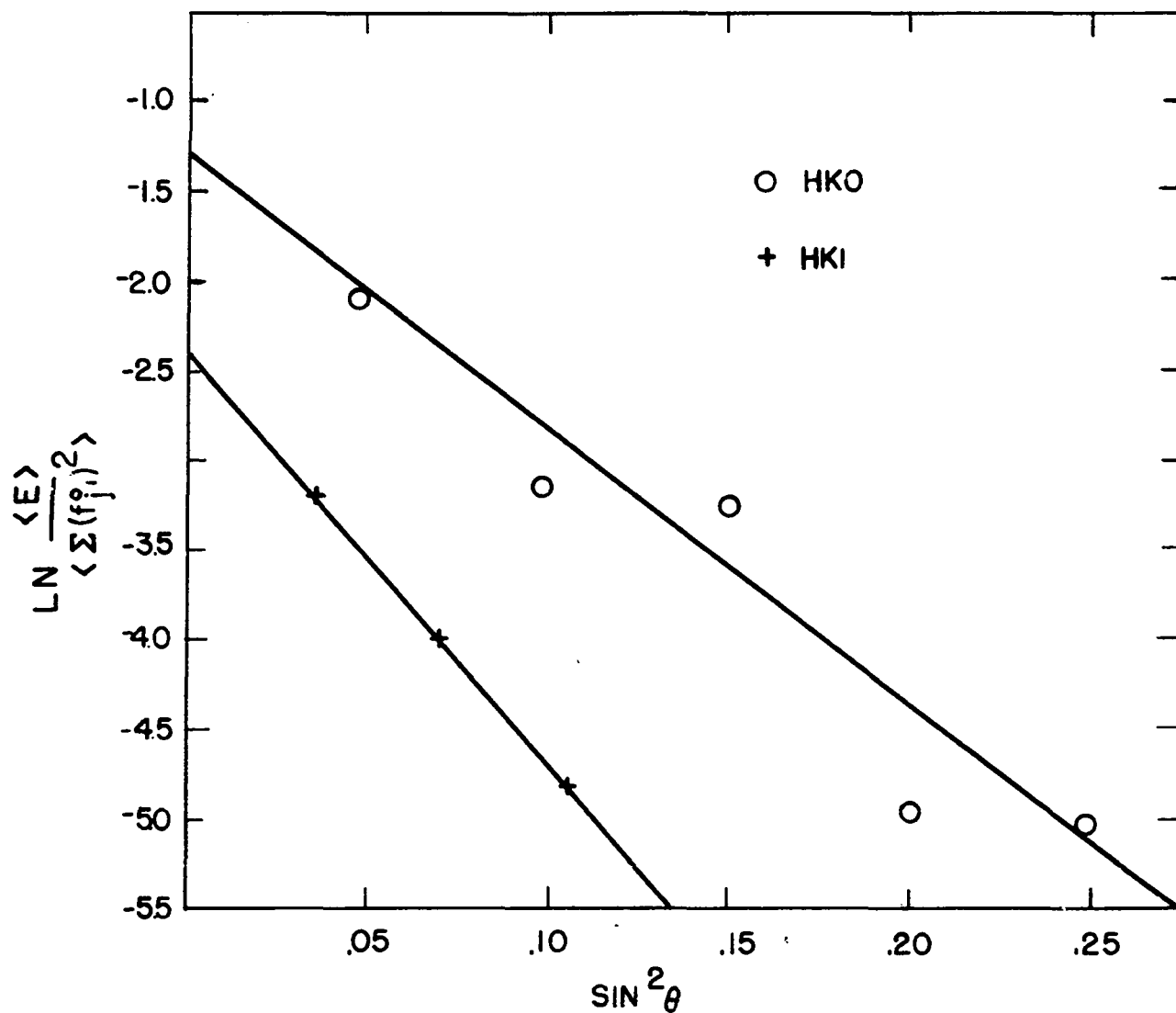


Figure 50. Determination of absolute scale and average temperature factor for {hk0} and {hkl} data for $(\text{C}_6\text{H}_5)_2\text{Mg} \cdot 2(\text{C}_4\text{H}_{10}\text{O})$

$$+ \frac{1}{V_c} \sum_{k=1}^{\infty} |F(0k0)|^2 \cos 2\pi kv \quad .$$

$$|F(\bar{h}k0)|^2 = |F(h\bar{k}0)|^2$$

A Patterson projection onto the (001) plane was calculated by means of the "MIFR 1" program for the 704. The vector map obtained is shown in Figure 51. Because of the B centering it is only necessary to consider one-half the unit cell in the \vec{a} direction. The two-fold axis at $a/4$ in projection permits the consideration of only one-half the unit cell in the h direction. The vectors for this projection are derived in Table 39 for the plane group P2.

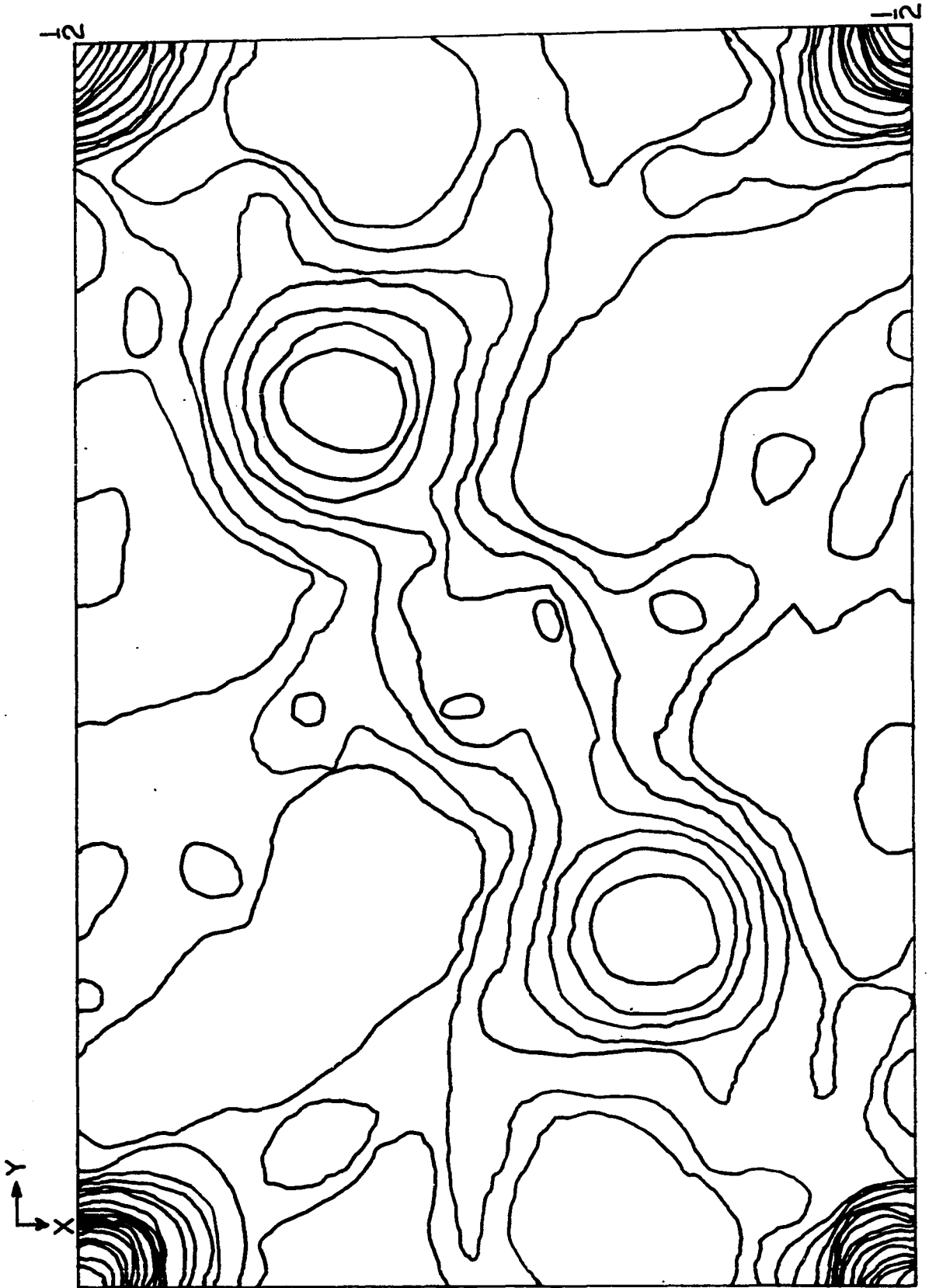
Table 39. Analysis of coordinates and vector distances for the plane group P2

Operation	Axis	Location	Coordinates	General vectors P2 : 2c	Special vectors
1	---	---	$x \ y$	$x_1 - x_2 \ y_1 - y_2$	00
2	001	000	$\bar{x} \ \bar{y}$	$x_1 + x_2 \ y_1 + y_2$	2x2y

The space group coordinates (x' , y') are related to the plane group coordinates (x , y) by

$$x' = 2x \qquad y' = y$$

Figure 51. (001) Patterson projection for $(C_6H_5)_2Mg \cdot 2(C_4H_{10}O)$



Note that in the plane group the translation distance is one unit cell. Table 38 is equally valid for space groups B2 and B 2/m, the only difference being the multiplicity of the vectors. The large peaks at $y = 1/2$ reflect the observation that $\{hk0\}$, k odd reflections are weak or missing. They correspond to atoms $\vec{b}/2$ from each other. The large diffuse peak in the $[110]$ direction is about 3.4 \AA from the origin. Rough intensity data were available from one timed exposure of $\{hh\}$ data. These data were judged using the $\{hh0\}$ reflections of the (001) projection as reference reflections. The observed intensities are listed in Table 40. The Patterson was computed as a two-dimensional projection by using the transformations

$$\vec{a}_2^* = \vec{a}_1^* + \vec{b}_1^*$$

$$\cos \gamma_2^* = .6938$$

$$\vec{b}_2^* = \vec{b}_1^*$$

$$\gamma_2^* = 50^\circ 14'$$

$$\vec{c}_2^* = \vec{c}_1^*$$

$$|\vec{a}_2^*| = .0916$$

$$|\vec{b}_2^*| = .0566$$

$$|\vec{c}_2^*| = .0704$$

Since the Miller indices transform as the real space vectors, it is necessary to determine this transformation matrix. If these are of the form

Table 40. $(C_6H_5)_2Mg \cdot 2(C_4H_{10}O)$ {hkl} intensities (uncorrected)
precession data, $\mu = 20^\circ$

Reflections						I(uncorrected)
h_1	k_1	l_1	h_2	k_2	l_2	
2	2	0	2	0	0	547
4	4	0	4	0	0	113
6	6	0	6	0	0	4
1	1	1	1	0	1	10
3	3	1	3	0	1	5
5	5	1	5	0	1	9
2	2	2	2	0	2	16
4	4	2	4	0	2	3
6	6	2	6	0	2	4
8	8	2	8	0	2	3
10	10	2	10	0	2	3
1	1	3	1	0	3	1
3	3	3	3	0	3	9
5	5	3	5	0	3	7
7	7	3	7	0	3	4
9	9	3	9	0	3	3
0	0	4	0	0	4	133
2	2	4	2	0	4	9
4	4	4	4	0	4	7
6	6	4	6	0	4	1
5	5	5	5	0	5	3
7	7	7	7	0	7	3

$$\vec{a}_2 = s_{11} \vec{a}_1 + s_{12} \vec{b}_1 + s_{13} \vec{c}_1$$

$$\vec{b}_2 = s_{21} \vec{a}_1 + s_{22} \vec{b}_1 + s_{23} \vec{c}_1$$

$$\vec{c}_2 = s_{31} \vec{a}_1 + s_{32} \vec{b}_1 + s_{33} \vec{c}_1$$

we have

$$\begin{aligned}
 \vec{a}_2 \cdot \vec{a}_1^* &= s_{11} = 1 & \vec{b}_2 \cdot \vec{a}_1^* &= s_{21} = -1 & \vec{c}_2 \cdot \vec{a}_1^* &= s_{31} = 0 \\
 \vec{a}_2 \cdot \vec{b}_1^* &= s_{12} = 0 & \vec{b}_2 \cdot \vec{b}_1^* &= s_{22} = 1 & \vec{c}_2 \cdot \vec{b}_1^* &= s_{32} = 0 \\
 \vec{a}_2 \cdot \vec{c}_1^* &= s_{13} = 0 & \vec{b}_2 \cdot \vec{c}_1^* &= s_{23} = 0 & \vec{c}_2 \cdot \vec{c}_1^* &= s_{33} = 1
 \end{aligned}$$

so that $h_2 = h_1$, $k_2 = k_1 - h_1$, $l_2 = l_1$.

This corresponds to a rotation about the z axis and an (010) projection. The corresponding Patterson function is

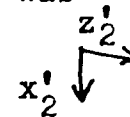
$$\begin{aligned}
 \rho(\text{UOW}) &= 2 \sum_{h=1}^{\infty} \sum_{l=1}^{\infty} |F(h0l)|^2 \cos 2\pi hu \cos 2\pi lw \\
 &+ \sum_{h=1}^{\infty} |F(h0l)|^2 \cos 2\pi hu \\
 &+ \sum_{h=1}^{\infty} |F(00l)|^2 \cos 2\pi lw .
 \end{aligned}$$

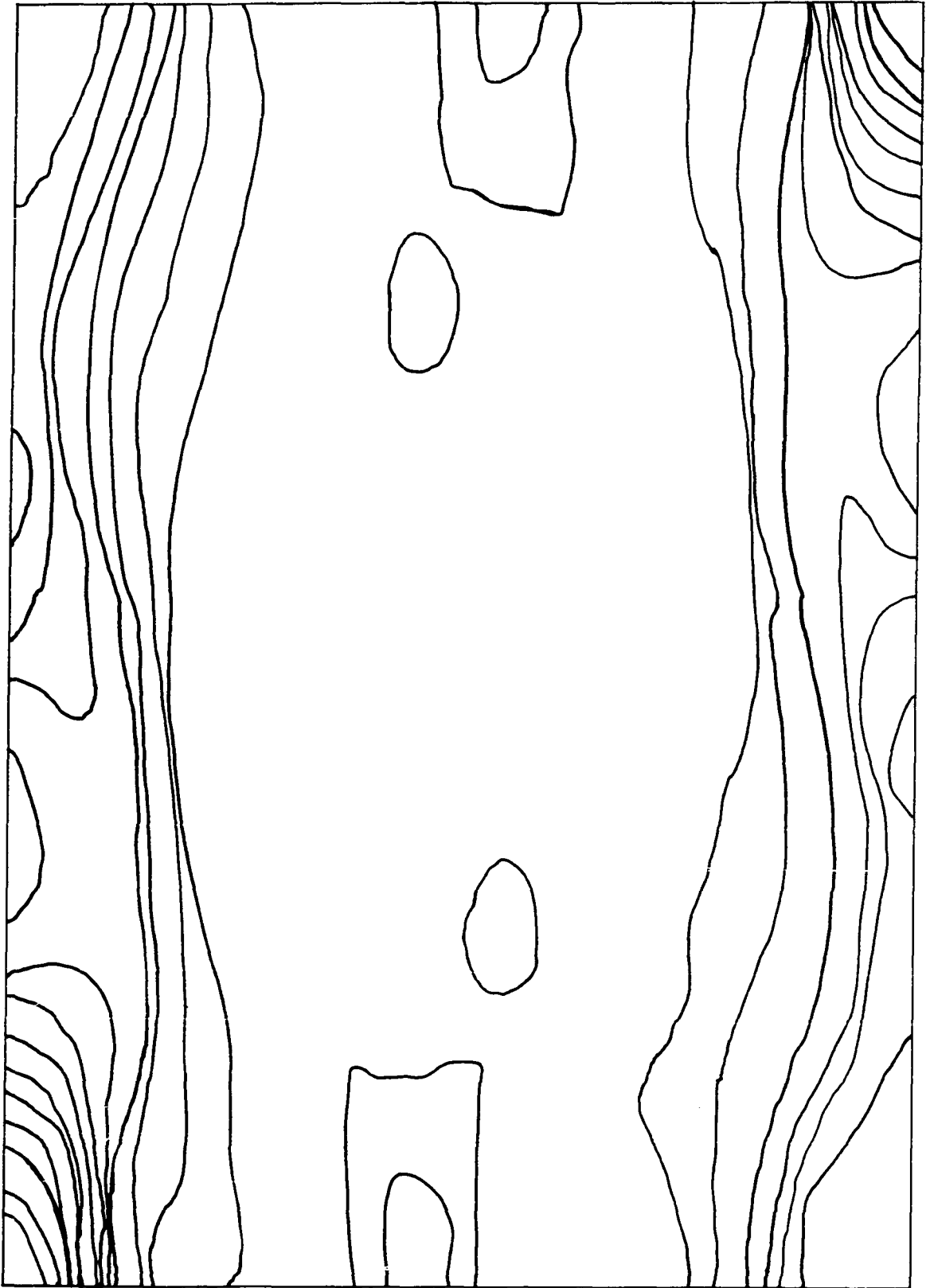
There were only 22 observable reflections in this zone, so the Patterson peaks (Figure 52) are quite diffuse. The extinctions for this zone are $h_2 + l_2 = 2n + 1$, so that the lattice is still B centered. The plane group projection symmetry is b_{mm} with

$$x_2' = x, \quad z_2' = z;$$

where x_2' , z_2' are the transformed space group coordinates.

Figure 52. $\{hkl\}$ Patterson projection for $(C_6H_5)_2Mg \cdot 2(C_4H_{10}O)$. Projection was calculated as (010). The transformed directions (for 010) are $1/2 \times 1/2$ of the unit cell is shown.





x_2' and z_2' are related to the original unit cell coordinates by

$$x_2' = x_1' + y_1'$$

$$y_2' = y_1'$$

$$z_2' = z_1' .$$

The vectors for this projection are derived in Table 41 for the plane group b_{mm} . From Table 41 the most prominent vectors between equivalent atoms should be at 0, 0 and 1/2, 1/2 with a multiplicity of 12. The next most intense peaks fall at $2x$ 0, 0 $2z$, 1/2 + $2x$ 1/2, and 1/2 1/2 + $2z$ all with a multiplicity of 2. The remaining vectors have a multiplicity of 1.

With the data available two more vector maps are of possible value. Consider the generalized projection (81, 82) defined by

$$P_L(u, v) = \int_0^1 cP(uvw) \exp 2\pi i Lw \, dw$$

where L is some particular value of the Miller indice l .

This reduces to

$$P_L(u, v) = \frac{1}{s} \sum_{hk}^{\infty} |F(hkL)| \exp 2\pi i (hu + kv)$$

Table 41. Analysis of coordinates and vector distances for the plane group bmm

Operation	Axis	Location	Coordinates		General 8(f) vectors:cmm		Special vectors		
1	-	-	x	z	$x_2 - x_1$	$z_2 - z_1$	8(a)	0	0
m_x	-	0,0	\bar{x}	z	$x_2 + x_1$	$z_2 - z_1$	4(d)	2x	0
m_z	-	0,0	x	\bar{z}	$x_2 - x_1$	$z_2 + z_1$	4(e)	0	2z
2	010	0,0	\bar{x}	\bar{z}	$x_2 + x_1$	$z_2 + z_1$	8(f)	2x	2z
2	010	a/4,c/4	$\frac{1}{2} - x$	$\frac{1}{2} - z$	$\frac{1}{2} + x_2 + x_1$	$\frac{1}{2} + z_2 + z_1$	8(f)	$\frac{1}{2} + 2x$	$\frac{1}{2} + z$
g	001	a/4	$\frac{1}{2} - x$	$\frac{1}{2} + z$	$\frac{1}{2} + x_2 + x_1$	$\frac{1}{2} + z_2 - z_1$	4(d)	$\frac{1}{2} + 2x$	$\frac{1}{2}$
g	100	c/4	$\frac{1}{2} + x$	$\frac{1}{2} - z$	$\frac{1}{2} + x_2 - x_1$	$\frac{1}{2} + z_2 + z_1$	4(e)	$\frac{1}{2}$	$\frac{1}{2} + 2z$
b	-	-	$\frac{1}{2} + x$	$\frac{1}{2} + z$	$\frac{1}{2} + x_2 - x_1$	$\frac{1}{2} + z_2 - z_1$	2(a)	$\frac{1}{2}$	$\frac{1}{2}$

where s is the area of the projection. For monoclinic structures and $\{hkl\}$ data this reduces to


$$P_1(uv) = \sum_{hk}^{\infty} |F(hkl)|^2 \cos 2\pi(hu + kv)$$

Curtis and Pasternak (83) have shown that if the weighting function of the zero level projection is $1 + \cos 2\pi z$, the corresponding function is

$$P_1'(uv) = \sum_{hk} \{ |F(hk0)|^2 + |F(hkl)|^2 \} \cos 2\pi(hu + kv)$$

for the monoclinic case. The Patterson maps for $P_1(uv)$ and $P_1'(uv)$ are shown in Figures 53 and 54. The symmetry of the vector space $P_1(uv)$ is that of $P(uv)$ if the absolute value of the peaks are taken. The symmetry of $P_1'(uv)$ is changed, however, to $P 2/m$. This necessitates the calculation of a full unit cell in the \vec{a} direction.

No consistent interpretation of the above vector maps was found. Part of the difficulty in interpretation is in the profusity of inter- and intramolecular benzene carbon-carbon interactions. Because of this and the fact that there is not much difference between the amounts of scattering produced by the various atoms, it is difficult to identify any one vector interaction. An additional factor is the pseudo translation of $\vec{b}/2$ which can also be expected to

Figure 53. {hkl} Patterson projection for
 $(C_6H_5)_2Mg \cdot 2(C_4H_{10}O)$. Dotted lines
indicate negative peaks. Coordinates
 . 1/2 by 1/2 of unit cell is
shown.

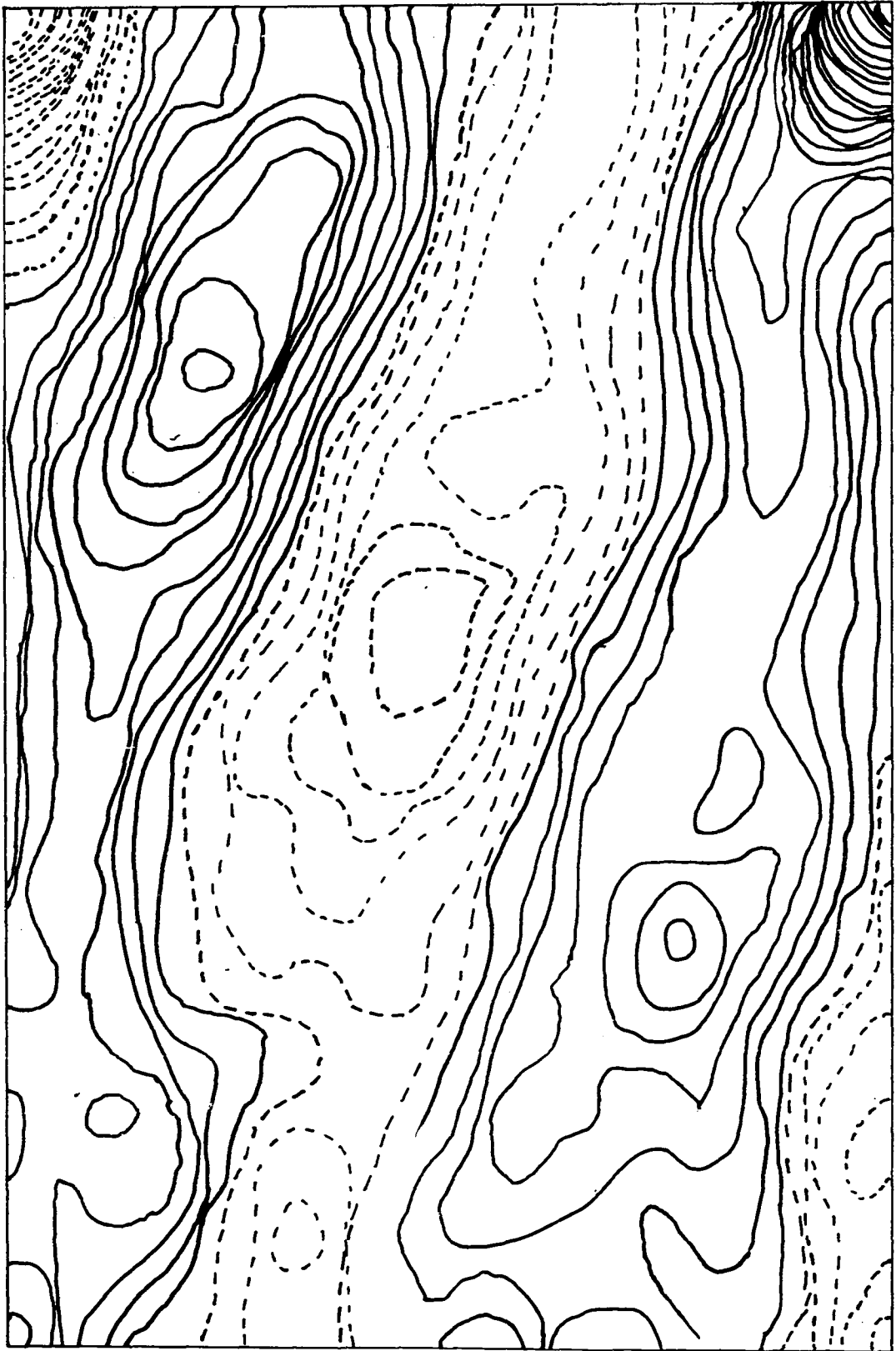
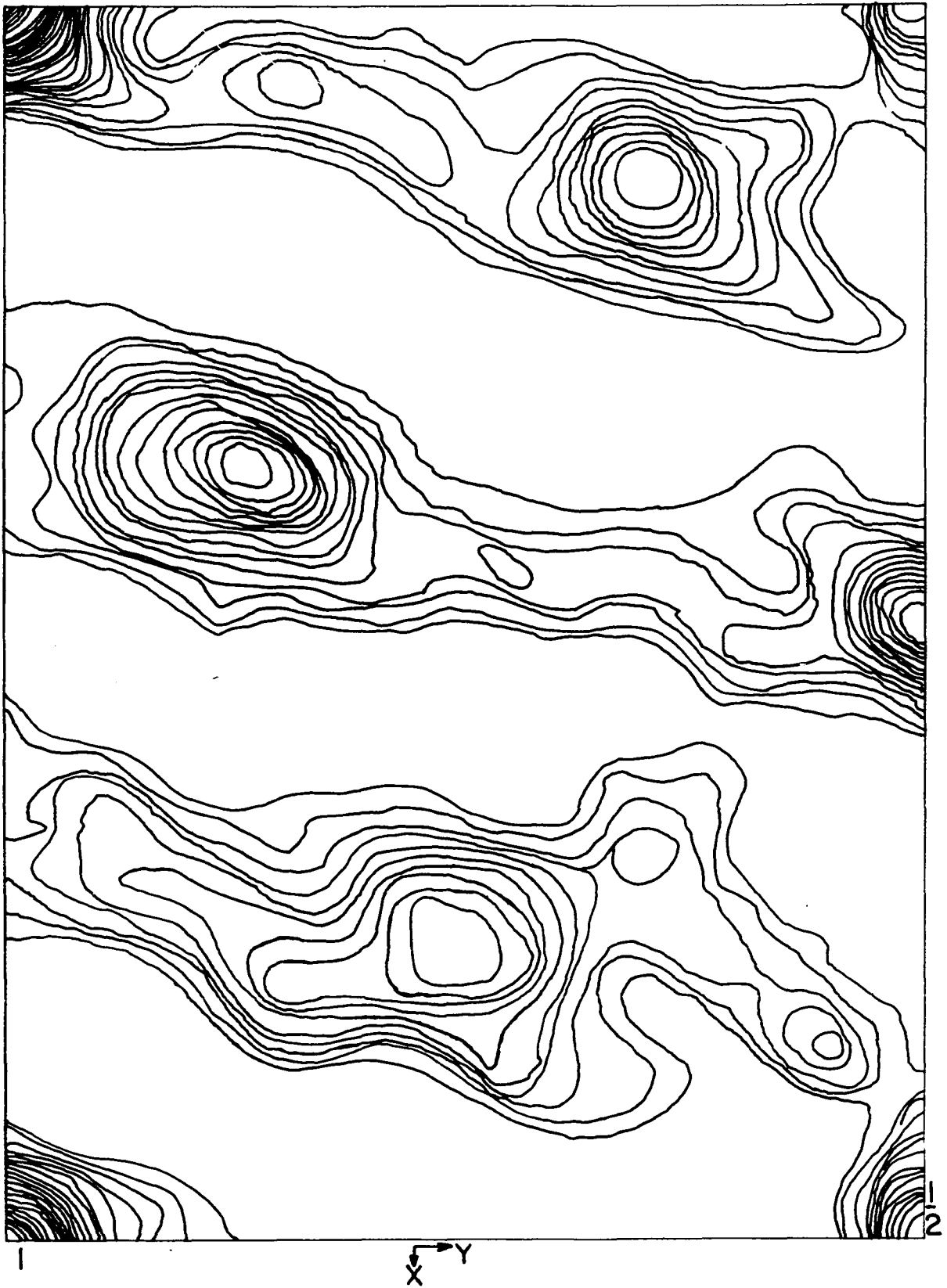


Figure 54. Patterson projection for $(C_6H_5)_2Mg \cdot 2(C_4H_{10}O)$
using $(|F(hk0)|^2 + |F(hkl)|^2)$ as coefficients



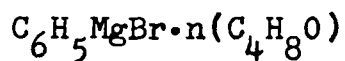
produce superposition of vectors. It would be hoped that the greater resolution available with three dimensional data would permit easier interpretation of the three-dimensional vector map.

Least Squares Analysis and Electron Density Projections

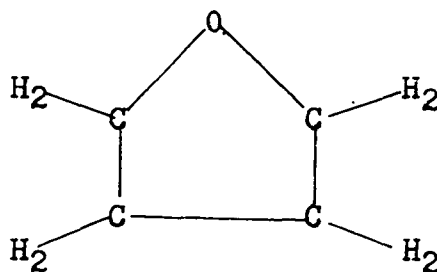
Out of a great number of models tried the best agreement for {hk0} data was obtained by including only magnesium atoms at 00 and 0 1/2. The agreement factor

$$R = \frac{\Sigma ||F_o| - |F_c||}{\Sigma |F_o|}$$

was 39%. Since all the signs of the structure factors are positive for these positions, the resulting Fourier map had the same features as the Patterson vector map (Figure 17). Several models were also tried using only the 15 strongest {hk0} reflections. The magnesium atom model gave R = 19%. The only parameter involved is the scale factor.



Tetrahydrofuran has some desirable features as a solvent for the Grignard reagent. It has a boiling point of 65°C as compared to the highly volatile diethylether which has a boiling point of 34.6°C . This greatly lessens experimental problems such as sealing capillaries and variation of pressure in a closed system. It is also a more pleasant molecule from the crystallographic viewpoint since it has the fixed geometric configuration shown below.



Hamelin and Gaypiron (84) measured the solubility of the Grignard reagent, ethylmagnesiumbromide, at room temperature in various solvents. They found that a "mixed" compound crystallized out of solution and that the composition of the compound was a function of the solvent used. They measured the "basic" magnesium, Mg_b , by titrating with water and then acid to determine the amount of R_2Mg present. They then measured the amount of "salt-like" magnesium, Mg_s , presumably as MgX_2 , by treating with silver nitrate. They characterized

the compound which precipitated out of solution by the ratio $[Mg_s]/[Mg_b]$. Their results are given in Table 42.

Table 42. Hamelin and Gaypiron's study of the C_2H_5MgBr in various solvents

Solvent	Solubility $n = \frac{[EtMgBr]}{[solvent]}$	$\frac{[Mg_s]}{[Mg_b]}$	No. moles solvent/mg
C_6H_6	insoluble	----	----
$C_6H_5OCH_3$	< .03	3.6	2.26
$(IPr)_2O$.14	1.25	1.23
Et_2O	.71	1.08	1.23
Bu_2O	.92	1.51	0.57
THF	.12	2.40	4.9
Dioxane	.00	> 10	----

The most interesting aspect of these results is the apparent variation of composition of the species in solution with the type of solvent used. The second point is the high degree of solvation attained by magnesium in tetrahydrofuran. Water has a solvation number of six about the magnesium atom and it is quite reasonable to expect that the tetrahydrofuran would be capable of a higher degree of association than the less basic diethylether.

Several preparations of phenylmagnesiumbromide in tetrahydrofuran were carried out. It was observed that the Grignard reagent or perhaps a magnesiumbromide solvate apparently crystallized out of tetrahydrofuran as soon as the solution in which it was prepared cooled to room temperature. An interesting effect was that the material could be redissolved but that once in solution again would not crystallize nearly as readily the second time. The solution gave a positive Gilman's test both before and after the crystals were redissolved. No quantitative analyses were carried out on these crystals.

By heating the tetrahydrofuran solution of the Grignard reagent to approximately the boiling point of the tetrahydrofuran and evaporating the reagent through a very small opening, beautiful, transparent, rectangular, rod-shaped crystals were obtained. The crystals had a density of approximately 1.5 gms/cm^3 . The lattice constants as determined by x-ray diffraction were

$$\begin{aligned} a &= 8.05 \overset{\circ}{\text{Å}} \\ b &= 9.89 \overset{\circ}{\text{Å}} \\ c &= 20.73 \overset{\circ}{\text{Å}} \end{aligned} \qquad B = 95^\circ 20'$$

The only extinctions observed were $\{h0l\}$, $l = 2n + 1$, indicating an apparent space group of Pc or $P 2/c$ (2nd setting). Gilman's test indicated that the material was not a true

organometallic. Since the preparation of this material followed that of the basic magnesium salt prepared from a phenylmagnesiumbromide solution of diethylether it seems not unlikely that the material is a more highly solvated version of the etherated compound.

SUMMARY

Structural investigations of the solvated compounds $\text{Mg}_4\text{Br}_6\text{O}\cdot 4(\text{C}_4\text{H}_{10}\text{O})$ and $\text{C}_6\text{H}_5\text{MgBr}\cdot 2(\text{C}_4\text{H}_{10}\text{O})$ were undertaken by means of x-ray diffraction techniques. In addition, initial structural studies were made on $(\text{C}_6\text{H}_5)_2\text{Mg}\cdot 2(\text{C}_4\text{H}_{10}\text{O})$ and the space group and lattice constants were determined for an oxy salt of the Grignard reagent solvated with tetrahydrofuran.

$\text{Mg}_4\text{Br}_6\text{O}\cdot 4(\text{C}_4\text{H}_{10}\text{O})$ was found to possess tetragonal symmetry; the lattice constants based on a primitive unit cell are:

$$\begin{aligned} a &= b = 10.68 \overset{\circ}{\text{A}} \\ c &= 15.34 \overset{\circ}{\text{A}} . \end{aligned}$$

There are two $\text{Mg}_4\text{Br}_6\text{O}\cdot 4(\text{C}_4\text{H}_{10}\text{O})$ species per unit cell.

Systematic absences indicated the space group $\text{P}\bar{4}2_1\text{c}$.

The structural analysis proceeded through a complete three-dimensional Fourier. The bromine atoms form an octahedron approximately 4.5 angstroms on an edge about the origin with the magnesium atoms in alternating faces of the octahedron, forming a tetrahedron of magnesium atoms. The magnesiums are five-fold coordinated to three bromines, a "basic" oxygen atom at the origin, and to an ether group packed against the face of the bromine octahedron. The only model compatible with the Fourier and least squares analysis and with packing considerations involves a disordered structure

in which the ether carbons can be packed in three equivalent ways against the faces of the octahedron formed by the bromine atoms. Packing considerations strongly imply that the ether oxygens are trigonally coordinated to the magnesium atom and that only two of the three possible ether orientations are utilized in the crystal.

$C_6H_5MgBr \cdot 2(C_4H_{10}O)$, a liquid at room temperature, was isolated by successive recrystallizations at low temperatures. The lattice constants for this orthorhombic system were found to be

$$\begin{aligned} a &= 12.25 \overset{\circ}{\text{A}} \\ b &= 12.81 \overset{\circ}{\text{A}} \\ c &= 11.02 \overset{\circ}{\text{A}} . \end{aligned}$$

The space group was uniquely determined to be $P2_12_12_1$, and the observed density and chemical analysis both suggested 4 molecules of $C_6H_5MgBr \cdot 2(C_4H_{10}O)$ per unit cell. Three-dimensional Patterson and two-dimensional Fourier analyses revealed that the basic molecular unit consisted of the phenyl group, the ether oxygens, and the bromine atom tetrahedrally coordinated to a single-magnesium atom. There was no evidence of intermolecular interaction between the monomeric molecules of $C_6H_5MgBr \cdot 2(C_4H_{10}O)$. Because of experimental difficulties in obtaining the data the carbon positions were not located by least squares refinement. Three-dimensional Fourier results implied, however, that the ether molecules are tetrahedrally

coordinated to the magnesium atom, although additional three-dimensional work will be needed to confirm the structural aspects relating to the carbon atoms. Since the magnesium-magnesium, magnesium-bromine, and bromine-bromine distances eliminate the possibility of $R_2Mg \cdot MgX_2$ type structures in the crystal, it would be surprising if recent proposals which disregarded the presence of the molecular species $RMgX \cdot 2ether$ in solution are correct.

$(C_6H_5)_2Mg \cdot 2(C_4H_{10}O)$ has monoclinic symmetry and lattice constants (1st setting) of

$$\begin{aligned} a &= 14.21 \text{ \AA} \\ b &= 17.69 \text{ \AA} \\ c &= 7.87 \text{ \AA} \end{aligned} \quad \gamma = 91^\circ 24'$$

The observed extinctions

$$\{hkl\} \quad h + l = 2n + 1$$

gave possible space groups of $B2$, $B 2/m$, or Bm . The ratio of ether groups to phenyl groups of one to one was confirmed by nuclear magnetic resonance studies. Density measurements made on the NMR samples gave $\rho = 1.09 \text{ gms/cm}^3$. This corresponds to four molecules of $(C_6H_5)_2Mg \cdot 2(C_4H_{10}O)$ per unit cell. Intensity data were taken of $\{hk0\}$ and $\{hkl\}$ reflections. No structural interpretation was found for these data.

The lattice constants and space group of a salt obtained by the oxidation of a solution of phenylmagnesium bromide in tetrahydrofuran were determined by x-ray techniques.

The lattice constants obtained (2nd setting) were

$$a = 8.05 \text{ \AA}$$

$$b = 9.89 \text{ \AA}$$

$$c = 20.73 \text{ \AA} .$$

$$\beta = 95^{\circ} 20'$$

The only extinctions were $\{h0l\}$ $l = 2n + 1$ implying a space group of Pc or $P 2/c$.

LITERATURE CITED

1. Kharasch, M.S. and Reinmuth, O. Grignard reactions of nonmetallic substances. New York, N.Y., Prentice-Hall. 1954.
2. Yoffé, S.T. and Nesmeyanov, A.N. Handbook of magnesium-organic compounds. 3 vols. London, Pergamon Press. 1957.
3. Rochow, E.G., Hurd, D.T. and Lewis, R.N. The chemistry of organometallic compounds. New York, N.Y., John Wiley and Sons. 1957.
4. Coates, G.E. Organo-metallic compounds. 2nd ed. New York, N.Y., John Wiley and Sons. 1960.
5. Runge, F. Organo-metallverbindungen. Stuttgart, Germany, Wissenschaftliche Verlagsgesellschaft M.B.H. 1944.
6. Gilman, H. and Brown, R.E. J. Am. Chem. Soc. 52: 3330. 1930.
7. Tschelinzeff, W.C. Berichte 39: 773. 1906.
8. Lifschitz, J. and Kalberer, O.E. Zeitschrift Physik. Chem. 102: 393. 1922.
9. Schlenk, W. and Schlenk, W. Jr. Berichte 62: 920. 1929.
10. Noller, C.R. and White, W.R. J. Am. Chem. Soc. 59: 1354. 1937.
11. Evans, W.V. and Pearson, R. J. Am. Chem. Soc. 64: 2865. 1942.
12. Dessy, R.E., Handler, G.S., Wotiz, J.H. and Hollingsworth, C.A. J. Am. Chem. Soc. 79: 3476. 1957.
13. _____ and _____. J. Am. Chem. Soc. 80: 5824. 1958.
14. Garrett, A.B., Sweet, A., Marshall, W.L., Riley, D. and Touma, A. Record of Chemical Progress 13: 155. 1952.

15. Lewis, P.H. and Rundle, R.E. *J. Chem. Phys.* 16: 552. 1948.
16. Allred, A.L. and McCoy, C.R. *Tetrahedron Letters* 27: 25. 1960.
17. Korshunov, I.A., Batalov, A.P. and Orlova, A.A. *Radiochemistry (Radiokhimiia)* 1: 280. 1960.
18. Sinotova, E.N., Vobetskii, Yu., Loginov, Yu.N. and Evtikheev, V.N. *Radiokhimiia* 1: 687-690. 1959. Original not available, abstracted in *Chem. Abs.* 54: 18038e. 1960.
19. Cope, A.C. *J. Am. Chem. Soc.* 57: 2238. 1933.
20. Slough, W. and Ubbelohde, A.R. *J. Chem. Soc.* 1955: 108. 1955.
21. McDonnell, F.R.M., Pink, R.C. and Ubbelohde, A.R. *J. Chem. Soc.* 1951: 191. 1951.
22. Rundle, R.E. and Goring, J.H. *J. Am. Chem. Soc.* 72: 5337. 1950.
23. Aston, J.G. and Bernhard, S.A. *Nature (London)* 165: 485. 1950.
24. Plum, W.B. *J. Chem. Phys.* 5: 172. 1937.
25. Zeil, W. *Zeitschrift für Elektrochem.* 56: 789. 1952.
26. Zerewitinoff, T. *Berichte* 41: 2244. 1908.
27. Meisenheimer, J. and Casper, J. *Berichte* 61: 710. 1928.
28. Gomberg, M. and Bachmann, W.E. *J. Am. Chem. Soc.* 52: 2455. 1930.
29. Schlenk, W. [Die Konstitution der Organomagnesium Verbindungen]: Unpublished Ph.D. thesis. Charlottenburg, Germany, Library, University of Charlottenburg. 1929.
30. Gilman, H. and Brown, R.E. *J. Am. Chem. Soc.* 52: 4480. 1930.

31. Gilman, H. *Rec. Trav. Chem.* 49: 202. 1930.
32. Bandaccio, C. The Grignard reagent. Italian patent 548,183. Sept. 19, 1956. Abstracted in *Chemical Abstracts* 53: 4134g. 1959.
33. Strohmeier, W. *Zeitschrift für Elektrochemie* 60: 58. 1956.
34. _____. *Berichte* 88: 1218. 1955.
35. Ziegler, K., Nagel, K. and Patheiger, M. *Zeitschrift anorg. Chem.* 282: 345. 1955.
36. Wiberg, E. and Bauer, R. *Zeitschrift Naturforsch* 56: 396. 1950.
37. Fleck, H. *Annalen* 276: 138. 1893.
38. Wittig, G., Meyer, F.J. and Lange, G. *Annalen* 571: 167. 1951.
39. Peterson, S.W. and Levy, H.A. *J. Chem. Phys.* 26: 220. 1957.
40. Busing, W.R. and Levy, H.A. A crystallographic least squares refinement program for the IBM 704. U.S. Atomic Energy Commission Report ORNL 59-4-3. [Oak Ridge National Laboratory, Tenn.] 1959.
41. Sly, W.G. and Shoemaker, D.P. MIFR 1: a two- and three-dimensional crystallographic Fourier summation program for the IBM 704 computer. Cambridge, Massachusetts, Massachusetts Institute of Technology.
42. Holyrod, G. *Proc. Chem. Soc.* 20: 38. 1904.
43. Zelinsky, J. *Chem. Centr.* ii: 227. 1903.
44. Nesmeyanow, A.N. Academy of Sciences of the U.S.S.R. Division of Chemical Science. *Bulletin (Akad. Nauk. SSSR., Otdel. Khim. Nauk. Izvestica)* 1955: 988. 1955.
45. Wuyts, M.H. *Comptes Rendus des Travaux de Chimie* 148: 930. 1909.
46. Porter, C.W. and Steel, C. *J. Am. Chem. Soc.* 42: 2650. 1920.

47. Gilman, H. and Wood, A. J. Am. Chem. Soc. 48: 806. 1926.
48. Meisenheimer, J. Berichte 61: 708. 1928.
49. Fieser, L.F. Experiments in organic chemistry. 2nd ed. New York, N.Y., D.C. Heath and Co. 1941.
50. Miller, F.A. and Wilkens, C.H. Analyt. Chem. 24: 1253. 1952.
51. Shriner, R.L., Fuson, R.C. and Curtin, D. The systematic identification of organic compounds. New York, N.Y., John Wiley and Sons. 1956.
52. Dahl, Larry F. Structures of some polynuclear metal carbonyls. Unpublished Ph.D. thesis. Ames, Iowa, Library, Iowa State University of Science and Technology. 1957.
53. Menshutkin, J. J. Russ. Phys.-Chem. Soc. 35: 610. 1903.
54. Evans, W. and Rowley, H. J. Am. Chem. Soc. 52: 3523. 1930.
55. Kitaigorodskii, A.I. Organic chemical crystallography. New York, N.Y., Consultants Bureau. 1961.
56. International tables for x-ray crystallography. 3 vols. Birmingham, England, Kynoch Press.
57. Margenau, H. and Murphy, G.E. The mathematics of physics and chemistry. 2nd ed. New York, N.Y., D. Van Nostrand. 1956.
58. Furnas, Thomas C., Jr. Single crystal orienter instruction manual. Milwaukee, Wisconsin, General Electric Company. 1957.
59. Pepinsky, R. Record of Chemical Progress 17: 145. 1956.
60. Jacobson, R., Wunderlich, J.A., and Lipcomb, W.N.L. Acta Cryst. 14: 598. 1961.
61. Donohue, J. and Trueblood, K.N. Acta Cryst. 5: 414 and 701. 1952.

62. Lipson, H. and Cochran, W. The determination of crystal structures. London, G. Bell and Sons.
63. Willett, R.D. The crystal structures and magnetic properties of some red cupric chloride complexes. Unpublished Ph.D. thesis. Ames, Iowa, Library, Iowa State University of Science and Technology. 1962.
64. Hamilton, C.W. Acta Cryst. 1: 185. 1962.
65. Pauling, L. Nature of the chemical bond. 3rd ed. Ithaca, New York, Cornell University Press. 1960.
66. Busing, W.R. and Levy, H.A. A crystallographic function and error program for the IBM 704. U.S. Atomic Energy Commission Report ORNL 59-12-3. [Oak Ridge National Laboratory, Tenn.] 1959.
67. Gilman, H. and Schulze, F. J. Amer. Chem. Soc. 47: 2002. 1925.
68. Waser, J. Rev. Scientific Instr. 22: 563. 1951.
69. Gilman, H. and Brown, R.E. Rec. Trav. Chem. 48: 1133. 1929.
70. Buerger, M.J. Vector space. New York, N.Y., John Wiley and Sons. 1959.
71. Howell, E.A., Phillips, D.C. and Rogers, D. Acta Cryst. 3: 210. 1950.
72. Wilson, A.J.C. Nature (London) 150: 152. 1942.
73. Ramachandran, G.N. and Srinivasan, R. Acta Cryst. 12: 410. 1959.
74. Srinivasan, R. Acta Cryst. 13: 388. 1960.
75. Howell, E.A., Phillips, D.C. and Rogers, D. Research 2: 338. 1949.
76. Wilson, A.J.C. Acta Cryst. 2: 318. 1949.
77. Rogers, D. and Wilson, A.J.C. Acta Cryst. 6: 439. 1953.
78. Herbstein, F.H. and Schoening, F.R.L. Acta Cryst. 10: 657. 1947.

79. Anderson, W.A. Phys. Rev. 102: 151. 1956.
80. Pople, J.A., Schneider, W.G. and Bernstein, H.J. High resolution nuclear magnetic resonance. New York, N.Y., McGraw-Hill Book Co. 1959.
81. Clews, C.J.B. and Cochran, W. Acta Cryst. 2: 46. 1949.
82. Raeuchle, R.F. and Rundle, R.E. Acta Cryst. 5: 85. 1952.
83. Curtis, R.M. and Pasternak, R.A. Acta Cryst. 9: 391. 1956.
84. Hamelin, R.M. and Gaypiron, S. Comptes Rendus des Travaux de Chimie 246: 2382. 1958.

ACKNOWLEDGEMENTS

The author wishes to express his deepest appreciation to Dr. R. E. Rundle for his encouragement, interest, and suggestions in regard to this research.

The assistance of Mr. Fred Hollenbeck in the use of the x-ray equipment, in plotting Fourier and Patterson maps, and in collecting data is also gratefully acknowledged.

Several conversations with Dr. D. R. Fitzwater regarding the computing aspects of crystallography were quite helpful and appreciated.

Finally, the author wishes to acknowledge the help of his wife, Kaaren, who spent many long hours in the preparation of this manuscript.